ISSN 1948-5182 (online)

World Journal of *Hepatology*

World J Hepatol 2018 July 27; 10(7): 452-529

Published by Baishideng Publishing Group Inc

World Journal of Hepatology

Contents

Monthly Volume 10 Number 7 July 27, 2018

REVIEW

452 Contemporary role of liver biopsy in hepatocellular carcinoma
Sparchez Z, Mocan T

MINIREVIEWS

462 MR with Gd-EOB-DTPA in assessment of liver nodules in cirrhotic patients
Inchingolo R, Faletti R, Grazioli L, Tricarico E, Gatti M, Pecorelli A, Ippolito D

474 Associations between nonalcoholic fatty liver disease and ischemic stroke
Alkagiet S, Papagiannis A, Tziomalos K

479 Status and perspective of laparoscopic repeat liver resection
Morise Z

485 Balloon-occluded transcatheter arterial chemoembolization for hepatocellular carcinoma
Hatanaka T, Arai H, Kakizaki S

ORIGINAL ARTICLE

Basic Study

496 Amelioration of hepatotoxicity by biocleavable aminothiol chimeras of isoniazid: Design, synthesis, kinetics and pharmacological evaluation
Bhilare NV, Dhaneshwar SS, Mahadik KR

CASE REPORT

509 Hepatitis B virus subgenotype F3 reactivation with vaccine escape mutations: A case report and review of the literature
Schlabe S, van Bremen K, Aldabbagh S, Glebe D, Bremer CM, Marsen T, Mellin W, Di Cristanziano V, Eis-Hübinger AM, Spengler U

517 Large primary hepatic gastrinoma in young patient treated with trisegmentectomy: A case report and review of the literature
Pipek LZ, Jardim YJ, Mesquita GHA, Nii F, Medeiros KAA, Carvalho BJ, Martines DR, Iuamoto LR, Waisberg DR, D'Albuquerque LAC, Meyer A, Andraus W

World Journal of Hepatology

Contents

Monthly Volume 10 Number 7 July 27, 2018

523 Hepatectomy for gallbladder-cancer with unclassified anomaly of right-sided ligamentum teres: A case report and review of the literature

Goto T, Terajima H, Yamamoto T, Uchida Y

Contents

World Journal of Hepatology
Volume 10 Number 7 July 27, 2018

ABOUT COVER

Editorial Board Member of *World Journal of Hepatology*, Ahmet Gurakar, MD, Associate Professor, Department of Medicine, Division of Gastroenterology and Hepatology, Johns Hopkins University, Baltimore, MA 21205, United States

AIM AND SCOPE

World Journal of Hepatology (*World J Hepatol*, *WJH*, online ISSN 1948-5182, DOI: 10.4254), is a peer-reviewed open access academic journal that aims to guide clinical practice and improve diagnostic and therapeutic skills of clinicians.

WJH covers topics concerning liver biology/pathology, cirrhosis and its complications, liver fibrosis, liver failure, portal hypertension, hepatitis B and C and inflammatory disorders, steatohepatitis and metabolic liver disease, hepatocellular carcinoma, biliary tract disease, autoimmune disease, cholestatic and biliary disease, transplantation, genetics, epidemiology, microbiology, molecular and cell biology, nutrition, geriatric and pediatric hepatology, diagnosis and screening, endoscopy, imaging, and advanced technology. Priority publication will be given to articles concerning diagnosis and treatment of hepatology diseases. The following aspects are covered: Clinical diagnosis, laboratory diagnosis, differential diagnosis, imaging tests, pathological diagnosis, molecular biological diagnosis, immunological diagnosis, genetic diagnosis, functional diagnostics, and physical diagnosis; and comprehensive therapy, drug therapy, surgical therapy, interventional treatment, minimally invasive therapy, and robot-assisted therapy.

We encourage authors to submit their manuscripts to *WJH*. We will give priority to manuscripts that are supported by major national and international foundations and those that are of great basic and clinical significance.

INDEXING/ABSTRACTING

World Journal of Hepatology is now indexed in Emerging Sources Citation Index (Web of Science), PubMed, PubMed Central, and Scopus.

NAME OF JOURNAL
World Journal of Hepatology

ISSN
ISSN 1948-5182 (online)

LAUNCH DATE
October 31, 2009

FREQUENCY
Monthly

World Journal of Hepatology
Baishideng Publishing Group Inc
7901 Stoneridge Drive, Suite 501,
Pleasanton, CA 94588, USA
Telephone: +1-925-2238242
Fax: +1-925-2238243
E-mail: editorialoffice@wjgnet.com
Help Desk: http://www.f6publishing.com/helpdesk
http://www.wjgnet.com

PUBLISHER
Baishideng Publishing Group Inc
7901 Stoneridge Drive, Suite 501,
Pleasanton, CA 94588, USA
Telephone: +1-925-2238242
Fax: +1-925-2238243
E-mail: bpgoffice@wjgnet.com
Help Desk: http://www.f6publishing.com/helpdesk
http://www.wjgnet.com

PUBLICATION DATE
July 27, 2018

INSTRUCTIONS TO AUTHORS
http://www.wjgnet.com/bpg/gerinfo/204

ONLINE SUBMISSION
http://www.f6publishing.com

World Journal of Hepatology

Submit a Manuscript: http://www.f6publishing.com

World J Hepatol 2018 July 27; 10(7): 452-461

DOI: 10.4254/wjh.v10.i7.452

ISSN 1948-5182 (online)

REVIEW

Contemporary role of liver biopsy in hepatocellular carcinoma

Zeno Sparchez, Tudor Mocan

Zeno Sparchez, Tudor Mocan, 3rd Medical Department, Institute for Gastroenterology and Hepatology, Iuliu Hatieganu University of Medicine and Pharmacy, Cluj-Napoca 400162, Romania

ORCID number: Zeno Sparchez (0000-0002-3813-1677); Tudor Mocan (0000-0001-7785-6403).

Author contributions: All authors equally contributed to this paper with conception and design of the study, literature review and analysis, drafting and critical revision and editing, and final approval of the final version.

Conflict-of-interest statement: No potential conflicts of interest. No financial support.

Manuscript source: Invited manuscript

Correspondence to: Tudor Mocan, MD, Associate Specialist, Doctor, 3rd Medical Department, Institute for Gastroenterology and Hepatology, Iuliu Hatieganu University of Medicine and Pharmacy, Croitorilor st. 19-21, Cluj-Napoca 400162, Romania. mocan_tudor@yahoo.com
Telephone: +4-799-861946

Received: March 29, 2018
Peer-review started: March 29, 2018
First decision: May 9, 2018
Revised: May 29, 2018
Accepted: June 26, 2018
Article in press: June 27, 2018
Published online: July 27, 2018

Abstract

A correct diagnosis of hepatocellular carcinoma (HCC) in cirrhotic patients with focal liver lesions is one of the most important issues nowadays. Probably one of the oldest debates in the hepatology community is whether to perform liver biopsy (LB) in all cirrhotic patients with focal liver lesions. We now face a time when oncology is moving towards personalized medicine. According to the current European Association for the study of Liver diseases HCC guidelines, LB has only a minor role in the management of HCC. However, the current recommendations were made more than five years ago. As time has passed, the development of high-throughput molecular technologies has helped reveal the main molecular mechanism involved in HCC development and progression. Several subtypes of HCC, with both molecular and histological characterization, have been described. Importantly, some of these subtypes have prognostic impact. In the context of personalized treatment, the role of LB will be carefully reconsidered. Until then, it is mandatory to know the various techniques of LB, their performances, complications and limitations. The balance of risk and benefit defines many of the decisions that we make as providers of medical care. In this review, we discuss not only the risks associated with LB, but also the benefits of biopsy in various clinical scenarios. Not long from now, the role of LB will be reconsidered. It is possible that we will go back in time and once again use biopsy for HCC diagnosis. Then again, we may move back to the future to try to improve the use of liquid biopsy in the follow-up of HCC patients after various treatment modalities.

Key words: Molecular classification; Bleeding; Seeding; Liver biopsy; Hepatocellular carcinoma

Core tip: We now face a time when oncology is moving towards personalized medicine. The development of high-throughput molecular technologies has allowed us to define the main molecular mechanism involved in hepatocellular carcinoma (HCC) development and progression. Several subtypes of HCC have been described using both molecular and histological characterization. In the context of histological HCC sub-classes, each with distinct molecular patterns and prognostic impacts, the need for liver biopsy in HCC management becomes a necessity. In this era of personalized medicine, knowing the strengths of each sampling technique is of the utmost importance.

Sparchez Z, Mocan T. Contemporary role of liver biopsy in hepatocellular carcinoma. *World J Hepatol* 2018; 10(7): 452-461 Available from: URL: http://www.wjgnet.com/1948-5182/full/v10/i7/452.htm DOI: http://dx.doi.org/10.4254/wjh.v10.i7.452

INTRODUCTION

The correct identification, either malignant or benign, of focal liver lesions is one of the most important issues in cirrhotic patients. Nodular lesions are frequently discovered during an ultrasound screening of these patients. Recent progress in ultrasound has led to an earlier discovery of these lesions. Moreover, the application of contrast agents has gained more and more attention. Compared to other imaging modalities, contrast enhanced ultrasound (CEUS) can be performed immediately after conventional ultrasound (US), providing a simple, easy-to-perform and immediately available dynamic imaging tool[1]. The use of CEUS might therefore shorten the diagnostic and therapeutic work-up of hepatocellular carcinoma (HCC) patients. The large applicability of CEUS for the diagnosis of HCC in cirrhosis was questioned due to the risk of false-positive diagnoses in cases of cholangiocarcinoma. This has caused the American College of Radiology to release a diagnostic scheme for the characterization of focal liver lesions in patients at risk for HCC, named CEUS LI-RADS®[2]. In a multicenter Italian study, the use of CEUS LI-RADS in small HCC showed that the LR-5 category was 98.5% predictive of HCC, with no risk of misdiagnosing pure cholangiocarcinoma[3].

Despite all the latest improvements in liver imaging, correctly identifying these lesions remains a challenge, especially when dealing with small focal lesions.

According to the AASLD and EASL guidelines, the images in certain situations may not be characteristic, or the results from two imaging techniques may be conflicting (a liver biopsy (LB) is required in these cases)[4]. In addition, the information from tumor tissue may provide prognostic data that are useful in the selection of therapy.

TECHNIQUES, PERFORMANCE, COMPLICATIONS

The invasive techniques used for the morphological diagnosis of HCC are ultrasound-guided fine-needle aspiration (FNA) and needle-core biopsy. The performance of these techniques is somewhat similar in the morphological diagnosis of HCC. Cytology sensitivity varies between 69%-95% across different studies (consistently lower in well-differentiated HCC), while specificity varies between 70%-100%[5–11]. The diagnostic accuracy of the method is lower in lesions < 3 cm (50%-83%) *vs* large ones (85%-95%)[7,12]. The smear cytology technique using Papanicolaou's method will decrease the number of both required passes and inadequate fragments. Flow cytometry and the various immunohistochemical techniques are extremely helpful in the characterization of neoplastic cells.

The difficulty of a correct differential diagnosis between a regenerative nodule and a well-differentiated HCC can only be overcome by using a relatively large tissue sample, which is obtainable only with the use of thick needles.

Core biopsy performed with large needles (1.1-1.6 mm outer diameter) ensures the recovery of an adequate tissue fragment; it also allows for a better preservation of tissue architecture, providing more information on the tumor tissue and facilitating certain special staining techniques. These advantages are, however, counterbalanced by the high risk of complications.

The rate of successful sampling using large needles is 85%-98.5%. It may be diminished by certain factors: the small size of the target (smaller lesions are harder to approach in liver with significant fibrosis), the location of the lesion in deeper segments (posterior and superior segments, such as segments Ⅳ B, Ⅶ and Ⅷ), and the presence of necrotic areas within the tumor[11]. Additionally, lesions that are poorly visible or invisible using conventional ultrasound are another cause of liver biopsy failure.

The sensitivity of core needle biopsy for HCC diagnosis is 86%-96%, which is increased in the case of multiple passes[11,13-16]. The specificity ranges between 95%-100%, especially when also sampling from an extra-nodular area (non-neoplastic neighboring parenchyma)[9,12]. The accuracy of the method varies between 85% and 91%[11,13,14,16].

Micro-histology combines the safety profile of fine-needle aspiration with a higher quality of tissue samples (similar to that provided by core needle biopsy); it has a higher sensitivity and specificity than conventional cytology: 92.6% and 100% *vs* 81.3% and 97.6%, respectively[7,9,11,17]. In addition, micro-histology has a high accuracy (89.6%) in diagnosing nodules < 2 cm and varies according to size: 88.6% for nodules ⩽ 10 mm, 86.2% for nodules between 11-15 mm and 91.3% for nodules between 16-20 mm in diameter[17].

Some needles (Histocut) allow the recovery of tissue fragments for both cytology and micro-histology during the same pass. The cytology-micro-histology combination increases the sensitivity of HCC diagnosis: 89.8%-90% *vs* 80%-85.6% for cytology, and 61%-66.1% for micro-histology[7,9].

Using real-time contrast-enhanced harmonic ultrasound (SonoVue) to guide the biopsy will increase its diagnostic sensitivity by targeting: (1) the enhanced, vascular areas of the tumor in the arterial phase, particularly in the case of large tumors that often display central necrosis[18]; and (2) the nodules that are poorly visible or invisible on conventional ultrasound, which become clearly visible after contrast injection in both the arterial or late phase[18,19].

The negative predictive value of liver biopsy remains low, and malignancy cannot be excluded from one negative result alone. The management of these patients includes long-term imaging, follow-up, and re-biopsy. If a re-biopsy is taken into consideration, it is imperative to recall its low chance of success when performed immediately after the first biopsy, with only a 35% increase in positive diagnosis[20]. If a tumor was not found in the first biopsy, the chances of success are higher (50%) than in cases with a non-diagnostic result (necrosis) (25%)[20]. In these cases, especially in nodules < 2 cm, imaging follow-up is recommended. Performing liver biopsy for the diagnosis of HCC is not without risks**.** Hemorrhage is more frequent when using thick needles (1.1% *vs* 0.5% for fine needle biopsy) and when sampling an HCC (2.5%)[11,21]. Risk factors for bleeding include: hemostatic abnormalities, the degree of liver failure, age, the presence of ascites, or the technique used. The risk is generally considered to increase with each additional pass, with a larger needle diameter, and with a smaller area of interposed parenchyma[22]. The actual recommendations are to use a needle < 1.2 mm in diameter for a maximum of two passes, and an oblique approach, which would allow at least 1 cm between the lesion and the liver capsule[15,23].

The incidence of needle-tract seeding varies in the literature between 0% and 7.69%, with a mean of 3.16% and a median of 2.66% (Table 1); this value is lower (1.43%) when considering the global incidence. A meta-analysis published in 2007 has established the median incidence of tumor cell seeding to be 2.7%[24]. Apparently, the larger the needle diameter and the number of passes, or the lower the degree of tumor differentiation, the higher the risk of seeding. There are no studies, however, to confirm this supposition. Seeding can occur in the thoraco-abdominal wall or intraperitoneally, sometimes several years after the biopsy and even after performing liver transplantation. The risk of seeding is not reduced by using the coaxial technique[25]. The treatment of needle-tract seeding, especially if parietal, is surgical; after surgery, most patients experience no recurrences. The occurrence of seeding does not alter global survival rates, which only depend on the progression of either the primary tumor or cirrhosis[26].

Liver cells are generally found in the blood after both liver biopsy and liver resection, as attested by the presence of mRNA AFP in the serum. It is not exactly known whether these are normal or tumor cells. No association between this phenomenon and tumor cell seeding has been demonstrated to date.

Mortality after biopsy is higher when using thick (0.15%-0.19%) *vs* fine needles (0.008%)[24,25, 27–37].

CURRENT INDICATIONS OF LB IN THE DIAGNOSIS OF HCC

Presently, the indications of performing LB in patients with liver cirrhosis and HCC are highly regulated. The two extreme perspectives that include recommending either biopsy in all cases (as was the norm before the introduction of non-invasive criteria), or the avoidance of biopsy at all costs when having good diagnostic imaging studies, have both been abandoned. The main factors that indicate, adjust or limit the use of biopsy in HCC are presented in Table 2.

In the following paragraphs, we will make a critical appraisal of the indicators of LB in the diagnosis of HCC for each of the BCLC stages.

BCLC stages 0 and A (very early and early HCC)

Correlation with imaging techniques. Nodules measuring between 1 and 2 cm are difficult to characterize using non-invasive methods[38,39], since up to 33% are benign, while HCC nodules frequently have no distinctive pattern of behavior. Only 33% of HCC nodules meet the precise diagnostic criteria recommended by the AASLD (hypervascularization in the arterial phase and washout in the portal/parenchymal phase using two imaging techniques)[38]. It follows that 50%-70% of patients will require a biopsy in order to receive an exact diagnosis[38,39]. US-guided LB may not be justified in patients with decompensated cirrhosis, despite the nature of the nodule, and liver transplantation might be considered. In contrast, in patients with a small nodule and compensated cirrhosis, US-guided LB should be performed before surgical resection, which carries morbidity and mortality rates higher than those of biopsy itself[14]. It is difficult to assess the differential between a well-differentiated HCC and a dysplastic nodule when using a fragment sampled by LB. The use of molecular markers (GPC3, HSP70, and GS) will identify the exact nature of nodules with 57% sensitivity and 100% specificity[40]. Compared to LB, new imaging techniques such as Gd-EOB-DTPA magnetic resonance imaging (MRI) might be more accurate in the differential diagnosis between early HCC and dysplastic nodules. Hyperintensity at diffusion-weighted imaging (DWI) was shown

Table 1 The incidence of needle-tract seeding after hepatocellular carcinoma biopsy

Ref.	Year	Lesion	Needle	No. of biopsies	No. of seeding	%
Yamashita *et al*[35]	1995	HCC	0.8-1.2 mm Bard	125	1	0.80
Huang *et al*[11]	1996	HCC	1.4-2 mm	455	9	2
Kanematsu *et al*[36]	1997	HCC	FNB 0.8 mm	50	2	4
Ch Yu *et al*[15]	1997	HCC	1.2 mm gun	139	0	0
Chapoutot *et al*[37]	1999	HCC	1.0-1.2 mm	150	4	2.66
Kim *et al*[28]	2000	HCC	1.1 mm gun	205	7	3.40
Takamori *et al*[27]	2000	HCC	FNB	59	3	5
Durand *et al*[14]	2001	HCC	1.2 mm	137	2	1.60
Kosugi *et al*[29]	2004	HCC	n.a	372	6	1.61
Ng *et al*[30]	2004	HCC	FNA	91	1	1.09
Shuto *et al*[31]	2004	HCC	n.a	480	5	1.04
Wang *et al*[32]	2005	HCC	FNA	90	0	0
Saborido *et al*[33]	2005	HCC	FNA	26	2	7.69
Maturen *et al*[25]	2006	HCC	1.2 mm, coaxial	128	0	0
Colecchia *et al*[34]	2012	HCC	0.95 mm	81	0	0
Total				2588	42	1.62

n.a: Not available; HCC: Hepatocellular carcinoma; %: Percent; FNA: Fine needle aspiration.

Table 2 Factors influencing the use of liver biopsy in hepatocellular carcinoma

1 Poor accuracy of contrast-enhanced methods in the diagnosis of HCC, especially in small lesions
2 The risks of LB, which are more severe in patients with cirrhosis and coagulopathy
3 Inadequate sampling of HCC lesions, especially in cases with very small or very large ones
4 The complex system of staging, treatment, and patient allocation to various therapy regimens (BCLC); the correct assessment of prognosis is important in the allocation of therapy, and is based mainly on pathology data
5 Modern therapies sometimes have limited applicability (transplantation), cost and effectiveness (systemic treatment); information resulting from histological analysis is necessary in order to increase effectiveness and personalize treatment

LB: Liver biopsy; HCC: Hepatocellular carcinoma; BCLC: Barcelona clinic liver cancer staging.

to be a useful feature for differentiating hypovascular early HCC from dysplastic nodules, which appear as hypointense nodules in Gd-EOB-DTPA MRI[41]. A more recent study reported a sensitivity of 94.7% and a specificity of 99.3% in classifying high-grade dysplastic nodules, which appear hypointense in the hepatobiliary (HB) phase without arterial phase hyperintensity and without DWI restriction[42]. More importantly, the benign nodules appeared hyperintense in the HB phase, and HCC rarely develops from hyperintense hepatic nodules in the HB phase. This suggests that these type of nodules do not require treatment or more intensive follow-up[43].

The degree of tumor differentiation in nodules measuring 1-2 cm can be identified with 60% accuracy, however the sensitivity of the histological examination in assessing vascular micro-invasion is low, especially after fine-needle biopsy[34]. Since vascular micro-invasion defines the prognosis of patients allocated to various therapies, its estimation (using nodule size and the degree of differentiation) is of the utmost importance[34].

Identifying the exact nature of the cirrhotic nodules gains additional importance in the context of liver transplantation. Several situations where LB may play a central role can be defined. For instance, identifying an HCC in a patient already on the transplant list using imaging studies will increase his or her priority score. In the first years of using the MELD score, 7%-31% of stage 1 HCC patients who received transplants were found to have no HCC in the explanted liver[44,45]. Secondly, although HCC is the most frequent tumor type to develop in cirrhotic liver, other tumors are also possible (especially cholangiocarcinoma). It is currently believed that ⩽ 20% of nodules developing in a cirrhotic liver, with imaging behavior typical for HCC, will actually have another histological structure[16]. The incidence of cholangiocarcinoma has increased considerably in the past years, and the imaging appearance of small peripheral lesions is very similar (or even identical) with that of HCC. Since the risk of recurrence after transplant is much higher for these tumors than for HCC, other patient selection criteria are required, as well as a more aggressive pre-transplant treatment[16]. Thirdly, HCC may sometimes occur in patients with chronic liver disease prior to the development of cirrhosis. The risk for HCC development is lower in these patients, and consequently any newly discovered nodule, even if hy-

pervascular, should be biopsied.

The fourth situation when a pre-transplant liver biopsy is warranted is related to the importance of assessing the degree of tumor differentiation and vascular invasion. It has been clearly proven that HCC tumor differentiation is strongly correlated to survival, both after resection and transplantation. The risk of recurrence is higher for poorly- or moderately-differentiated *vs* well-differentiated tumors[16,46]. This is also applicable for tumors outside of the Milan criteria, but within the Up-to-seven criteria. This means that the patients with well-differentiated HCC, and without vascular invasion, have a very good prognosis (1- and 3-year survival rates of 84.2% and 67.4%, respectively)[47].

Vascular micro-invasion is difficult to ascertain by liver biopsy, and its risk can only be estimated at best. For instance, for a poorly differentiated tumor > 4 cm, the risk of vascular micro-invasion is 61%[46]. For well-differentiated tumors, the size and extent of vascular invasion do not appear to influence prognosis[46]. In situations where vascular micro-invasion cannot be estimated, the use of imagistic methods might be of real importance. Diffusion-weighted imaging (DWI), an emerging technique in hepatic MRI, provided a sensitivity of 93.5% and a specificity of 72.2% for the prediction of micro-vascular invasion during the preoperative evaluation of HCC[48]. Consequently, knowing the exact type of tumor appears to be very important for optimizing patient selection for transplantation[46,47].

In conclusion, choosing to perform a pre-transplant biopsy in patients with liver cirrhosis and HCC depends on the tumor stage and the severity of cirrhosis. For instance, in patients with compensated cirrhosis and HCC diagnosed with the Milan criteria, LB should be performed in order to correctly confirm or exclude an HCC, therefore avoiding the granting of additional MELD points. In patients with decompensated cirrhosis, liver biopsy is not indicated since transplantation is already an immediate necessity. For patients outside of the Milan but within the Up-to-seven criteria, liver biopsy is very useful in selecting patients with well-differentiated tumors who would benefit the most from transplantation[44,49].

An argument for the use of LB before resection concerns a poor correlation (sometimes below 50% for large biopsied tumors) between the degree of differentiation found on biopsy and on the resected tumor[34,50]. This can be explained by the high heterogeneity of larger tumors, which relates to their varying degrees of differentiation. Secondly, performing a biopsy before a resection will expose the patient to a higher risk of peritoneal metastases (12.5% *vs* 1.6%) and will decrease 5-year disease-free survival (24% *vs* 52%)[51]. However, some authors claim that fine-needle aspiration before resection does not affect either mortality or survival rates[30].

Thirdly, we must not ignore the risk of complications (seeding, bleeding), as well as the contraindications and limitations of LB (ascites, coagulopathy or isoechoic nodules). The negative predictive value of LB does not reach 100%, and a new biopsy or imaging follow-up is recommended in the case of negative results. This approach will prolong the time to resection and will expose the patient to additional risks[52]. The current approach states that LB should be indicated and performed only in tertiary centers that are equipped with state-of-the-art imaging techniques, high imaging expertise, interventional techniques, and pathology labs[47]. In other conditions, performing liver biopsy before resection should be avoided, except in cases where the biopsy result is expected to substantially alter the therapy[53].

BCLC intermediate and advanced stages

In each of these stages, the indication to perform LB is made based on the following issues: (1) choosing the optimal therapy from a variety of possible treatment courses. For instance, patients in the intermediate stage may benefit not only from chemoembolization, but also from curative options such as resection, percutaneous ablation or liver transplantation. Curative treatment is indicated in the presence of favorable prognostic factors, such as well-differentiated HCC or the lack of vascular micro-invasion[54]; (2) diagnosing a portal thrombus as benign using liver biopsy may suggest the need for liver transplantation or resection for a patient in an advanced stage; and (3) Considering the poor efficacy of current antiangiogenic therapies (Sorafenib), which can be attributed to its severe adverse effects and high cost, it is essential to exclude other tumors that may form in a cirrhotic liver (cholangiocarcinoma, mixed types - hepatocholangiocarcinoma) and that would require a different therapy[49]. The lack of histological confirmation in the Sharp studies, as well other similar ones, raises the question of whether or not some cases of hepatocholangiocarcinoma may have been wrongly diagnosed as HCC in the study groups.

Molecular testing is a staple nowadays in oncology. The selection of systemic treatments is made by considering the tumor molecular biology (as in breast or lung cancer). The concept of non-invasive diagnosis of HCC (which is the only tumor that does not require morphological examination) was established before the introduction of new therapeutic agents. Several authors speculate whether this lack of histological data may explain the limited efficacy of Sorafenib, considering that certain studies fail to prove the efficacy of other systemic therapies in HCC[55]. In the future, the multitude of studies performed on systemic therapy for HCC will have to make use of pathological, molecular and genetic information provided by the tissue fragment in order to accurately establish the prognosis and to individualize the therapy[49,53]. Current progress in molecular biology will soon allow for guided treatment based on the expression of tumor genes[53]. At present, molecular genetic

tests are costly, and their widespread use is limited by their ongoing validation and standardization, as well as by the lack of consensus in their guidelines[53].

LIVER BIOPSY IN THE CONTEXT OF PERSONALIZED MEDICINE

The role of liver biopsy for the management of patients with HCC is one of the most active debates in the liver cancer community[56,57]. Over the last decade, the emergence of high-throughput molecular technologies has provided the ability to interrogate the main molecular mechanism involved in HCC development and progression. HCC is best considered a highly heterogeneous entity that is composed of distinct transcriptomic subgroups with various genetic alterations[58,59]. Importantly, a high degree of heterogeneity can also be observed at the histological level. For instance, fibrolamellar carcinoma is already a well-accepted morphological and molecular subtype of HCC[60]. Furthermore, the chromophobe subtype shows a distinct morphology, while also utilizing a specific molecular mechanism to overcome replicative senescence, which is in contrast to the telomerase activation seen in most HCCs[61]. Several histological subtypes, which feature distinctive and recognizable morphological features, have also been reported, such as the steatohepatitic, cirrhotic, lymphoepithelioma-like, and inflammatory HCCs[61-63]. Indeed, the molecular mechanism behind these histological subtypes awaits clarification, however this is only a matter of time considering the rapid advancement of molecular technologies. It is estimated that 20%-30% of HCCs belong to a recognizable morphological/molecular subtype[57]. A recent paper, published in *Hepatology*, described another HCC subtype that displays distinct histological and molecular features[64]. The macrotrabecullar-massive HCC (MTM-HCC) was identified in 12% of the total cohort (16% of surgically-resected samples, 8.5% of liver biopsy samples). In multivariate analysis, the MTM-HCC subtype was an independent predictor of early and overall recurrence. From the molecular point of view, MTM- HCC was characterized by high expression of angiopoietin 2 and vascular endothelial growth factor A (VEGFA)[65]. Bi-specific, anti-angiopoietin 2 and anti-VEGFA antibodies may represent potent treatments for this subclass of HCC.

Taking into account this new, recently-described MTM-HCC subclass, we now have an estimated 36%-46% of HCCs that belong to a recognizable morphological or molecular subtype. For the remaining HCCs, molecular subtypes likely exist[66]. Tumor heterogeneity will not be fully reflected in all liver biopsies, however many HCCs can be sub-classified appropriately. The discovery of different histological subtypes, each with distinct molecular features, is still in its infancy. Until further evidence is revealed, no recommendations can be made regarding how to best treat different subtypes. For the time being, HCC should instead be considered as one disease. On the contrary, once all the signaling pathways for each HCC subtype have been described, liver biopsy will indeed be necessary for the correct identification of such signaling pathways. Moreover, the identification of distinct signaling pathways for different subtypes of HCC will allow for the development of new treatments. In this ideal and close-approaching scenario, liver biopsy will allow for the correct diagnosis of HCC subtypes, the corresponding upregulated signaling pathways, and the proper choice of specific molecules. This will ultimately open the path for personalized medicine.

The balance of risk and benefit defines many of the decisions that we make as providers of medical care. With respect to the use of liver biopsy in diagnosing HCC, the risks are well-defined and quantifiable. Common arguments against liver tumor biopsy have included the risk of bleeding and tumor seeding (Table 1). Up to 20% of focal liver lesions developed on a background of liver cirrhosis are not HCC (14), and almost 46% of HCCs have a distinct histological or molecular signature that might benefit from targeted therapies. We are all afraid of the invasive nature of liver biopsy, but must also consider the risks and benefits of treating a non-HCC patient as though they had HCC. What is the benefit of targeting a molecular pathway in a patient with HCC when that targeted pathway is not activated? We do not believe that the current guidelines are wrong, because the data that form the basis of the existing guidelines are against liver biopsy. Nevertheless, due to advancements in molecular biology, more and more molecular and histological classes of HCC have been, and will continue to be, described. We believe that there will come a time when diagnostic biopsies will be commonly performed. This will improve the diagnosis of HCC and increase our ability to provide better patient care in the future.

LIQUID BIOPSY: THE FUTURE OF LIVER BIOPSY

In the past few decades, several studies have demonstrated the utility of circulating cancer byproducts known as "liquid biopsy", which could provide accessible, accurate, and dynamic information to evaluate tumor progression. Circulating tumor cells (CTCs), circulating cell-free DNA, circulating miRNA, and circulating tumor associated microparticles (MPs) can all be united under the term "liquid biopsy". Compared to liver biopsy, liquid biopsy is a noninvasive method used for the identification of CTCs, circulating MPs, or circulating miRNA/DNA in the blood of patients with HCC. Moreover, it is well accepted by the patients, since only 1 mL of blood is enough for proper identification in flow cytometry or cell search systems. Similar to conventional biopsies, CTSs or MPs can be stained for various surface markers specific for HCC. A detailed description of all cancer

byproducts is beyond the scope of this review and has already been nicely reviewed elsewhere[67]. We will only provide some brief examples.

CTCs were detected in blood samples from 45 out of 69 HCC patients, compared to 0 out of 31 controls. Moreover, CTC numbers correlated significantly with tumor size, PVT and survival[68]. Others have found that patients with preoperative detectable EpCAM^{mRNA+} CTCs had significantly shorter TTR (median of 10.9 mo *vs* not reached) and higher recurrence rates (59.6% *vs* 25.7%) than those without detectable EpCAM^{mRNA+} CTCs[69]. Chan *et al*[70] confirmed the existence of typical DNA copy number variations in the peripheral blood of four HCC patients, which primarily disappeared after surgical resection. Circulating miRNA is probably the most studied form of liquid biopsy in HCC. Several miRNAs have been reported to have a role in diagnosis, prognosis and follow-up[67]. More recently, another form of liquid biopsy has gained particular attention. Circulating tumor microparticles that are positive for a combination of antigens, particularly AnexinV$^+$EpCAM$^+$ASGPR1$^+$ CD133$^+$, allowed for the distinction of liver malignancies (HCC or CCA) and cirrhosis from tumor-free individuals and, more importantly, from patients carrying other non-liver cancers. In addition, AnexinV$^+$EpCAM$^+$ASGPR1$^+$ microparticles were increased in liver cancer-bearing patients compared to patients with cirrhosis that lacked any detectable liver malignancy[71].

The term liquid biopsy has only recently been introduced, and the technology for cancer byproduct identification is still in its infancy. Until more and more data becomes available, liquid biopsy cannot be performed in daily practice and should instead be used for research intents. Time will decide the limits of liquid biopsies and whether it can replace conventional biopsies. The reported sensitivity and specificity of liquid biopsy in HCC is rather modest. Better performance was reported for liquid biopsy as a tool to monitor treatment outcomes. Indeed, a lot of work must be done in this field before we can draw any conclusions. Continuously improving the detection and characterization of CTCs, circulating free DNA, and MPs is of the utmost importance, since liquid biopsy has several advantages over conventional biopsy: (1) it is a non-invasive procedure; (2) it can be easily repeated over time, which offers a more complete portrait of the disease; (3) it could better reveal the genetic complexity of a highly heterogeneous tumor; and (4) it is much faster[72].

CONCLUSION

Presently, morphological examination during HCC diagnosis is very carefully adjusted, as one must consider the availability of non-invasive techniques and, on the other hand, the need for prognostic criteria and individualized therapy. Improving the biopsy technique (higher needle performance, more accurate guidance in the active, hypervascular areas of the tumor, and the use of techniques with a lower seeding risk) will increase the sensitivity of the procedure and decrease the complication rate. With recent advances in high-throughput molecular technologies, which have allowed for the identification of novel HCC subclasses with prognostic impact, the role of liver biopsy will gain increasingly more attention and reconsideration.

REFERENCES

1 **Giorgio A**, Montesarchio L, Gatti P, Amendola F, Matteucci P, Santoro B, Merola MG, Merola F, Coppola C, Giorgio V. Contrast-Enhanced Ultrasound: a Simple and Effective Tool in Defining a Rapid Diagnostic Work-up for Small Nodules Detected in Cirrhotic Patients during Surveillance. *J Gastrointestin Liver Dis* 2016; **25**: 205-211 [PMID: 27308652 DOI: 10.15403/jgld.2014.1121.252.chu]

2 **Kono Y**, Lyshchik A, Cosgrove D, Dietrich CF, Jang HJ, Kim TK, Piscaglia F, Willmann JK, Wilson SR, Santillan C, Kambadakone A, Mitchell D, Vezeridis A, Sirlin CB. Contrast Enhanced Ultrasound (CEUS) Liver Imaging Reporting and Data System (LI-RADS®): the official version by the American College of Radiology (ACR). *Ultraschall Med* 2017; **38**: 85-86 [PMID: 28249328 DOI: 10.1055/s-0042-124369]

3 **Terzi E**, Iavarone M, Pompili M, Veronese L, Cabibbo G, Fraquelli M, Riccardi L, De Bonis L, Sangiovanni A, Leoni S, Zocco MA, Rossi S, Alessi N, Wilson SR, Piscaglia F; CEUS LI-RADS Italy study group collaborators:. Contrast ultrasound LI-RADS LR-5 identifies hepatocellular carcinoma in cirrhosis in a multicenter restropective study of 1,006 nodules. *J Hepatol* 2018; **68**: 485-492 [PMID: 29133247 DOI: 10.1016/j.jhep.2017.11.007]

4 **Ye SL**, Chen RX. [Comments on management of hepatocellular carcinoma: an update]. *Zhonghua Gan Zang Bing Za Zhi* 2011; **19**: 251-253 [PMID: 21805733 DOI: 10.1002/hep.24199]

5 **Bru C**, Maroto A, Bruix J, Faus R, Bianchi L, Calvet X, Ayuso C, Vilana R, Gilabert R, Rodés J. Diagnostic accuracy of fine-needle aspiration biopsy in patients with hepatocellular carcinoma. *Dig Dis Sci* 1989; **34**: 1765-1769 [PMID: 2555123 DOI: 10.1007/BF01540056]

6 **Bolondi L**, Gaiani S, Benzi G, Zironi G, Rigamonti A, Fusconi F, Barbara L. Ultrasonography and guided biopsy in the diagnosis of hepatocellular carcinoma. *Ital J Gastroenterol* 1992; **24**: 46-49 [PMID: 1315177]

7 **Fornari F**, Filice C, Rapaccini GL, Caturelli E, Cavanna L, Civardi G, Di Stasi M, Buscarini E, Buscarini L. Small (< or = 3 cm) hepatic lesions. Results of sonographically guided fine-needle biopsy in 385 patients. *Dig Dis Sci* 1994; **39**: 2267-2275 [PMID: 7924754 DOI: 10.1007/BF02090383]

8 **Duysburgh I**, Michielsen P, Fierens H, Van Marck E, Pelckmans P. Fine needle trucut biopsy of focal liver lesions: a new technique. *Dig Dis Sci* 1997; **42**: 2077-2081 [PMID: 9365138 DOI: 10.1023/A:1018870501882]

9 **Caturelli E**, Bisceglia M, Fusilli S, Squillante MM, Castelvetere M, Siena DA. Cytological *vs* microhistological diagnosis of hepatocellular carcinoma: comparative accuracies in the same fine-needle biopsy specimen. *Dig Dis Sci* 1996; **41**: 2326-2331 [PMID: 9011437 DOI: 10.1007/BF02100122]

10 **Livraghi T**, Sangalli G, Giordano F, Vettori C. Fine aspiration versus fine cutting needle, and comparison between smear cytology, inclusion cytology and microhistology in abdominal lesions. *Tumori* 1988; **74**: 361-364 [PMID: 3041658 DOI: 10.1177/030089168807400321]

11 **Huang GT**, Sheu JC, Yang PM, Lee HS, Wang TH, Chen DS. Ultrasound-guided cutting biopsy for the diagnosis of hepatocellular carcinoma-a study based on 420 patients. *J Hepatol* 1996; **25**: 334-338 [PMID: 8895013 DOI: 10.1016/S0168-8278(96)80120-6]

12 **Borzio M**, Borzio F, Macchi R, Croce AM, Bruno S, Ferrari A, Servida E. The evaluation of fine-needle procedures for the diagnosis of focal liver lesions in cirrhosis. *J Hepatol* 1994; **20**: 117-121 [PMID: 8201212 DOI: 10.1016/S0168-8278(05)80477-5]

13 **Radu B, Zeno S.** Biopsia leziunilor focale pe ficatul cirotic: indicații, tehnică, performanțe, complicații. *Med Ultrason* 2001; **3**: 21-25

14 **Durand F**, Regimbeau JM, Belghiti J, Sauvanet A, Vilgrain V, Terris B, Moutardier V, Farges O, Valla D. Assessment of the benefits and risks of percutaneous biopsy before surgical resection of hepatocellular carcinoma. *J Hepatol* 2001; **35**: 254-258 [PMID: 11580148 DOI: 10.1016/S0168-8278(01)00108-8]

15 **Ch Yu S**, Metreweli C, Lau WY, Leung WT, Liew CT, Leung NW. Safety of percutaneous biopsy of hepatocellular carcinoma with an 18 gauge automated needle. *Clin Radiol* 1997; **52**: 907-911 [PMID: 9413963 DOI: 10.1016/S0009-9260(97)80222-X]

16 **Durand F,** Belghiti J, Paradis V. Liver transplantation for hepatocellular carcinoma: Role of biopsy. *Liver Transplant* 2007; **13**: S17-S23 [PMID: 17969095 DOI: 10.1002/lt.21326]

17 **Caturelli E**, Solmi L, Anti M, Fusilli S, Roselli P, Andriulli A, Fornari F, Del Vecchio Blanco C, de Sio I. Ultrasound guided fine needle biopsy of early hepatocellular carcinoma complicating liver cirrhosis: a multicentre study. *Gut* 2004; **53**: 1356-1362 [PMID: 15306600 DOI: 10.1136/gut.2003.032359]

18 **Schlottmann K**, Klebl F, Zorger N, Feuerbach S, Schölmerich J. Contrast-enhanced ultrasound allows for interventions of hepatic lesions which are invisible on convential B-mode. *Z Gastroenterol* 2004; **42**: 303-310 [PMID: 15095120 DOI: 10.1055/s-2004-812712]

19 **Sparchez Z**, Radu P, Zaharia T, Kacso G, Grigorescu I, Botis G, Badea R. Usefulness of contrast enhanced ultrasound guidance in percutaneous biopsies of liver tumors. *J Gastrointestin Liver Dis* 2011; **20**: 191-196 [PMID: 21725517]

20 **Caturelli E**, Biasini E, Bartolucci F, Facciorusso D, Decembrino F, Attino V, Bisceglia M. Diagnosis of hepatocellular carcinoma complicating liver cirrhosis: utility of repeat ultrasound-guided biopsy after unsuccessful first sampling. *Cardiovasc Intervent Radiol* 2002; **25**: 295-299 [PMID: 12324817 DOI: 10.1007/s00270-001-0123-6]

21 **Souto E**, Gores GJ. When should a liver mass suspected of being a hepatocellular carcinoma be biopsied? *Liver Transpl* 2000; **6**: 73-75 [PMID: 10648581 DOI: 10.1002/lt.500060108]

22 **Little AF**, Ferris JV, Dodd GD 3rd, Baron RL. Image-guided percutaneous hepatic biopsy: effect of ascites on the complication rate. *Radiology* 1996; **199**: 79-83 [PMID: 8633176 DOI: 10.1148/radiology.199.1.8633176]

23 **Blanc JF**. Traitement du carcinome hépatocellulaire: Un tournant? *Hepatogastroenterology* 2016; **23**: 79-85 [DOI: 10.1684/hpg.2015.1244]

24 **Silva MA**, Hegab B, Hyde C, Guo B, Buckels JA, Mirza DF. Needle track seeding following biopsy of liver lesions in the diagnosis of hepatocellular cancer: a systematic review and meta-analysis. *Gut* 2008; **57**: 1592-1596 [PMID: 18669577 DOI: 10.1136/gut.2008.149062]

25 **Maturen KE**, Nghiem HV, Marrero JA, Hussain HK, Higgins EG, Fox GA, Francis IR. Lack of tumor seeding of hepatocellular carcinoma after percutaneous needle biopsy using coaxial cutting needle technique. *AJR Am J Roentgenol* 2006; **187**: 1184-1187 [PMID: 17056903 DOI: 10.2214/AJR.05.1347]

26 **Torzilli G**, Minagawa M, Takayama T, Inoue K, Hui AM, Kubota K, Ohtomo K, Makuuchi M. Accurate preoperative evaluation of liver mass lesions without fine-needle biopsy. *Hepatology* 1999; **30**: 889-893 [PMID: 10498639 DOI: 10.1002/hep.510300411]

27 **Takamori R**, Wong LL, Dang C, Wong L. Needle-tract implantation from hepatocellular cancer: is needle biopsy of the liver always necessary? *Liver Transpl* 2000; **6**: 67-72 [PMID: 10648580 DOI: 10.1002/lt.500060103]

28 **Kim SH**, Lim HK, Lee WJ, Cho JM, Jang HJ. Needle-tract implantation in hepatocellular carcinoma: frequency and CT findings after biopsy with a 19.5-gauge automated biopsy gun. *Abdom Imaging* 2000; **25**: 246-250 [PMID: 10823443 DOI: 10.1007/s002610000025]

29 **Kosugi C**, Furuse J, Ishii H, Maru Y, Yoshino M, Kinoshita T, Konishi M, Nakagohri T, Inoue K, Oda T. Needle tract implantation of hepatocellular carcinoma and pancreatic carcinoma after ultrasound-guided percutaneous puncture: clinical and pathologic characteristics and the treatment of needle tract implantation. *World J Surg* 2004; **28**: 29-32 [PMID: 14648043 DOI: 10.1007/s00268-003-7003-y]

30 **Ng KK**, Poon RT, Lo CM, Liu CL, Lam CM, Ng IO, Fan ST. Impact of preoperative fine-needle aspiration cytologic examination on clinical outcome in patients with hepatocellular carcinoma in a tertiary referral center. *Arch Surg* 2004; **139**: 193-200 [PMID: 14769580 DOI: 10.1001/archsurg.139.2.193]

31 **Shuto T**, Yamamoto T, Tanaka S, Kanazawa A, Takemura S, Tanaka H, Kubo S, Hirohashi K, Sakaguchi H, Seki S. Resection of needle-tract implantation after percutaneous puncture for hepatocellular carcinoma. *J Gastroenterol* 2004; **39**: 907-908 [PMID: 15565415 DOI: 10.1007/s00535-003-1411-5]

32 **Wang CW**, Lin ZY, Chuang WL, Wang LY, Yu ML, Chen SC, Hsieh MY, Tsai JF, Chang WY. Safety of fine-needle aspiration in patients with small hepatocellular carcinoma. *Hepatol Res* 2005; **31**: 31-35 [PMID: 15652468 DOI: 10.1016/j.hepres.2004.11.002]

33 **Saborido BP**, Díaz JC, de Los Galanes SJ, Segurola CL, de Usera MA, Garrido MD, Elola-Olaso AM, Sánz RG, Romero CJ, Garcia García I, González EM. Does preoperative fine needle aspiration-biopsy produce tumor recurrence in patients following liver transplantation for hepatocellular carcinoma? *Transplant Proc* 2005; **37**: 3874-3877 [PMID: 16386569 DOI: 10.1016/j.transproceed.2005.09.169]

34 **Colecchia A**, Scaioli E, Montrone L, Vestito A, Di Biase AR, Pieri M, D'Errico-Grigioni A, Bacchi-Reggiani ML, Ravaioli M, Grazi GL, Festi D. Pre-operative liver biopsy in cirrhotic patients with early hepatocellular carcinoma represents a safe and accurate diagnostic tool for tumour grading assessment. *J Hepatol* 2011; **54**: 300-305 [PMID: 21056498 DOI: 10.1016/j.jhep.2010.06.037]

35 **Yamashita Y**, Matsukawa T, Arakawa A, Hatanaka Y, Urata J, Takahashi M. US-guided liver biopsy: predicting the effect of interventional treatment of hepatocellular carcinoma. *Radiology* 1995; **196**: 799-804 [PMID: 7644646 DOI: 10.1148/radiology.196.3.7644646]

36 **Kanematsu M**, Hoshi H, Takao H, Sugiyama Y. Abdominal wall tumor seeding at sonographically guided needle-core aspiration biopsy of hepatocellular carcinoma. *AJR Am J Roentgenol* 1997; **169**: 1198-1199 [PMID: 9308498 DOI: 10.2214/ajr.169.4.9308498]

37 **Chapoutot C**, Perney P, Fabre D, Taourel P, Bruel JM, Larrey D, Domergue J, Ciurana AJ, Blanc F. [Needle-tract seeding after ultrasound-guided puncture of hepatocellular carcinoma. A study of 150 patients]. *Gastroenterol Clin Biol* 1999; **23**: 552-556 [PMID: 10429862]

38 **Forner A**, Vilana R, Ayuso C, Bianchi L, Solé M, Ayuso JR, Boix L, Sala M, Varela M, Llovet JM, Brú C, Bruix J. Diagnosis of hepatic nodules 20 mm or smaller in cirrhosis: Prospective validation of the noninvasive diagnostic criteria for hepatocellular carcinoma. *Hepatology* 2008; **47**: 97-104 [PMID: 18069697 DOI: 10.1002/hep.21966]

39 **Sersté T**, Barrau V, Ozenne V, Vullierme MP, Bedossa P, Farges O, Valla DC, Vilgrain V, Paradis V, Degos F. Accuracy and disagreement of computed tomography and magnetic resonance imaging for the diagnosis of small hepatocellular carcinoma and dysplastic nodules: role of biopsy. *Hepatology* 2012; **55**: 800-806 [PMID: 22006503 DOI: 10.1002/hep.24746]

40 **Tremosini S**, Forner A, Boix L, Vilana R, Bianchi L, Reig M, Rimola J, Rodríguez-Lope C, Ayuso C, Solé M, Bruix J. Prospective validation of an immunohistochemical panel (glypican 3, heat shock protein 70 and glutamine synthetase) in liver biopsies for diagnosis of very early hepatocellular carcinoma. *Gut* 2012; **61**: 1481-1487 [PMID: 22287594 DOI: 10.1136/gutjnl-2011-301862]

41 **Hwang J**, Kim YK, Jeong WK, Choi D, Rhim H, Lee WJ. Nonhypervascular Hypointense Nodules at Gadoxetic Acid-enhanced MR Imaging in Chronic Liver Disease: Diffusion-weighted Imaging

for Characterization. *Radiology* 2015; **276**: 137-146 [PMID: 25734551 DOI: 10.1148/radiol.15141350]
42 **Renzulli M**, Biselli M, Brocchi S, Granito A, Vasuri F, Tovoli F, Sessagesimi E, Piscaglia F, D'Errico A, Bolondi L, Golfieri R. New hallmark of hepatocellular carcinoma, early hepatocellular carcinoma and high-grade dysplastic nodules on Gd-EOB-DTPA MRI in patients with cirrhosis: a new diagnostic algorithm. *Gut* 2018; **pii**: gutjnl-2017-315384[PMID: 29437912 DOI: 10.1136/gutjnl-2017-315384]
43 **Sano K**, Ichikawa T, Motosugi U, Ichikawa S, Morisaka H, Enomoto N, Matsuda M, Fujii H. Outcome of hypovascular hepatic nodules with positive uptake of gadoxetic acid in patients with cirrhosis. *Eur Radiol* 2017; **27**: 518-525 [PMID: 27255397 DOI: 10.1007/s00330-016-4423-2]
44 **Marsh JW**, Dvorchik I. Should we biopsy each liver mass suspicious for hepatocellular carcinoma before liver transplantation?--yes. *J Hepatol* 2005; **43**: 558-562 [PMID: 16112246 DOI: 10.1016/j.jhep.2005.07.014]
45 **Hayashi PH**, Trotter JF, Forman L, Kugelmas M, Steinberg T, Russ P, Wachs M, Bak T, Kam I, Everson GT. Impact of pretransplant diagnosis of hepatocellular carcinoma on cadveric liver allocation in the era of MELD. *Liver Transpl* 2004; **10**: 42-48 [PMID: 14755776 DOI: 10.1002/lt.20020]
46 **Ramos Rubio E**, Llado Garriga L. [Usefulness of pre-surgical biopsy in selecting patients with hepatocellular carcinoma for liver transplant]. *Cir Esp* 2010; **87**: 133-138 [PMID: 20074710 DOI: 10.1016/j.ciresp.2009.11.026]
47 **Cresswell AB**, Welsh FK, Rees M. A diagnostic paradigm for resectable liver lesions: to biopsy or not to biopsy? *HPB* (Oxford) 2009; **11**: 533-540 [PMID: 20495704 DOI: 10.1111/j.1477-2574.2009.00081.x]
48 **Suh YJ**, Kim MJ, Choi JY, Park MS, Kim KW. Preoperative prediction of the microvascular invasion of hepatocellular carcinoma with diffusion-weighted imaging. *Liver Transpl* 2012; **18**: 1171-1178 [PMID: 22767394 DOI: 10.1002/lt.23502]
49 **Parisi G**. Should a radiological diagnosis of hepatocellular carcinoma be routinely confirmed by a biopsy? Yes. *Eur J Intern Med* 2012; **23**: 34-36 [PMID: 22153528 DOI: 10.1016/j.ejim.2011.10.015]
50 **Pawlik TM**, Gleisner AL, Anders RA, Assumpcao L, Maley W, Choti MA. Preoperative assessment of hepatocellular carcinoma tumor grade using needle biopsy: implications for transplant eligibility. *Ann Surg* 2007; **245**: 435-442 [PMID: 17435551 DOI: 10.1097/01.sla.0000250420.73854.ad]
51 **Young AL**, Malik HZ, Abu-Hilal M, Guthrie JA, Wyatt J, Prasad KR, Toogood GJ, Lodge JP. Large hepatocellular carcinoma: time to stop preoperative biopsy. *J Am Coll Surg* 2007; **205**: 453-462 [PMID: 17765162 DOI: 10.1016/j.jamcollsurg.2007.04.033]
52 **Stigliano R**, Burroughs AK. Should we biopsy each liver mass suspicious for HCC before liver transplantation?--no, please don't. *J Hepatol* 2005; **43**: 563-568 [PMID: 16120469 DOI: 10.1016/j.jhep.2005.07.015]
53 **Heuman DM**, Gilles HS, Solomon C, Bajaj JS. Should a radiological diagnosis of hepatocellular carcinoma be routinely confirmed by a biopsy? No. *Eur J Intern Med* 2012; **23**: 37-39 [PMID: 22153529 DOI: 10.1016/j.ejim.2011.09.014]
54 **Bolondi L**, Burroughs A, Dufour JF, Galle PR, Mazzaferro V, Piscaglia F, Raoul JL, Sangro B. Heterogeneity of patients with intermediate (BCLC B) Hepatocellular Carcinoma: proposal for a subclassification to facilitate treatment decisions. *Semin Liver Dis* 2012; **32**: 348-359 [PMID: 23397536 DOI: 10.1055/s-0032-1329906]
55 **Schirmacher P**, Bedossa P, Roskams T, Tiniakos DG, Brunt EM, Zucman-Rossi J, Manns MP, Galle PR. Fighting the bushfire in HCC trials. *J Hepatol* 2011; **55**: 276-277 [PMID: 21439335 DOI: 10.1016/j.jhep.2011.03.004]
56 **Sherman M**, Bruix J. Biopsy for liver cancer: how to balance research needs with evidence-based clinical practice. *Hepatology* 2015; **61**: 433-436 [PMID: 25308482 DOI: 10.1002/hep.27563]
57 **Torbenson M,** Schirmacher P. Liver cancer biopsy - back to the future?! *Hepatology* 2015; **61**: 431-433 [PMID: 25271144 DOI: 10.1002/hep.27545]
58 **Zucman-Rossi J**, Villanueva A, Nault JC, Llovet JM. Genetic Landscape and Biomarkers of Hepatocellular Carcinoma. *Gastroenterology* 2015; **149**: 1226-1239.e4 [PMID: 26099527 DOI: 10.1053/j.gastro.2015.05.061]
59 **Hoshida Y**, Nijman SM, Kobayashi M, Chan JA, Brunet JP, Chiang DY, Villanueva A, Newell P, Ikeda K, Hashimoto M, Watanabe G, Gabriel S, Friedman SL, Kumada H, Llovet JM, Golub TR. Integrative transcriptome analysis reveals common molecular subclasses of human hepatocellular carcinoma. *Cancer Res* 2009; **69**: 7385-7392 [PMID: 19723656 DOI: 10.1158/0008-5472.CAN-09-1089]
60 **Rieber A**. [Fibrolamellar carcinoma]. *Z Gastroenterol* 1994; **32**: 651-653 [PMID: 7886976 DOI: 10.1097/PCR.0000000000000063]
61 **Solinas A**, Calvisi DF. Lessons from rare tumors: hepatic lymphoepithelioma-like carcinomas. *World J Gastroenterol* 2015; **21**: 3472-3479 [PMID: 25834311 DOI: 10.3748/wjg.v21.i12.3472]
62 **Salomao M**, Yu WM, Brown RS Jr, Emond JC, Lefkowitch JH. Steatohepatitic hepatocellular carcinoma (SH-HCC): a distinctive histological variant of HCC in hepatitis C virus-related cirrhosis with associated NAFLD/NASH. *Am J Surg Pathol* 2010; **34**: 1630-1636 [PMID: 20975341 DOI: 10.1097/PAS.0b013e3181f31caa]
63 **Seok JY**, Na DC, Woo HG, Roncalli M, Kwon SM, Yoo JE, Ahn EY, Kim GI, Choi JS, Kim YB, Park YN. A fibrous stromal component in hepatocellular carcinoma reveals a cholangiocarcinoma-like gene expression trait and epithelial-mesenchymal transition. *Hepatology* 2012; **55**: 1776-1786 [PMID: 22234953 DOI: 10.1002/hep.25570]
64 **Ziol M**, Poté N, Amaddeo G, Laurent A, Nault JC, Oberti F, Costentin C, Michalak S, Bouattour M, Francoz C, Pageaux GP, Ramos J, Decaens T, Luciani A, Guiu B, Vilgrain V, Aubé C, Derman J, Charpy C, Zucman-Rossi J, Barget N, Seror O, Ganne-Carrié N, Paradis V, Calderaro J. Macrotrabecular-massive hepatocellular carcinoma: A distinctive histological subtype with clinical relevance. *Hepatology* 2017 [Epub ahead of print] [PMID: 29281854 DOI: 10.1002/hep.29762]
65 **Calderaro J**, Couchy G, Imbeaud S, Amaddeo G, Letouzé E, Blanc JF, Laurent C, Hajji Y, Azoulay D, Bioulac-Sage P, Nault JC, Zucman-Rossi J. Histological subtypes of hepatocellular carcinoma are related to gene mutations and molecular tumour classification. *J Hepatol* 2017; **67**: 727-738 [PMID: 28532995 DOI: 10.1016/j.jhep.2017.05.014]
66 **Boyault S**, Rickman DS, de Reyniès A, Balabaud C, Rebouissou S, Jeannot E, Hérault A, Saric J, Belghiti J, Franco D, Bioulac-Sage P, Laurent-Puig P, Zucman-Rossi J. Transcriptome classification of HCC is related to gene alterations and to new therapeutic targets. *Hepatology* 2007; **45**: 42-52 [PMID: 17187432 DOI: 10.1002/hep.21467]
67 **Yin CQ**, Yuan CH, Qu Z, Guan Q, Chen H, Wang FB. Liquid Biopsy of Hepatocellular Carcinoma: Circulating Tumor-Derived Biomarkers. *Dis Markers* 2016; **2016**: 1427849 [PMID: 27403030 DOI: 10.1155/2016/1427849]
68 **Ogle LF**, Orr JG, Willoughby CE, Hutton C, McPherson S, Plummer R, Boddy AV, Curtin NJ, Jamieson D, Reeves HL. Imagestream detection and characterisation of circulating tumour cells - A liquid biopsy for hepatocellular carcinoma? *J Hepatol* 2016; **65**: 305-313 [PMID: 27132171 DOI: 10.1016/j.jhep.2016.04.014]
69 **Vona G**, Estepa L, Béroud C, Damotte D, Capron F, Nalpas B, Mineur A, Franco D, Lacour B, Pol S, Bréchot C, Paterlini-Bréchot P. Impact of cytomorphological detection of circulating tumor cells in patients with liver cancer. *Hepatology* 2004; **39**: 792-797 [PMID: 14999698 DOI: 10.1002/hep.20091]
70 **Chan KC**, Jiang P, Zheng YW, Liao GJ, Sun H, Wong J, Siu SS, Chan WC, Chan SL, Chan AT, Lai PB, Chiu RW, Lo YM. Cancer genome scanning in plasma: detection of tumor-associated copy number aberrations, single-nucleotide variants, and tumoral heterogeneity by massively parallel sequencing. *Clin Chem* 2013; **59**: 211-224 [PMID: 23065472 DOI: 10.1373/clinchem.2012.196014]
71 **Julich-Haertel H**, Urban SK, Krawczyk M, Willms A, Jankowski K, Patkowski W, Kruk B, Krasnodębski M, Ligocka J, Schwab R, Richardsen I, Schaaf S, Klein A, Gehlert S, Sänger H, Casper M,

Banales JM, Schuppan D, Milkiewicz P, Lammert F, Krawczyk M, Lukacs-Kornek V, Kornek M. Cancer-associated circulating large extracellular vesicles in cholangiocarcinoma and hepatocellular carcinoma. *J Hepatol* 2017; **67**: 282-292 [PMID: 28267620 DOI: 10.1016/j.jhep.2017.02.024]

72 **Friedlander TW**, Premasekharan G, Paris PL. Looking back, to the future of circulating tumor cells. *Pharmacol Ther* 2014; **142**: 271-280 [PMID: 24362084 DOI: 10.1016/j.pharmthera.2013.12.011]

P- Reviewer: Dietrich cf, Tajiri k, Zheng sj **S- Editor**: Ma YJ
L- Editor: Filipodia **E- Editor**: Tan WW

World Journal of Hepatology

Submit a Manuscript: http://www.f6publishing.com

World J Hepatol 2018 July 27; 10(7): 462-473

DOI: 10.4254/wjh.v10.i7.462

ISSN 1948-5182 (online)

MINIREVIEWS

MR with Gd-EOB-DTPA in assessment of liver nodules in cirrhotic patients

Riccardo Inchingolo, Riccardo Faletti, Luigi Grazioli, Eleonora Tricarico, Marco Gatti, Anna Pecorelli, Davide Ippolito

Riccardo Inchingolo, Eleonora Tricarico, Division of Interventional Radiology, Department of Radiology, Madonna delle Grazie Hospital, Matera 75100, Italy

Riccardo Faletti, Marco Gatti, Department of Surgical Sciences, Radiology Unit, University of Turin, Turin 10126, Italy

Luigi Grazioli, Department of Radiology, University of Brescia "Spedali Civili", Brescia 25123, Italy

Anna Pecorelli, Davide Ippolito, Department of Diagnostic Radiology, School of Medicine, University of Milano-Bicocca, Monza 20900, Italy

ORCID number: Riccardo Inchingolo (0000-0002-0253-5936); Riccardo Faletti (0000-0002-8865-8637); Luigi Grazioli (0000-0002-2345-1571); Eleonora Tricarico (0000-0001-9805-2551); Marco Gatti (0000-0001-8168-5280); Anna Pecorelli (0000-0001-9791-6709); Davide Ippolito (0000-0002-2696-7047).

Author contributions: All authors equally contributed to this paper with conception and design of the study, literature review and analysis, drafting and critical revision and editing, and final approval of the final version.

Conflict-of-interest statement: All the authors are aware of the content of the manuscript and have no conflict of interest.

Manuscript source: Invited manuscript

Correspondence to: Riccardo Inchingolo, MD, Doctor, Division of Interventional Radiology, Department of Radiology, Madonna delle Grazie Hospital, Via Montescaglioso, Matera 75100, Italy. riccardoin@hotmail.it
Telephone: +39-333-4601735
Fax: +39-835-253857

Received: March 26, 2018
Peer-review started: March 27, 2018
First decision: April 18, 2018
Revised: April 25, 2018
Accepted: May 30, 2018
Article in press: May 30, 2018
Published online: July 27, 2018

Abstract

To date the imaging diagnosis of liver lesions is based mainly on the identification of vascular features, which are typical of overt hepatocellular carcinoma (HCC), but the hepatocarcinogenesis is a complex and multistep event during which, a spectrum of nodules develop within the liver parenchyma, including benign small and large regenerative nodule (RN), low-grade dysplastic nodule (LGDN), high-grade dysplastic nodule (HGDN), early HCC, and well differentiated HCC. These nodules may be characterised not only on the basis of their respective different blood supplies, but also on their different hepatocyte function. Recently, in liver imaging the introduction of hepatobiliary magnetic resonance imaging contrast agent offered the clinicians the possibility to obtain, at once, information not only related to the vascular changes of liver nodules but also information on hepatocyte function. For this reasons this new approach becomes the most relevant diagnostic clue for differentiating low-risk nodules (LGDN-RN) from high-risk nodules (HGDN/early HCC or overt HCC) and consequently new diagnostic algorithms for HCC have been proposed. The use of hepatobiliary contrast agents is constantly increasing and gradually changing the standard of diagnosis of HCC. The main purpose of this review is to

underline the added value of Gd-EOB-DTPA in early-stage diagnoses of HCC. We also analyse the guidelines for the diagnosis and management of HCC, the key concepts of HCC development, growth and spread and the imaging appearance of precursor nodules that eventually may transform into overt HCC.

Key words: Hepatobiliary contrast materials; Cirrhosis; Gadoxetic acid; Magnetic resonance imaging; Liver

Core tip: Hepatobiliary contrast agents improve detection and characterization of focal liver lesions in patients with cirrhotic liver. Gd-EOB-DTPA provides information not only on vascular changes but also on hepatocyte function. Based on the recent advances in liver magnetic resonance imaging (MRI) technology, in this review, we discuss the pivotal role of Gd-EOB-DTPA enhanced MRI for the future of hepatocellular carcinoma's management.

Inchingolo R, Faletti R, Grazioli L, Tricarico E, Gatti M, Pecorelli A, Ippolito D. MR with Gd-EOB-DTPA in assessment of liver nodules in cirrhotic patients. *World J Hepatol* 2018; 10(7): 462-473 Available from: URL: http://www.wjgnet.com/1948-5182/full/v10/i7/462.htm DOI: http://dx.doi.org/10.4254/wjh.v10.i7.462

INTRODUCTION

Liver cancer is the fifth most common cancer in men, the ninth in women and is the second most common cause of death from cancer worldwide[1]. Hepatocellular carcinoma (HCC) is a primary tumour of the liver and several risk factors for its development have been identified. These include hepatitis C viral (HCV) infection, hepatitis B virus (HBV) infection, hereditary hemochromatosis and cirrhosis of almost any cause[2].

The diagnosis of HCC can be difficult and often requires the use of one or more imaging modalities[3-6]. Surveillance for HCC aims to reduce disease-related mortality because an accurate and early detection and characterization of focal liver nodule is mandatory since the management of HCC patients differs to other malignant or benign nodules and the prognosis of HCC depends mostly on the stage at which the tumour is identified[7].

Liver cirrhosis is the underlying and common condition associated with hepatocarcinogenesis. Cirrhosis develops after a long period of chronic liver disease when the risk of HCC is still low. The nodules that could be potentially find in a cirrhotic liver comprise: regenerative nodule (RN), low-grade dysplastic nodule (LGDN), high-grade dysplastic nodule (HGDN), early HCC, well differentiated HCC and moderately-poorly differentiated HCC. Hepatocarcinogenesis is a multistep event during which cell density increase, Kuppfer cells decrease, nodules enlarge and hemodynamics changes occur. To date, the imaging diagnosis of HCC is based on the characterization of vascular features, which are typical for overt HCC[3,6,8]. In fact, in the final step of hepatocarcinogenesis, the tumor blood supply consists of nontriadal or unpaired arteries and sinusoidal capillarization, with reduced or absent portal blood supply[9]. However, an atypical vascular behaviour is quite common in small (< 2 cm) nodule and almost one-third of these are malignant ("the one-third rule")[10]. These features depends on intra-nodular perfusional changes during carcinogenesis, starting with arterial hypovascularity with portal supply still present, followed by a decrease of both arterial and portal blood flow and, subsequently, to an hypervascular pattern[5].

At the same time organic anionic transporting polypeptide (OATP), transporters of bile salts, simultaneously and gradually decrease. OATP is expressed in RNs and LGDNs and its levels are lower in many HGDNs, early HCCs and progressed HCCs. The hemodynamic changes are well depict during dynamic multi detector computed tomography (MDCT) and magnetic resonance imaging (MRI) and both European and American guidelines have endorsed this techniques for the diagnosis of HCC > 1 cm, based on the typical hallmarks of hypervascularity in arterial phase with wash-out in portal phase, avoiding liver biopsy[10,11]. Moreover, OATP8 expression level reduces prior to complete neoangiogenesis[12] and the use of hepatospecific contrast media in MRI is considered a "new" HCC diagnostic tools that allows either to increase sensitivities for detection of HCC of all sizes[13] or would make it possible to identify preneoplastic lesions, such as HGDNs[14]. Furthermore, MRI offers additional imaging sequences that can be helpful in nodule characterization, including T2-weighted imaging (T2-WI) and diffusion-weighted imaging (DWI), which provides information on cellularity and has shown additional value to gadolinium-enhanced MRI by increasing the detection rate of HCC[15]. However, precise differentiation of preneoplastic lesions remain uncertain to date. The recent introduction of hepatobiliary MRI contrast agent gadolinium-ethoxybenzyl-dieth-ylenetriamine pentaacetic acid (Gd-EOB-DTPA, Primovist®; Bayer Schering Pharma, Berlin, Germany) which gives information not only on vascular changes but also on hepatocyte function, raises the sensitivity for the detection of early HCC to 91%-93%[16]. Many authors[9,16-21] suggested that Gd-EOB-DTPA-enhanced MRI is itself the most relevant diagnostic tool for differentiating low-risk nodules (LGDN, RN) from high-risk nodules (HGDN, early HCC, overt HCC) and hence new diagnostic algorithms for HCC have been proposed[4,22].

Based on the recent advances in MRI imaging technology and since early-stage diagnoses of HCC have increased and opened the possibilities to curative therapy, the purpose of these review is to the analyze the guidelines for the diagnosis and management of HCC; the basic MRI protocol and the advanced techniques, the key concepts of HCC development, growth and spread and the imaging appearance of precursor nodules that eventually may transform into overt HCC in order to eluci-

date the pivotal role of Gd-EOB-DTPA-enhanced MRI for the future of HCC's management, through a review of the published literature.

INTERNATIONAL GUIDELINES

Many studies have examined the clinical management of HCC, detecting guidelines to define a standardized approach to surveillance, diagnosis and treatment, with the aim of improve timely diagnosis and early intervention.

Guidelines in fact could be a roadmap to develop decision making algorithms, improving quality of treatment and patients' outcomes according with support of regional or national resources. From 2001 to 2017 at least 20 guidelines have been published worldwide, with some differences in surveillance and diagnostic criteria[23].

The American Association for the Study of Liver Diseases (AASLD) was founded in 1950, providing recommendation for surveillances, diagnosis, staging and treatment of HCC, in a similar way of European Association for the Study of the Liver (EASL)[8], while the first edition of practice guidelines for HCC in Japan was published in 2005[24]. Most of the guidelines devises the form of surveillance depending on risk factors for HCC and on individuating patients with risk factor that have to be monitored. Risk factors are divided into those that are cirrhosis-related (HBV, HCV, alcoholic cirrhosis, genetic causes such as hemochromatosis, non-alcoholic steatohepatitis, stage IV primary biliary cirrhosis, alpha one antitrypsin deficiency) and those that are non-cirrhosis related, (being an HBV carrier with family history of HCC, being Asian and > 40 years old, being African/North American black infected with HBV). The distribution of risk factors is different among the world, being HBV the leading cause of HCC in Africa and East Asia, instead HCV is the main cause in Europe, Japan and North American. However, cirrhosis of any aetiology, is the strongest predictor of HCC[25,26].

The main differences in surveillance among guidelines is represented by the use of serologic markers [alpha-fetoprotein (AFP), agglutinin-reactive fraction of AFP, des-gamma-carboxy prothrombin (DCP)] and grouping the patients depending on risk to develop HCC[23,27]. The use of serologic markers in HCC surveillance is still recommended only by the Japan Society of Hepatology (JSH) Guideline and Japan-HCC (J-HCC) Guideline[4,24], while guidelines in many western countries, such as the AASLD Guideline, the National Comprehensive Cancer Network (NCCN) Guideline and the EASL guideline have excluded serologic markers from surveillance criteria[3,8,28].

Guidelines have some differences in definition of high-risk population: JSH Guideline and J-HCC Guideline divide patients in very-high risk population, including individuals with HBV and HCV cirrhosis, and high risk population, including individuals with cirrhosis with other causes or with chronic HBV or HCV infection. The two groups of patients have a different surveillance protocol: very high-risk patients undergo ultrasound (US) and measurement of serologic markers every 3-4 mo, or dynamic CT/MRI every 6-12 mo for patients that are not suitable for US examination, while high-risk patients undergo US and measurement of tumour markers every 6 mo[23].

The NCCN guideline and EASL guideline divide patients in cirrhosis group and non-cirrhosis group, including liver function for EASL guideline. NCCN Guideline considers only cirrhotic patients as candidates for surveillance, while EASL Guideline recommends surveilling the non-cirrhosis group for chronic HCV with advanced fibrosis[3].

In NCCN, EASL and AASLD guidelines surveillance is performed with only US scan every 6 mo. If a nodule $\leqslant$ 1 cm is found at US, EASL and AASLD guidelines recommend another ultrasound examination performed every 3 or 4 mo; if the lesion grows and exceed 1 cm, CT or MRI are performed, instead a stable lesion undergo US follow-up every 3 or 4 mo for 1 or 2 years, with regular checking every 6 mo thereafter. NCCN Guideline recommends CT, MRI or US examination with contrast enhancement (CEUS) at 3 to 6 mo if a nodule < 1 cm is found. MDCT or MRI examinations are mandatory if the nodule at first US examination exceeds 1 cm, and the non-invasive diagnosis of HCC is possible if the nodule shows arterial enhancement and venous equilibrium phase washout. A difference between EASL guideline and AASLD guidelines is that EASL guideline states that typical feature of HCC have to be identified in both CT and MRI for 1 to 2 cm nodules in other than centres of excellence; a single imaging modality is sufficient for 1 to 2 cm nodules for AASLD guideline, independently from the centre of examination. If the typical pattern of HCC is not observed the patient undergo the other imaging modality, and if this is not diagnostic too, biopsy is recommended and if it is inconclusive, US is performed after 4 mo.

All these pathways examined, extensively used in western countries are "size based", while J-HCC, JSH and APASL guidelines' algorithms are "non-size based", with all patients undergo dynamic imaging regardless of nodule size. If dynamic CT/MRI reveal typical HCC pattern a definitive diagnosis can be made. JSH Guideline includes Gd-EOB-DTPA MRI (gadoxetic acid disodium, a liver-specific contrast agent) as a tool for first-line surveillance and diagnosis of HCC. Otherwise, J-HCC guidelines recommend the use of Gd-EOB-DTPA MRI, together with SPIO-MRI, CEUS, CTA and biopsy for nodules larger than 1 cm revealing only hypervascularity with no wash-out, while only US follow-up at 3 mo is suggested for nodule < 1 cm[24].

The APASL Guideline recommend SPIO-enhanced MRI or Sonazoid CEUS for patients with atypical vascular pattern: diagnosis of HCC can be made if there is not uptake, otherwise follow-up is recommended[27].

On summary, the main differences among guidelines are represented by the use or serologic markers for surveillance, the distribution of patients in different risk categories and finally in the use of more detailed

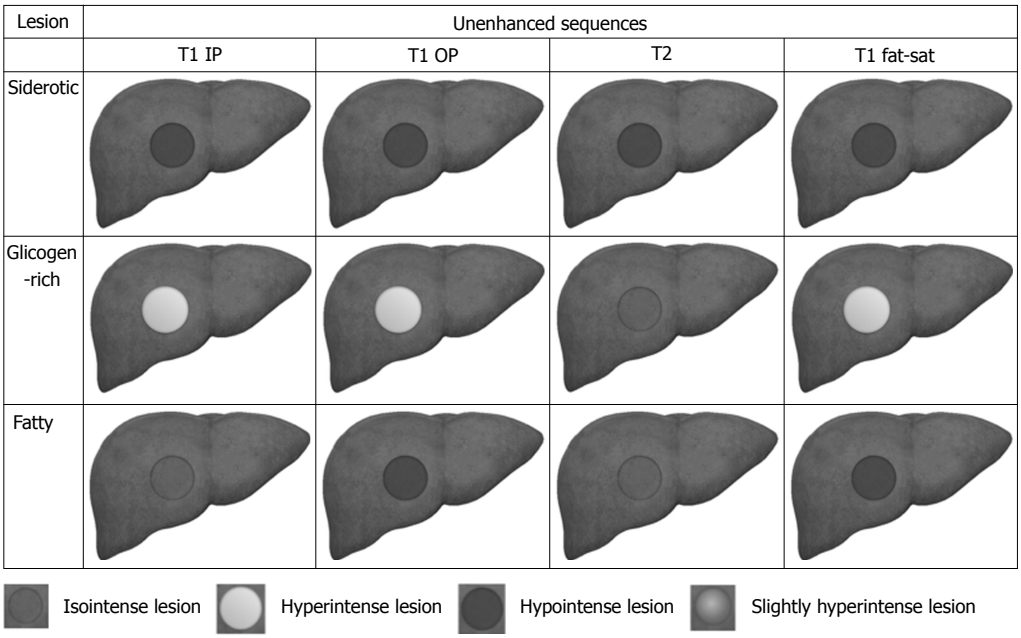

Figure 1 Schematic representation showing pre-contrast magnetic resonance imaging features of cirrhotic nodules such as siderotic (iron reach), glicogen rich and fatty nodule. T1 IP: T1-weighted in-phase image; T1 OP: T1-weighted out-of-phase image.

algorithm in J-HCC, JSH and APASL guidelines in case of hypervascular and hypovascular nodules, which maybe makes them more defined pathways.

RNS AND LGDNS

HCC is a complicated disease with a multi-step process from preneoplastic lesions, including cirrhosis, RN, LGDN, HGDN to HCC[29]. A RN is a well-defined area of liver parenchyma that has enlarged in response to necrosis, altered perfusion or other stimuli and consist of proliferating normal liver cells surrounded by a fibrous stroma[30].

Because of their histopathological nature, RNs are often not visible on T1 and T2 WI. However, they may appear hypointense, isointense or hyperintense related to the background liver on T1-WI or to the presence of paramagnetic materials a glycogen which contributes to T1-WI hyperintensity (Figure 1). On T2-WI, the signal intensity of the RNs is not hyper (unlike HCC) and they are often hypointense or isointense; low signal intensity may be due to iron deposition[9,31]. On DWI, RNs could be iso or less than a few times mild hyperintense compared to the surrounding parenchyma and the likely explanation for this mild hyperintensity was local areas of active fibrosis or infarction[32,33].

These nodules preserve hepatocellular function and lack neoangiogenesis. Thus, after extracellular contrast agent injection, enhancement is similar to, or slightly lower than that of the surrounding liver parenchyma while, after hepatobiliary MRI contrast agent injection, they usually appear iso- or hyper-intense on hepatobiliary phase images when compared to the surrounding liver[9,31].

The pre-malignant potentiality of RNs was controversial, but recently Sato *et al*[34] reported a rate of progression to malignancy of 13.6% at 50 mo and 32% at 100 mo for large RNs and these data stressed the outcome reported by Kobayashi *et al*[35] who reported an evolution rate into HCC of 12.4% in a 5-year period.

A DN is a focal area of hepatocytes $\geqslant$ 1 mm in diameter with dysplasia, without definite histologic malignant features[30]. They are classified into LGDNs and HGDNs based on cytological and architectural atypia as seen on microscopic evaluation.

In LGDNs, the hepatocytes rarely show a clonal population, there is minimal nuclear atypia and only an initial increase in the nuclear/cytoplasmic ratio. Large cell change is often present, but mitotic figures are absent. Without obvious clonal population, the distinction between LGDN and a large RN is difficult and does not comport any practical consequences as long as features of HGDN are absent[30].

The combination of iso- or hyper-intensity on T1-WI and iso- or hypo-intensity on T2-WI strongly suggests a DN. The reasons for the high intensity on T1 images include fatty change, intratumoral copper and increased zinc in the surrounding parenchyma. As RNs, LGDNs are iso or mild hyperintense compared to the surrounding parenchyma on DWI[32,33]. LGDNs display enhancement characteristics similar to that of the background liver parenchyma on all dynamic phases; because they remain mainly supplied by the portal circulation. LGDNs have been recently demonstrated as the tipping point (*i.e.*, pre-HCC state rather than HCC state) of hepatocarcinogenesis[36] and the evolution of dysplastic nodules into early HCC includes appearance of arterial blood supply and stromal invasion[37]. Channual

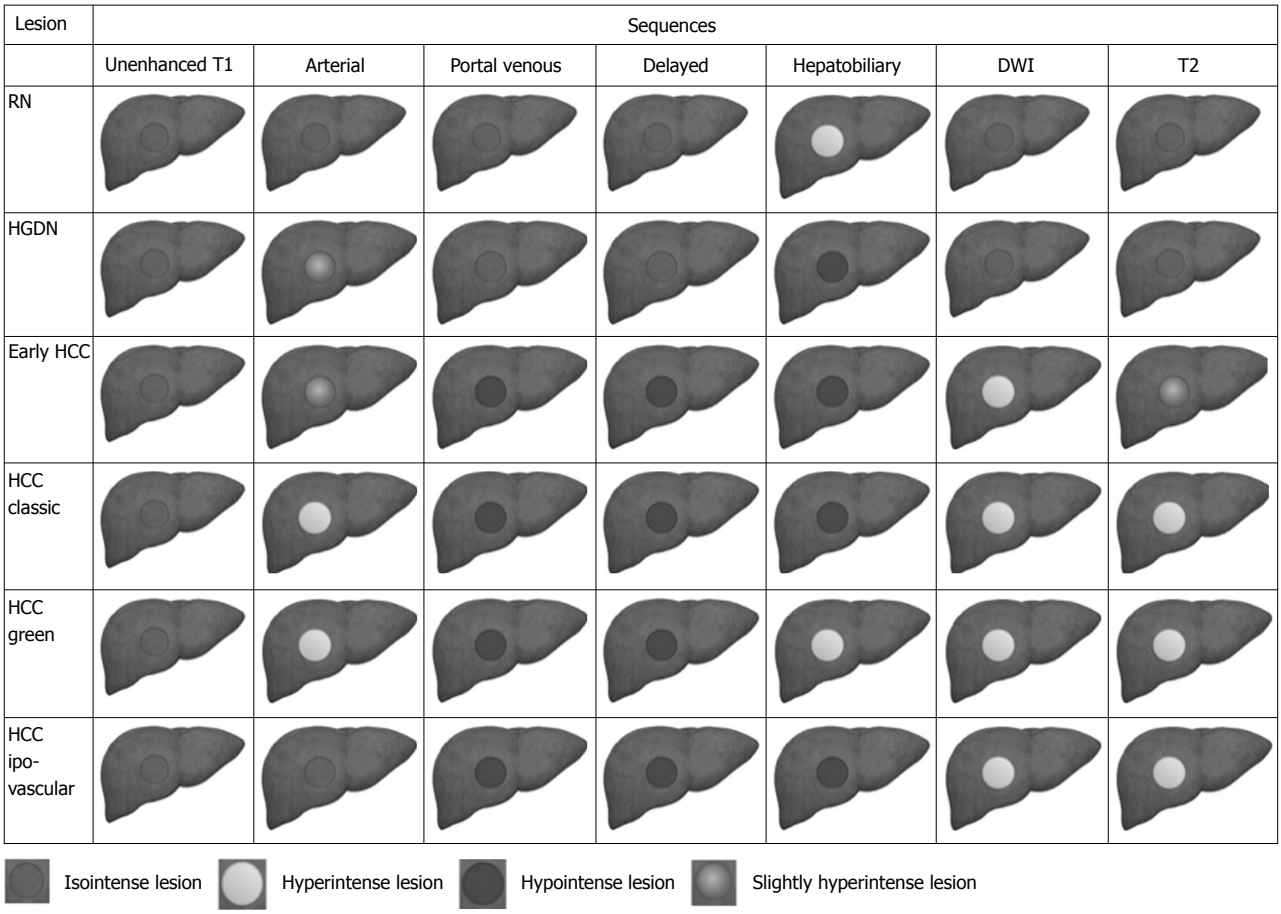

Figure 2 Schematic representation showing dynamic, diffusion weighted images and T2-weighted features, of regenerative nodules, high-grade dysplastic nodule, early hepatocellular carcinoma, classic hepatocellular carcinoma, green hepatocellular carcinoma and hypovascular hepatocellular carcinoma. DWI: Diffusion weighted images; HGDN: High-grade dysplastic nodule; RN: Regenerative nodule; HCC: Hepatocellular carcinoma.

et al[19] recently reported that LGDNs show lower relative intensity ratio on T2-WI and higher unenhanced to arterial signal intensities when compared with HGDNs and HCC.

All LGDNs demonstrated OATP1B3 expression similar to or higher than that of the surrounding liver and because of this OATP1B3 expression, commonly show iso/hyperintensity relative to surrounding liver in the hepatobiliary (HB) phase (Figure 2). According to the latest EASL and AASLD guidelines[3,5], DNs should not be treated or managed as cancers, nevertheless also LGDNs should be followed by regular imaging studies, since as firstly reported by Kobayashi *et al*[35] there is an annual transition rate of 10% for patients with LGDN and a 5-year cumulative transition rate of 30.2 and more recently Sato *et al*[34] studied founded a 50-mo transition rate of 40% in DNs.

Many authors demonstrated that reduction of signal intensity on both the late dynamic and hepatobiliary phase should then be considered an high feature of malignancy and could predict malignant transformation[16,38,39]. Therefore, a more frequent surveillance imaging is fundamental in these cases taking into account that the difference in the rates of malignant transformation between RNs and DNs is also important and highlighting the importance of classifying non-HCC lesions in cirrhotic liver into RNs and DNs. MRI features proposed by different authors for LGDN are summarized in Table 1.

HGDN

HGDNs usually have a vaguely nodular shape and lack of a capsule. Their cells are structured in an irregular trabecular pattern and are increased in density (2 times higher than the normal surrounding parenchyma). HGDNs often contain fat and sometimes copper and/or iron. Unpaired arteries are present even if in small number, and feeding portal veins are diminishing but still present. Finally organic anionic transporting polypeptide (OATP) expression progressively decrease[35]. The histopathological features of HGDNs are responsible for the lack of typical enhancement hallmark of HCC, that is arterial enhancement and delayed wash-out, and for their different appearance on the radiological imaging. MRI, better than other imaging techniques, is able to depict all this hepatocarcinogenesis changes[40].

Depending on iron or fat concentration, HDGNs can differently appear on pre-contrast sequences. Non-siderotic dysplastic nodules typically are hyperintense on T1-weighted sequence and iso-hypointense on T2-

Table 1 Magnetic resonance imaging features of low-grade dysplastic nodules according to various authors

	No. of nodules	T1w	T2w	Arterial phase	Delayed phase	DWI	HB
Golfieri *et al*[10]	38		=/-	=	=		=/-
Bartolozzi *et al*[17]	32	NA		=/+	=/+		+/=
Golfieri *et al*[16]	27	=/+	=/+	=	=		=/+
Chen *et al*[33]	10	+	=/-	=/+	=/-	=/+	
Di Martino *et al*[21]	29	+	-	=/-	=		=/+
Shin *et al*[44]	6	=/-	=/-	=	=	=	

+: Hyperintense; =: Isointense; -: Hypointense; NA: Not available; DWI: Diffusion-weighted imaging; HB: Hepatobiliary.

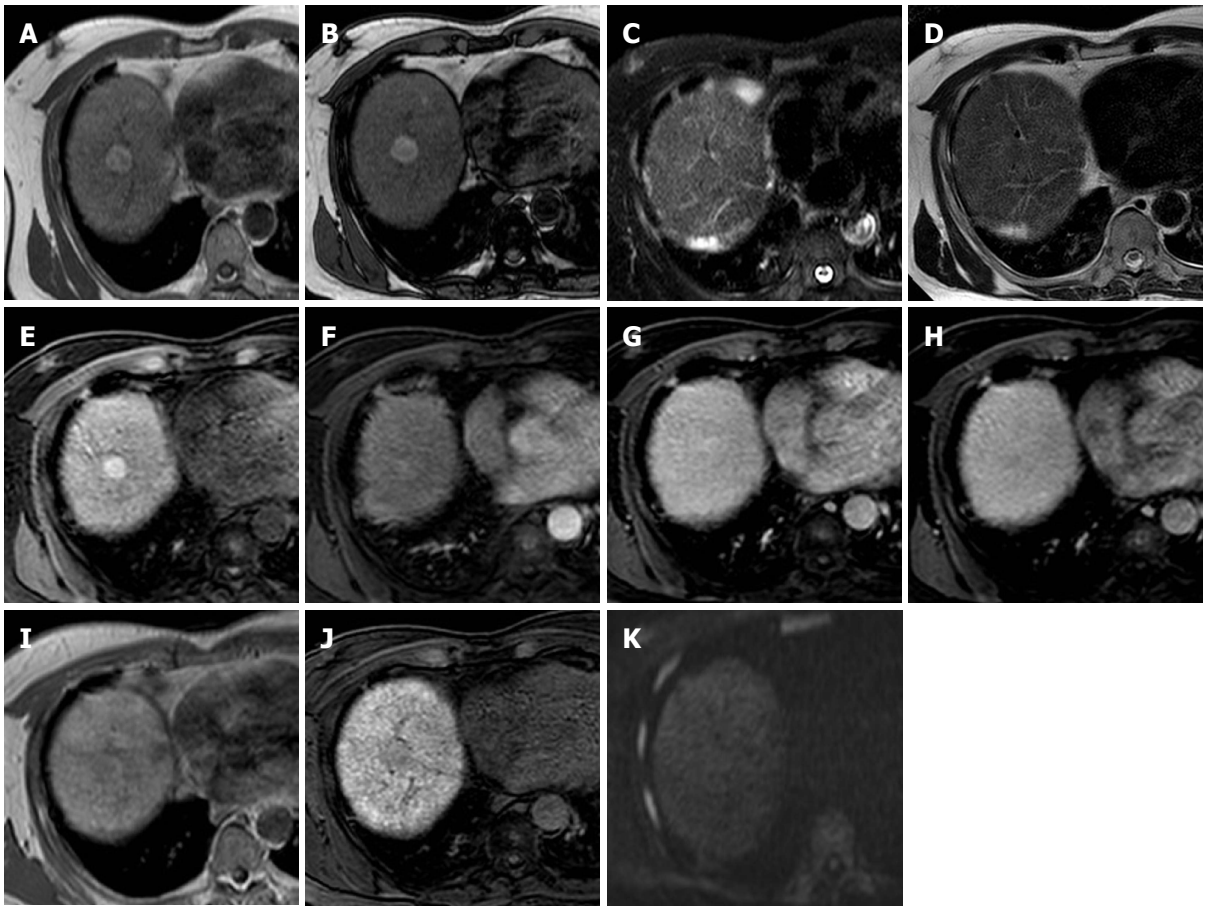

Figure 3 High-grade dysplastic nodule. Gd-EOB-DTPA enhanced MR images of a 57 years old cirrhotic patient with a liver nodule in the Ⅷ segment. A and B: Axial T1-weighted sequences both "in phase" and "out of phase" show a hyperintense nodule; C and D: On T2-weighted image with and without fat saturation the nodule appears as isointense; E-H: during the dynamic contrast-enhanced images the nodule shows a slight enhancement in the arterial phase, without wash-out in portal and delayed phases; I and J: Diffusion weighted image demonstrate no restriction to the diffusion; K: In hepatobiliary phase the nodule is hypointense in comparison to the surrounding liver parenchyma. The MRI features, suggestive of high grade dysplastic nodule, have been later confirmed by the histological examination. MRI: Magnetic resonance imaging.

weighted sequence[41]. With the increase of iron concentration HGDNs will appear as hypointense both on T1w and T2w images, although hyperintensity on T1w in siderotic nodules has been described which is related to low amount of iron[42] (Figure 3). Fat-rich HGDNs show hyperintensity on T1w in-phase images with a signal drop on out-of-phase images[43]. However intracellular fat is typical also in early HCC and can even found in overt HCC. In DWI, which provides information about cellular density, HGDNs have no restriction. For all this reason a correct characterization only based on pre-contrast images is not possible and the use of hepatospecific contrast agent to differentiate pre-neoplastic lesions and HCC is essential. A PubMed search using "high grade displastic nodules", "HGDN", "Gd-EOB-DTPA" and "Primovist" as keywords, identified 9 studies from 2011 to 2017, of whom only 4 focused on vascular pattern[1,11,16,17,44-48]. Typically, after hepatobiliary contrast agent injection, dysplastic nodules appear iso or hypointense on the arterial phase due to the uncomplete capillarization, and hypointense in delayed phase. Bartolozzi *et al*[17], in their study correlated dynamic MRI with histological findings on explanted cirrhotic lesions. They found 30 HGDNs of whom the majority (20/30) were iso-

hypointense on arterial phase and hypointense on late phase and the remaining 10 cases were iso-hyperintense on both arterial and late phases[17]. Kim *et al*[45] confirmed the prevalence of the iso-hypointense appearance of HGDNs in arterial phase. However vascular changes are a dynamic event and HGDNs may show hypervascular arterial enhancement[45]. Golfieri *et al*[10,16] in two different studies (2011 and 2012) reported a non-negligible amount of hypervascular enhancement in arterial phase, probably related to the fact that in both series HGDNs and early HCC were considered in the same group. The different radiological appearance clearly reflect the hemodynamic changes: Hypointense nodules in arterial phase are those lesions with arterial hypovascularity and a normal portal perfusion, isointense nodules are lesions with a perfect balance in the decrease of both arterial and portal blood supply and finally hyperintense nodules are lesions with an increase in arterial vascularity and the complete disappear of portal perfusion. In all studies the majority of HGDNs were hypointense on hepatobiliary phase (HBP). During hepatocarcinogenesis, OATP expression reduces prior to complete neoangiogenesis and increased arterial flow and so dysplastic nodules appear non-hypervascular and hypointense on HBP[9]. HB hypointensity is the most sensitive MRI feature to discriminate benign from malignant/pre-malignant lesions[49]. Moreover according to the literature non-hypervascular nodules with hypointensity on HBP have been shown to develop subsequent hypervascularization (range, 31%-35%) during the follow-up period of 1–3 years, being a risk factor for the development of HCC[50]. The probability to become hypervascular nodule increases with the nodule's dimension. According Kumada *et al*[51] a tumour diameter of 15 mm is the critical threshold for the vascularization of hypointense nodule since, at this size, nodules proliferate more actively and develop unpaired arteries. Akai *et al*[52] confirm these results. In fact, in their series hypointense nodules = 15 mm has a higher risk to progress to overt HCC in comparison to hypointense nodules > 15 mm (HR = 3.55; 95%CI: 0.79.12.3), although no significant difference was observed. As previously reported HGDNs have no restriction in the DWI. Shin *et al*[44] demonstrated that hyperintensity in DWI, combined with high signal intensity on T2, was the most specific feature to differentiate atypical HCCs from dysplastic nodules (sensitivity 80.0%, specificity 100%, positive predictive value 100%, negative predictive value 78.3%) due to the low cellularity of HGDNs when compared to HCC.

To conclude the combination of all MRI features (lesion size, intranodular fat, T2 and T1 intensity, DWI, HBP intensity), improves the characterization of lesions developed in a cirrhotic liver without the typical vascular pattern of HCC[53].

EARLY HCC

The multistep process of hepatocarcinogenesis, from RN to overt HCC, passes through an early stage of HCC. From a pathological point of view cancer cells of early HCC show unremarkable cellular atypia however nuclear-cytoplasmic ratio is increased and cellular density may be more than twice that of the surrounding non-cancerous liver tissue[54]. Early HCC proliferates by replacing adjacent hepatocytes in a trabecular pattern at the boundary with surrounding normal liver tissues, resulting in a poorly demarcated margin[55]. The pathologic features of early HCC closely resemble those of high grade dysplastic nodule (HGDN) and a distinct pathological differentiation between them is still lacking. According the International Consensus Group for Hepatocellular Neoplasia (ICGHN), stromal invasion should be considered as the most characteristics pathologic findings of early HCC[56]. The challenge for the radiologists is not only to differentiate between early HCC and HGDN but also with progressed HCC since early HCC shows a longer time to recurrence and a higher 5-year survival rate[57]. In this setting, magnetic resonance imaging using hepatospecific such as Gd-EOB-DTPA represents a major breakthrough in the proper characterization of liver nodules. In the last years some authors have described the MRI findings of histologically proven early HCC[10,58]. The largest series, published by Sano *et al*[59], described the MRI behaviour of 180 resected early HCC. In this study authors demonstrated that early HCC (n = 30) mostly appear as isointense on T1-WIand isointense or hyperintense on T2-WI. In some cases it may contain fat and appear as hypointense on T1-weighted sequences "out of phase" (Figure 4). Regarding contrast enhancement behaviour early-HCC is mainly hypovascular during arterial phase due to the lack of unpaired arteries. However some early HCCs may show hypervascular foci within them and this is the so called "nodule in nodule" appearance. During portal and delayed phases early HCC mostly appears as hypointense due to the progressive reduction of portal blood flow and in hepatobiliary phase is typically hypointense, because of the absence or the reduction of OATP1B3 carriers[59]. However, hypointensity in the hepatobiliary phase is not an peculiar finding of early or progressed HCC but can also be seen in dysplastic nodules, particularly in high grade[38]. In this setting, hyperintensity on DWI is the more accurate imaging feature to differentiate between early HCC/HCC and HGDN, with a sensitivity of 72.0%, higher than that of hyperintensity on T2 weighted images which is about 40.0% as reported by Hwang *et al*[60]. This finding has been recently confirmed by Renzulli *et al*[61]. In their series of 420 liver nodules, all the 24 histologically proven early-HCC were hypointense on hepatobiliary phase, hypovascular during arterial phase and hyperintense on DWI[61]. The explanation of the restriction to the diffusion, which is responsible for the hyperintensity on DWI, may rely on the increased cellular density during the histologic transition from dysplastic nodule to HCC. MRI features proposed by different authors for HGDN and early-HCC are summarized in Table 2.

HCC

HCC may arise from pre-existing DN or from an early

Table 2 Magnetic resonance imaging features of high-grade dysplastic nodules and early hepatocellular carcinoma according to various authors

	No. of nodules	T2w	Arterial phase	Delayed phase	DWI	HB
High grade dysplastic nodules						
Golfieri *et al*[10]	20	+	+/=	=		-
Golfieri *et al*[16]	41		+/=	=		-
Bartolozzi *et al*[17]	30		-/=	-		-
Choi *et al*[48]	17					-
Sugimori *et al*[46]	7					-
Kim *et al*[45]	17		-/=			-
Shin *et al*[44]	12	-/=			-	
Early HCC						
Sano *et al*[59]	180	=/+	+/=	-		-
Renzulli *et al*[61]	24	=/+	+	-	+	-

+: Hyperintense; =: Isointense; -: Hypointense; DWI: Diffusion-weighted imaging; HB: Hepatobiliary; HCC: Hepatocellular carcinoma.

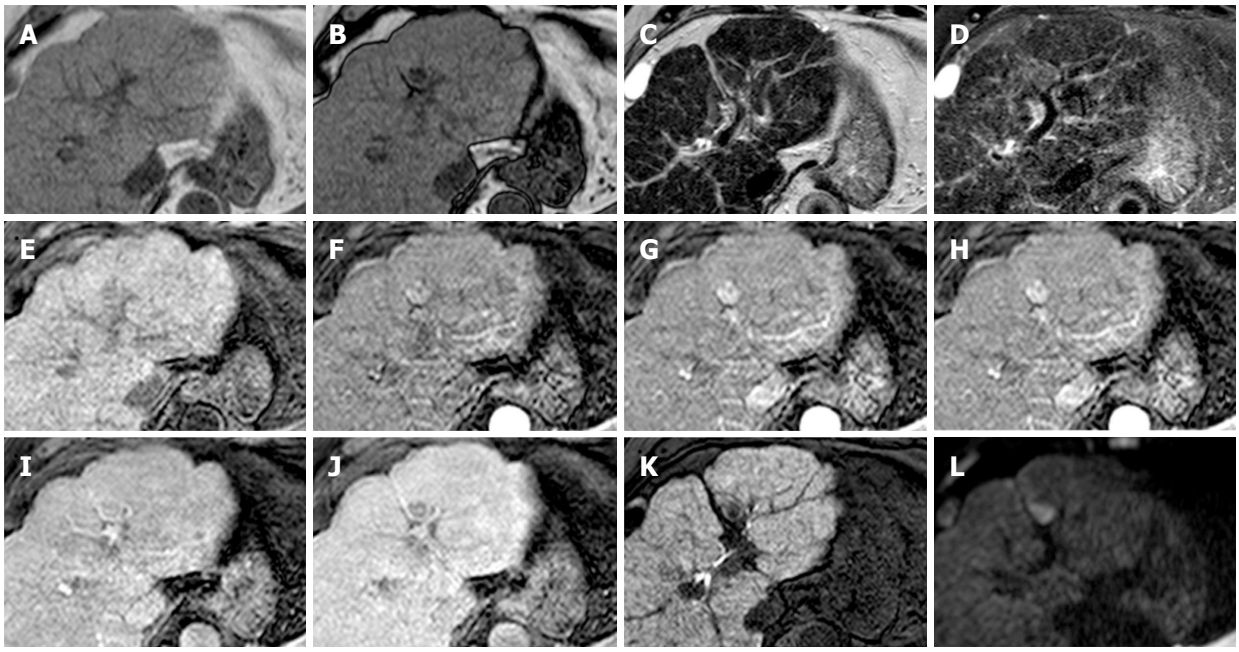

Figure 4 Typical case of lipid-rich hepatocellular carcinoma. A and B: The signal loss of nodule on opposed-phase compared to in-phase indicates intralesional fat; C and D: There is mild signal intensity on T2 and DWI restriction (L); E: The nodule appears hypointense in pre-contrast phase; G-J: Note the typical arterial phase hyperenhancement (G and H) followed by washout appearance in the portal venous (I) and/or delayed phase (J) that is the key diagnostic feature of HCC; K: The lesion also demonstrate hypointensity in the hepatobiliary phase; F-H: Note how the multi-arterial phase imaging (F and H) able improve the conspicuity of the HCC, especially in the late arterial phase (H). DWI: Diffusion weighted images; HCC: Hepatocellular carcinoma.

HCC. In both cases, it can take the macroscopic and radiological feature of the well-known "nodule in nodule". At the earliest stage, progressed HCC can be small, less than 2 cm and it is rarely a diagnostic dilemma either from a radiological and histological point of view. It is characterized by a destructive growth pattern with neoarterialization and microscopic vascular invasion in 1/4 of the cases. Portal tracts are no visible anymore and the borders of the tumour are usually rimmed by fibrosis that create a tumour capsule. Histologically, small but progressed HCC is usually well to moderately differentiated (G1/G2)[62].

According to the AASLD practice guidelines, typical enhancement of HCC during dynamic phases was defined as a combination of iso- to hypo-intensity on precontrast images, hyperintensity on arterial phase images, and hypointensity on PVP or delayed phase images, which represents washout[5]. This is based on previous studies that have demonstrated that HCCs contain solely arterial blood, whereas the normal liver parenchyma contains both arterial and portal blood[63]. However, many nodules in cirrhotic liver may have atypical enhancement patterns especially smaller ones (< 2 cm), and following "the one-third rule", approximately 30% of these are malignant[10].

In fact, HCC nodules smaller than 20 mm may be hypovascular, showing isointensity during the arterial and portal venous phases or may not have wash-out in portal phase[64]. Yoon *et al*[64] reported that the probability to have arterial phase enhancement was not only related to the size of the tumor, but also to the degree

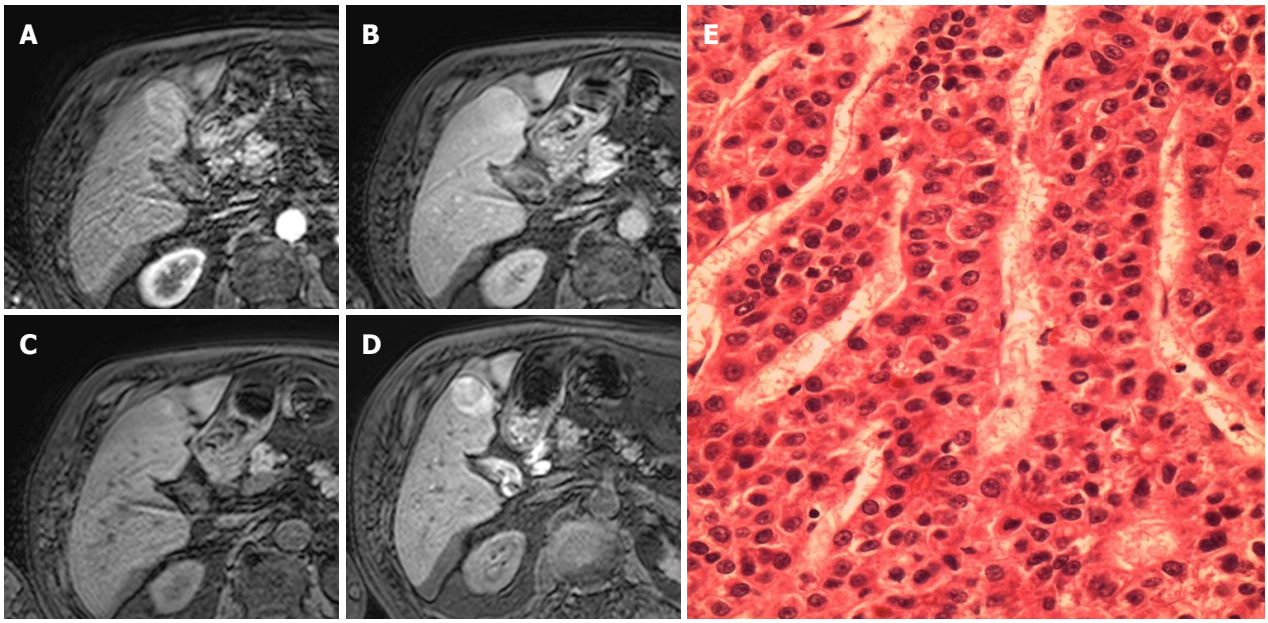

Figure 5 Atypical hepatocellular carcinoma. A and B: There is arterial phase (A) mild hyperenhancement and absence of washout appearance in the portal venous phase (B); C and D: In the delayed phase (C), there is a minimum hypointensity of the nodule, suspected for washout. The nodule resulted hyperintense in hepatobiliary phase (D); E: The lesion was biopsied and the specimen diagnosis was HCC solid-trabecular; G2, pT3a in non-cirrhotic liver with mild (< 5%) macrovescicular steatosis with portal fibrous enlargement and without septae formation.

of tumor differentiation, with poor differentiated HCC nodules having more probability to have arterial phase enhancement. In the same studies, the authors show that also the wash-out in portal phase was also related the degree of dedifferentiation with moderately and poorly differentiated HCCs have more probability to have wash-out than well-differentiated tumors. The atypical enhancement of small HCCs and well-differentiated HCCs during dynamic phase MR imaging may be explained by their immature arterialization during hepatocarcinogenesis[34,35,65,66].

Several previous studies[49,67] have demonstrated that HB phase imaging of hepatocyte-specific contrast agents such as Gd-EOB-DTPA can improve the detection and characterization of small nodules in the cirrhotic liver in comparison with dynamic phase imaging. However, Choi *et al*[68] have shown in their study that 10%-27% of HCCs remain iso- to hyper-intense on HBP images (Figure 5). The signal intensity on HBP may not depend on tumor differentiation, but rather on the degree of OATP8 expression and other potential genetic alterations, with possibility of poor differentiated HCC showing a high degree of OATP8 expression[12,69]. Furthermore, HCC can produce bile, thus appearing macroscopically green after fixing with formalin, the so called "green HCC"[55]. Asayama *et al*[70] in their study, significantly correlated the uptake of Gd-EOB-DTPA with green HCC, even if it was found that the location of uptake of Gd-EOB-DTPA in the tumor did not macroscopically correspond to the greenish areas.

Atypical enhancement pattern on dynamic phase images and iso- to hyperintensity on HBP images were more frequently detected in patients with worse Child Pugh class. The reason is that both the tumor and liver characteristics can affect the relative signal intensity of HCC and the gadoxetic acid uptake in the liver at HBP can particularly be diminished and delayed in the cirrhotic liver[67]. Therefore in cirrhotic patients the imaging interpretation of HCCs has to include a multiparametric assessment with other MR sequences.

However, Renzulli *et al*[61], in a recent study, included HBP hypointensity as an hallmark sufficient for diagnosis of HCC together with arterial phase hyperintensity and DWI restriction, purposing that only these three elements allow the diagnosis, excluding portal venous and delayed phase evaluation. Their diagnostic algorithm shows higher sensitivity and a specificity not very lower than that of the AASLD even for lesion smaller than 2 cm in cirrhotic patients evaluated with Gd-EOB-DTPA MRI, suggesting the increase value of the HBP signal intensity for diagnosis of HCC.

CONCLUSION

In summary, the use of MR with Gd-EOB-DTPA is increasing and progressively changing the standard of diagnosis of HCC and some international groups have boosted its role in new diagnostic algorithms for HCC. Indeed, to date the use of Gd-EOB-DTPA should be considered as an integral part and first line approach in diagnostic management of liver nodules in patients with liver cirrhosis, because it offers information not only related to the vascular pattern but also significant information on hepatocellular function. In most of cases the Gadoxetic acid improves detection of focal liver lesions and the categorization from LGDN form HGDN

and early HCCs lesions, avoiding the liver biopsy, an invasive procedure, that should be considered only in very few and specific cases. Moreover the identification of the borderline nodules from those with progression to HCC on the basis of the imaging appearance, related to hepatocellular function, is critical for determining the better management strategy of these patients and MR with Gd-EOB-DTPA can thus play a crucial role for the correct and non-invasive of HCC's management.

ACKNOWLEDGMENTS

We wish to thank Professor Adam Cassels for his contribution in amending and polishing the language of this manuscript.

REFERENCES

1 **Ferlay J**, Soerjomataram I, Dikshit R, Eser S, Mathers C, Rebelo M, Parkin DM, Forman D, Bray F. Cancer incidence and mortality worldwide: sources, methods and major patterns in GLOBOCAN 2012. *Int J Cancer* 2015; **136**: E359-E386 [PMID: 25220842 DOI: 10.1002/ijc.29210]

2 **Sun S**, Wang GL, Huang Y, Diwu HL, Luo YC, Su J, Xiao YH. The effects of 2-hydroxyethyl methacrylate on matrix metalloproteinases 2 and 9 in human pulp cells and odontoblast-like cells in vitro. *Int Endod J* 2018; **51** Suppl 2: e157-e166 [PMID: 28667765 DOI: 10.1111/iej.12812]

3 **European Association For The Study Of The Liver**; European Organisation For Research And Treatment Of Cancer. EASL-EORTC clinical practice guidelines: management of hepatocellular carcinoma. *J Hepatol* 2012; **56**: 908-943 [PMID: 22424438 DOI: 10.1016/j.jhep.2011.12.001]

4 **Kudo M**, Matsui O, Izumi N, Iijima H, Kadoya M, Imai Y, Okusaka T, Miyayama S, Tsuchiya K, Ueshima K, Hiraoka A, Ikeda M, Ogasawara S, Yamashita T, Minami T, Yamakado K; Liver Cancer Study Group of Japan. JSH Consensus-Based Clinical Practice Guidelines for the Management of Hepatocellular Carcinoma: 2014 Update by the Liver Cancer Study Group of Japan. *Liver Cancer* 2014; **3**: 458-468 [PMID: 26280007 DOI: 10.1159/000343875]

5 **Bruix J**, Sherman M; American Association for the Study of Liver Diseases. Management of hepatocellular carcinoma: an update. *Hepatology* 2011; **53**: 1020-1022 [PMID: 21374666 DOI: 10.1002/hep.24199]

6 **Mitchell DG**, Bruix J, Sherman M, Sirlin CB. LI-RADS (Liver Imaging Reporting and Data System): summary, discussion, and consensus of the LI-RADS Management Working Group and future directions. *Hepatology* 2015; **61**: 1056-1065 [PMID: 25041904 DOI: 10.1002/hep.27304]

7 **Fateen W**, Ryder SD. Screening for hepatocellular carcinoma: patient selection and perspectives. *J Hepatocell Carcinoma* 2017; **4**: 71-79 [PMID: 28553624 DOI: 10.2147/JHC.S105777]

8 **Adachi K**, Honma Y, Miyake T, Kawakami K, Takahashi T, Suzumiya J. Tamoxifen enhances the differentiation-inducing and growth-inhibitory effects of all-trans retinoic acid in acute promyelocytic leukemia cells. *Int J Oncol* 2016; **48**: 1095-1102 [PMID: 26797574 DOI: 10.3892/ijo.2016.3348]

9 **Park HJ**, Choi BI, Lee ES, Park SB, Lee JB. How to Differentiate Borderline Hepatic Nodules in Hepatocarcinogenesis: Emphasis on Imaging Diagnosis. *Liver Cancer* 2017; **6**: 189-203 [PMID: 28626731 DOI: 10.1159/000455949]

10 **Golfieri R**, Renzulli M, Lucidi V, Corcioni B, Trevisani F, Bolondi L. Contribution of the hepatobiliary phase of Gd-EOB-DTPA-enhanced MRI to Dynamic MRI in the detection of hypovascular small (≤2 cm) HCC in cirrhosis. *Eur Radiol* 2011; **21**: 1233-1242 [PMID: 21293864 DOI: 10.1007/s00330-010-2030-1]

11 **Kitao A**, Matsui O, Yoneda N, Kozaka K, Shinmura R, Koda W, Kobayashi S, Gabata T, Zen Y, Yamashita T, Kaneko S, Nakanuma Y. The uptake transporter OATP8 expression decreases during multistep hepatocarcinogenesis: correlation with gadoxetic acid enhanced MR imaging. *Eur Radiol* 2011; **21**: 2056-2066 [PMID: 21626360 DOI: 10.1007/s00330-011-2165-8]

12 **Tsuboyama T**, Onishi H, Kim T, Akita H, Hori M, Tatsumi M, Nakamoto A, Nagano H, Matsuura N, Wakasa K, Tomoda K. Hepatocellular carcinoma: hepatocyte-selective enhancement at gadoxetic acid-enhanced MR imaging--correlation with expression of sinusoidal and canalicular transporters and bile accumulation. *Radiology* 2010; **255**: 824-833 [PMID: 20501720 DOI: 10.1148/radiol.10091557]

13 **Eisenberg E**, Burstein Y, Suzan E, Treister R, Aviram J. Spinal cord stimulation attenuates temporal summation in patients with neuropathic pain. *Pain* 2015; **156**: 381-385 [PMID: 25599230 DOI: 10.1097/01.j.pain.0000460342.69718.a2]

14 **Choi JY**, Lee JM, Sirlin CB. CT and MR imaging diagnosis and staging of hepatocellular carcinoma: part II. Extracellular agents, hepatobiliary agents, and ancillary imaging features. *Radiology* 2014; **273**: 30-50 [PMID: 25247563 DOI: 10.1148/radiol.14132362]

15 **Gluskin JS**, Chegai F, Monti S, Squillaci E, Mannelli L. Hepatocellular Carcinoma and Diffusion-Weighted MRI: Detection and Evaluation of Treatment Response. *J Cancer* 2016; **7**: 1565-1570 [PMID: 27471573 DOI: 10.7150/jca.14582]

16 **Golfieri R**, Grazioli L, Orlando E, Dormi A, Lucidi V, Corcioni B, Dettori E, Romanini L, Renzulli M. Which is the best MRI marker of malignancy for atypical cirrhotic nodules: hypointensity in hepatobiliary phase alone or combined with other features? Classification after Gd-EOB-DTPA administration. *J Magn Reson Imaging* 2012; **36**: 648-657 [PMID: 22592930 DOI: 10.1002/jmri.23685]

17 **Bartolozzi C**, Battaglia V, Bargellini I, Bozzi E, Campani D, Pollina LE, Filipponi F. Contrast-enhanced magnetic resonance imaging of 102 nodules in cirrhosis: correlation with histological findings on explanted livers. *Abdom Imaging* 2013; **38**: 290-296 [PMID: 23053453 DOI: 10.1007/s00261-012-9952-9]

18 **Külpmann WR**, Lagemann J, Sander R, Maibaum P. A comparison of reference method values for sodium, potassium and chloride with method-dependent assigned values. *J Clin Chem Clin Biochem* 1985; **23**: 865-874 [PMID: 3831226 DOI: 10.1515/cclm.1985.23.12.865]

19 **Channual S**, Tan N, Siripongsakun S, Lassman C, Lu DS, Raman SS. Gadoxetate Disodium-Enhanced MRI to Differentiate Dysplastic Nodules and Grade of Hepatocellular Carcinoma: Correlation With Histopathology. *AJR Am J Roentgenol* 2015; **205**: 546-553 [PMID: 26295640 DOI: 10.2214/AJR.14.12716]

20 **Cho HJ**, Kim B, Lee JD, Kang DR, Kim JK, Lee JH, Shin SJ, Lee KM, Yoo BM, Lee KJ, Kim SS, Cheong JY, Cho SW. Development of Risk Prediction Model for Hepatocellular Carcinoma Progression of Indeterminate Nodules in Hepatitis B Virus-Related Cirrhotic Liver. *Am J Gastroenterol* 2017; **112**: 460-470 [PMID: 27779194 DOI: 10.1038/ajg.2016.480]

21 **Di Martino M**, Anzidei M, Zaccagna F, Saba L, Bosco S, Rossi M, Ginanni Corradini S, Catalano C. Qualitative analysis of small (≤2 cm) regenerative nodules, dysplastic nodules and well-differentiated HCCs with gadoxetic acid MRI. *BMC Med Imaging* 2016; **16**: 62 [PMID: 27835984 DOI: 10.1186/s12880-016-0165-5]

22 **Renzulli M**, Golfieri R; Bologna Liver Oncology Group (BLOG). Proposal of a new diagnostic algorithm for hepatocellular carcinoma based on the Japanese guidelines but adapted to the Western world for patients under surveillance for chronic liver disease. *J Gastroenterol Hepatol* 2016; **31**: 69-80 [PMID: 26312574 DOI: 10.1111/jgh.13150]

23 **Song P**, Cai Y, Tang H, Li C, Huang J. The clinical management of hepatocellular carcinoma worldwide: A concise review and comparison of current guidelines from 2001 to 2017. *Biosci Trends* 2017; **11**: 389-398 [PMID: 28904327 DOI: 10.5582/bst.2017.01202]

24 **Japan Society of Hepatology**. Clinical practice guidelines for hepatocellular carcinoma (2013 version). Available from: URL: https://www.jsh.or.jp/English/guidelines_en/Guidelines_for_hepatocellular_carcinoma_2013

25 **Fattovich G**, Stroffolini T, Zagni I, Donato F. Hepatocellular carcinoma in cirrhosis: incidence and risk factors. *Gastroenterology* 2004; **127**: S35-S50 [PMID: 15508101 DOI: 10.1053/j.gastro.2004.09.014]

26 **Sherman M**. Hepatocellular carcinoma: epidemiology, surveillance,

and diagnosis. *Semin Liver Dis* 2010; **30**: 3-16 [PMID: 20175029 DOI: 10.1055/s-0030-1247128]
27 **Omata M**, Cheng AL, Kokudo N, Kudo M, Lee JM, Jia J, Tateishi R, Han KH, Chawla YK, Shiina S, Jafri W, Payawal DA, Ohki T, Ogasawara S, Chen PJ, Lesmana CRA, Lesmana LA, Gani RA, Obi S, Dokmeci AK, Sarin SK. Asia-Pacific clinical practice guidelines on the management of hepatocellular carcinoma: a 2017 update. *Hepatol Int* 2017; **11**: 317-370 [PMID: 28620797 DOI: 10.1007/s12072-017-9799-9]
28 **Benson AB 3rd**, D'Angelica MI, Abrams TA, Are C, Bloomston PM, Chang DT, Clary BM, Covey AM, Ensminger WD, Iyer R, Kelley RK, Linehan D, Malafa MP, Meranze SG, Park JO, Pawlik T, Posey JA, Scaife C, Schefter T, Sigurdson ER, Tian GG, Vauthey JN, Venook AP, Yen Y, Zhu AX, Hoffmann KG, McMillian NR, Sundar H. Hepatobiliary cancers, version 2.2014. *J Natl Compr Canc Netw* 2014; **12**: 1152-1182 [PMID: 25099447 DOI: 10.6004/jnccn.2014.0112]
29 **Niu ZS**, Niu XJ, Wang WH, Zhao J. Latest developments in precancerous lesions of hepatocellular carcinoma. *World J Gastroenterol* 2016; **22**: 3305-3314 [PMID: 27022212 DOI: 10.3748/wjg.v22.i12.3305]
30 **International Working Party**. Terminology of nodular hepatocellular lesions. *Hepatology* 1995; **22**: 983-993 [PMID: 7657307 DOI: 10.1016/0270-9139(95)90324-0]
31 **Choi BI**, Lee JM, Kim TK, Dioguardi Burgio M, Vilgrain V. Diagnosing Borderline Hepatic Nodules in Hepatocarcinogenesis: Imaging Performance. *AJR Am J Roentgenol* 2015; **205**: 10-21 [PMID: 26102378 DOI: 10.2214/AJR.14.12655]
32 **Lee MH**, Kim SH, Park MJ, Park CK, Rhim H. Gadoxetic acid-enhanced hepatobiliary phase MRI and high-b-value diffusion-weighted imaging to distinguish well-differentiated hepatocellular carcinomas from benign nodules in patients with chronic liver disease. *AJR Am J Roentgenol* 2011; **197**: W868-W875 [PMID: 22021534 DOI: 10.2214/AJR.10.6237]
33 **Chen ML**, Zhang XY, Qi LP, Shi QL, Chen B, Sun YS. Diffusion-weighted images (DWI) without ADC values in assessment of small focal nodules in cirrhotic liver. *Chin J Cancer Res* 2014; **26**: 38-47 [PMID: 24653625 DOI: 10.3978/j.issn.1000-9604.2014.01.07]
34 **Sato T**, Kondo F, Ebara M, Sugiura N, Okabe S, Sunaga M, Yoshikawa M, Suzuki E, Ogasawara S, Shinozaki Y, Ooka Y, Chiba T, Kanai F, Kishimoto T, Nakatani Y, Fukusato T, Yokosuka O. Natural history of large regenerative nodules and dysplastic nodules in liver cirrhosis: 28-year follow-up study. *Hepatol Int* 2015; **9**: 330-336 [PMID: 25788204 DOI: 10.1007/s12072-015-9620-6]
35 **Kobayashi M**, Ikeda K, Hosaka T, Sezaki H, Someya T, Akuta N, Suzuki F, Suzuki Y, Saitoh S, Arase Y, Kumada H. Dysplastic nodules frequently develop into hepatocellular carcinoma in patients with chronic viral hepatitis and cirrhosis. *Cancer* 2006; **106**: 636-647 [PMID: 16369988 DOI: 10.1002/cncr.21607]
36 **Lu L**, Jiang Z, Dai Y, Chen L. Low-Grade Dysplastic Nodules Revealed as the Tipping Point during Multistep Hepatocarcinogenesis by Dynamic Network Biomarkers. *Genes* (Basel) 2017; **8**: [PMID: 29027943 DOI: 10.3390/genes8100268]
37 **Kojiro M**, Roskams T. Early hepatocellular carcinoma and dysplastic nodules. *Semin Liver Dis* 2005; **25**: 133-142 [PMID: 15918142 DOI: 10.1055/s-2005-871193]
38 **Kogita S**, Imai Y, Okada M, Kim T, Onishi H, Takamura M, Fukuda K, Igura T, Sawai Y, Morimoto O, Hori M, Nagano H, Wakasa K, Hayashi N, Murakami T. Gd-EOB-DTPA-enhanced magnetic resonance images of hepatocellular carcinoma: correlation with histological grading and portal blood flow. *Eur Radiol* 2010; **20**: 2405-2413 [PMID: 20490505 DOI: 10.1007/s00330-010-1812-9]
39 **Park MJ**, Kim YK, Lee MW, Lee WJ, Kim YS, Kim SH, Choi D, Rhim H. Small hepatocellular carcinomas: improved sensitivity by combining gadoxetic acid-enhanced and diffusion-weighted MR imaging patterns. *Radiology* 2012; **264**: 761-770 [PMID: 22843769 DOI: 10.1148/radiol.12112517]
40 **Lee JM**, Yoon JH, Kim KW. Diagnosis of hepatocellular carcinoma: newer radiological tools. *Semin Oncol* 2012; **39**: 399-409 [PMID: 22846858 DOI: 10.1053/j.seminoncol.2012.05.010]
41 **Hanna RF**, Aguirre DA, Kased N, Emery SC, Peterson MR, Sirlin CB. Cirrhosis-associated hepatocellular nodules: correlation of histopathologic and MR imaging features. *Radiographics* 2008; **28**: 747-769 [PMID: 18480482 DOI: 10.1148/rg.283055108]
42 **Gaffuri G**. [Use of a preparation with a base of L-citrulline and L-acetylaspartic acid in minors with "mental fatigue" and slight "mental retardation"]. *G Psichiatr Neuropatol* 1966; **94**: 701-713 [PMID: 4381170]
43 **Martín J**, Sentís M, Zidan A, Donoso L, Puig J, Falcó J, Bella R. Fatty metamorphosis of hepatocellular carcinoma: detection with chemical shift gradient-echo MR imaging. *Radiology* 1995; **195**: 125-130 [PMID: 7892452 DOI: 10.1148/radiology.195.1.7892452]
44 **Shin SK**, Kim YS, Choi SJ, Shim YS, Jung DH, Kwon OS, Choi DJ, Kim JH. Characterization of small (⩽3cm) hepatic lesions with atypical enhancement feature and hypointensity in hepatobiliary phase of gadoxetic acid-enhanced MRI in cirrhosis: A STARD-compliant article. *Medicine* (Baltimore) 2017; **96**: e7278 [PMID: 28723741 DOI: 10.1097/MD.0000000000007278]
45 **Kim BR**, Lee JM, Lee DH, Yoon JH, Hur BY, Suh KS, Yi NJ, Lee KB, Han JK. Diagnostic Performance of Gadoxetic Acid-enhanced Liver MR Imaging versus Multidetector CT in the Detection of Dysplastic Nodules and Early Hepatocellular Carcinoma. *Radiology* 2017; **285**: 134-146 [PMID: 28609205 DOI: 10.1148/radiol.2017162080]
46 **Sugimori K**, Numata K, Okada M, Nihonmatsu H, Takebayashi S, Maeda S, Nakano M, Tanaka K. Central vascular structures as a characteristic finding of regenerative nodules using hepatobiliary phase gadolinium ethoxybenzyl diethylenetriaminepentaacetic acid-enhanced MRI and arterial dominant phase contrast-enhanced US. *J Med Ultrason* (2001) 2017; **44**: 89-100 [PMID: 27771842 DOI: 10.1007/s10396-016-0750-9]
47 **Sugimoto K**, Moriyasu F, Shiraishi J, Saito K, Taira J, Saguchi T, Imai Y. Assessment of arterial hypervascularity of hepatocellular carcinoma: comparison of contrast-enhanced US and gadoxetate disodium-enhanced MR imaging. *Eur Radiol* 2012; **22**: 1205-1213 [PMID: 22270142 DOI: 10.1007/s00330-011-2372-3]
48 **Choi SH**, Byun JH, Lim YS, Yu E, Lee SJ, Kim SY, Won HJ, Shin YM, Kim PN. Diagnostic criteria for hepatocellular carcinoma ⩽3 cm with hepatocyte-specific contrast-enhanced magnetic resonance imaging. *J Hepatol* 2016; **64**: 1099-1107 [PMID: 26820629 DOI: 10.1016/j.jhep.2016.01.018]
49 **Ahn SS**, Kim MJ, Lim JS, Hong HS, Chung YE, Choi JY. Added value of gadoxetic acid-enhanced hepatobiliary phase MR imaging in the diagnosis of hepatocellular carcinoma. *Radiology* 2010; **255**: 459-466 [PMID: 20413759 DOI: 10.1148/radiol.10091388]
50 **Yoon JH**, Lee JM, Yang HK, Lee KB, Jang JJ, Han JK, Choi BI. Non-hypervascular hypointense nodules ⩾1 cm on the hepatobiliary phase of gadoxetic acid-enhanced magnetic resonance imaging in cirrhotic livers. *Dig Dis* 2014; **32**: 678-689 [PMID: 25376284 DOI: 10.1159/000368000]
51 **Kumada T**, Toyoda H, Tada T, Sone Y, Fujimori M, Ogawa S, Ishikawa T. Evolution of hypointense hepatocellular nodules observed only in the hepatobiliary phase of gadoxetate disodium-enhanced MRI. *AJR Am J Roentgenol* 2011; **197**: 58-63 [PMID: 21701011 DOI: 10.2214/AJR.10.5390]
52 **Akai H**, Matsuda I, Kiryu S, Tajima T, Takao H, Watanabe Y, Imamura H, Kokudo N, Akahane M, Ohtomo K. Fate of hypointense lesions on Gd-EOB-DTPA-enhanced magnetic resonance imaging. *Eur J Radiol* 2012; **81**: 2973-2977 [PMID: 22280873 DOI: 10.1016/j.ejrad.2012.01.007]
53 **Merkle EM**, Zech CJ, Bartolozzi C, Bashir MR, Ba-Ssalamah A, Huppertz A, Lee JM, Ricke J, Sakamoto M, Sirlin CB, Ye SL, Zeng M. Consensus report from the 7th International Forum for Liver Magnetic Resonance Imaging. *Eur Radiol* 2016; **26**: 674-682 [PMID: 26070500 DOI: 10.1007/s00330-015-3873-2]
54 **Dondelinger RF**, Kurdziel JC. Biliary endoprostheses adapted from percutaneous drainage catheters. *Ann Radiol* (Paris) 1986; **29**: 142-147 [PMID: 3740734]
55 **Liver Cancer Study Group of Japan**. General rules for the clinical and pathological study of primary liver cancer. 3rd English edition. Tokyo: Kanehara Co. Ltd., 2010

56 **International Consensus Group for Hepatocellular Neoplasia**, The International Consensus Group for Hepatocellular Neoplasia. Pathologic diagnosis of early hepatocellular carcinoma: a report of the international consensus group for hepatocellular neoplasia. *Hepatology* 2009; **49**: 658-664 [PMID: 19177576 DOI: 10.1002/hep.22709]

57 **Sakamoto M**, Hirohashi S, Shimosato Y. Early stages of multistep hepatocarcinogenesis: adenomatous hyperplasia and early hepatocellular carcinoma. *Hum Pathol* 1991; **22**: 172-178 [PMID: 1848205 DOI: 10.1016/0046-8177(91)90039-R]

58 **Rhee H**, Kim MJ, Park YN, Choi JS, Kim KS. Gadoxetic acid-enhanced MRI findings of early hepatocellular carcinoma as defined by new histologic criteria. *J Magn Reson Imaging* 2012; **35**: 393-398 [PMID: 21990116 DOI: 10.1002/jmri.22828]

59 **Sano K**, Ichikawa T, Motosugi U, Sou H, Muhi AM, Matsuda M, Nakano M, Sakamoto M, Nakazawa T, Asakawa M, Fujii H, Kitamura T, Enomoto N, Araki T. Imaging study of early hepatocellular carcinoma: usefulness of gadoxetic acid-enhanced MR imaging. *Radiology* 2011; **261**: 834-844 [PMID: 21998047 DOI: 10.1148/radiol.11101840]

60 **Hwang J**, Kim YK, Jeong WK, Choi D, Rhim H, Lee WJ. Nonhypervascular Hypointense Nodules at Gadoxetic Acid-enhanced MR Imaging in Chronic Liver Disease: Diffusion-weighted Imaging for Characterization. *Radiology* 2015; **276**: 137-146 [PMID: 25734551 DOI: 10.1148/radiol.15141350]

61 **Renzulli M**, Biselli M, Brocchi S, Granito A, Vasuri F, Tovoli F, Sessagesimi E, Piscaglia F, D'Errico A, Bolondi L, Golfieri R. New hallmark of hepatocellular carcinoma, early hepatocellular carcinoma and high-grade dysplastic nodules on Gd-EOB-DTPA MRI in patients with cirrhosis: a new diagnostic algorithm. *Gut* 2018 [PMID: 29437912 DOI: 10.1136/gutjnl-2017-315384]

62 **Roncalli M**, Terracciano L, Di Tommaso L, David E, Colombo M; Gruppo Italiano Patologi Apparato Digerente (GIPAD); Società Italiana di Anatomia Patologica e Citopatologia Diagnostica/International Academy of Pathology, Italian division (SIAPEC/IAP). Liver precancerous lesions and hepatocellular carcinoma: the histology report. *Dig Liver Dis* 2011; **43** Suppl 4: S361-S372 [PMID: 21459342 DOI: 10.1016/S1590-8658(11)60592-6]

63 **Baron RL**, Peterson MS. From the RSNA refresher courses: screening the cirrhotic liver for hepatocellular carcinoma with CT and MR imaging: opportunities and pitfalls. *Radiographics* 2001; **21** Spec No: S117-S132 [PMID: 11598252 DOI: 10.1148/radiographics.21.suppl_1.g01oc14s117]

64 **Yoon SH**, Lee JM, So YH, Hong SH, Kim SJ, Han JK, Choi BI. Multiphasic MDCT enhancement pattern of hepatocellular carcinoma smaller than 3 cm in diameter: tumor size and cellular differentiation. *AJR Am J Roentgenol* 2009; **193**: W482-W489 [PMID: 19933622 DOI: 10.2214/AJR.08.1818]

65 **Willatt JM**, Hussain HK, Adusumilli S, Marrero JA. MR Imaging of hepatocellular carcinoma in the cirrhotic liver: challenges and controversies. *Radiology* 2008; **247**: 311-330 [PMID: 18430871 DOI: 10.1148/radiol.2472061331]

66 **Kitao A**, Zen Y, Matsui O, Gabata T, Nakanuma Y. Hepatocarcinogenesis: multistep changes of drainage vessels at CT during arterial portography and hepatic arteriography--radiologic-pathologic correlation. *Radiology* 2009; **252**: 605-614 [PMID: 19703890 DOI: 10.1148/radiol.2522081414]

67 **Cruite I**, Schroeder M, Merkle EM, Sirlin CB. Gadoxetate disodium-enhanced MRI of the liver: part 2, protocol optimization and lesion appearance in the cirrhotic liver. *AJR Am J Roentgenol* 2010; **195**: 29-41 [PMID: 20566795 DOI: 10.2214/AJR.10.4538]

68 **Choi JW**, Lee JM, Kim SJ, Yoon JH, Baek JH, Han JK, Choi BI. Hepatocellular carcinoma: imaging patterns on gadoxetic acid-enhanced MR Images and their value as an imaging biomarker. *Radiology* 2013; **267**: 776-786 [PMID: 23401584 DOI: 10.1148/radiol.13120775]

69 **Vavricka SR**, Jung D, Fried M, Grützner U, Meier PJ, Kullak-Ublick GA. The human organic anion transporting polypeptide 8 (SLCO1B3) gene is transcriptionally repressed by hepatocyte nuclear factor 3beta in hepatocellular carcinoma. *J Hepatol* 2004; **40**: 212-218 [PMID: 14739090 DOI: 10.1016/j.jhep.2003.10.008]

70 **Asayama Y**, Tajima T, Nishie A, Ishigami K, Kakihara D, Nakayama T, Okamoto D, Fujita N, Aishima S, Shirabe K, Honda H. Uptake of Gd-EOB-DTPA by hepatocellular carcinoma: radiologic-pathologic correlation with special reference to bile production. *Eur J Radiol* 2011; **80**: e243-e248 [PMID: 21109378 DOI: 10.1016/j.ejrad.2010.10.032]

P- Reviewer: Jarcuska P, Kaya M, Takahashi T **S- Editor**: Ji FF
L- Editor: A **E- Editor**: Yin SY

World Journal of Hepatology

Submit a Manuscript: http://www.f6publishing.com

World J Hepatol 2018 July 27; 10(7): 474-478

DOI: 10.4254/wjh.v10.i7.474

ISSN 1948-5182 (online)

MINIREVIEWS

Associations between nonalcoholic fatty liver disease and ischemic stroke

Stelina Alkagiet, Achilleas Papagiannis, Konstantinos Tziomalos

Stelina Alkagiet, Achilleas Papagiannis, Konstantinos Tziomalos, First Propedeutic Department of Internal Medicine, Medical School, Aristotle University of Thessaloniki, AHEPA Hospital, Thessaloniki 54636, Greece

ORCID number: Stelina Alkagiet (0000-0001-5089-1161); Achilleas Papagiannis (0000-0001-7285-4724); Konstantinos Tziomalos (0000-0002-3172-1594).

Author contributions: Alkagiet S and Papagiannis A drafted the review; Tziomalos K critically revised the draft.

Conflict-of-interest statement: All authors declare no conflict of interest related to this publication.

Manuscript source: Invited manuscript

Correspondence to: Konstantinos Tziomalos, MD, PhD, Assistant Professor, First Propedeutic Department of Internal Medicine, Medical School, Aristotle University of Thessaloniki, AHEPA Hospital, 1 Stilponos Kyriakidi Street, Thessaloniki 54636, Greece. ktziomalos@yahoo.com
Telephone: +30-2310-994621
Fax: +30-2310-994773

Received: March 27, 2018
Peer-review started: March 28, 2018
First decision: April 13, 2018
Revised: April 22, 2018
Accepted: May 30, 2018
Article in press: May 31, 2018
Published online: July 27, 2018

Abstract

Nonalcoholic fatty liver disease (NAFLD) is the commonest chronic liver disease and affects a considerable proportion of the general population. NAFLD is independently associated with increased risk for cardiovascular events, particularly coronary heart disease. Importantly, even though NAFLD is more prevalent in patients with major cardiovascular risk factors (*e.g.*, type 2 diabetes mellitus, obesity and hypertension), the association between NAFLD and cardiovascular disease appears to be independent of these risk factors. However, NAFLD also appears to increase the risk for ischemic stroke, a leading cause of mortality and long-term disability worldwide. It also appears that nonalcoholic steatohepatitis is more strongly related to the risk of ischemic stroke than isolated hepatic steatosis. Moreover, emerging data suggest that patients with NAFLD experience more severe ischemic stroke and have more unfavorable prognosis after an acute ischemic stroke in terms of functional dependency and short- and long-term mortality. These associations have major public health implications, since ischemic stroke is the second leading cause of death worldwide and an important cause of long-term disability. The aim of the present review is to summarize the current knowledge regarding the relationship between NAFLD and ischemic stroke incidence, severity and outcome. Given these associations, it might be useful to evaluate patients with acute ischemic stroke for the presence of NAFLD and to manage those with NAFLD more aggressively.

Key words: Nonalcoholic fatty liver disease; Ischemic stroke; Risk; Incidence; Severity; Outcome; Functional dependency

Core tip: Accumulating data suggest that nonalcoholic

fatty liver disease (NAFLD) is independently associated with increased risk for ischemic stroke, a leading cause of mortality and long-term disability worldwide. Moreover, emerging evidence shows that patients with NAFLD experience more severe ischemic stroke and have more unfavorable prognosis after an acute ischemic stroke in terms of functional dependency and short- and long-term mortality.

Alkagiet S, Papagiannis A, Tziomalos K. Associations between nonalcoholic fatty liver disease and ischemic stroke. *World J Hepatol* 2018; 10(7): 474-478 Available from: URL: http://www.wjgnet.com/1948-5182/full/v10/i7/474.htm DOI: http://dx.doi.org/10.4254/wjh.v10.i7.474

INTRODUCTION

Nonalcoholic fatty liver disease (NAFLD) is the most frequent chronic liver disease, affects approximately 25% of the general population and is the leading cause of abnormal liver function tests[1,2]. Moreover, the prevalence of NAFLD is even higher in elderly subjects and in patients with type 2 diabetes mellitus (T2DM), obesity, hypertension and/or metabolic syndrome[2,3]. Nonalcoholic steatohepatitis (NASH), a more advanced form of NAFLD, is present in up to 10% of adults[4]. NAFLD can progress to cirrhosis, hepatocellular cancer or liver failure, and is a major cause of liver transplantation[3,5].

Several studies showed that NAFLD is a risk factor for cardiovascular disease (CVD)[6,7]. Importantly, even though NAFLD is more prevalent in patients with major cardiovascular risk factors (*e.g.*, T2DM, obesity and hypertension), the association between NAFLD and CVD appears to be independent of these risk factors (Figure 1)[6,7].

In this context, accumulating data suggest that NAFLD is also associated with increased incidence of ischemic stroke. Moreover, emerging evidence suggests that NAFLD might also be related with more severe stroke and with worse outcome of patients with acute ischemic stroke. These associations have major public health implications, since ischemic stroke is the second leading cause of death worldwide and an important cause of long-term disability[8,9]. The aim of the present review is to summarize the current knowledge regarding the relationship between NAFLD and ischemic stroke incidence, severity and outcome.

NAFLD AND INCIDENCE OF ISCHEMIC STROKE

Several studies reported that elevated aminotransferase and g-glutamyltransferase (gGT) levels, which are mostly due to NAFLD, are associated with increased incidence of ischemic stroke (Table 1). In a small case-control study in 103 patients with acute ischemic stroke and 200 controls, alanine or aspartate aminotransferase levels were independently associated with increased odds ratio for ischemic stroke[10]. In a larger prospective study in 6997 men without established CVD or T2DM, gGT levels, a more specific marker of NAFLD, was independently associated with higher risk of ischemic stroke, even in subjects at low- or moderate cardiovascular risk[11]. In EUROSTROKE, a nested-case control study performed in 3 European countries (Finland, Netherlands and United Kingdom), the association between gGT levels and ischemic stroke risk appeared to be stronger in patients without T2DM[12]. Importantly, gGT appears to play a role in atherogenesis[13]. Indeed, gGT has been isolated from atheromatic plaques, macrophages and foam cells[14] and appears to contribute to atherosclerosis by inducing oxidative stress[15]. It was shown than gGT promotes oxidization of low-density lipoprotein and that it plays a crucial role in the catabolism of glutathione and the release of reactive oxygen species[16,17]. In a recent cross-sectional study, NAFLD diagnosed with ultrasonography was associated with increased prevalence of lacunar infarcts in non-obese subjects but not in obese patients[18]. In contrast, in another recent case-cohort study in 572 patients with incident ischemic stroke and 1017 controls, NAFLD defined as fatty liver index > 60 was associated with lower risk in men but there was no association in women[19]. In a meta-analysis of 9 case-control and cohort studies, NAFLD was independently associated with 2.3 times higher risk for ischemic stroke (95%CI: 1.84-2.93)[20]. The strength of this association was comparable in Caucasian and Asian patients[20]. Importantly, this association was independent of traditional cardiovascular risk factors, including dyslipidemia, obesity and T2DM[20].

It appears that NASH is more strongly related to the risk of ischemic stroke than isolated hepatic steatosis. Indeed, in a case-control study in 295 patients with acute ischemic stroke and 1942 subjects who underwent a health check-up, the degree of liver fibrosis, evaluated with transient elastography, was independently associated with increased stroke risk[21]. In contrast, isolated steatosis was not related with the risk of stroke[21].

NAFLD AND SEVERITY AND OUTCOME OF ISCHEMIC STROKE

There are very few data regarding the impact of NAFLD on the severity and outcome of ischemic stroke (Table 1). In an early prospective study in 200 patients admitted with acute ischemic stroke, NAFLD (defined as elevated aminotransferase levels in the absence of other causes) was present in 42.5% of patients[22]. Patien-

Table 1 Major studies that evaluated the association between nonalcoholic fatty liver disease and ischemic stroke

Ref.	Design	Mean age (yr)	Follow-up	Outcome
[7]	Prospective observational study in 1637 healthy Japanese men/women	47.8	2 yr	Higher incidence of CVD including stroke in patients with NAFLD compared with controls
[22]	Prospective study in 242 patients admitted with acute stroke	66	2 yr	Increased risk of acute stroke, more severe stroke and worse outcome in patients with NAFLD
[11]	Prospective study in 6997 men with no history of CVD or diabetes mellitus	40-59	24 yr	Association between gGT and higher incidence of fatal, major stroke events and total CVD mortality
[10]	Cross sectional study in adults with suspected acute stroke	20-27	Not applicable	Elevated ALP and ALT levels independently associated with higher risk of acute stroke
[12]	Case-control study using data from 3 European cohort studies in 13177 subjects	40-60	3-8 yr	Elevated gGT levels associated with higher risk of stroke
[21]	Case-control study in 295 patients with acute stroke and 1942 healthy subjects	60	Not applicable	Liver fibrosis was associated with higher incidence of ischemic stroke
[20]	Meta analysis of 9 studies that examined relation of NAFLD and stroke	Not reported	Not applicable	Higher risk of ischemic stroke and hemorrhagic stroke in patients with NAFLD
[23]	Retrospective study in 306 patients with confirmed brainstem infractions	65	Not applicable	Higher incidence of brainstem infracts in patients with NAFLD
[24]	Study in 415 patients admitted with acute ischemic stroke	78.8	Duration of hospitalization	NAFLD was not associated with stroke severity at admission or outcome during hospitalization
[19]	Case-cohort study in 572 patients with stroke and 1017 controls	> 45	5.8 yr	Fatty liver index associated with increased risk for ischemic stroke in women and with lower risk in women
[20]	Cross-sectional study in 1277 subjects who underwent brain magnetic resonance imaging and abdominal ultrasound during check-up	> 40 yr	Not applicable	NAFLD diagnosed with ultrasonography was associated with increased prevalence of lacunar infarcts in non-obese subjects but not in obese patients

CVD: Cardiovascular disease; gGT: G-glutamyltransferase; ALP: Alkaline phosphatase; ALT; Alanine aminotransferase; NAFLD: Nonalcoholic fatty liver disease.

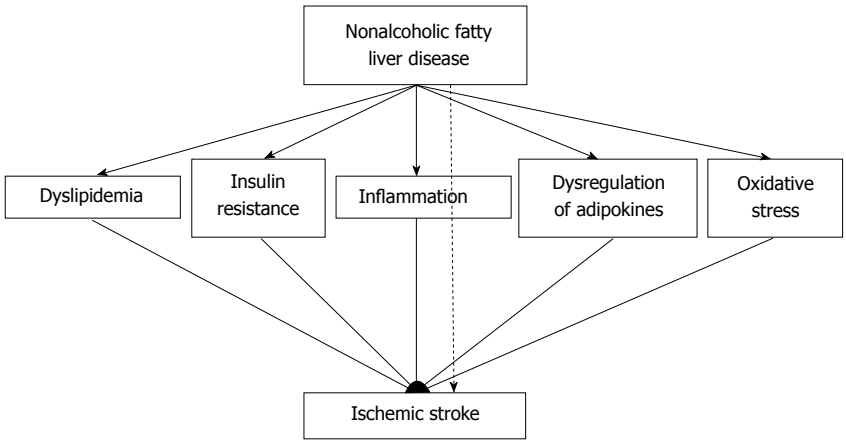

Figure 1 Mechanisms underpinning the association between nonalcoholic fatty liver disease and ischemic stroke (broken line suggests the independent association between nonalcoholic fatty liver disease and ischemic stroke).

ts with NAFLD had more severe stroke at admission and worse functional outcome at discharge[22]. However, patients with NAFLD were more obese, had higher prevalence of T2DM and had higher low-density lipoprotein cholesterol and triglyceride levels than patients without NAFLD; these differences were not adjusted for in the comparisons of stroke severity and outcome between the 2 groups[22]. In a more recent retrospective study in 306 patients with brainstem infarction, a similar prevalence of NAFLD (defined as elevated aminotransferase levels in the absence of other causes) was reported (42.5%)[23]. Patients with NAFLD had more severe stroke at admission and higher risk for neurological deterioration during hospitalization, independently of other risk factors[23]. In contrast, in a prospective study in 415 consecutive patients with acute ischemic stroke, stroke severity at admission, functional outcome at discharge and in-hospital mortality did not differ between patients with NAFLD (defined as elevated aminotransferase levels without another apparent cause) and those without NAFLD after adjustment for other cardiovascular risk factors[24]. However, only 32 patients (7.7% of the study population) had NAFLD[24]. Therefore, this study might have lacked the power to

identify an association between NAFLD and stroke severity and outcome[24].

CONCLUSION

Accumulating data suggest that NAFLD is independently associated with increased risk for ischemic stroke. Moreover, it appears that patients with NAFLD experience more severe stroke and have more adverse functional outcome than patients without NAFLD. Therefore, it might be useful to evaluate patients with acute ischemic stroke for the presence of NAFLD and to manage those with NAFLD more aggressively. It remains to be established whether management of NAFLD will also reduce the risk and improve the outcome of ischemic stroke.

REFERENCES

1 **Armstrong MJ**, Houlihan DD, Bentham L, Shaw JC, Cramb R, Olliff S, Gill PS, Neuberger JM, Lilford RJ, Newsome PN. Presence and severity of non-alcoholic fatty liver disease in a large prospective primary care cohort. *J Hepatol* 2012; **56**: 234-240 [PMID: 21703178 DOI: 10.1016/j.jhep.2011.03.020]

2 **Younossi ZM**, Koenig AB, Abdelatif D, Fazel Y, Henry L, Wymer M. Global epidemiology of nonalcoholic fatty liver disease-Meta-analytic assessment of prevalence, incidence, and outcomes. *Hepatology* 2016; **64**: 73-84 [PMID: 26707365 DOI: 10.1002/hep.28431]

3 **Chalasani N**, Younossi Z, Lavine JE, Diehl AM, Brunt EM, Cusi K, Charlton M, Sanyal AJ. The diagnosis and management of non-alcoholic fatty liver disease: practice Guideline by the American Association for the Study of Liver Diseases, American College of Gastroenterology, and the American Gastroenterological Association. *Hepatology* 2012; **55**: 2005-2023 [PMID: 22488764 DOI: 10.1002/hep.25762]

4 **Caballería L**, Pera G, Arteaga I, Rodríguez L, Alumà A, Morillas RM, de la Ossa N, Díaz A, Expósito C, Miranda D, Sánchez C, Prats RM, Urquizu M, Salgado A, Alemany M, Martinez A, Majeed I, Fabrellas N, Graupera I, Planas R, Ojanguren I, Serra M, Torán P, Caballería J, Ginès P. High Prevalence of Liver Fibrosis Among European Adults With Unknown Liver Disease: A Population-Based Study. *Clin Gastroenterol Hepatol* 2018; **16**: 1138-1145.e5 [PMID: 29452268 DOI: 10.1016/j.cgh.2017.12.048]

5 **Bhala N**, Angulo P, van der Poorten D, Lee E, Hui JM, Saracco G, Adams LA, Charatcharoenwitthaya P, Topping JH, Bugianesi E, Day CP, George J. The natural history of nonalcoholic fatty liver disease with advanced fibrosis or cirrhosis: an international collaborative study. *Hepatology* 2011; **54**: 1208-1216 [PMID: 21688282 DOI: 10.1002/hep.24491]

6 **Targher G**, Bertolini L, Rodella S, Tessari R, Zenari L, Lippi G, Arcaro G. Nonalcoholic fatty liver disease is independently associated with an increased incidence of cardiovascular events in type 2 diabetic patients. *Diabetes Care* 2007; **30**: 2119-2121 [PMID: 17519430 DOI: 10.2337/dc07-0349]

7 **Hamaguchi M**, Kojima T, Takeda N, Nagata C, Takeda J, Sarui H, Kawahito Y, Yoshida N, Suetsugu A, Kato T, Okuda J, Ida K, Yoshikawa T. Nonalcoholic fatty liver disease is a novel predictor of cardiovascular disease. *World J Gastroenterol* 2007; **13**: 1579-1584 [PMID: 17461452 DOI: 10.3748/wjg.v13.i10.1579]

8 **Mendis S**, Puska P, Norrving B, editors. Globes Atlas on cardiovascular disease prevention and control. Geneva: World Health Organization, 2011

9 **Menken M**, Munsat TL, Toole JF. The global burden of disease study: implications for neurology. *Arch Neurol* 2000; **57**: 418-420 [PMID: 10714674 DOI: 10.1001/archneur.57.3.418]

10 **Ying I**, Saposnik G, Vermeulen MJ, Leung A, Ray JG. Non-alcoholic fatty liver disease and acute ischemic stroke. *Epidemiology* 2011; **22**: 129-130 [PMID: 21150361 DOI: 10.1097/EDE.0b013e3181feb50a]

11 **Wannamethee SG**, Lennon L, Shaper AG. The value of gamma-glutamyltransferase in cardiovascular risk prediction in men without diagnosed cardiovascular disease or diabetes. *Atherosclerosis* 2008; **201**: 168-175 [PMID: 18378241 DOI: 10.1016/j.atherosclerosis.2008.01.019]

12 **Bots ML**, Salonen JT, Elwood PC, Nikitin Y, Freire de Concalves A, Inzitari D, Sivenius J, Trichopoulou A, Tuomilehto J, Koudstaal PJ, Grobbee DE. Gamma-glutamyltransferase and risk of stroke: the EUROSTROKE project. *J Epidemiol Community Health* 2002; **56** Suppl 1: i25-i29 [PMID: 11815641 DOI: 10.1136/jech.56.suppl_1.i25]

13 **Emdin M**, Passino C, Franzini M, Paolicchi A, Pompella A. gamma-glutamyltransferase and pathogenesis of cardiovascular diseases. *Future Cardiol* 2007; **3**: 263-270 [PMID: 19804218 DOI: 10.2217/14796678.3.3.263]

14 **Franzini M**, Corti A, Martinelli B, Del Corso A, Emdin M, Parenti GF, Glauber M, Pompella A, Paolicchi A. Gamma-glutamyltransferase activity in human atherosclerotic plaques-biochemical similarities with the circulating enzyme. *Atherosclerosis* 2009; **202**: 119-127 [PMID: 18486136 DOI: 10.1016/j.atherosclerosis.2008.03.023]

15 **Koenig G**, Seneff S. Gamma-Glutamyltransferase: A Predictive Biomarker of Cellular Antioxidant Inadequacy and Disease Risk. *Dis Markers* 2015; **2015**: 818570 [PMID: 26543300 DOI: 10.1155/2015/818570]

16 **Paolicchi A**, Minotti G, Tonarelli P, Tongiani R, De Cesare D, Mezzetti A, Dominici S, Comporti M, Pompella A. Gamma-glutamyl transpeptidase-dependent iron reduction and LDL oxidation--a potential mechanism in atherosclerosis. *J Investig Med* 1999; **47**: 151-160 [PMID: 10198571]

17 **Stark AA**, Zeiger E, Pagano DA. Glutathione metabolism by gamma-glutamyltranspeptidase leads to lipid peroxidation: characterization of the system and relevance to hepatocarcinogenesis. *Carcinogenesis* 1993; **14**: 183-189 [PMID: 8094645 DOI: 10.1093/carcin/14.2.183]

18 **Kwak MS**, Kim KW, Seo H, Chung GE, Yim JY, Kim D. Non-obese fatty liver disease is associated with lacunar infarct. *Liver Int* 2018; **38**: 1292-1299[PMID: 29220869 DOI: 10.1111/liv.13663]

19 **Alexander KS**, Zakai NA, Lidofsky SD, Callas PW, Judd SE, Tracy RP, Cushman M. Non-alcoholic fatty liver disease, liver biomarkers and stroke risk: The Reasons for Geographic and Racial Differences in Stroke cohort. *PLoS One* 2018; **13**: e0194153 [PMID: 29529073 DOI: 10.1371/journal.pone.0194153]

20 **Hu J**, Xu Y, He Z, Zhang H, Lian X, Zhu T, Liang C, Li J. Increased risk of cerebrovascular accident related to non-alcoholic fatty liver disease: a meta-analysis. *Oncotarget* 2017; **9**: 2752-2760 [PMID: 29416808 DOI: 10.18632/oncotarget.22755]

21 **Kim SU**, Song D, Heo JH, Yoo J, Kim BK, Park JY, Kim DY, Ahn SH, Kim KJ, Han KH, Kim YD. Liver fibrosis assessed with transient elastography is an independent risk factor for ischemic stroke. *Atherosclerosis* 2017; **260**: 156-162 [PMID: 28222857 DOI: 10.1016/j.atherosclerosis.2017.02.005]

22 **Abdeldyem SM**, Goda T, Khodeir SA, Abou Saif S, Abd-Elsalam S. Nonalcoholic fatty liver disease in patients with acute ischemic stroke is associated with more severe stroke and worse outcome. *J Clin Lipidol* 2017; **11**: 915-919 [PMID: 28579247 DOI: 10.1016/j.jacl.2017.04.115]

23 **Li H**, Hu B, Wei L, Zhou L, Zhang L, Lin Y, Qin B, Dai Y, Lu Z. Non-alcoholic fatty liver disease is associated with stroke severity and progression of brainstem infarctions. *Eur J Neurol* 2018; **25**: 577-e34 [PMID: 29281159 DOI: 10.1111/ene.13556]

24 **Tziomalos K**, Giampatzis V, Bouziana SD, Spanou M, Pap-

adopoulou M, Pavlidis A, Kostaki S, Bozikas A, Savopoulos C, Hatzitolios AI. Association between nonalcoholic fatty liver disease and acute ischemic stroke severity and outcome. *World J Hepatol* 2013; **5**: 621-626 [PMID: 24303090 DOI: 10.4254/wjh.v5.i11.621]

P- Reviewer: Abd-Elsalam S, Arslan N, Chen CJ **S- Editor**: Ji FF
L- Editor: A **E- Editor**: Tan WW

World Journal of Hepatology

Submit a Manuscript: http://www.f6publishing.com

World J Hepatol 2018 July 27; 10(7): 479-484

DOI: 10.4254/wjh.v10.i7.479

ISSN 1948-5182 (online)

MINIREVIEWS

Status and perspective of laparoscopic repeat liver resection

Zenichi Morise

Zenichi Morise, Department of Surgery, Fujita Health University School of Medicine, Toyoake 470-1192, Aichi, Japan

ORCID number: Zenichi Morise (0000-0001-6382-6502).

Author contributions: Morise Z collected the data and wrote this paper.

Conflict-of-interest statement: Morise Z declares no conflicts of interest related to this publication.

Manuscript source: Invited manuscript

Correspondence to: Zenichi Morise, MD, PhD, Professor, Department of Surgery, Fujita Health University School of Medicine, 1-98 Kutsukakecho Toyoake 470-1192, Aichi, Japan. zmorise@fujita-hu.ac.jp
Telephone: +81-562-939246
Fax: +81-562-935125

Received: March 26, 2018
Peer-review started: March 27, 2018
First decision: April 13, 2018
Revised: April 18, 2018
Accepted: May 30, 2018
Article in press: May 30, 2018
Published online: July 27, 2018

Abstract

Liver resection (LR) is now actively applied to intrahepatic recurrence of liver metastases and hepatocellular carcinoma. Although indications of laparoscopic LR (LLR) have been expanded, there are increased risks of intraoperative complications and conversion in repeat LLR. Controversy still exists for the indication. There are 16 reports of small series to date. These studies generally reported that repeat LLR has better short-term outcomes than open (reduced bleedings, less or similar morbidity and shorter hospital stay) without compromising the long-term outcomes. The fact that complete adhesiolysis can be avoided in repeat LLR is also reported. In the comparison of previous procedures, it is reported that the operation time for repeat LLR was shorter for the patients previously treated with LLR than open. Furthermore, it is speculated that LLR for minor repeat LR of cirrhotic liver can be minimized the deterioration of liver function by LR. However, further experience and evaluation of anatomical resection or resections exposing major vessels as repeat LLR, especially after previous anatomical resection, are needed. There should be a chance to prolong the overall survival of the patients by using LLR as a powerful local therapy which can be applied repeatedly with minimal deterioration of liver function.

Key words: Hepatocellular carcinoma; Laparoscopic liver resection; Repeat surgery; Metastasis

Core tip: There are 16 reports of repeat laparoscopic liver resection (LLR). They reported that it has better short-term outcomes than open (reduced bleedings, less or similar morbidity and shorter hospital stay). The fact that complete adhesiolysis can be avoided in repeat LLR is also reported. It is speculated that LLR for minor repeat LR of cirrhotic liver can be minimized the deterioration of liver function by LR. Repeated application of LLR as a powerful local therapy, which can be applied repeatedly with minimal deterioration of liver function, could improve the overall survival of the patients.

Morise Z. Status and perspective of laparoscopic repeat liver resection. *World J Hepatol* 2018; 10(7): 479-484 Available from: URL: http://www.wjgnet.com/1948-5182/full/v10/i7/479.htm DOI: http://dx.doi.org/10.4254/wjh.v10.i7.479

INTRODUCTION

The neoplastic liver background of hepatocellular carcinoma (HCC) with chronic liver disease (CLD) develops multifocal and metachronous liver tumors repeatedly. Also, metastases of various tumors can occur repeatedly in the liver. Repeat treatments for HCC and metastases, especially of colorectal cancer, are often needed.

Nowadays, liver resection (LR) is often performed to such lesions, if they are resectable without other uncontrollable/distant disease, and the reports for repeat LR has increased[1-4]. Furthermore, indications of laparoscopic LR (LLR) are expanding with the accumulation of experiences and technical/instrumental developments[5-8]. In LLR, surgeons should overcome restricted manipulation, lack of tactile sensation and three-dimensional (3D) vision (which is recently partially resolved by 3D-laparoscope), and disorientation from the lack of an overview of operative field, during liver mobilization, pedicle control and parenchymal transection, which is a trade-off to magnified fine local view[9,10]. Postoperative adhesions with the need for adhesiolysis are known to increase the operation time of subsequent surgeries and the incidence of bowel injury[11,12]. Therefore, increased rates of complications and conversion from laparoscopic to open surgery had been reported in repeat laparoscopic surgery[13]. A previous history of surgery had been among the contraindications for laparoscopic surgery. However, many laparoscopic procedures with previous surgical history, such as cholecystectomy[12,13], appendectomy[14], colectomy[15], and gastrectomy[16], can be performed nowadays with technical and instrumental improvements. On the other, LLR itself remains a demanding procedure and the indications of repeat LLR are under discussion. Adequate dissection of adhesion and mobilization of the involved liver should be performed before repeat LR. Adhesion can disrupt the dissection of hilar area and hepatoduodenal ligament, which is often crucial in LR. The deformity of the liver and surrounding scars and adhesion makes the localization of tumors and the important structures (vessels) difficult. The fact that liver capsule bleeds easily during adhesiolysis and mobilization leads to increase the intraoperative bleeding and create a suboptimal operative field[17]. These changes after previous surgery can increase the risks of intraoperative injury to vascular or biliary structures.

STUDIES OF REPEAT LLR

Only 16 reports of small series were found out under Medline-search with the words "repeat" and "laparoscopic liver resection" and their re-quotations[18-33] (Table 1), although they are gradually increasing. Belli *et al*[20] reported that LLR with its magnifies view facilitates more meticulous dissection of adhesions strained by the pneumoperitoneum. An additional possible advantage of repeat LLR is reported that complete adhesiolysis can be avoided when the adhesion does not affect the current operative procedure[24,29]. Generally, these studies reported that repeat LLR has better short-term outcomes (similar or longer operation time, reduced bleedings, less blood transfusion, less or similar morbidity and shortened hospital stay) with the comparable long-term outcomes. Each study concluded that repeat LLR is feasible and safe for selected patients, although those studies are the mixtures of the patients with HCC and metastases. The settings of the patients with HCC and metastases are different in LR. The patients with metastases sometimes undergo major LR with the handling of Glissonian pedicles on the soft liver with congestion and/or steatosis. Minor LR on the fibrous hard liver with poor functional reserve and surrounding collateral vessels is often performed for HCC patients. Five studies of repeat LLR, which only include HCC patients[20,24,26,27,31], reported the outcomes for the series of 12, 6, 3, 20 and 8 patients. The conclusions of all studies are that repeat LLR for recurrent HCC in CLD backgrounds is a safe and feasible procedure. It is mentioned that the adhesiolysis was easier and the operation time was shorter in repeat LLR for the patients with previous LLR compared to open LR[20]. Belli *et al*[20] referred the advantages of LLR for the management during the long history with repeat oncogenesis in cirrhotic patients. Kanazawa *et al*[27] mentioned that the complication rate and the hospital stay had been decreased in their institute by the introduction of LLR for recurrent HCC patients.

LLR CHARACTERISTICS

It is previously reported that LLR is especially beneficial for severe CLD patients[34]. LLR with minimal laparotomy and mobilization can minimize the destruction of blood and lymphatic collaterals, as well as the parenchymal injury by compression. It reduces postoperative ascites and liver failure for CLD patients[35]. In LR, resection of the liver inside the subphrenic rib cage is performed. The cage is opened with a big subcostal incision and then the liver is picked up with mobilization in open LR. On the other, laparoscope and forceps intrude into the cage directly from the caudal direction ("Caudal approach"[36-38], Figure 1) and perform LR in the small targeted area without damages to the surrounding area in LLR. LLR also facilitates the usage of postural change and the gravity for handling organs/tumors, since the same surgical view under position changes can be established by the adjustments of laparoscope's positioning and rotation. That reduces compression on the liver during surgery. Our previous

Table 1 Summary of previous reports of repeat laparoscopic liver resection

n	Disease	Previous LR (open:lap)	Procedure	Bleeding (mL)	Operating time (min)	Conversion (*n*)	Postoperative hospital stay (d)	Morbidity	Mortality	Ref.
12	HCC	4:8	LLS (*n* = 5), Pt (*n* = 4), Seg (*n* = 3)	297 ± 134 272.2 ± 120	114.4 ± 11.0 63.9 ± 13.3	1	7.4 ± 2.5 6.2 ± 3.0	26.60%	0%	[20]
2	Met	ND	ND	ND	ND	ND	ND	ND	ND	[21]
6	HCC	3:3 (Lap RFA, *n* = 2)	LLS (*n* = 2), Pt (*n* = 4)	283.3 ± 256.3	140.8 ± 35.7	0	5.67 ± 1.63	16.7%	0%	[24]
76	Met (*n* = 63), HCC (*n* = 3), others (*n* = 10)	28:44	LLS (*n* = 4), Pt, seg (*n* = 53), above-seg (*n* = 19)	300 (0–5000)	180 (80–570)	8	6 (2–42)	26%	0%	[23]
4	HCC (*n* = 3), Met (*n* =1)	0:4	LLS (*n* = 1), Pt (*n* = 3)	481.7 ± 449.5	312.3 ± 158.4	1	10.6 ± 7.4	23.4%	0%	[22]
3	HCC	0:3	ND	281.3 (mean)	264.6 (mean)	0	8.6 (mean)		0%	[26]
17	ND	ND	ND	ND	ND	ND	ND	ND	ND	[25]
20	HCC	15:5	Pt	78 (1–1500)	239 (69–658)	2 (HALS)	9 (5–22)	5%	0%	[27]
20	HCC (*n* = 2), Met (*n* = 16), others (*n* = 2)	0:20	Minor (*n* = 14), major (*n* = 6)	400 (IQR 150-200 mL)	285 (IQR 195-360)	3	4 (1-57)	10%	0%	[30]
12	HCC (*n* = 8), Met (*n* = 2), others (*n* = 2)	8:4	Pt (*n* = 9), Subseg (*n* = 3)	50 (NC–840)	301 (104–570)	0	12 (9–30)	0%	0%	[29]
11	HCC	6:5	LLS = 2 Subseg = 9	100 (50-500)	200 (131-352)	0	6 (3-17)	18.2%	0%	[33]
27	Met	ND	Major = 25 Minor = 2	ND (4 patients received transfusion)	252.5 (180-300)	1	9 (IQR 8-18)	48.1%	0%	[32]
8	HCC	6:2	Sec = 2 Seg = 2 Subseg = 4	200 (30-5000)	343 (120-530)	1	3.5 (3-8)	12.5%	0%	[31]
20	HCC (*n* = 15) Met (*n* = 5)	12:8	Anatomical = 1 Non-anatomical = 19	159 +/- 256	225 +/- 85	1	14.2 +/- 5.4	0%	0%	[19]
33	HCC and combined (*n* = 18) Met (*n* = 15)	21:12	Anatomical = 11 Non-anatomical = 22	30 (NC-1012)	217 (43-356)	0	6.5 (3-47)	6.1%	3%	[18]

Data are expressed as median (range) or mean ± SD, unless stated otherwise. In the paper from Belli, operation time, bleeding and postoperative hospital stay are described separately for patients whose previous hepatectomy was open (upper) or laparoscopic (lower). LLR: Laparoscopic liver resection; LR: Liver resection; HCC: Hepatocellular carcinoma; LLS: Left lateral sectorectomy; Met: Metastasis; Minor: Resection of 2 segments or less; Major: Resection of 3 segments or more; ND: Not documented; Pt: Partial resection; Sec: Sectionectomy; Seg: Segmentectomy; Subseg: Subsegmentectomy; IQR: Interquartile range; NC: Not countable.

report of the caudal approach posterior sectionectomy in the left lateral position[36] posed the novel concept of "caudal approach" in LLR. Although the supine to semi-lateral positioning had been employed for the other resections, the transection plane of posterior sectionectomy was horizontal and gravity obstructs the exposure of the plane in the supine position. A clear view from the caudal direction and an easy access to postural changes is among the advantages of LLR (Figure 1). We perform parenchymal transection prior to mobilization in the left lateral position for laparoscopic posterior sectionectomy. It facilitates exposure of the cutting plane during the transection in caudal-to-cranial one direction. The transection plane is well-opened between the retroperitoneal-fixed posterior section and the remnant liver falling down to left by gravity. Moreover, the resection of segment(s) 7 should be performed in the deeper and smaller cranial subphrenic space and S6 is an obstacle under the laparoscopic caudal view even in the left lateral position. Semi-prone position with only partial dissection of the retroperitoneum is employed for those resections[39]. Our key aim in LLR is to carry out minimal dissection around the liver with the intrusion and manipulation of laparoscope and forceps to the small target area under postural changes. In the same context, repeat LLR requires smaller (than open) working space between adhesions. Direct approach to the tumor after

Table 2 The summary of present status and future perspectives of repeat laparoscopic liver resection

Present status
There are 16 reports of small series. Controversy still exists in the indication of repeat LLR
These studies generally reported that it has better short-term outcomes without compromising the long-term outcomes (similar or longer operation time, reduces bleedings, reduced blood transfusion rate, less or similar morbidity and shorter hospital stay)
It facilitates more meticulous dissection of adhesions strained by the pneumoperitoneum using magnified laparoscopic view
Complete adhesiolysis can be avoided when the adhesion does not affect the current operative procedure
Operation time was shorter and the adhesiolysis was easier for the patients previously treated with LLR than open LR
It requires smaller (than open) working space between adhesions (this fact allows for minimal adhesiolysis, and operation time and bleeding amount were similar in primary and repeat LLR, although those from open LR are longer and increased)
Future perspectives
Further evaluations of anatomical resection or resections exposing major vessels after previous anatomical resection are needed
One of the possible advantages for minor repeat LR of CLD liver is that the deterioration of liver function can be minimized
It could prolong the overall survival of the HCC patients with CLD as a powerful local therapy which can be applied repeatedly with minimal deterioration of liver function

LLR: Laparoscopic liver resection; LR: Liver resection; HCC: Hepatocellular carcinoma; CLD: Chronic liver disease.

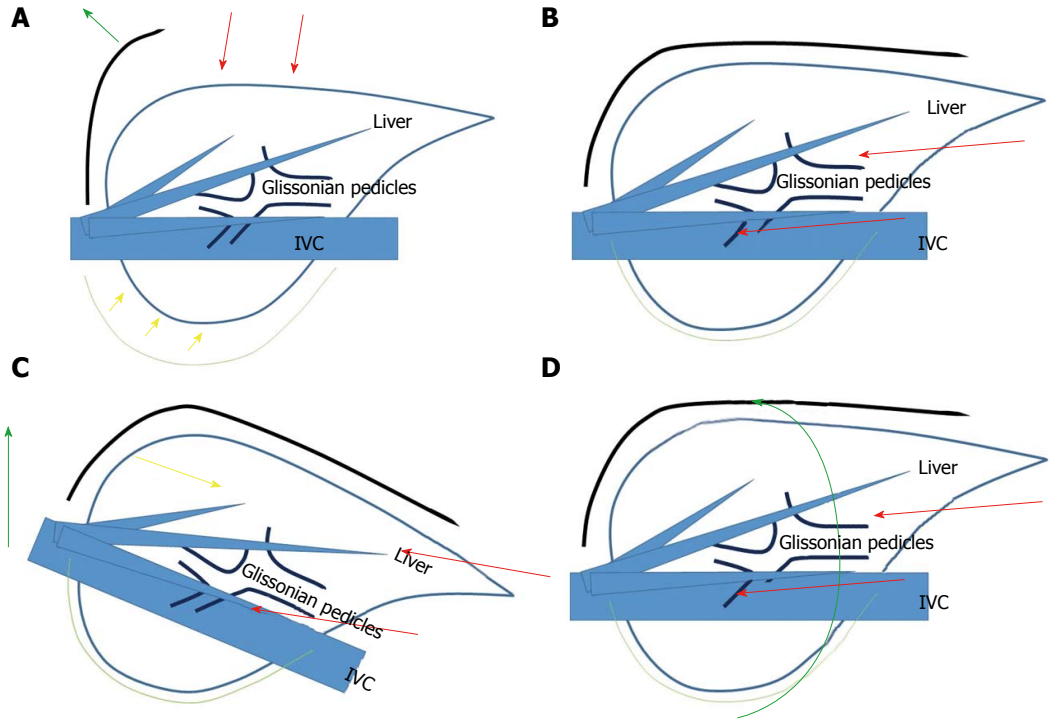

Figure 1 Schema of open liver resection (A), laparoscopic liver resection (B), position change in laparoscopic liver resection (tilting the bed for head-up position, C) and position change in laparoscopic liver resection (rotation from supine to semi-prone position, D). Red arrows indicate the directions of the view and manipulation in each approach. A: In the open approach, the subcostal cage containing the liver is opened with a large subcostal incision, and instruments are used to lift the costal arch up. The liver is dissected and mobilized (picked up) from the retroperitoneum; B: In the laparoscopic caudal approach, the laparoscope and forceps are placed into the subcostal cage from caudal direction, and surgery is performed with minimal alteration and destruction of the associated structures; C and D: In the laparoscopic approach, the same surgical view under position changes (tilting the bed and rotation of the patient's body), acquired by the adjustments of laparoscope's positioning and rotation, allows for handling large-volume liver/tumor by postural changes.

minimal adhesiolysis for the space where laparoscope and forceps can intrude and do manipulation can be allowed especially in repeat small LLR[23,24,29]. That is why some studies showed that operation time and bleeding amount were similar in primary and repeat LLR[18,29]. The operation time and blood loss are usually much longer and larger in open repeat than open primary LR. Operation time and bleeding amount of repeat partial resection could be reduced under laparoscopic approach.

OUR EXPERIENCES AND FUTURE PERSPECTIVES OF REPEAT LLR

Most reported cases of repeat LLR underwent minor resection of HCC with CLD, as mentioned above. The impact of alterations from the previous surgery on hepatic parenchyma and intrahepatic structure could be smaller in such cases. There were three repeat cases with anatomical resection or resections exposing major vessels (including S8 segmentectomy after

4-times LLR[40]) after previous anatomical resection who developed bile leakage and > 30 d hospital stay, among our 33 repeat and 12 three or more-time repeat LLR cases. Anatomical alterations surrounded by the scars and adhesions on major vessel structures could have big impacts on subsequent anatomical resection or resections exposing major vessels, experiences and evaluations of such setting of repeat LLR are required for the settlement (Table 2).

REFERENCES

1 **Petrowsky H**, Gonen M, Jarnagin W, Lorenz M, DeMatteo R, Heinrich S, Encke A, Blumgart L, Fong Y. Second liver resections are safe and effective treatment for recurrent hepatic metastases from colorectal cancer: a bi-institutional analysis. *Ann Surg* 2002; **235**: 863-871 [PMID: 12035044 DOI: 10.1097/00000658-200206000-00015]

2 **Wanebo HJ**, Chu QD, Avradopoulos KA, Vezeridis MP. Current perspectives on repeat hepatic resection for colorectal carcinoma: a review. *Surgery* 1996; **119**: 361-371 [PMID: 8643998 DOI: 10.1016/S0039-6060(96)80133-4]

3 **Morise Z**, Sugioka A, Fujita J, Hoshimoto S, Kato T, Hasumi A, Suda T, Negi H, Hattori Y, Sato H, Maeda K. Does repeated surgery improve the prognosis of colorectal liver metastases? *J Gastrointest Surg* 2006; **10**: 6-11 [PMID: 16368485 DOI: 10.1016/j.gassur.2005.09.006]

4 **Itamoto T**, Nakahara H, Amano H, Kohashi T, Ohdan H, Tashiro H, Asahara T. Repeat hepatectomy for recurrent hepatocellular carcinoma. *Surgery* 2007; **141**: 589-597 [PMID: 17462458 DOI: 10.1016/j.surg.2006.12.014]

5 **Nguyen KT**, Gamblin TC, Geller DA. World review of laparoscopic liver resection-2,804 patients. *Ann Surg* 2009; **250**: 831-841 [PMID: 19801936 DOI: 10.1097/SLA.0b013e3181b0c4df]

6 **Buell JF**, Thomas MT, Rudich S, Marvin M, Nagubandi R, Ravindra KV, Brock G, McMasters KM. Experience with more than 500 minimally invasive hepatic procedures. *Ann Surg* 2008; **248**: 475-486 [PMID: 18791368 DOI: 10.1097/SLA.0b013e318185e647]

7 **Wakabayashi G**, Cherqui D, Geller DA, Buell JF, Kaneko H, Han HS, Asbun H, O Rourke N, Tanabe M, Koffron AJ, Tsung A, Soubrane O, Machado MA, Gayet B, Troisi RI, Pessaux P, Van Dam RM, Scatton O, Abu Hilal M, Belli G, Kwon CH, Edwin B, Choi GH, Aldrighetti LA, Cai X, Cleary S, Chen KH, Schön MR, Sugioka A, Tang CN, Herman P, Pekolj J, Chen XP, Dagher I, Jarnagin W, Yamamoto M, Strong R, Jagannath P, Lo CM, Clavien PA, Kokudo N, Barkun J, Strasberg SM. Recommendations for laparoscopic liver resection: a report from the second international consensus conference held in Morioka. *Ann Surg* 2015; **261**: 619-629 [PMID: 25742461 DOI: 10.1097/SLA.0000000000001184]

8 **Morise Z**, Wakabayashi G. First quarter century of laparoscopic liver resection. *World J Gastroenterol* 2017; **23**: 3581-3588 [PMID: 28611511 DOI: 10.3748/wjg.v23.i20.3581]

9 **Buell JF**, Thomas MJ, Doty TC, Gersin KS, Merchen TD, Gupta M, Rudich SM, Woodle ES. An initial experience and evolution of laparoscopic hepatic resectional surgery. *Surgery* 2004; **136**: 804-811 [PMID: 15467665 DOI: 10.1016/j.surg.2004.07.002]

10 **Vibert E**, Perniceni T, Levard H, Denet C, Shahri NK, Gayet B. Laparoscopic liver resection. *Br J Surg* 2006; **93**: 67-72 [PMID: 16273531 DOI: 10.1002/bjs.5150]

11 **Beck DE**, Ferguson MA, Opelka FG, Fleshman JW, Gervaz P, Wexner SD. Effect of previous surgery on abdominal opening time. *Dis Colon Rectum* 2000; **43**: 1749-1753 [PMID: 11156462 DOI: 10.1007/BF02236862]

12 **Karayiannakis AJ**, Polychronidis A, Perente S, Botaitis S, Simopoulos C. Laparoscopic cholecystectomy in patients with previous upper or lower abdominal surgery. *Surg Endosc* 2004; **18**: 97-101 [PMID: 14569455 DOI: 10.1007/s00464-003-9001-4]

13 **Wiebke EA**, Pruitt AL, Howard TJ, Jacobson LE, Broadie TA, Goulet RJ Jr, Canal DF. Conversion of laparoscopic to open cholecystectomy. An analysis of risk factors. *Surg Endosc* 1996; **10**: 742-745 [PMID: 8662431 DOI: 10.1007/BF00193048]

14 **Wu JM**, Lin HF, Chen KH, Tseng LM, Tsai MS, Huang SH. Impact of previous abdominal surgery on laparoscopic appendectomy for acute appendicitis. *Surg Endosc* 2007; **21**: 570-573 [PMID: 17103279 DOI: 10.1007/s00464-006-9027-5]

15 **Law WL**, Lee YM, Chu KW. Previous abdominal operations do not affect the outcomes of laparoscopic colorectal surgery. *Surg Endosc* 2005; **19**: 326-330 [PMID: 15624064 DOI: 10.1007/s00464-004-8114-8]

16 **Nunobe S**, Hiki N, Fukunaga T, Tokunaga M, Ohyama S, Seto Y, Yamaguchi T. Previous laparotomy is not a contraindication to laparoscopy-assisted gastrectomy for early gastric cancer. *World J Surg* 2008; **32**: 1466-1472 [PMID: 18340481 DOI: 10.1007/s00268-008-9542-8]

17 **Szomstein S**, Lo Menzo E, Simpfendorfer C, Zundel N, Rosenthal RJ. Laparoscopic lysis of adhesions. *World J Surg* 2006; **30**: 535-540 [PMID: 16555020 DOI: 10.1007/s00268-005-7778-0]

18 **Ome Y**, Hashida K, Yokota M, Nagahisa Y, Yamaguchi K, Okabe M, Kawamoto K. The feasibility and efficacy of pure laparoscopic repeat hepatectomy. *Surg Endosc* 2018 [PMID: 29344784 DOI: 10.1007/s00464-018-6066-7]

19 **Noda T**, Eguchi H, Wada H, Iwagami Y, Yamada D, Asaoka T, Gotoh K, Kawamoto K, Takeda Y, Tanemura M, Umeshita K, Doki Y, Mori M. Short-term surgical outcomes of minimally invasive repeat hepatectomy for recurrent liver cancer. *Surg Endosc* 2018; **32**: 46-52 [PMID: 28639044 DOI: 10.1007/s00464-017-5632-8]

20 **Belli G**, Cioffi L, Fantini C, D'Agostino A, Russo G, Limongelli P, Belli A. Laparoscopic redo surgery for recurrent hepatocellular carcinoma in cirrhotic patients: feasibility, safety, and results. *Surg Endosc* 2009; **23**: 1807-1811 [PMID: 19277781 DOI: 10.1007/s00464-009-0344-3]

21 **Nguyen KT**, Laurent A, Dagher I, Geller DA, Steel J, Thomas MT, Marvin M, Ravindra KV, Mejia A, Lainas P, Franco D, Cherqui D, Buell JF, Gamblin TC. Minimally invasive liver resection for metastatic colorectal cancer: a multi-institutional, international report of safety, feasibility, and early outcomes. *Ann Surg* 2009; **250**: 842-848 [PMID: 19806058 DOI: 10.1097/SLA.0b013e3181bc789c]

22 **Ahn KS**, Han HS, Yoon YS, Cho JY, Kim JH. Laparoscopic liver resection in patients with a history of upper abdominal surgery. *World J Surg* 2011; **35**: 1333-1339 [PMID: 21452069 DOI: 10.1007/s00268-011-1073-z]

23 **Shafaee Z**, Kazaryan AM, Marvin MR, Cannon R, Buell JF, Edwin B, Gayet B. Is laparoscopic repeat hepatectomy feasible? A tri-institutional analysis. *J Am Coll Surg* 2011; **212**: 171-179 [PMID: 21276531 DOI: 10.1016/j.jamcollsurg.2010.10.012]

24 **Hu M**, Zhao G, Xu D, Liu R. Laparoscopic repeat resection of recurrent hepatocellular carcinoma. *World J Surg* 2011; **35**: 648-655 [PMID: 21184074 DOI: 10.1007/s00268-010-0919-0]

25 **Cannon RM**, Brock GN, Marvin MR, Buell JF. Laparoscopic liver resection: an examination of our first 300 patients. *J Am Coll Surg* 2011; **213**: 501-507 [PMID: 21624840 DOI: 10.1016/j.jamcollsurg.2011.04.032]

26 **Tsuchiya M**, Otsuka Y, Maeda T, Ishii J, Tamura A, Kaneko H. Efficacy of laparoscopic surgery for recurrent hepatocellular carcinoma. *Hepatogastroenterology* 2012; **59**: 1333-1337 [PMID: 22591625 DOI: 10.5754/hge12302]

27 **Kanazawa A**, Tsukamoto T, Shimizu S, Kodai S, Yamamoto S, Yamazoe S, Ohira G, Nakajima T. Laparoscopic liver resection for treating recurrent hepatocellular carcinoma. *J Hepatobiliary Pancreat Sci* 2013; **20**: 512-517 [PMID: 23404252 DOI: 10.1007/s00534-012-0592-9]

28 **Montalti R**, Berardi G, Laurent S, Sebastiani S, Ferdinande L, Libbrecht LJ, Smeets P, Brescia A, Rogiers X, de Hemptinne B, Geboes K, Troisi RI. Laparoscopic liver resection compared to open approach in patients with colorectal liver metastases improves further resectability: Oncological outcomes of a case-control matched-pairs analysis. *Eur J Surg Oncol* 2014; **40**: 536-544 [PMID: 24555996 DOI: 10.1016/j.ejso.2014.01.005]

29 **Isetani M**, Morise Z, Kawabe N, Tomishige H, Nagata H, Kawase

J, Arakawa S. Pure laparoscopic hepatectomy as repeat surgery and repeat hepatectomy. *World J Gastroenterol* 2015; **21**: 961-968 [PMID: 25624731 DOI: 10.3748/wjg.v21.i3.961]

30 **Shelat VG**, Serin K, Samim M, Besselink MG, Al Saati H, Gioia PD, Pearce NW, Abu Hilal M. Outcomes of repeat laparoscopic liver resection compared to the primary resection. *World J Surg* 2014; **38**: 3175-3180 [PMID: 25138071 DOI: 10.1007/s00268-014-2728-3]

31 **Goh BKP**, Teo JY, Chan CY, Lee SY, Cheow PC, Chung AYF. Laparoscopic repeat liver resection for recurrent hepatocellular carcinoma. *ANZ J Surg* 2017; **87**: E143-E146 [PMID: 27117542 DOI: 10.1111/ans.13628]

32 **Hallet J**, Sa Cunha A, Cherqui D, Gayet B, Goéré D, Bachellier P, Laurent A, Fuks D, Navarro F, Pessaux P; French Colorectal Liver Metastases Working Group, Association Française de Chirurgie. Laparoscopic Compared to Open Repeat Hepatectomy for Colorectal Liver Metastases: a Multi-institutional Propensity-Matched Analysis of Short- and Long-Term Outcomes. *World J Surg* 2017; **41**: 3189-3198 [PMID: 28717911 DOI: 10.1007/s00268-017-4119-z]

33 **Chan AC**, Poon RT, Chok KS, Cheung TT, Chan SC, Lo CM. Feasibility of laparoscopic re-resection for patients with recurrent hepatocellular carcinoma. *World J Surg* 2014; **38**: 1141-1146 [PMID: 24305932 DOI: 10.1007/s00268-013-2380-3]

34 **Morise Z**, Sugioka A, Kawabe N, Umemoto S, Nagata H, Ohshima H, Kawase J, Arakawa S, Yoshida R. Pure laparoscopic hepatectomy for hepatocellular carcinoma patients with severe liver cirrhosis. *Asian J Endosc Surg* 2011; **4**: 143-146 [PMID: 22776279 DOI: 10.1111/j.1758-5910.2011.00081.x]

35 **Morise Z**, Ciria R, Cherqui D, Chen KH, Belli G, Wakabayashi G. Can we expand the indications for laparoscopic liver resection? A systematic review and meta-analysis of laparoscopic liver resection for patients with hepatocellular carcinoma and chronic liver disease. *J Hepatobiliary Pancreat Sci* 2015; **22**: 342-352 [PMID: 25663288 DOI: 10.1002/jhbp.215]

36 **Tomishige H**, Morise Z, Kawabe N, Nagata H, Ohshima H, Kawase J, Arakawa S, Yoshida R, Isetani M. Caudal approach to pure laparoscopic posterior sectionectomy under the laparoscopy-specific view. *World J Gastrointest Surg* 2013; **5**: 173-177 [PMID: 23977419 DOI: 10.4240/wjgs.v5.i6.173]

37 **Soubrane O**, Schwarz L, Cauchy F, Perotto LO, Brustia R, Bernard D, Scatton O. A Conceptual Technique for Laparoscopic Right Hepatectomy Based on Facts and Oncologic Principles: The Caudal Approach. *Ann Surg* 2015; **261**: 1226-1231 [PMID: 24854453 DOI: 10.1097/SLA.0000000000000737]

38 **Wakabayashi G**, Cherqui D, Geller DA, Han HS, Kaneko H, Buell JF. Laparoscopic hepatectomy is theoretically better than open hepatectomy: preparing for the 2nd International Consensus Conference on Laparoscopic Liver Resection. *J Hepatobiliary Pancreat Sci* 2014; **21**: 723-731 [PMID: 25130985 DOI: 10.1002/jhbp.139]

39 **Morise Z**. Laparoscopic liver resection for posterosuperior tumors using caudal approach and postural changes: A new technical approach. *World J Gastroenterol* 2016; **22**: 10267-10274 [PMID: 28058008 DOI: 10.3748/wjg.v22.i47.10267]

40 **Morise Z**, Isetani M, Kawabe N, Tomishige H, Nagata H, Arakawa S, Ikeda M, Kamio K. Case report of the fourth laparoscopic liver resection and review of repeat laparoscopic resection for recurrent hepatocellular carcinoma in cirrhotic liver. *Hepatoma Res* 2016; **2**: 253-258 [DOI: 10.20517/2394-5079.2016.09]

P- Reviewer: Aurello P, Bian AZL, Donadon M **S- Editor**: Ji FF
L- Editor: A **E- Editor**: Tan WW

World Journal of Hepatology

Submit a Manuscript: http://www.f6publishing.com

World J Hepatol 2018 July 27; 10(7): 485-495

DOI: 10.4254/wjh.v10.i7.485

ISSN 1948-5182 (online)

MINIREVIEWS

Balloon-occluded transcatheter arterial chemoembolization for hepatocellular carcinoma

Takeshi Hatanaka, Hirotaka Arai, Satoru Kakizaki

Takeshi Hatanaka, Department of Gastroenterology, Saiseikai Maebashi Hospital, Gunma 371-0821, Japan

Hirotaka Arai, Department of Gastroenterology, Maebashi Red Cross Hospital, Gunma 371-0014, Japan

Satoru Kakizaki, Department of Gastroenterology and Hepatology, Gunma University Graduate School of Medicine, Gunma 371-8511, Japan

ORCID number: Takeshi Hatanaka (0000-0003-3656-285X); Hirotaka Arai (0000-0003-1119-8588); Satoru Kakizaki (0000-0002-1508-584X).

Author contributions: All authors have contributed to the study concept, data analyzing, manuscript writing, editing and approval of the final manuscript for publication.

Conflict-of-interest statement: No potential conflicts of interest. No financial support.

Manuscript source: Invited manuscript

Correspondence to: Satoru Kakizaki, MD, PhD, Associate Professor, Department of Gastroenterology and Hepatology, Gunma University Graduate School of Medicine, Showa-machi, 3-39-15, Maebashi, Gunma 371-8511, Japan. kakizaki@gunma-u.ac.jp
Telephone: +81-27-2208127
Fax: +81-27-2208136

Received: March 27, 2018
Peer-review started: March 27, 2018
First decision: April 11, 2018
Revised: June 24, 2018
Accepted: June 28, 2018
Article in press: June 28, 2018
Published online: July 27, 2018

Abstract

Transcatheter arterial chemoembolization (TACE) is widely accepted as a treatment for patients with hepatocellular carcinoma (HCC) in the intermediate stage according to the Barcelona Clinic Liver Cancer (BCLC) guidelines. Recently, balloon-occluded TACE (B-TACE) was developed in Japan. Despite the lack of a clear definition, B-TACE is generally defined as the infusion of emulsion of chemotherapeutic agents with lipiodol followed by gelatin particles under the occlusion of feeding arteries by a microballoon catheter, which leads to the dense lipiodol emulsion (LE) accumulation in HCC nodules. This phenomenon cannot be explained only by the prevention of proximal migration and leakage of embolization materials; it further involves causing local changes in the hemodynamics of the surrounding occlusion artery and targeted HCC nodules. Balloon-occluded arterial stump pressure plays an important role in the dense LE accumulation in targeted HCC nodules. Although randomized controlled trials comparing the therapeutic effect and the prognosis of B-TACE to those of the other TACE procedures, such as conventional-TACE and drug-eluting beads TACE, are still lacking, B-TACE is thought to be a promising treatment. The purpose of this review is to summarize the mechanism, therapeutic effect, indication, prognosis and complications of B-TACE.

Key words: Hepatocellular carcinoma; Treatment effect; Transcatheter arterial chemoembolization; Prognosis; Balloon-occluded arterial stump pressure; Dense lipiodol emulsion accumulation; Balloon-occluded transcatheter arterial chemoembolization; Microballoon catheter

Core tip: Balloon-occluded transcatheter arterial chemoembolization (B-TACE) was recently developed in Japan. Despite the lack of a clear definition, B-TACE is generally defined as the infusion of emulsion of chemotherapeutic agents with lipiodol followed by gelatin particles under the occlusion of feeding arteries by a microballoon catheter. Although randomized controlled trials comparing the therapeutic effect and the prognosis of B-TACE to those of the other TACE procedures are still lacking, B-TACE is thought to be a promising treatment. The purpose of this review is to summarize the mechanism, therapeutic effect, indication, prognosis and complications of B-TACE.

Hatanaka T, Arai H, Kakizaki S. Balloon-occluded transcatheter arterial chemoembolization for hepatocellular carcinoma. *World J Hepatol* 2018; 10(7): 485-495 Available from: URL: http://www.wjgnet.com/1948-5182/full/v10/i7/485.htm DOI: http://dx.doi.org/10.4254/wjh.v10.i7.485

INTRODUCTION

Liver cancer ranks sixth as the common malignant neoplasm and second as the cause of death worldwide[1], and hepatocellular carcinoma (HCC) is the most common type of malignant liver tumors[2]. According to the Barcelona Clinic Liver Cancer (BCLC) guidelines, transcatheter arterial chemoembolization (TACE) is an established treatment for patients with HCC in the intermediate stage[3]. The median survival of untreated patients at the intermediate stage, who present with multinodular without vascular invasion or extrahepatic metastasis, performance status 0 and Child-Pugh class A or B, is reported to be 16 mo[4,5], and TACE prolongs their overall survival compared to that of a control group[6,7].

TACE is performed through the injection of single or multiple chemotherapeutic agents after the catheterization of tumor-feeding arteries, followed by the embolization of the same vessels in order to gain a synergistic effect of cytotoxicity and ischemia[3,8]. Conventional-TACE (C-TACE) is defined as the injection of a mixture of anticancer agents with lipiodol followed by embolic materials, such as gelatin particles, calibrated microspheres or polyvinyl alcohol, and drug-eluting beads TACE (DEB-TACE) is defined as the infusion of microspheres onto which chemotherapeutic agents is loaded or adsorbed to achieve a sustained *in vivo* drug release[8,9].

Recently, balloon-occluded TACE (B-TACE), which was first reported by Irie *et al*[10], has been developed in Japan. Although it is not mentioned in several guidelines[3,11,12] and its clear definition has not been established, it is generally defined as the infusion of emulsion of chemotherapeutic agents with lipiodol followed by gelatin particles under the occlusion of feeding arteries by a microballoon catheter. The occlusion of the feeding arteries result in the dense lipiodol emulsion (LE) accumulation in targeted nodules[10]. The therapeutic effect of B-TACE was better than that of C-TACE according to several previous reports[13-15], although those were retrospective and small in scale. In addition, randomized controlled trials (RCTs) comparing the therapeutic effect and the prognosis of B-TACE to those of other TACE procedures are still lacking.

Table 1 depicts the key findings of the therapeutic effect and overall survival of B-TACE. With this potential limitation in mind, in the present review, we describe the current understanding of the mechanism, therapeutic effect, indication, overall survival and complications of B-TACE.

BALLOON-OCCLUDED TACE PROCEDURE

Microballoon catheters

A 3-Fr microballoon catheter was used in the study reported by Irie *et al*[10]. However, it is sometimes difficult to advance a microballoon catheter into the targeted tumor-feeding arteries selectively[16]. Moreover, a 5- or 6-Fr guiding catheter was required when we used a 3-Fr microballoon catheter for B-TACE, which is more invasive than C-TACE[16]. Microballoon catheters have improved in recent years, and a 1.8-Fr microballoon catheter (Logos, Piolax, Kanagawa, Japan; or Attendant, Terumo Clinical Supply, Tokyo, Japan) is now available, enabling us to insert the catheter more selectively and more peripherally[16]. We are able to coaxially advanced these microballoon catheters through a typical 4-Fr parent catheter[16]. The proximal side consists of two ports in these microballoon catheters: the microballoon lumen and the microguidewire lumen, the diameter of which is 0.017-0.018 inches[16].

B-TACE procedure

Although a clear definition of B-TACE has not been established and several details concerning the procedure vary markedly among institutions, we will attempt to briefly describe the main points of B-TACE.

The right femoral artery is punctured under local anesthesia. A 4- or 5-Fr parent catheter is then placed in the celiac artery (CeA) or superior mesenteric artery (SMA), and angiography is carried out to assess the anatomy of the hepatic artery, tumor stains, the feeding arteries and arteriovenous shunting. In some institutions, cone-beam computed tomography (CBCT) and angiography-assisted computed tomography (CT) is performed to diagnose the HCC and evaluate the tumor-feeding arteries. A microballoon catheter is inserted into the tumor-feeding arteries over the guidewire as selectively as possible. When the selective insertion of the microballoon catheter into the targeted arteries is difficult, such as in patients with tortuous anatomies

Table 1 Summary of retrospective studies of therapeutic effect and overall survival of balloon-occluded transcatheter arterial chemoembolization for hepatocellular carcinoma

Ref.	Year	No. of patients	Antitumor agent and embolic materials	Therapeutic effect	Overall survival	Commentary
Hatanaka *et al*[43]	2018	66	Miriplatin-lipiodol suspension + gelatin particle	CR 53.0%, PR 10.6%, SD 19.7%, PD 16.7%, RR 63.6%	The 1-, 2-, and 3-yr survival rates were 76.8%, 57.3%, and 46.7%, respectively	The number of tumors and α-fetoprotein level were predictive factors for the tumor response and serum albumin and overall response (CR + PR) were predictive factors for prognosis
Kawamura *et al*[40]	2017	30	Miriplatin-lipiodol suspension + gelatin particle	TE4 51.0%, TE3 8.5%, TE2 19.1%, TE1 21.3%, RR 59.6%	NA	The presence of portal vein visualization, tumor on the subcapsular portion, and successful subsegmental artery embolization were predictive factors for the tumor response
Maruyama *et al*[20]	2016	50	Epirubicin-lipiodol suspension + gelatin particle	There was no statistically significant difference between the B-TACE group and the C-TACE group	NA	
Irie *et al*[15]	2016	28	Doxorubicin, mytomysin-lipiodol suspension + gelatin particle	TE4 89.3%, TE3 10.7%, TE2 0%, TE1 0%, RR 100%. The local recurrence rates at 1, 3, and 5 yr were 92.4%, 69.9%, and 69.9%, respectively	The 1-, 3-, and 5-yr survival rates were 96.4%, 60.3% and 31.1%, respectively	B-TACE was an independent factor for improving both the control rate of the primary nodule and the overall survival rates
Asayama *et al*[32]	2016	29	Miriplatin-lipiodol suspension + gelatin particle	TE4 8.6%, TE3 48.6%, TE2 17.1%, TE1 25.7%, RR 57.1%	NA	
Ogawa *et al*[14]	2015	33	Miriplatin-lipiodol suspension + gelatin particle	TE4 49.2%	NA	The percentage of TE4 in B-TACE was significantly higher than that in the C-TACE
Minami *et al*[41]	2015	27	Miriplatin-lipiodol suspension + gelatin particle (epirubicin was used in 3 patients)	Countable HCC (n = 17): TE4 43.8%, TE3 12.5%, TE2 37.5%, TE1 6.3%, RR 56.3%, Uncountable HCC (n = 10): CR 0%, PR 0%, SD 10%, PD 90%	NA	
Arai *et al*[13]	2014	49	Miriplatin-lipiodol suspension + gelatin particle	TE4 55.1%, TE3 38.8%, TE2 4.1%, TE1 2.0%, RR 93.9%	NA	
Ishikawa *et al*[44]	2014	51	Miriplatin-lipiodol suspension + gelatin particle	The local recurrence rates at 6, 12 mo were 11.1 %, 26.2%, respectively. The medan recurrence time was 9 mo	NA	The CT value just after B-TACE was a predictive factor for the tumor response

According to Response Evaluation Criteria in Cancer of the Liver (RECICL), the treatment effect (TE) was defined as follows: TE4, tumor necrosis of 100% or 100% reduction; TE3, tumor necrosis of 50%-100% or 50%-100% reduction in tumor size; TE1, tumor enlargement of > 50% regardless of necrosis; TE2, effect other than TE3 or TE1. B-TACE: Balloon-occluded transcatheter arterial chemoembolization; CR: Complete response; PR: Partial response; SD: Stable disease; PD: Progressive disease; RR: Response rate; NA: Not available; C-TACE: Conventional transcatheter arterial chemoembolization; CT: Computed tomography.

of the CeA or SMA, using a microballoon catheter as an anchor might be useful for achieving deep cannulation with the parent catheter[17]. The tumor-feeding artery is then occluded, and the emulsion of lipiodol and anticancer drugs is infused under radiographic guidance. The proportion of lipiodol to anticancer drugs was as follow: 70 mg of Miriplatin[18,19], which is most commonly used in B-TACE, was suspended with 3.5 mL of lipiodol (20 mg/mL); 10 mg of epirubicin[20] with 1-2 mL of lipiodol (5-10 mg/mL); 10 mg of doxorubicin hydrochloride and 2 mg of mitomycin C with 5-10 ml of lipiodol (5-10 mg/mL and 1-2 mg/mL, respectively)[10,15]. Digital angiography is sometimes useful for checking for the flow of LE droplets outside the target areas. LE is infused until sufficient filling of the targeted nodule, overflow into the intrahepatic collateral arteries or the presence of portal vein visualization is observed. The fragmented gelatin sponge slurry is then injected into

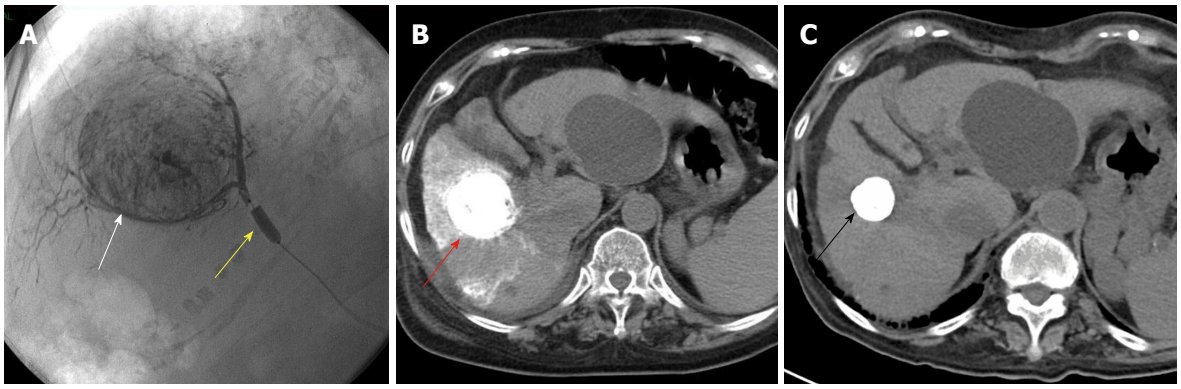

Figure 1 A 71-year-old female patient with hepatitis-C related hepatocellular carcinoma 45 mm in diameter underwent balloon-occluded transcatheter arterial chemoembolization. A: A 3-Fr microballoon catheter was inserted into a tumor-feeding artery. After achieving occlusion with the microballoon catheter (yellow arrowhead), emulsion of lipiodol and miriplatin was infused until the cancer nodule (white arrowhead) was sufficiently filled. Fragmented gelatin sponge slurry was then injected; B: Just after B-TACE, computed tomography (CT) showed a dense lipiodol emulsion (LE) accumulation in HCC nodules (red arrowhead); C: Four years after B-TACE, CT showed that the volume of the LE accumulation was reduced (black arrowhead) with no local recurrence. HCC: Hepatocellular carcinoma; B-TACE: Balloon-occluded transcatheter arterial chemoembolization.

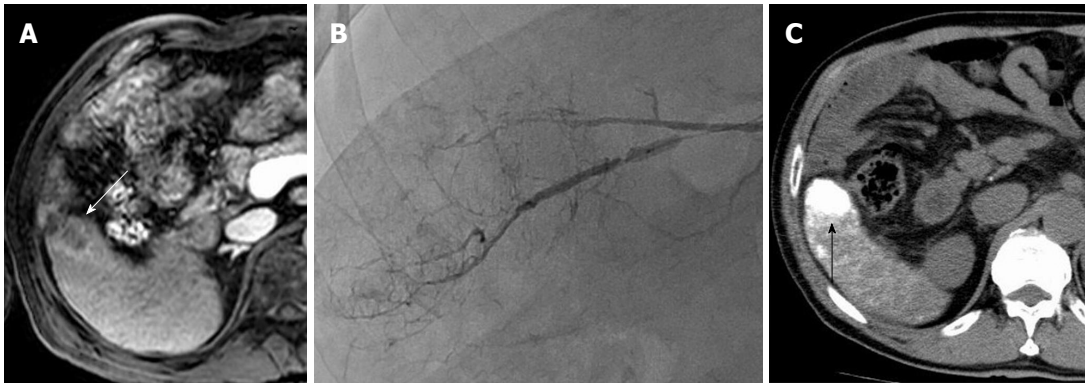

Figure 2 A 75-year-old man with hepatitis-B related hepatocellular carcinoma. A: Gadolinium-ethoxybenzyl-diethylenetriamine pentaacetic acid-enhanced magnetic resonance imaging (EOB-MRI) showed that HCC was slightly enhanced in the arterial phase (white arrowhead); B: While angiography did not show the tumor stain obviously, we injected the lipiodol emulsion (LE) and fragmented gelatin sponge slurry from tumor-feeding artery under occlusion with microballoon inflation; C: A favorable LE accumulation (black arrowhead) was seen on computed tomography one day after balloon-occluded transcatheter arterial chemoembolization. HCC: Hepatocellular carcinoma.

the blood vessels until the distal vessel is embolized. We describe a typical B-TACE procedure in Figures 1-3.

MECHANISM OF B-TACE

Irie *et al*[10] reported that they found dense lipiodol emulsion (LE) accumulation in HCC nodules when they used a 3-Fr microballoon catheter in selective TACE with occlusion of feeding arteries. Denser LE accumulation in targeted HCC nodules means more accumulation of anticancer drugs, leading to more therapeutic effect[21,22]. Therefore, revealing this mechanism is important for hepatologists and interventional radiologists in daily clinical practice.

Relationship between the balloon-occluded arterial stump pressure and the dense LE accumulation

The dense LE accumulation caused by the occlusion of feeding arteries cannot be explained only by the prevention of proximal migration and leakage of embolization materials; it also involves causing local changes in the hemodynamics of the surrounding occlusion artery and targeted tumors. Irie *et al*[10] reported that the pulsatile movement of LE droplets was observed after the inflation of the tip of a balloon catheter, with the peripheral arterial blood flow unable to be stopped. Because stasis of an LE droplet was observed even at the tip of the microballoon catheter, the authors speculated that the distal arterial blood flow did not come from leakage though the space between the balloon and the occluded artery. The intrahepatic collateral arteries, such as the peribiliary plexus[23], interlobar communicating arcade[24] and isolated artery[25], were considered to help maintain the distal arterial blood flow, based on the observation of anastomotic vessels with collateral arteries on digital subtraction angiography (DSA) under occlusion[10]. Consequently, the BOASP is reduced compared to the mean arterial pressure without balloon occlusion and more decreased BOASP allows the injection of LE under higher pressure. He

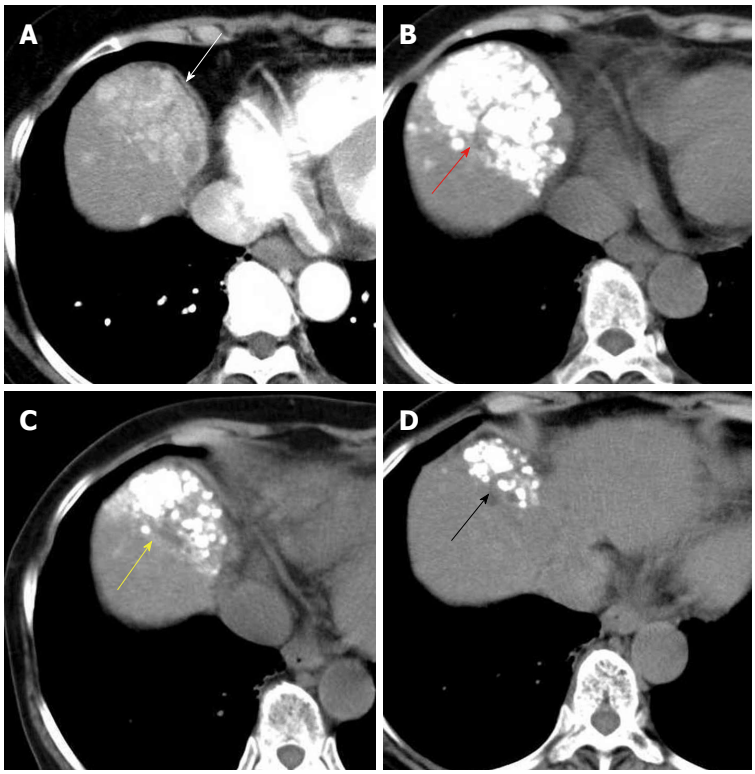

Figure 3 A 74-year-old woman with hepatitis-C related multiple hepatocellular carcinoma. A: Contrast-enhanced computed tomography (CT) showed that multiple HCC nodules were observed, aggregated at segment 8 (white arrowhead); B: Computed tomography showed that the dense lipiodol emulsion (LE) accumulations (red arrowhead) were observed just after balloon-occluded transcatheter arterial chemoembolization (B-TACE) for multiple HCC; C: We carried out additional B-TACE because local recurrence was detected on follow-up CT. Favorable LE accumulations were observed just after additional B-TACE (yellow arrowhead); D: Three month after additional B-TACE, local recurrence was not observed, and the LE accumulations were shrinking (black arrowhead). HCC: Hepatocellular carcinoma.

also demonstrated that BOASP is responsible for the dense LE accumulation and the BOASP ⩾ 64 mmHg is predictive for the presence of thick collateral arteries and less dense LE accumulation[10].

Matsumoto *et al*[26] reported that they used a 1.8-Fr microballoon catheter and measured the BOASP at each lobar, segmental and subsegmental arteries before B-TACE treatment. He showed that the BOASP ⩾ 64 mmHg was founded at A1, A4, A8, anterior segment artery, right hepatic artery (RHA) and left hepatic artery (LHA) whereas the BOASP ⩾ 64 mmHg was never seen at the other segmental and subsegmental arteries and the BOASP was independent of the size and number of tumors[26]. He presumed that this result was affected by the presence of intrahepatic collateral arteries, especially the communicating arcade in the hilum which is a relatively thick anastomosis between the right and left hepatic arteries and originates mainly from A4 and from anterior segment artery or the right hepatic artery[24,26]. BOASP ⩾ 64 mmHg at A1 artery could be explained by the studies reported by Miyayama *et al*[27,28] in which the right branch of the communicating artery in the hilum might have been A1[26]. So, B-TACE treatment in A1, A4, A8, anterior segment artery, RHA and LHA possibly caused less dense LE accumulation in targeted HCC nodules[26]. However, this study is small sample size in measured hepatic arteries and lack of the statistical analysis. A large number of validation studies are needed.

Kakuta *et al*[29] examined the changes in the stump pressure with and without balloon occlusion as well as after B-TACE treatment. The mean blood pressure at the targeted occluded artery was 97 mmHg before balloon occlusion and decreased to 49.1 mmHg immediately after balloon occlusion, with a statistically significance[29]. Five minutes after balloon occlusion, the mean blood pressure was 50.4 mmHg, and the maintenance of a decreased blood pressure was observed[29]. After the injection of LE and gelatin sponge particles, the mean blood pressure increased to 70.6 mmHg, which was significantly higher than that immediately after balloon occlusion ($P < 0.001$)[29]. The mean arterial blood pressure without balloon occlusion after B-TACE was not significantly different from that without balloon occlusion before B-TACE ($P = 0.9107$)[29]. Although no significant differences were observed among the stump pressures at the first-, second- and third-order branches, the proportion of stump pressure < 64 mmHg at third-order branches tended to be higher than that at first- or second-order branches[29]. Advancing a microballoon catheter to a more peripheral artery appeared to cause the stump pressure to decrease more[29]. A further investigation is needed to determine whether or not the occlusion of a more distal artery results in a more de-

creased BOASP.

Although these previous studies[10,26,29] have provided only preliminary and limited data, the findings indicate that the BOASP plays an important role in the dense LE accumulation in targeted HCC nodules. Further studies regarding whether or not the BOSAP can predict the long-term therapeutic effect should be conducted.

Hemodynamic changes assessed by CBCT and angio-assisted CT

Three reports[30-32] have explored the hemodynamic changes assessed by balloon occlusion using CBCT and angiography-assisted CT. Ishikawa *et al*[30] reported that the CBCT pixel values of tumor enhancement increased after balloon occlusion in 37 of the 52 nodules, whereas it decreased in the remaining 15 nodules. Yoshimatsu *et al*[31] showed that the degree of tumor enhancement on selective CT during hepatic angiography (CTHA) increased after balloon occlusion in 3 of the 27 nodules, while it decreased in 11 nodules. Asayama *et al*[32] also reported that 15 of the 35 nodules showed decreased enhancement or perfusion defects on CTHA with balloon occlusion. While the percentage of decreased tumor enhancement varied markedly among those studies, it remained a negative predictive factor for a dense LE accumulation[30,31] and short-term therapeutic effect[32]. It can be presumed that the blood flow from the occluded artery reduced and the blood flow from the collateral arteries relatively increased[31,32]. In relation to this, a discrepancy was noted between the tumor enhancement on selective CTHA with balloon occlusion and a dense LE accumulation after B-TACE, which was higher than the tumor enhancement grade[31]. Although CBCT[33-35] and CTHA[36,37] are well known to be useful tools for identifying the tumor-feeding arteries, evaluating the embolized area and avoiding nontargeted embolization, the same findings were reported in selective C-TACE[38]. A validation study will be needed to confirm whether or not a decreased tumor enhancement after balloon occlusion can predict the short- and long-term therapeutic effects.

With regard to the analysis of CT findings during arterial portography (CTAP), the reduction in size of the tumorous portal perfusion defects on CTAP with balloon occlusion was observed in 90% (18/20) of nodules. Its mean size significantly decreased from 21.9 to 19.1 mm in diameter (P = 0.0001). No decrease in the tumorous portal perfusion defect area significantly influenced the poor dense LE accumulation in the tumor[31]. The authors speculated that the decrease in the BOASP enabled the pressure gradient from the hepatic artery to the portal vein to also decrease, thus resulting in a relative increase in the blood flow from the portal vein in the surrounding tumor[31]. In other words, no change in the size of the tumorous portal perfusion defect may indicate no decrease in the BOASP[31]. To facilitate our understanding of the mechanism of B-TACE, we summarize the main findings mentioned above and present them in a schematic illustration in Figure 4.

THERAPEUTIC EFFECT OF B-TACE

Short-term therapeutic effect and local recurrence rate

In many previous studies, the short-term therapeutic effect of B-TACE was evaluated mainly by the Response Evaluation Criteria in Cancer of the Liver (RECICL) proposed by the Liver Cancer Study Group of Japan[39]. The treatment effect (TE) was determined by the radiological findings 1-3 mo after B-TACE treatment and defined as follows: TE4, tumor necrosis of 100% or 100% reduction; TE3, tumor necrosis of 50%-100% or 50%-100% reduction in tumor size; TE1, tumor enlargement of > 50% regardless of necrosis; TE2, effect other than TE3 or TE1[39]. According to previous reports[13,15,32,40,41], the rate of TE4 of targeted HCC nodules treated with B-TACE was 8.6%-89.3%, and that of TE3 was 8.5%-48.6%, with a response rate of 56.3%-100%.

Kawamura *et al*[40] showed that the presence of portal vein visualization during treatment was associated with an objective response, which is consistent with findings of the study reported by Miyayama *et al*[42]. However, the evaluation of the therapeutic effect of B-TACE in these studies[13,15,32,40,41] was limited to only targeted lesions and did not include the appearance of new lesions. According to a study[43] evaluated based on the overall response, including target lesions, non-target lesions and the appearance of new lesion, 35 patients (53.0%) experienced complete response (CR), 7 patients (10.6%) partial response (PR), 13 patients (19.7%) stable disease, and 11 patients (16.7%) progressive disease. The rate of a response rate and a disease control rate were 63.6% and 83.3%, respectively. Furthermore, a multivariate analysis showed that a solitary tumor and serum α-fetoprotein level were significantly relevant to the tumor response[43].

Regarding the analysis of the local recurrence rate, Ishikawa *et al*[44] showed that the median recurrence time and the local recurrence rate at 6 mo and 12 mo were 9 mo and 11.1% and 26.2%. The authors further revealed that only the CT value just after B-TACE was significantly relevant to local recurrence in a multivariate analysis[44]. CBCT was also deemed useful as a substitute for conventional CT to evaluate the degree of dense LE accumulation quantitatively in targeted HCC nodules[45]. Irie *et al*[15] also showed that the control rates of primary nodule treated by B-TACE at 1, 3 and 5 years were 92.4%, 69.9% and 69.9%, respectively. However, these were retrospective studies, and the number of nodules per patient was small (many patients had solitary nodules). The results should therefore be interpreted with caution when extrapolating to HCC patients with more nodules. A summary of the previous studies is shown in Table 1. A prospective validation study is warranted.

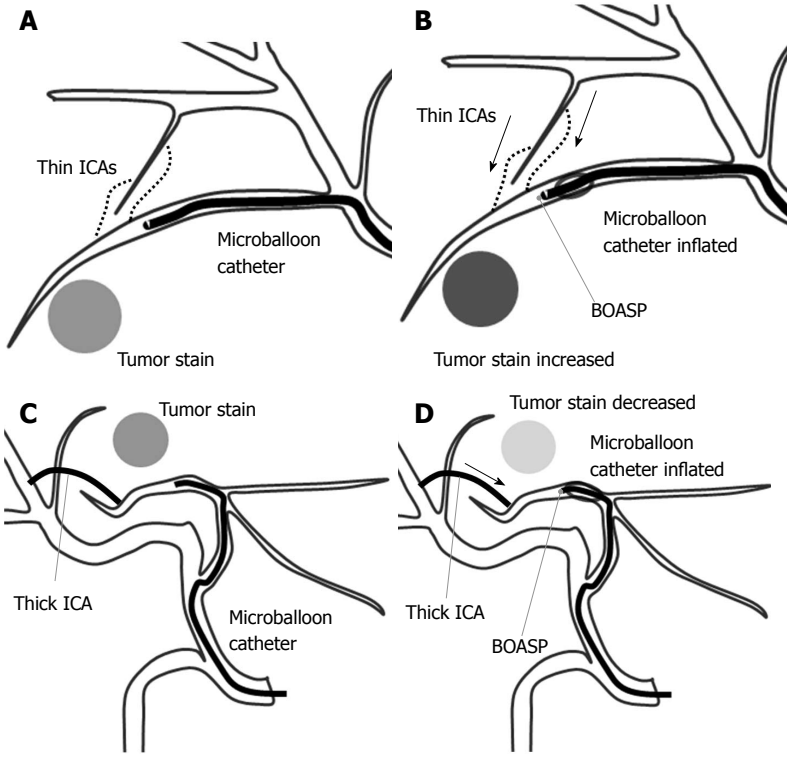

Figure 4 A schematic illustration of the balloon-occluded transcatheter arterial chemoembolization procedure. A: A microballoon catheter is inserted into the tumor-feeding artery and inflated to occlude it. If the distal arterial blood flow cannot be stopped, the intrahepatic collateral arteries (ICAs) may be maintaining the distal arterial blood flow; B: When the ICAs are thin, the balloon-occluded arterial stump pressure (BOASP) is remarkably reduced compared to the arterial pressure without balloon occlusion. In this situation, we might observe increased tumor enhancement on selective computed tomography during hepatic angiography (CTHA) after balloon occlusion. A remarkable reduction in the BOASP is thought to allow us to inject the lipiodol emulsion (LE) under higher pressure, leading to the denser LE accumulation in targeted tumors. The BOASP after the injection of LE and gelatin particles is significantly higher than that before treatment; C and D: When the ICAs are thick, the BOASP is expected to be mildly reduced or unchanged because of the adequate blood flow from a thick ICA. In this situation, we might observe decreased tumor enhancement on CTHA after balloon occlusion. We would probably inject the LE under lower pressure in such a situation, thereby achieving a less-dense LE accumulation.

Suitable anticancer agents

The anticancer agents that have been used in B-TACE are as follows: Miriplatin[13,14,31,32,40,41,44], which was the most commonly used; cisplatin[29,31]; epirubicin[20] and a mixture of doxorubicin hydrochloride and mitomycin[10,15]. Miriplatin, which is a lipophilic platinum complex[18,19], has been used in C-TACE[46]. A retrospective study[47] showed that the local recurrence rate was significantly higher after superselective TACE with miriplatin than with epirubucin and mitomycin. This may be attributed to its high viscosity, and warmed miriplatin may reduce its viscosity, possibly overcoming its disadvantages and increasing its therapeutic effect[48,49]. Therefore, B-TACE with warmed miriplatin may exert a better therapeutic effect than that with miriplatin at room temperature. In this connection, arterial vascular damage is less severe in patients treated with miriplatin than in those treated with epirubicin[50]. Although no RCT has compared antitumor agents, miriplatin might be suitable as an anticancer agent in B-TACE. Further studies should be conducted.

Comparing the effectiveness of B-TACE and C-TACE

Reliable data on the comparative efficacy between B-TACE and C-TACE are still lacking, with only four retrospective studies reported. Arai *et al*[13] reported that the targeted therapeutic effect of B-TACE with miriplatin was better than that of C-TACE, and the mean total dose of miriplatin in B-TACE was higher than that of C-TACE. They presumed that inflating the microballoon catheter decreased the arterial pressure proximal of the tip of the catheter and blocked the backflow of miriplatin, resulting in a higher total dose of miriplatin and a better therapeutic effect on targeted nodules than with C-TACE. Ogawa *et al*[14] also reported that TE4 was observed in 29 patients (49.2%) treated with B-TACE and in 10 patients (27%) treated with C-TACE, indicating that local efficacy of B-TACE was significantly better than that of C-TACE. Irie *et al*[15] reported that the short-term treatment effect based on RECICL criteria was significantly better in B-TACE group than that in the C-TACE group, and the tumor control rates of the targeted nodule were significantly improved in the B-TACE group compared to C-TACE group. However, Maruyama *et al*[20] reported that the local control rate in B-TACE group were not significantly better than in the C-TACE group. The major cause of this was the lack of a significant difference between the two groups

in the analysis of the LE ratio. The LE ratio, which was calculated as the ratio of the LE concentration in the targeted tumor to that in the surrounding embolized non-cancerous area, was considered to be an indicator of the selectivity of the LE accumulation in HCC[10]. Alternatively, this finding may have been observed because most patients received B-TACE treatment at the lobar or segmental level, resulting in a less-marked decrease in the BOASP and therefore a less-marked therapeutic effect[26]. More large-scale prospective studies are warranted.

INDICATIONS OF B-TACE

Since no definitive indications of B-TACE have been established to date, we explored potential factors and conditions supporting the performance of B-TACE. Summarizing the findings of the previous studies mentioned above, the following factors and conditions are known to be related to a dense LE accumulation in targeted HCC nodules and the therapeutic effect of B-TACE: a BOASP $\geqslant$ 64 mmHg[10]; microballoon occlusion at A1, A4, A8, anterior segment artery, RHA or LHA[26]; decreased tumor enhancement on CBCT and CTHA[30-32]; no decrease in the tumorous portal perfusion defect on CTAP[31]; tumor location on the subcapsular portion[40]; successful subsegmental feeding artery embolization[40]; the presence of portal vein visualization[40]; a high CT value just after B-TACE[44]; solitary tumor[43] and a low serum α-fetoprotein level[43]. Based on studies[13-15] showing that patients with fewer tumor nodules experienced a better therapeutic effect with B-TACE than with C-TACE, B-TACE might be a better indication than C-TACE in patients with fewer tumor nodules. Prospective validation studies are needed to clarify the indications of B-TACE.

The contraindications of B-TACE were thought to be almost the same as those for C-TACE treatment: Child-Pugh class C, no tumor thrombosis in the first branch or main portal vein, extrahepatic metastasis, refractory ascites, hepatic encephalopathy, presence of high-flow arterioportal or arteriovenous shunts, and allergy to contrast medium.

OVERALL SURVIVAL OF B-TACE

Hatanaka *et al*[43] reported that the survival rates at 1, 3 and 5 years in patients after B-TACE were 76.8%, 57.3% and 46.7%, respectively, and the median survival time was 902 d. They also revealed that a serum albumin level $\geqslant$ 3.4 g/dL and an overall response of CR+PR were favorable prognostic factors in a multivariate analysis[43]. Serum albumin is one of the most well-known prognostic factors for patients with HCC and has been adopted and integrated into several staging systems, including the BCLC staging system[3], Cancer of the Liver Italian Program (CLIP) score[51] and Japan Integrated Staging score (JIS score)[52]. According to previous studies of TACE[53,54], the overall response has been reported to be an independent factor affecting for the survival of HCC patients. Although the findings reported by Hatanaka *et al*[43] were consistent with those of previous studies[53,54], the results were based on a single-arm and single-institution study. Additional validation studies are therefore warranted.

One problem that remains to be solved is whether or not B-TACE improves the overall survival compared to other TACE treatments. Unfortunately, no RCTs have compared B-TACE with other TACE treatments, such as C-TACE and DEB-TACE, and only one historical control study[15] with patients who had solitary or two nodules has been reported. However, while it was small in scale, that study found that B-TACE was a significant factor predicting for the overall survival in a multivariate analysis[15]. A large-scale prospective study is therefore warranted.

COMPLICATIONS OF B-TACE

According to previous reports[13,20,43,44] evaluated by the Common Terminology Criteria for Adverse Effects (CTCAE), all grades of fever were reported as complications in 44.2%-68% of cases, nausea in 16.3%-28%, abdominal pain in 14%-36.7%, ascites in 12.2%-15.2%, elevated total bilirubin in 34%-62.2%, elevated alanine aminotransferase (ALT) in 78.8%-96%, elevated serum creatine in 8.1%-9.1%, leukocytopenia in 53.1%-59%, thrombocytopenia in 71.3%-87.7%, anorexia in 31.3% and vagovagal reflex in 12%, while a grade 3/4 fever was reported as a complication in 0%-6% of cases, elevated total bilirubin in 0%-6.1%, elevated ALT in 9.1%-18%, leukocytopenia in 0%-12.1% and thrombocytopenia in 7.6%-12.2%. In an analysis comparing the adverse events of B-TACE with those of C-TACE, the rate of increased levels of ALT was significantly higher in the B-TACE group, with no significant differences in the clinical symptoms or other laboratory data between the two groups[13,20].

Hatanaka *et al*[43] reported no mortalities, but the development of biloma requiring percutaneous transhepatic biliary drainage after B-TACE was observed in 1 patient (1.5%) who had intrahepatic dilation on preoperative CT. Maruyama *et al*[20] reported that liver abscess was observed in 3 patients (6%), and liver infarction was observed in 1 patient (2%), with bile duct dilation indicated as a significant predictive factor in a multivariate analysis. Careful consideration must be given to perform the B-TACE for the patients with bile duct dilation[43]. Large-scale validation studies are therefore needed to confirm these findings.

CONCLUSION

B-TACE represents a feasible and promising therapy for the treatment of HCC patients, especially those with few nodules. Although no definitive indication of B-TACE in the common clinical practice has yet been established, leaving the decision to perform this procedure up to

gastroenterologist or radiologist based on their expertise with or the availability of microballoon catheters, B-TACE may represent an established treatment in HCC patients.

REFERENCES

1 **Ferlay J**, Soerjomataram I, Dikshit R, Eser S, Mathers C, Rebelo M, Parkin DM, Forman D, Bray F. Cancer incidence and mortality worldwide: sources, methods and major patterns in GLOBOCAN 2012. *Int J Cancer* 2015; **136**: E359-E386 [PMID: 25220842 DOI: 10.1002/ijc.29210]

2 **McGlynn KA**, Petrick JL, London WT. Global epidemiology of hepatocellular carcinoma: an emphasis on demographic and regional variability. *Clin Liver Dis* 2015; **19**: 223-238 [PMID: 25921660 DOI: 10.1016/j.cld.2015.01.001]

3 **European Association For The Study Of The Liver**; European Organisation For Research And Treatment Of Cancer. EASL-EORTC clinical practice guidelines: management of hepatocellular carcinoma. *J Hepatol* 2012; **56**: 908-943 [PMID: 22424438 DOI: 10.1016/j.jhep.2011.12.001]

4 **Llovet JM**, Bruix J. Systematic review of randomized trials for unresectable hepatocellular carcinoma: Chemoembolization improves survival. *Hepatology* 2003; **37**: 429-442 [PMID: 12540794 DOI: 10.1053/jhep.2003.50047]

5 **Llovet JM**, Burroughs A, Bruix J. Hepatocellular carcinoma. *Lancet* 2003; **362**: 1907-1917 [PMID: 14667750 DOI: 10.1016/s0140-6736(03)14964-1]

6 **Lo CM**, Ngan H, Tso WK, Liu CL, Lam CM, Poon RT, Fan ST, Wong J. Randomized controlled trial of transarterial lipiodol chemoembolization for unresectable hepatocellular carcinoma. *Hepatology* 2002; **35**: 1164-1171 [PMID: 11981766 DOI: 10.1053/jhep.2002.33156]

7 **Llovet JM**, Real MI, Montaña X, Planas R, Coll S, Aponte J, Ayuso C, Sala M, Muchart J, Solà R, Rodés J, Bruix J; Barcelona Liver Cancer Group. Arterial embolisation or chemoembolisation versus symptomatic treatment in patients with unresectable hepatocellular carcinoma: a randomised controlled trial. *Lancet* 2002; **359**: 1734-1739 [PMID: 12049862 DOI: 10.1016/s0140-6736(02)08649-x]

8 **Brown DB**, Gould JE, Gervais DA, Goldberg SN, Murthy R, Millward SF, Rilling WS, Geschwind JF, Salem R, Vedantham S, Cardella JF, Soulen MC; Society of Interventional Radiology Technology Assessment Committee and the International Working Group on Image-Guided Tumor Ablation. Transcatheter therapy for hepatic malignancy: standardization of terminology and reporting criteria. *J Vasc Interv Radiol* 2009; **20**: S425-S434 [PMID: 19560030 DOI: 10.1016/j.jvir.2009.04.021]

9 **Brown DB**, Nikolic B, Covey AM, Nutting CW, Saad WE, Salem R, Sofocleous CT, Sze DY; Society of Interventional Radiology Standards of Practice Committee. Quality improvement guidelines for transhepatic arterial chemoembolization, embolization, and chemotherapeutic infusion for hepatic malignancy. *J Vasc Interv Radiol* 2012; **23**: 287-294 [PMID: 22284821 DOI: 10.1016/j.jvir.2011.11.029]

10 **Irie T**, Kuramochi M, Takahashi N. Dense accumulation of lipiodol emulsion in hepatocellular carcinoma nodule during selective balloon-occluded transarterial chemoembolization: measurement of balloon-occluded arterial stump pressure. *Cardiovasc Intervent Radiol* 2013; **36**: 706-713 [PMID: 22996589 DOI: 10.1007/s00270-012-0476-z]

11 **Heimbach JK**, Kulik LM, Finn RS, Sirlin CB, Abecassis MM, Roberts LR, Zhu AX, Murad MH, Marrero JA. AASLD guidelines for the treatment of hepatocellular carcinoma. *Hepatology* 2018; **67**: 358-380 [PMID: 28130846 DOI: 10.1002/hep.29086]

12 **Omata M**, Cheng AL, Kokudo N, Kudo M, Lee JM, Jia J, Tateishi R, Han KH, Chawla YK, Shiina S, Jafri W, Payawal DA, Ohki T, Ogasawara S, Chen PJ, Lesmana CRA, Lesmana LA, Gani RA, Obi S, Dokmeci AK, Sarin SK. Asia-Pacific clinical practice guidelines on the management of hepatocellular carcinoma: a 2017 update. *Hepatol Int* 2017; **11**: 317-370 [PMID: 28620797 DOI: 10.1007/s12072-017-9799-9]

13 **Arai H**, Abe T, Takayama H, Toyoda M, Ueno T, Kakizaki S, Sato K. Safety and efficacy of balloon-occluded transcatheter arterial chemoembolization using miriplatin for hepatocellular carcinoma. *Hepatol Res* 2015; **45**: 663-666 [PMID: 25132539 DOI: 10.1111/hepr.12403]

14 **Ogawa M**, Takayasu K, Hirayama M, Miura T, Shiozawa K, Abe M, Matsumoto N, Nakagawara H, Ohshiro S, Yamamoto T, Tanaka N, Moriyama M, Mutou H, Yamamoto Y, Irie T. Efficacy of a microballoon catheter in transarterial chemoembolization of hepatocellular carcinoma using miriplatin, a lipophilic anticancer drug: Short-term results. *Hepatol Res* 2016; **46**: E60-E69 [PMID: 25974615 DOI: 10.1111/hepr.12527]

15 **Irie T**, Kuramochi M, Kamoshida T, Takahashi N. Selective balloon-occluded transarterial chemoembolization for patients with one or two hepatocellular carcinoma nodules: Retrospective comparison with conventional super-selective TACE. *Hepatol Res* 2016; **46**: 209-214 [PMID: 26224032 DOI: 10.1111/hepr.12564]

16 **Matsumoto T**, Endo J, Hashida K, Ichikawa H, Kojima S, Takashimizu S, Watanabe N, Yamagami T, Hasebe T. Balloon-occluded transarterial chemoembolization using a 1.8-French tip coaxial microballoon catheter for hepatocellular carcinoma: technical and safety considerations. *Minim Invasive Ther Allied Technol* 2015; **24**: 94-100 [PMID: 25263680 DOI: 10.3109/13645706.2014.951657]

17 **Shibuya K**, Tahara H, Takeuchi S, Koyama Y, Tsushima Y. New Method of Parent Catheter Advancement in the Balloon Anchor Technique during Balloon-Occluded Transarterial Chemoembolization for Hepatic Tumors. *Case Rep Radiol* 2016; **2016**: 1957129 [PMID: 27340582 DOI: 10.1155/2016/1957129]

18 **Kishimoto S**, Noguchi T, Yamaoka T, Fukushima S, Takeuchi Y. In vitro release of SM-11355, cis[((1R,2R)-1,2-cyclohexanediamine-N,N')bis(myristato)] platinum(II) suspended in lipiodol. *Biol Pharm Bull* 2000; **23**: 637-640 [PMID: 10823679 DOI: 10.1248/bpb.23.637]

19 **Hanada M**, Baba A, Tsutsumishita Y, Noguchi T, Yamaoka T, Chiba N, Nishikaku F. Intra-hepatic arterial administration with miriplatin suspended in an oily lymphographic agent inhibits the growth of tumors implanted in rat livers by inducing platinum-DNA adducts to form and massive apoptosis. *Cancer Chemother Pharmacol* 2009; **64**: 473-483 [PMID: 19104812 DOI: 10.1007/s00280-008-0895-3]

20 **Maruyama M**, Yoshizako T, Nakamura T, Nakamura M, Yoshida R, Kitagaki H. Initial Experience with Balloon-Occluded Transcatheter Arterial Chemoembolization (B-TACE) for Hepatocellular Carcinoma. *Cardiovasc Intervent Radiol* 2016; **39**: 359-366 [PMID: 26711804 DOI: 10.1007/s00270-015-1237-6]

21 **Takayasu K**, Muramatsu Y, Maeda T, Iwata R, Furukawa H, Muramatsu Y, Moriyama N, Okusaka T, Okada S, Ueno H. Targeted transarterial oily chemoembolization for small foci of hepatocellular carcinoma using a unified helical CT and angiography system: analysis of factors affecting local recurrence and survival rates. *AJR Am J Roentgenol* 2001; **176**: 681-688 [PMID: 11222205 DOI: 10.2214/ajr.176.3.1760681]

22 **Hayashi K**, Ina H, Tezuka M, Okada Y, Irie T. Local therapeutic results of computed tomography-guided transcatheter arterial chemoembolization for hepatocellular carcinoma: results of 265 tumors in 79 patients. *Cardiovasc Intervent Radiol* 2007; **30**: 1144-1155 [PMID: 17909884 DOI: 10.1007/s00270-007-9169-4]

23 **Cho KJ**, Lunderquist A. The peribiliary vascular plexus: the microvascular architecture of the bile duct in the rabbit and in clinical cases. *Radiology* 1983; **147**: 357-364 [PMID: 6836115 DOI: 10.1148/radiology.147.2.6836115]

24 **Tohma T**, Cho A, Okazumi S, Makino H, Shuto K, Mochiduki R, Matsubara K, Gunji H, Ochiai T. Communicating arcade between the right and left hepatic arteries: evaluation with CT and angiography during temporary balloon occlusion of the right or left

hepatic artery. *Radiology* 2005; **237**: 361-365 [PMID: 16118153 DOI: 10.1148/radiol.2371040919]
25 **Ekataksin W**. The isolated artery: an intrahepatic arterial pathway that can bypass the lobular parenchyma in mammalian livers. *Hepatology* 2000; **31**: 269-279 [PMID: 10655246 DOI: 10.1002/hep.510310203]
26 **Matsumoto T**, Endo J, Hashida K, Mizukami H, Nagata J, Ichikawa H, Kojima S, Takashimizu S, Yamagami T, Watanabe N, Hasebe T. Balloon-occluded arterial stump pressure before balloon-occluded transarterial chemoembolization. *Minim Invasive Ther Allied Technol* 2016; **25**: 22-28 [PMID: 26406612 DOI: 10.3109/13645706.2015.1086381]
27 **Miyayama S**, Matsui O, Taki K, Minami T, Ryu Y, Ito C, Nakamura K, Inoue D, Takamatsu S. Arterial blood supply to the posterior aspect of segment IV of the liver from the caudate branch: demonstration at CT after iodized oil injection. *Radiology* 2005; **237**: 1110-1114 [PMID: 16251397 DOI: 10.1148/radiol.2373041660]
28 **Miyayama S**, Yamashiro M, Okuda M, Yoshie Y, Nakashima Y, Ikeno H, Orito N, Notsumata K, Watanabe H, Toya D, Tanaka N, Matsui O. Main bile duct stricture occurring after transcatheter arterial chemoembolization for hepatocellular carcinoma. *Cardiovasc Intervent Radiol* 2010; **33**: 1168-1179 [PMID: 20058008 DOI: 10.1007/s00270-009-9781-6]
29 **Kakuta A**, Shibutani K, Ono S, Miura H, Tsushima F, Kakehata S, Basaki K, Fujita H, Seino H, Fujita T, Takai Y. Temporal variations in stump pressure and assessment of images obtained from cone-beam computed tomography during balloon-occluded transarterial chemoembolization. *Hepatol Res* 2016; **46**: 468-476 [PMID: 26333025 DOI: 10.1111/hepr.12579]
30 **Ishikawa T**, Imai M, Owaki T, Sato H, Nozawa Y, Sano T, Iwanaga A, Seki K, Honma T, Yoshida T, Kudo M. Hemodynamic Changes on Cone-Beam Computed Tomography during Balloon-Occluded Transcatheter Arterial Chemoembolization Using Miriplatin for Hepatocellular Carcinoma: A Preliminary Study. *Dig Dis* 2017; **35**: 598-601 [PMID: 29040993 DOI: 10.1159/000480255]
31 **Yoshimatsu R**, Yamagami T, Ishikawa M, Kajiwara K, Aikata H, Chayama K, Awai K. Change in Imaging Findings on Angiography-Assisted CT During Balloon-Occluded Transcatheter Arterial Chemoembolization for Hepatocellular Carcinoma. *Cardiovasc Intervent Radiol* 2016; **39**: 865-874 [PMID: 26711803 DOI: 10.1007/s00270-015-1279-9]
32 **Asayama Y**, Nishie A, Ishigami K, Ushijima Y, Takayama Y, Okamoto D, Fujita N, Morita K, Honda H. Hemodynamic changes under balloon occlusion of hepatic artery: predictor of the short-term therapeutic effect of balloon-occluded transcatheter arterial chemolipiodolization using miriplatin for hepatocellular carcinoma. *Springerplus* 2016; **5**: 157 [PMID: 27026854 DOI: 10.1186/s40064-016-1880-7]
33 **Tognolini A**, Louie JD, Hwang GL, Hofmann LV, Sze DY, Kothary N. Utility of C-arm CT in patients with hepatocellular carcinoma undergoing transhepatic arterial chemoembolization. *J Vasc Interv Radiol* 2010; **21**: 339-347 [PMID: 20133156 DOI: 10.1016/j.jvir.2009.11.007]
34 **Miyayama S**, Yamashiro M, Hattori Y, Orito N, Matsui K, Tsuji K, Yoshida M, Matsui O. Efficacy of cone-beam computed tomography during transcatheter arterial chemoembolization for hepatocellular carcinoma. *Jpn J Radiol* 2011; **29**: 371-377 [PMID: 21786092 DOI: 10.1007/s11604-011-0568-8]
35 **Miyayama S**, Yamashiro M, Okuda M, Yoshie Y, Sugimori N, Igarashi S, Nakashima Y, Matsui O. Usefulness of cone-beam computed tomography during ultraselective transcatheter arterial chemoembolization for small hepatocellular carcinomas that cannot be demonstrated on angiography. *Cardiovasc Intervent Radiol* 2009; **32**: 255-264 [PMID: 19067043 DOI: 10.1007/s00270-008-9468-4]
36 **Takayasu K**, Maeda T, Iwata R. Sensitivity of superselective arteriography for small hepatocellular carcinoma compared with proximal arteriography and computed tomography during superselective arteriography. *Jpn J Clin Oncol* 2002; **32**: 191-195 [PMID: 12110634 DOI: 10.1093/jjco/hyf046]
37 **Sze DY**, Razavi MK, So SK, Jeffrey RB Jr. Impact of multidetector CT hepatic arteriography on the planning of chemoembolization treatment of hepatocellular carcinoma. *AJR Am J Roentgenol* 2001; **177**: 1339-1345 [PMID: 11717079 DOI: 10.2214/ajr.177.6.1771339]
38 **Fujita T**, Ito K, Tanabe M, Yamatogi S, Sasai H, Matsunaga N. Iodized oil accumulation in hypervascular hepatocellular carcinoma after transcatheter arterial chemoembolization: comparison of imaging findings with CT during hepatic arteriography. *J Vasc Interv Radiol* 2008; **19**: 333-341 [PMID: 18295691 DOI: 10.1016/j.jvir.2007.10.020]
39 **Kudo M**, Ueshima K, Kubo S, Sakamoto M, Tanaka M, Ikai I, Furuse J, Murakami T, Kadoya M, Kokudo N; Liver Cancer Study Group of Japan. Response Evaluation Criteria in Cancer of the Liver (RECICL) (2015 Revised version). *Hepatol Res* 2016; **46**: 3-9 [PMID: 26041564 DOI: 10.1111/hepr.12542]
40 **Kawamura Y**, Ikeda K, Fujiyama S, Hosaka T, Kobayashi M, Saitoh S, Sezaki H, Akuta N, Suzuki F, Suzuki Y, Arase Y, Kumada H. Usefulness and limitations of balloon-occluded transcatheter arterial chemoembolization using miriplatin for patients with four or fewer hepatocellular carcinoma nodules. *Hepatol Res* 2017; **47**: 338-346 [PMID: 27249401 DOI: 10.1111/hepr.12754]
41 **Minami Y**, Minami T, Chishina H, Arizumi T, Takita M, Kitai S, Yada N, Hagiwara S, Tsurusaki M, Yagyu Y, Ueshima K, Nishida N, Murakami T, Kudo M. Balloon-Occluded Transcatheter Arterial Chemoembolization for Hepatocellular Carcinoma: A Single-Center Experience. *Oncology* 2015; **89** Suppl 2: 27-32 [PMID: 26584033 DOI: 10.1159/000440628]
42 **Miyayama S**, Matsui O, Yamashiro M, Ryu Y, Kaito K, Ozaki K, Takeda T, Yoneda N, Notsumata K, Toya D, Tanaka N, Mitsui T. Ultraselective transcatheter arterial chemoembolization with a 2-f tip microcatheter for small hepatocellular carcinomas: relationship between local tumor recurrence and visualization of the portal vein with iodized oil. *J Vasc Interv Radiol* 2007; **18**: 365-376 [PMID: 17377182 DOI: 10.1016/j.jvir.2006.12.004]
43 **Hatanaka T**, Arai H, Shibasaki M, Tojima H, Takizawa D, Toyoda M, Takayama H, Abe T, Sato K, Kakizaki S, Yamada M. Factors predicting overall response and overall survival in hepatocellular carcinoma patients undergoing balloon-occluded transcatheter arterial chemoembolization: A retrospective cohort study. *Hepatol Res* 2018; **48**: 165-175 [PMID: 28500686 DOI: 10.1111/hepr.12912]
44 **Ishikawa T**, Abe S, Inoue R, Sugano T, Watanabe Y, Iwanaga A, Seki K, Honma T, Nemoto T, Takeda K, Yoshida T. Predictive factor of local recurrence after balloon-occluded TACE with miriplatin (MPT) in hepatocellular carcinoma. *PLoS One* 2014; **9**: e103009 [PMID: 25047920 DOI: 10.1371/journal.pone.0103009]
45 **Ishikawa T**, Abe S, Hoshii A, Yamada Y, Iiduka A, Nemoto T, Takeda K, Yoshida T. Cone-Beam Computed Tomography Correlates with Conventional Helical Computed Tomography in Evaluation of Lipiodol Accumulation in HCC after Chemoembolization. *PLoS One* 2016; **11**: e0145546 [PMID: 26752696 DOI: 10.1371/journal.pone.0145546]
46 **Okusaka T**, Okada S, Nakanishi T, Fujiyama S, Kubo Y. Phase II trial of intra-arterial chemotherapy using a novel lipophilic platinum derivative (SM-11355) in patients with hepatocellular carcinoma. *Invest New Drugs* 2004; **22**: 169-176 [PMID: 14739665 DOI: 10.1023/B:DRUG.0000011793.72775.d1]
47 **Miyayama S**, Yamashiro M, Shibata Y, Hashimoto M, Yoshida M, Tsuji K, Toshima F, Matsui O. Comparison of local control effects of superselective transcatheter arterial chemoembolization using epirubicin plus mitomycin C and miriplatin for hepatocellular carcinoma. *Jpn J Radiol* 2012; **30**: 263-270 [PMID: 22223074 DOI: 10.1007/s11604-011-0043-6]
48 **Seko Y**, Ikeda K, Kawamura Y, Fukushima T, Hara T, Sezaki H, Hosaka T, Akuta N, Suzuki F, Kobayashi M, Suzuki Y, Saitoh S, Arase Y, Kumada H. Antitumor efficacy of transcatheter arterial chemoembolization with warmed miriplatin in hepatocellular carcinoma. *Hepatol Res* 2013; **43**: 942-949 [PMID: 23301851 DOI: 10.1111/hepr.12041]
49 **Kora S**, Urakawa H, Mitsufuji T, Osame A, Higashihara H,

Yoshimitsu K. Warming effect on miriplatin-lipiodol suspension as a chemotherapeutic agent for transarterial chemoembolization for hepatocellular carcinoma: preliminary clinical experience. *Cardiovasc Intervent Radiol* 2013; **36**: 1023-1029 [PMID: 23238851 DOI: 10.1007/s00270-012-0537-3]

50 **Iwazawa J**, Hashimoto N, Ohue S, Muramoto O, Mitani T. Chemoembolization-induced arterial damage: Evaluation of three different chemotherapeutic protocols using epirubicin and miriplatin. *Hepatol Res* 2014; **44**: 201-208 [PMID: 23551984 DOI: 10.1111/hepr.12104]

51 The Cancer of the Liver Italian Program (CLIP) investigators. A new prognostic system for hepatocellular carcinoma: a retrospective study of 435 patients: *Hepatology* 1998; **28**: 751-755 [PMID: 9731568 DOI: 10.1002/hep.510280322]

52 **Kudo M**, Chung H, Haji S, Osaki Y, Oka H, Seki T, Kasugai H, Sasaki Y, Matsunaga T. Validation of a new prognostic staging system for hepatocellular carcinoma: the JIS score compared with the CLIP score. *Hepatology* 2004; **40**: 1396-1405 [PMID: 15565571 DOI: 10.1002/hep.20486]

53 **Gillmore R**, Stuart S, Kirkwood A, Hameeduddin A, Woodward N, Burroughs AK, Meyer T. EASL and mRECIST responses are independent prognostic factors for survival in hepatocellular cancer patients treated with transarterial embolization. *J Hepatol* 2011; **55**: 1309-1316 [PMID: 21703196 DOI: 10.1016/j.jhep.2011.03.007]

54 **Shim JH**, Lee HC, Kim SO, Shin YM, Kim KM, Lim YS, Suh DJ. Which response criteria best help predict survival of patients with hepatocellular carcinoma following chemoembolization? A validation study of old and new models. *Radiology* 2012; **262**: 708-718 [PMID: 22187634 DOI: 10.1148/radiol.11110282]

P- Reviewer: Guan YS, Lee JI **S- Editor**: Ji FF **L- Editor**: A
E- Editor: Tan WW

World Journal of Hepatology

Submit a Manuscript: http://www.f6publishing.com

World J Hepatol 2018 July 27; 10(7): 496-508

DOI: 10.4254/wjh.v10.i7.496

ISSN 1948-5182 (online)

ORIGINAL ARTICLE

Basic Study

Amelioration of hepatotoxicity by biocleavable aminothiol chimeras of isoniazid: Design, synthesis, kinetics and pharmacological evaluation

Neha Vithal Bhilare, Suneela Sunil Dhaneshwar, Kakasaheb Ramoo Mahadik

Neha Vithal Bhilare, Suneela Sunil Dhaneshwar, Kakasaheb Ramoo Mahadik, Department of Pharmaceutical Chemistry, Poona College of Pharmacy, Bharati Vidyapeeth University, Maharashtra 411038, India

ORCID number: Neha Vithal Bhilare (0000-0002-9144-9422); Suneela Sunil Dhaneshwar (0000-0001-7646-642X); Kakasaheb Ramoo Mahadik (0000-0001-7622-6899).

Author contributions: Bhilare NV and Dhaneshwar SS equally contributed to the conception and design of the study, the acquisition, analysis and interpretation of the data, and drafted the article and made revisions related to the intellectual content of the manuscript; Mahadik KR performed critical revision of the manuscript and approved the final version of the article to be published.

Institutional review board statement: No humans were used in this study and IRB approval was not required.

Institutional animal care and use committee statement: All animal experimentation was approved by the Institutional Animal Ethics Committee (IAEC-approval number: CPCSEA/PCH/02/2016-17) of Poona College of Pharmacy, Bharati Vidyapeeth University, Erandwane, Pune- 411038, India.

Conflict-of-interest statement: The authors declare no conflicts of interest.

Data sharing statement: There are no additional data available in relation to this manuscript.

ARRIVE guidelines statement: The ARRIVE guidelines have been adopted in the study.

Manuscript source: Unsolicited manuscript

Correspondence to: Suneela Sunil Dhaneshwar, PhD, Professor, Department of Pharmaceutical Chemistry, Poona College of Pharmacy, Bharati Vidyapeeth University, Erandwane, Maharashtra 411038, India. suneeladhaneshwar@rediffmail.com
Telephone: +91-20-25437237
Fax: +91-20-25439382

Received: March 11, 2018
Peer-review started: March 12, 2018
First decision: March 29, 2018
Revised: April 6, 2018
Accepted: April 9, 2018
Article in press: April 9, 2018
Published online: July 27, 2018

Abstract

AIM

To overcome the hazardous effects on liver caused by long-term use of antitubercular agent isoniazid (INH) by developing a novel hepatoprotective prodrug strategy by conjugating INH with aminothiols as antioxidant promoieties for probable synergistic effect.

METHODS

INH was conjugated with N-acetyl cysteine (NAC) and N-(2)-mercaptopropionyl glycine using the Schotten-Baumann reaction and with L-methionine using Boc-anhydride through a biocleavable amide linkage. Synthesized prodrugs were characterized by spectral analysis, and *in vitro* and *in vivo* release studies were carried out using HPLC. Their hepatoprotective potential was evaluated in male Wistar rats by performing liver function tests, mea-

suring markers of oxidative stress and carrying out histopathology studies.

RESULTS

Prodrugs were found to be stable in acidic (pH 1.2) and basic (pH 7.4) buffers and in rat stomach homogenates, whereas they were hydrolysed significantly (59.43%-94.93%) in intestinal homogenates over a period of 6 h. Upon oral administration of prodrug NI to rats, 52.4%-61.3% INH and 47.4%-56.8% of NAC were recovered in blood in 8-10 h. Urine and faeces samples pooled over a period of 24 h exhibited 1.3%-2.5% and 0.94%-0.9% of NAC, respectively, without any presence of intact NI or INH. Prodrugs were biologically evaluated for hepatoprotective activity. All the prodrugs were effective in abating oxidative stress and re-establishing the normal hepatic physiology. The effect of prodrug of INH with NAC in restoring the levels of the enzymes superoxide dismutase and glutathione peroxidase and abrogating liver damage was noteworthy especially.

CONCLUSION

The findings of this investigation demonstrated that the reported prodrugs can add safety and efficacy to future clinical protocols of tuberculosis treatment.

Key words: Aminothiols; Antioxidants; N-acetyl cysteine; N-(2-mercaptopropionyl) glycine; Isoniazid; L-methionine; Liver injury; Tuberculosis

Core tip: To overcome the deleterious effects caused by long-term use of isoniazid (INH), a novel hepatoprotective prodrug strategy was developed by integrating the antioxidant property of aminothiols with INH moiety to improve its therapeutic safety. The anticipated prodrugs were synthesized using facile method of synthesis, wherein aminothiols were tethered to the INH molecule *via* biocleavable amide linkage. Upon hepatoprotective potential assessment, the prodrug NI displayed noteworthy effects, whereas prodrugs MGI and MI exhibited moderate effects. The findings of this study strongly suggest that concept-based design of hepatoprotective prodrugs can be applied effectively in reversing toxic effects of INH and its metabolites on liver.

Bhilare NV, Dhaneshwar SS, Mahadik KR. Amelioration of hepatotoxicity by biocleavable aminothiol chimeras of isoniazid: Design, synthesis, kinetics and pharmacological evaluation. *World J Hepatol* 2018; 10(7): 496-508 Available from: URL: http://www.wjgnet.com/1948-5182/full/v10/i7/496.htm DOI: http://dx.doi.org/10.4254/wjh.v10.i7.496

INTRODUCTION

Tuberculosis (TB) is a worldwide pandemic and has existed for millennia. According to the Global Tuberculosis Report 2016 published by the World Health Organization, 10.4 million new TB cases (including 1.2 million among human immunodeficiency virus-positive people) occurred in 2015 and an astounding 1.4 million perished from TB that year. Overall, 10% of cases were children, whereas 90% were adults. TB disproportionately afflicts developing nations; India, Indonesia, China, Nigeria, Pakistan and South Africa were the countries that accounted for 60% of the global burden[1]. TB was one of the top 10 causes of death worldwide in 2015, despite the existence of curative chemotherapy.

Standard treatment recommended for adult respiratory TB is a 2-mo regime of isoniazid (INH), rifampicin, pyrazinamide and ethambutol, followed by INH and rifampicin for 4 mo[2]. Unfortunately, INH, the drug for the intensive phase of conventional anti-TB treatment, is highly hepatotoxic, with incidence varying between 4%-11%[3]. INH and/or its metabolites trigger systemic lupus erythematosus, peripheral neuropathy, steatosis, neurological disorders and hepatic necrosis[4]. N-arylaminoacetyl transferases (NATs) are the enzymes that metabolize INH in humans through acetylation at N2-center in the hydrazinic chain and release free radicals, which are implicated in the hepatotoxicity[4-7].

A well-established drug therapy to prevent or cure this hepatotoxicity does not exist, except discontinuing the treatment for a while and restoring it steadily later on when liver enzymes return to normal level. Such discontinuation of treatment may result in morbidity or prolonged disability. Therefore, clinical safety in long term treatment with INH is questionable and continues to be a subject of grave concern in the field of medicine[3]. In the past, considerable focus has been put on the development of INH conjugates with lower hepatotoxicity, improved hydrolytic stability, enhanced bioavailability and antitubercular activity. These include conjugation with polymers like gelatine[8], peptide[9], polyethyleneglycol[10], β-cyclodextrin conjugate[11] and antioxidants like cinnamic acids[12], curcumin[13], Schiff bases[14] and phenolic acids[15].

Resurgence of INH as a clinically safe drug appears to rely on its appropriate modification that can block acetylation by NATs and overcome toxicity. To engender these anticipated drug properties in INH, it can be structurally modified at N2-center in the hydrazinic chain[2,14]. The molecular mechanism of cytotoxicity is attributed to CYP2E1-induced oxidative stress as protein carbonyl formation and rise in reactive oxygen species occur before the beginning of hepatocyte toxicity[16,17].

Since nitrogen-centred free radicals play a critical role in instigating oxidative stress, by augmenting the hepatocellular antioxidant defence system, especially glutathione (GSH), cells can be protected against the INH-induced oxidative injury, as evidenced in previous reports[18]. Thiol-containing antioxidants have earned great interest of researchers because of the profound part played by intracellular GSH in redox regulation and antioxidant

cell defence machinery. In the present study, GSH depletion is the rationale for the selection of protective amino thiol antioxidants as carriers for conjugation with INH. As precursors of GSH, sulfhydryl group-containing compounds either increase hepatic stores of reduced GSH or substitute for it in the liver[19]. Among the sulphur-containing antioxidants, N-acetyl cysteine (NAC), N-(2-mercaptopropionyl) glycine (MPG) and L-methionine (Met) are known to be nontoxic and have been used in the treatment of various disorders[20-24].

Met plays a vital role in detoxification by acting as an amino acid precursor for GSH synthesis, which protects cells from oxidative damage[25]. NAC helps in maintaining intracellular GSH levels and scavenging reactive oxygen species and its potential in attenuating INH and rifampicin-induced hepatotoxicity has already been reported[20]. Protective effects of MPG have been reported in paracetamol-induced hepatic necrosis[26].

On these grounds, a novel series of prodrugs was designed with the aim of combining antioxidant properties of aminothiols (NAC, MPG and Met) with INH to yield codrugs with lower hepatotoxicity. The hypothesis behind this concept was based on transient masking of the hydrazinic chain of INH at the N2 position to block oxidation by CYP2E1 and acetylation by NAT. Release kinetics were studied to confirm the biocleavable nature of this newly formed amide bond, and hepatoprotective efficacy was assessed.

MATERIALS AND METHODS

INH was received as gift sample from Lupin Research Park (Lupin Ltd., Aurangabad, India). NAC was generously provided by Zim Laboratories Ltd (Nagpur, India). MPG and Met were purchased from Sigma Chemical Co. (St Louis, MO, United States). Precoated silica gel plates (60 F254; Merck, Kenilworth, NJ, United States) with fluorescent indicator were used for thin-layer chromatography, and ultraviolet (UV) light (254 nm) was used for spot detection. Programmable melting point apparatus (Veego, India) was used to record melting points and are uncorrected. The V530, UV-visible double-beam spectrophotometer (JASCO, Oklahoma City, OK, United States) was used to determine the λ_{max} of the synthesized compounds.

Spectroscopic methods were used for confirmation of structures. The infrared (IR) spectrum was recorded on a JASCO V-530 FTIR in potassium bromide (anhydrous IR grade). Proton- and ^{13}C-NMR were recorded in $CDCl_3$ and DMSO referring chemical shifts to TMS as the internal standard using an Avance Ⅱ 400 instrument (Bruker, Billerica, MA, United States) at 400 MHz, with super conducting magnet, at VIT University (Vellore, Tamilnadu, India). The mass spectra were recorded by employing an Agilent 1260 Infinity HPLC-MASS Analyzer 6460 Triple Quad LC/MS at the Poona College of Pharmacy, Food Testing Laboratory (Pune, India). The elemental analysis of synthesized prodrugs was performed on an elemental analyser (Vario Micro Cube; Elementar, Frankfurt, Germany) at the Poona College of Pharmacy.

In vitro and *in vivo* release studies were carried out on a JASCO PU HPLC model 2080, with UV detector UV-Vis 2070, using a Thermo C18 column (Hypersil gold, 250 mm × 4.36 mm, 5 μm). For pharmacological screening of synthesized prodrugs (CPCSEA/PCH/02/2016-17), Institutional Animal Ethical Committee-approved experimental protocols were followed and all procedures were carried out at the CPCSEA-approved animal facilities of Poona College of Pharmacy (Reg. No.100/1999/CPCSEA). The animals were bought from the National Institute of Biosciences (Pune, India).

Synthesis of aminothiol prodrugs of INH

Synthesis of prodrugs of INH with NAC (NI) and MPG (MGI): To the solution of amino acid (1) (0.005 mol/L) in THF (10 mL) thionyl chloride (2) (0.005 mol/L) was added drop-wise and stirred for 2 h at 55 ℃. The reaction was monitored by thin-layer chromatography using ethyl acetate:methanol:glacial acetic acid (GAA) (0.5:1.5:0.02 v/v/v). At the end of 2 h, the reaction mixture was evaporated using a rotary evaporator, and the residue of acid chloride (3) was dried under vacuum. It was then dissolved in THF and poured into a round-bottom flask which was placed in an ice bath and kept for stirring. To an ice-cold mixture of INH (4) in THF, TEA (0.5 mL) was added and the resultant solution was added drop-wise to the round-bottom flask containing acid chloride, and the temperature of the ice bath was maintained at 0 ℃. At the end of 4 h, the precipitated amide (5) was separated from the mixture by filtration and was recrystallized using mixture of ethanol:water (2:1 v/v). It was further purified by preparative thin-layer chromatography using the same mobile phase mentioned above. The reaction scheme is shown in Figure 1.

Synthesis of prodrug of INH with Met (MI): To a stirred solution of Met (6) (2 mmol) in THF (20 mL), a saturated solution of potassium carbonate (5 mL) was added. Di-*tert*-butyl dicarbonate (Boc_2O; 2 mmoL) was then added to this solution and the resultant reaction mixture was refluxed for 4 h (7) and monitored by thin-layer chromatography using ethyl acetate:hexane:GAA (0.7:0.3:0.01 v/v/v). INH (4) (2 mmol) was added to the reaction flask and the resulting mixture was refluxed for a further 6 h. Removal of solvent yielded a pale orange paste, which was further extracted using hexane: ethyl acetate (3:2 v/v) to remove excess Boc_2O and with water:DCM (1:5 v/v) to obtain a product which was dried over anhydrous magnesium sulphate.

Deprotection at the N-terminal (8) was done by addition of a solution of HCl in MeOH (10 mL) to the pale orange product obtained from the previous step. The resulting reaction mixture was stirred at room-temperature for 12 h, after which its pH was adjusted to 9 with 2 N NaOH[27]. The mixture was extracted with DCM (2 × 10 mL). The combined organics were washed with saturated aqueous brine (2 × 15 mL), dried over sodium sulphate

Table 1 Doses of test and standard drugs

S.N.	Compound	Dose[1], mg/kg/per day
1	H	0.9% saline (1 mL)
2	INH	150
3	NI	309
4	MGI	311
5	MI	293
6	INH + NAC	150 + 159
7	INH + MPG	150 + 161
8	INH + Met	150 + 143

[1]All doses were calculated on an equimolar basis to the dose of INH. H: Healthy control; INH: Isoniazid; NI: Prodrug of INH and N-acetyl cysteine; MGI: Prodrug of INH and N-(2-mercaptopropionyl) glycine; MI: Prodrug of INH and L-methionine; INH + NAC: Physical mixture of INH+N-acetyl cysteine; INH + MPG: Physical mixture of INH + N-(2-mercaptopropionyl) glycine; INH + Met: Physical mixture of INH and L-methionine.

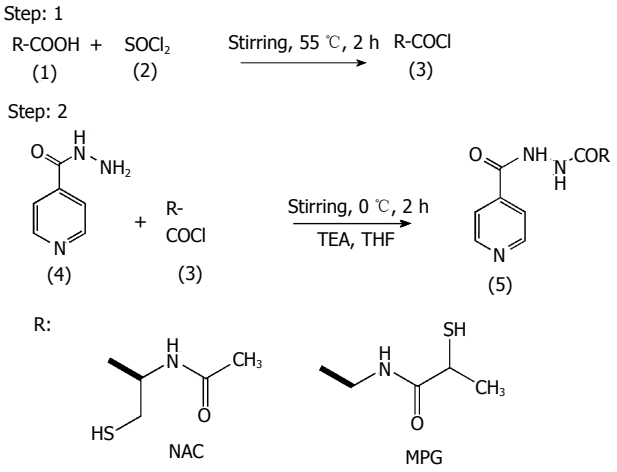

Figure 1 Scheme of synthesis for NI and MGI.

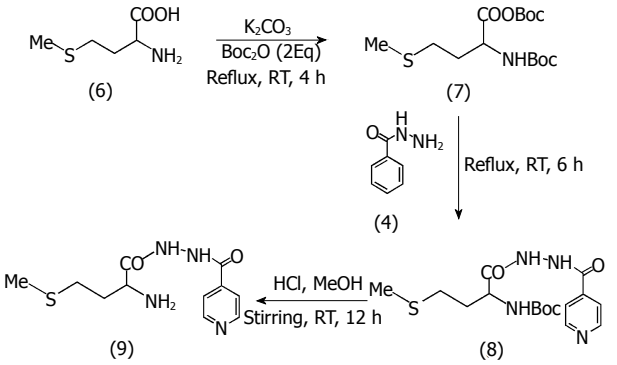

Figure 2 Scheme of synthesis for MI.

and concentrated *in vacuo*, to yield the final product (9) as a pale yellow solid. Further purification was carried out using preparative thin-layer chromatography with mobile phase ethyl acetate:hexane:GAA (0.7:0.3:0.01 v/v/v). The reaction scheme is shown in Figure 2.

In vitro stability and release studies

In vitro stability studies were performed in aqueous buffers of varied pH range and tissue homogenates of stomach and intestine of rats to ensure bioreversibility of the synthesized prodrugs. Triplicate samples were analysed and methods were validated as per ICH guidelines. Novel HPLC methods were developed for simultaneous estimation of prodrugs in the presence of their released active metabolite, INH. Percentage of hydrolysed prodrugs and release of INH was calculated using equations generated from calibration curves. Prodrugs in the presence of their hydrolysed products were estimated by simultaneous estimation method developed on reverse-phase HPLC. The method developed for estimation of NI and its hydrolysed products was comprised of water: methanol (80:20 v/v adjusted to pH 3.0 with OPA at flow rate 1 mL/min on a Thermo C_{18} column at 204 nm). For MGI, the mobile phase was comprised of acetonitrile: water (65:35; v/v adjusted to pH 2.5 with OPA at flow rate 1 mL/min on a Thermo C18 column at 365 nm). For the MI mobile phase, water:acetonitrile:methanol (20:20:60 v/v/v at flow rate 1mL/min on a Thermo C_{18} column at 205 nm) was used.

Calibration curves of prodrugs and INH were constructed in HCl buffer (pH 1.2) and phosphate buffer (pH 7.4) in the range of 10-100 μg/mL. Release study was performed in HCl buffer (pH 1.2) and stomach homogenates till 3 h and in phosphate buffer (pH 7.4) and intestinal homogenates till 6 h respectively. Prodrug (10 mg) was introduced in 100 mL of 0.05 mol/L HCl (pH 1.2) or 0.05 mol/L phosphate buffer (pH 7.4) in a beaker kept in a constant-temperature bath at 37 ± 1 ℃ with occasional stirring. Aliquots (5 mL) were withdrawn and replaced with fresh aqueous buffer at regular intervals of 0, 15, 30, 45, 60 min and every 30 min thereafter till 3 h for HCl buffer and 6 h for phosphate buffer, and 50 μL sample reconstituted with the mobile phase was injected in the column and analysed by HPLC.

In vivo release studies

In vivo behaviour of the orally-administered prodrug NI was investigated in Wistar rats (200-250 g; n = 3) housed in metabolic cages individually under normal conditions (at 27 ± 0.5 ℃ and a relative humidity of 70% ± 0.5% under natural light/dark conditions). To study the *in vivo* behaviour, an HPLC method was developed for simultaneous estimation of INH, NI and NAC. The same HPLC system, column and mobile phase were used for this purpose, as mentioned in the *in vitro* release study section above. All the kinetic studies were carried out in triplicate.

Equimolar dose of NI (Table 1) was orally administered to the 6 male Wistar rats kept in individual metabolic cages. Male Wistar rats were fasted for 24 h prior to use and were administered water *ad libitum*. Blood (0.5 mL) was withdrawn by retro-orbital puncture and the reading was considered as the 0-min reading. A suspension of NI in 1.0 mL of physiological saline was administered to the animals (Table 1). Blood samples were collected in EDTA-coated tubes at an interval of 15 min for the first 1 h. Then, subsequent blood collection

was made on a bihourly basis till the 10th h and finally at the 24th h. These EDTA-coated tubes were centrifuged for 10 min at 5000 rpm with temperature set at 0-5 ℃. The supernatant solution (0.1 mL) of centrifuged blood was added to an Eppendorf tube (1 mL capacity) and methanol (0.9 mL) was added to it for instant plasma protein precipitation. After vortexing all the solutions for 2 min, they were again centrifuged at 5000 rpm for 10 min at 0-5 ℃ in order to precipitate any solid matter or impurities present in the biological samples. These samples were then analysed by HPLC, using the procedure described above.

Urine/faeces samples were also collected at various time intervals and pooled together over a period of 24 h and analysed similarly by HPLC.

Biological evaluation

Animals: For screening of prodrugs for hepatoprotective potential, Wistar rats (male, 180-200 g) were used. Solid-bottom polypropylene cages were used to house the animals and were maintained at 24 ± 1 ℃, with a relative humidity of 45%-55% and 12:12 h dark/light cycle. They were acclimatized to laboratory conditions for 1 wk. The animals had free access to food (standard chow pellets; Chakan Oil Mills, Sangli, India) and water. The doses of prodrugs were calculated on an equimolar basis to INH and are presented in Table 1. The standard and the test compounds were administered orally as a suspension in 1% sodium CMC.

Evaluation of hepatoprotective potential: Rats were randomly divided into eight groups, after an acclimatization period of 1 wk, with each group consisting of 6 animals. Doses as mentioned in the Table 1 were administered for 21 d to the respective groups. Body weights and relative liver weights of animals from prodrug-treated groups and physical mixture-treated groups were calculated at the end of study. After completion of 21 d, on the 22nd d, the animals were fasted overnight and sacrificed immediately after withdrawal of blood from the retrobulbar venous plexus. Afterwards, centrifugation of whole blood was carried out to obtain serum samples. Liver samples were dissected out and washed immediately with ice-cold saline to remove as much blood as possible. One fraction of the liver samples was excised, fixed in a 10% formalin solution and sent for histopathological analysis; another fraction was immediately stored at -80 ℃ for future analysis. The histopathologist was unaware of the protocols to ensure unbiased analysis.

Assessment of antioxidant parameters: Liver tissues were washed with normal saline to remove any blood or clots, and homogenized on ice in Tris-HCl (5 mmol/L containing 2 mmol/L EDTA, pH 7.4). Homogenates were centrifuged at 1000 × *g* for 15 min at 4 ℃. Aliquoted samples of the supernatants were used immediately for the assays of superoxide dismutase (SOD) and glutathione peroxidase (GSHPx). SOD activity was estimated by the method described by Marklund and Marklund (1974). GSHPx content was determined by the method of Moron *et al*[28-30] (1979).

Assay of lipid peroxidation products: The extent of lipid peroxidation was assessed by estimating the concentration of thiobarbituric acid reactive product malondialdehyde (MDA) as described by Ohkawa *et al*[31] (1979). MDA concentrations were measured using 1,1,3,3-tetraethoxypropane as standard and expressed as micromoles per gram of tissue[31].

Estimation of alanine aminotransferase and aspartate aminotransferase: Serum levels of alanine aminotransferase (ALT) and aspartate aminotransferase (AST) were estimated with help of commercially available kits (Coral Clinical Systems, Mumbai, Maharashtra, India) using Reitman and Frankel's colorimetric method[32].

Biochemical parameters

Commercially available spectrophotometric kits (Coral Clinical Systems) were used to measure triglycerides and cholesterol levels. For determination of triglycerides in plasma, glycerol-3-phosphate-oxidase enzymatic colorimetric (GPO/PAP) method was used. CHOD/PAP method based on estimation of D4 cholestenone after enzymatic cleavage of cholesterol ester by cholesterol esterase was used for the determination of cholesterol in plasma[33].

Histopathological analysis

Histopathology of rat liver was carried out at SAI Research Laboratories (Pune, India). The sections were stained by haematoxylin and eosin. Coloured photomicrographs of the sections were taken on Nikon Optical Microscope, Eclipse E-200 (resolution of 10 × 10 X), with an attached trinocular camera.

Statistical analysis

An average of six readings was calculated and data were expressed as mean ± SEM; *n* referred to number of animals in each group. Statistical differences between the groups were calculated by one-way ANOVA followed by Dunnett's post-hoc test. Differences were considered at *P* values of < 0.001-0.05 when compared with the INH group.

RESULTS

Partition coefficient and aqueous solubility

The log P_{oct} of INH was found to be -0.71 and aqueous solubility was 135 mg/mL. The partition coefficients of NI, MGI and MI were found to be 0.11, 0.27 and 0.06 respectively and their aqueous solubilities were 104 mg/mL, 94 mg/mL and 114 mg/mL respectively.

Spectral analysis

For confirming the structures of synthesized prodrugs, they were subjected to spectral analysis by IR, NMR,

Table 2 *In vitro* release kinetics data

Prodrug	Incubation medium						
	HCl buffer, pH 1.2	Phosphate buffer, pH 7.4	Stomach homogenates	Intestinal homogenates			
				K ± SD, min-1[1]	$t_{1/2}$, min	% Prodrug hydrolysed	% INH released
NI	Stable	Stable	Negligible	3.4×10^{-3}	233.42	94.93	46.10
MGI	Stable	Stable	Negligible	3.3×10^{-3}	217.34	70.11	33.83
MI	Stable	Stable	Negligible	5.1×10^{-3}	181.36	86.55	44.26

[1]Average of three readings; follows first-order kinetics.

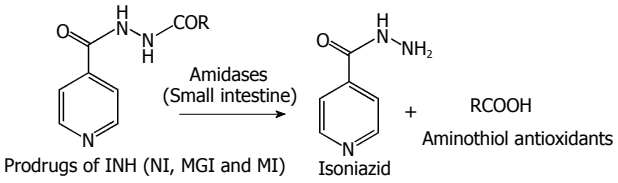

Figure 3 Proposed activation mechanism of prodrugs.

mass spectroscopy and elemental analysis.

Amide NI: N-{1-mercaptomethyl-2-oxo-2-[N'-(pyridine-4-carbonyl)-hydrazino]-ethyl}-acetamide, M.P.: 175-178 ℃ (uncorrected), R_f: 0.58 (ethyl acetate: methanol:GAA; 0.5:1.5:0.02 v/v/v), Aq. Sol. : 104 mg/mL, Log P_{oct}: 0.11, IR (anhydrous KBr; cm-1): 3300 (NH, sec amide, str), 2545 (SH, str), 1704 (C=O, CHCONH, str), 1663 (C=O, aromatic CONH, str.), 1532 (C-N, pyridine ring, str), 1406 (CH_2, bend), 751 (N-N, hydrazine, sym wag) ^{1}HNMR ($CDCl_3$; 400 MHz): δ 2.02 [s, 3H]-CH_3O, 3.05-3.06 [d, 2H]-CH_2S, 4.68-4.71 [t, 1H]-CH_2-CH_2-SH, 7.82-7.83 [d, 2H]-pyridine ring, 8.78-8.79 [d, 2H]-pyridine ring, 9.84 [s, 3H]-NH ^{13}C-NMR ($CDCl_3$; 400 MHz): 19.07, 28.85, 63.75, 121.31, 134.41, 140.51, 150.22, 163.75, 164.22, 170.22 MS: m/z ratio: 282.09 ($C_{11}H_{14}N_4O_3S$, predicted: 282.32). Elemental analysis: Calculated for $C_{11}H_{14}N_4O_3S$: C, 46.80; H, 5.00; N, 19.85; S, 11.36; Found: C, 46.77; H, 5.03; N, 19.87; S, 11.32.

Amide MGI: 2-Mercapto-N-{2-oxo-2-[N'-(pyridine-4-carbonyl)-hydrazino]-ethyl}-propionamide, M.P.: 189-191 ℃ (uncorrected), R_f: 0.66 (ethyl acetate:methanol:GAA; 0.5:1.5:0.02 v/v/v), Aq. Sol. : 94 mg/mL, Log P_{oct}: 0.27, IR (anhydrous KBr; cm-1): 3583 (NH, sec amide, str), 2560 (SH, str), 1692 (C=O, CHCONH, str), 1679 (C=O, aromatic CONH, str.), 1533 (C-N, pyridine ring, str), 1401 (CH_2, bend), 760 (N-N, hydrazine, sym wag) ^{1}HNMR ($CDCl_3$; 400MHz) δ 1.20-1.21[d, 3H]-CH_3, 3.04-3.07 [1H, m]-CH-CH_3, 4.04 [2H, s]-CH_2CO, 7.94-7.96 [d, 2H]-pyridine ring, 8.861-8.863 [d, 2H]-pyridine ring, 10.21 [s, 3H]-NH. ^{13}C-NMR ($CDCl_3$; 400 MHz): 18.03, 45.81, 59.18, 122.43, 139.18, 150.03, 164.38, 170.03, 175.97 MS: m/z ratio: 283.89 ($C_{11}H_{14}N_4O_3S$, predicted: 282.32). Elemental analysis: Calculated for $C_{11}H_{14}N_4O_3S$: C, 46.80; H, 5.00; N, 19.55; S, 11.36; Found: C, 46.79; H, 5.01; N, 19.88; S, 11.34

Amide MI: Isonicotinic acid N'-(2-amino-4-methylsulfanyl-butyryl)-hydrazide, M.P.: 199-201 ℃ (uncorrected), R_f: 0.66 (ethyl acetate:hexane:GAA; 0.7:0.3:0.01 v/v/v), Aq. Sol.: 114 mg/mL, Log P_{oct}: 0.06, IR (anhydrous KBr; cm^{-1}): 3461 (NH, sec amide, str), 2830, 2911 (CH, str), 1701 (C=O, CHCONH, str), 1692 (C=O, aromatic CONH, str.), 1538 (C-N, pyridine ring, str), 1325 (S-CH_3, str), 754 (N-N, hydrazine, sym wag), 661 (C-S-C, str) ^{1}HNMR ($CDCl_3$; 400MHz) δ 1.88-2.12[m, 2H]-CH_2-CH_2-S, 2.46[s, 3H]-CH_3S, 2.76-2.96 [2H, t]-CH_2-S, 3.85-3.88 [1H, t]-CH-NH_2, 7.88-7.89 [d, 2H]-pyridine ring, 8.82-8.83 [d, 2H]-pyridine ring, 10.06 [s, 4H]-NH. ^{13}C-NMR ($CDCl_3$; 400MHz): 18.36, 28.77, 29.98, 58.36, 122.36, 122.56, 140.40, 150.53, 150.63, 164.57, 170.17 MS: m/z ratio: 268.19 ($C_{11}H_{16}N_4O_2S$, predicted: 268.34). Elemental analysis: Calculated for $C_{11}H_{16}N_4O_2S$: C, 49.21; H, 6.07; N, 20.85; S, 11.89; Found: C, 49.25; H, 6.04; N, 20.89; S, 11.96.

In vitro release kinetics in aqueous buffers and tissue homogenates of rats

Kinetic parameters like rate constants, half-lives and order of kinetics of hydrolysis were also calculated (Table 2). No change in the peak of prodrugs was noted for the 0.05 M HCl buffer (pH 1.2) and phosphate buffer (pH 7.4). All the three prodrugs showed negligible release of INH in stomach homogenates of rats. They were readily hydrolysed in intestinal homogenates by first-order kinetics. There was gradual increase in the percentage of prodrugs hydrolysed in intestinal homogenates (59.43%-94.93%; Table 2); thus, confirming their activation by intestinal amidases (Figure 3).

In vivo release kinetics

Prodrug NI was selected as a representative of the three synthesized prodrugs to investigate the *in vivo* behaviour. NI appeared in blood between 2-2.5 h after oral administration, indicating absorption of intact prodrug through stomach (Figure 4). There was consistent rise in the concentration of NI in blood till 4.5-5 h, indicating absorption of intact prodrug from the small intestine also. INH and NAC appeared in the blood from 4 h onwards, indicating hydrolytic activation of NI in the small intestine. The concentration of intact NI in the blood started declining from 5.5-6.5 h and completely disappeared at 7.5-9 h. The concentration of INH and

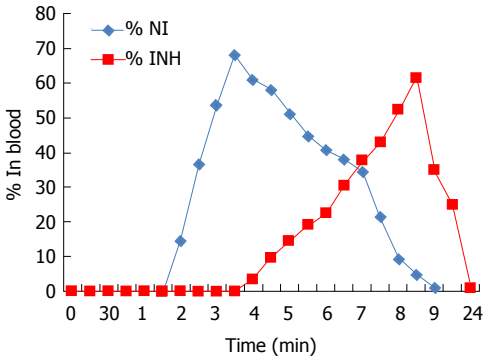

Figure 4 ***In vivo*** **pharmacokinetics after oral administration of the prodrug NI (blood).** NI: Prodrug of INH and N-acetyl cysteine.

NAC reached a maximum of 52.4%-61.3% at 9.5-10 h and 47.4%-56.8% at 8-9 h respectively. Intact NI was not observed in urine and faeces samples, whereas 1.3%-2.5% and 0.94%-0.9% of NAC was detected in 24 h pooled samples of urine and faeces respectively.

Biological evaluation

The body weights and relative liver weights of animals from prodrug-treated groups and physical mixture-treated groups calculated at the end of study had no statistical significance when compared to those of the INH-treated group.

Antioxidant markers (SOD, GSHPx and MDA): The SODs are a group of closely associated enzymes that catalyse the breakdown of the superoxide anion into hydrogen peroxide and oxygen. The function of GSHPx is to reduce free hydrogen peroxide to water and reduce lipid hydroperoxides to their corresponding alcohols[34]. Elevating GSH levels aids the productivity of the GSHPx and *vice versa*. The process of oxidative degradation of lipids is brought about by the enzyme lipid peroxidase. In this course, free radicals steal electrons from the lipids that are present in cell membranes, causing cell damage. This process progresses through a free radical chain reaction mechanism[35,36]. Polyunsaturated fatty acids are most often affected by this reaction, as they possess multiple double bonds within which are methylene groups that contain specifically reactive hydrogen. It is a free radical-mediated destructive autocatalytic process, whereby polyunsaturated fatty acids undergo degradation to form MDA. Raised MDA levels in liver signify enhanced lipid peroxidation causing hepatic tissue damage and breakdown of antioxidant defence mechanisms to obviate the excessive free radical formation. In the group treated with INH, the level of SOD and GSHPx was significantly lower and the MDA level was significantly higher. This finding confirmed the induction of oxidative stress due to administration of INH[37,38].

Treatment with NI, MGI and MI significantly re-established the levels of SOD to 93.39%, 71.98% and 88.69% respectively and GSHPx to 100%, 91.83% and 93.87% respectively (Figure 5A and B). Physical mixture INH + NAC had significant effect, whereas the effect of INH + MPG and INH + MI on both the enzymes was moderate. MDA levels were significantly decreased by prodrugs compared to the INH-treated group (Figure 5C). The effect of NI and MGI in reducing the MDA level was better compared to that achieved with MI. Physical mixtures moderately decreased the MDA level. Thus, prodrugs were found to restore the levels of antioxidant enzymes, demonstrating their hepatoprotective potential.

ALT and AST: Raised levels of ALT and AST, bilirubinuria, bilirubinaemia, jaundice and rarely severe and occasionally fatal hepatitis often occur with normal dosing procedures of antitubercular drugs. ALT and AST levels are often used to assess hepatic damage. Hepatic injury causes necrosis or membrane damage, which permits intracellular enzymes to circulate and, hence, to be detected in serum. Elevated concentration of these enzymes in the serum is an indication of loss of functional integrity of the hepatic membrane[39,40]. Elevated ALT level, especially, is a signal of hepatocellular necrosis and has been used as a surrogate marker of liver injury[41].

In the present study, drastic elevation in ALT and AST levels (144 ± 7.70 U/L and 148 ± 7.60 U/L respectively) occurred in the INH-treated group, indicating pathological conditions in liver (Figure 5D and E). Physical mixtures as well as prodrug-treated groups displayed decline in ALT and AST levels, signifying restoration of these enzymes. The effect of prodrugs compared to physical mixtures was significantly superior; the effect of prodrug NI was especially noteworthy as it restored levels of ALT and AST to 48 ± 4.50 and 46 ± 7.30 U/L respectively. This is in agreement with the generally established observation that levels of transaminases return to normal with the healing of hepatic parenchyma and regeneration of hepatocytes.

Triglycerides and cholesterol: Previous studies have documented a strong association between hypercholesterolemia and increased free radical production[42]. Increase in cholesterol levels in the liver might be due to increased uptake of low-density lipoprotein from the blood by the tissues[43]. Earlier studies state that treatment with INH resulted in accumulation of triglycerides (TGs) in the liver of INH-treated animals. This was found to be a consequence of decreased lipoprotein synthesis, causing impaired mobilization of lipids[44]. Moreover, the levels of total cholesterol also increased, indicating that INH induces the hypercholesterolemic condition. Increased uptake of low-density lipoprotein from the blood by the tissues and inhibition of bile secretion might be the reason behind this increase in cholesterol levels[45]. Hepatotoxic agents like INH have also been reported to disrupt the membrane fluidity and thus affect the normal hepatocellular functions[45].

In groups administered with prodrugs, TG and cholesterol level decreased remarkably in comparison to the group administered with INH (Figure 5F and G). TG and cholesterol level decreased, to a lesser extent, in

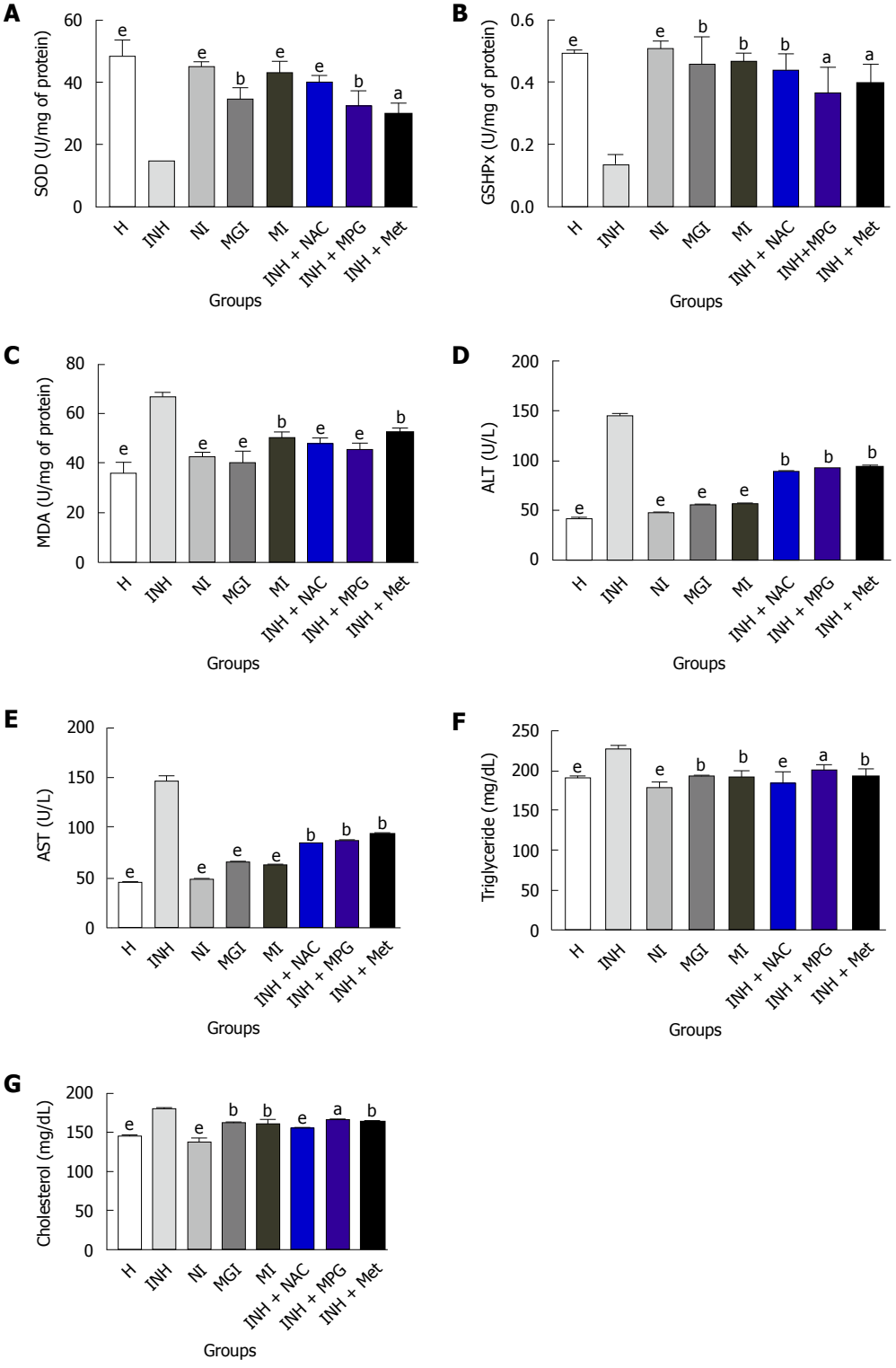

Figure 5 Effect of prodrugs on markers of liver function and oxidative stress and biochemical parameters. Average of six readings; One-way ANOVA followed by Dunnett's multiple comparison test, statistical significance considered at $^{a}P < 0.05$, $^{b}P < 0.01$, $^{e}P < 0.001$ and ns: non-significant, when *vs* INH-treated group. H: Healthy control; INH: Isoniazid; NI: Prodrug of INH and N-acetyl cysteine; MGI: Prodrug of INH and N-(2-mercaptopropionyl) glycine; MI: Prodrug of INH and L-methionine; INH + NAC: Physical mixture of INH + N-acetyl cysteine; INH + MPG: Physical mixture of INH + N-(2-mercaptopropionyl) glycine; INH + Met: Physical mixture of INH and L-methionine.

the groups treated with physical mixtures INH + MPG and INH + Met, whereas the effect of INH + NAC was more significant. Prodrugs provided remarkable defence against INH-induced aberrations in liver.

Histopathological analysis

Microscopic examination of liver sections of healthy rats showed intact parenchymal cells and normal lobular architecture (Figure 6). Polygonal hepatocytes (single headed black arrow) arranged in hexagonal lobules and portal triads at vertices were also visible. Inside each lobule, adjacent blood sinusoids (white triangle) separated the hepatocytes and Kupffer cells (two headed black arrow), along with abundant eosinophilic cytoplasm

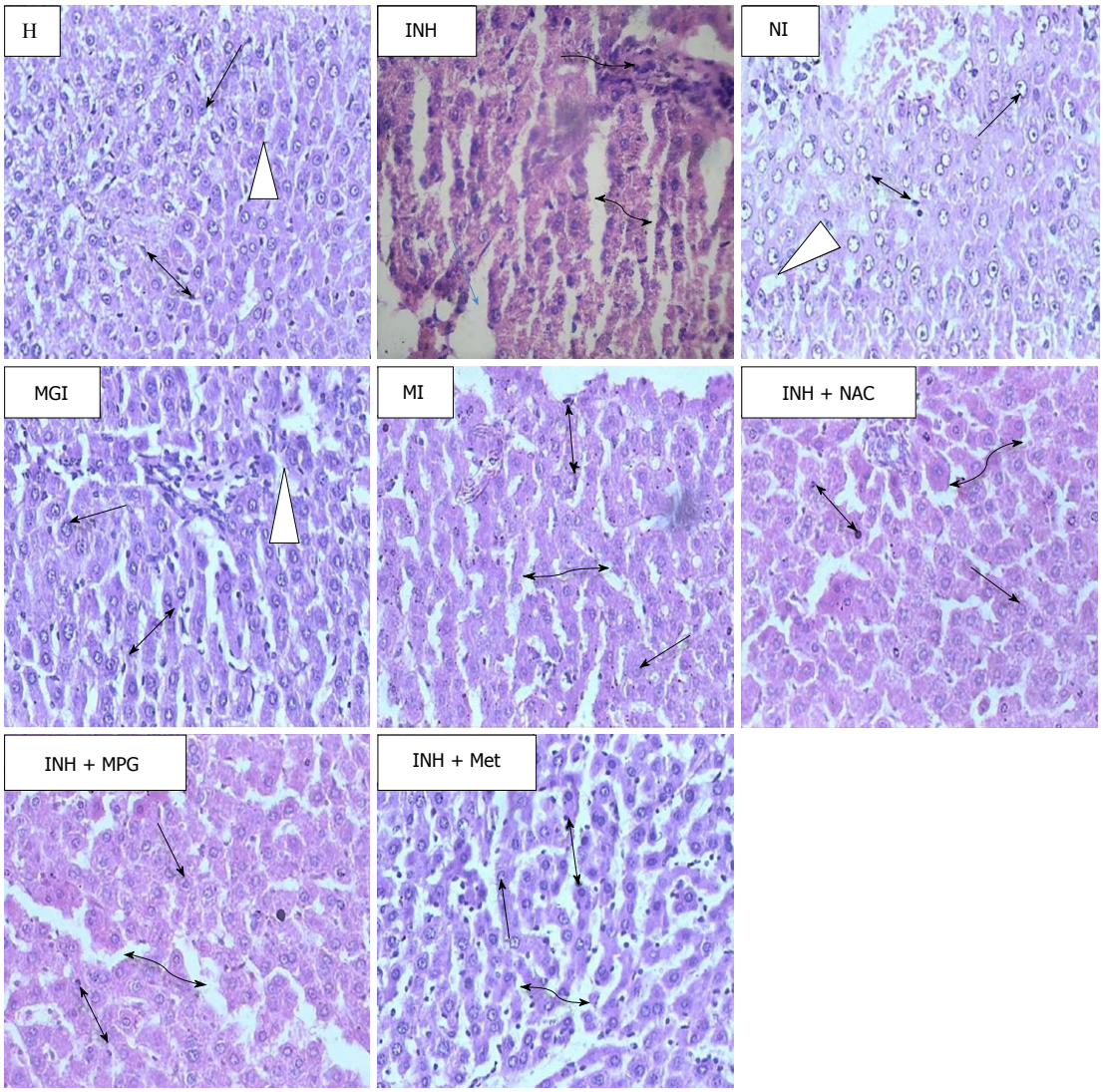

Figure 6 Photomicrographs of haematoxylin and eosin-stained histological sections of normal, isoniazid-intoxicated, prodrugs- and physical mixtures-treated rat livers.

being observable.

Membrane disintegration, degenerated nuclei, intense vacuolation accompanied by cytoplasmic rarefication leading to loss of the polyhedral structure is generally seen in liver sections of rats treated with INH. Blood sinusoidal dilatation (double headed curved black arrow), portal triaditis, multifocal area of necrosis (single headed blue arrow) and inflammatory cells (single headed curved black arrow) with granular swelling are also the prominent features in the histopathology of INH-damaged liver[46]. In the present study, all these pathological changes were noticed in liver sections of INH-treated rats (Figure 6).

The liver of rats treated with NI showed reversal of such pathology, with no evidence of necrosis, inflammation or fibrosis. Normal lobular structural design of the liver with well-preserved cytoplasm and blood sinusoids running in between normal hepatocytes were seen. Liver sections of groups treated with prodrug MGI and MI showed minimal inflammation, with minimal portal triaditis and mild dilation of blood sinusoids. The lobular architecture and hepatocytes were normal, and overall normal hepatic morphology with no histopathological derangements was observed.

Histological observations of rats administered with physical mixtures INH+NAC and INH+MPG displayed slight degenerative alterations in the parenchymal lining. Moderate sinusoidal dilatation was also observed. However, liver sections of the INH+ Met-treated group exhibited hepatocytic vacuolation, necrotic areas, moderate inflammation and severe blood sinusoidal dilatation.

DISCUSSION

Synthesis and characterization

Amide prodrugs of INH and three different sulphur containing amino acids (NI, MGI and NI) were synthesized. NI and MGI were synthesized using Schotten-Baumann reaction as described in the above section of synthesis of NI, and MGI and MI were synthesized by using the Boc-

anhydride as a protecting as well as an activating group in amide formation, as described in section of synthesis of MI. Reactions were monitored by thin-layer chromatography (ethyl acetate:methanol:GAA; 0.5:1.5:0.02 v/v/v for NI and MGI and ethyl acetate:hexane:GAA; 0.7:0.3:0.01 v/v/v for MI). Partition coefficients and aqueous solubilities of standard drugs and synthesized conjugates were determined experimentally. Log P_{oct} of INH was found to be -0.71 and aqueous solubility was 135 mg/mL. Partition coefficients of prodrugs were in the range of 0.06-0.27. The results of partition coefficients of prodrugs were in accordance with their determined aqueous solubilities (94-114 mg/mL). Increased partition coefficients might enhance the penetration and bioavailability of prodrugs.

The synthesized prodrugs were characterized by FTIR, ^{1}H-NMR, ^{13}C-NMR, elemental analysis and mass spectroscopy. Formation of amide prodrugs was confirmed through IR by carbonyl stretching between 1663-1692 cm^{-1} and NH stretching of secondary amide between 3300-3583 cm^{-1}. Chemical shifts of protons of INH and amino acids backbones were confirmed by ^{1}H-NMR, in which number of protons matched with the anticipated structures. ^{13}C-NMR confirmed formation of amide linkage between one molecule of INH and one molecule of amino acid. Mass spectroscopy also exhibited molecular ion peaks in accordance with the molecular weights (268-283) of respective prodrugs. Elemental analysis results were within the permissible range that confirmed molecular weights of prodrugs.

In vitro release kinetics

All prodrugs when incubated with HCl buffer (pH 1.2) and stomach homogenates resisted hydrolysis for 3 h and when incubated with phosphate buffer (pH 7.4) resisted hydrolysis for 6 h, as HPLC analysis did not show any peaks of INH, aminothiols or unknown hydrolysis products except for the peaks of intact prodrugs. Prodrugs were readily hydrolysed in intestinal homogenates by first-order kinetics, confirming their activation by intestinal amidases. The rate constant values increased while half-lives of the prodrugs decreased, as shown in Table 2. The extent of hydrolysis was highest for NI (94.93%; Table 2).

In vivo release kinetics

In vivo pharmacokinetic properties and factors influencing it are the guiding principles for effective prodrug design and hence need to be accurately estimated. Appearance of INH and NAC in blood from 4 h onwards indicated enzymatic activation of NI in the small intestine. From these results, we hypothesize that NI must have been activated in the small intestine by enzymatic (amidase) hydrolysis. Interestingly, many unknown metabolites were detected in urine and faeces, which might be the consequence of metabolism of INH and NAC.

Biological evaluation

Results of estimations of antioxidant markers, including SOD, GSHPx and MDA, of liver function markers, including ALT and AST, and biochemical parameters, including cholesterol and TG, clearly indicated the abrogating effect of synthesized prodrugs. Histopathological observations correlated with the biochemical findings, thus confirming that prodrugs were more effective than physical mixtures in re-establishing the normal hepatic cytoarchitecture[47,48].

The ameliorative effect of prodrugs observed in this study can be accredited to the thiol-containing amino acids which were used as carriers. They can cause hepatotropic detoxification by augmenting synthesis of GSH, which is an endogenous antioxidant and is usually depleted as a consequence of increased oxidative stress[49]. They also act either by maintaining GSH in the reduced state or providing an alternative nucleophilic target and, thus, protect protein-SH groups[18].

In summary, to address the issue of INH-induced hepatotoxicity, prodrugs of INH with aminothiol antioxidants were successfully synthesized employing simple methods for amide synthesis. *In vitro* and *in vivo* release studies confirmed the bioactivation of these prodrugs. Observations obtained from hepatoprotective potential assessment demonstrated that the prodrugs had remarkable restorative effect on levels of enzymes and biochemical parameters involved in liver injury, to normal. Further confirmation was obtained from histological micrographs of liver that displayed complete reparation of hepatic tissue. The underlying mechanism of this protective action of prodrugs involved the suppression of oxidative stress, cell membrane stabilization and reinforcement of cellular antioxidant defences, as evidenced from interpretations of hepatoprotective activity. Findings of this study proved the success of concept-based prodrug design in abating the deleterious effects of INH and its metabolites on liver.

We believe that these novel prodrugs may offer a new therapeutic strategy in TB treatment by preventing complications associated with long-term use of INH. However, further studies to explore their *in vivo* antimycobacterial efficacy are required and are under progress in our laboratory, the results of which will be communicated in our future publications.

ARTICLE HIGHLIGHTS

Research background

Tuberculosis (TB) is widely viewed as a disease of the developing world and death rates are often attributed to failure of overburdened public health systems to deliver appropriate care to infected individuals. The logistics of delivering the complex regimen and ensuring patient compliance with the full course of chemotherapy challenge the resources of the public health sector, even in the most developed countries. TB drug development has made substantial progress in the past decade. There are currently at least 10 drugs being evaluated in clinical trials. Some belong to chemical classes already employed in first- or second-line treatment regimens and are being explored for more optimized use at higher doses or in new drug combinations (oxazolidinones, rifamycins and fluoroquinolones), while others represent potential novel members of the TB drug arsenal, killing *Mycobacterium tuberculosis* through previously untried mechanisms of action (diarylquinolines, nitroimidazoles, pyrroles and ethylene diamines). The typical challenges of drug development are augmented in TB by the complexity of the disease, the requirement for multi-drug regimens,

the relative lack of TB drug development for the past several decades, and inadequate resources being brought to bear despite the urgency of the global medical need. Yet, in the face of these challenges, none of the drugs have succeeded to reach the patients. The urgent need for innovation and persistent efforts to tap novel resources cannot be denied. A fine balance needs to be achieved between protecting novel drugs or modified derivatives of existing drugs so that resistance, side effects and toxicity could be minimized, ensuring that regimens are low-cost, safe, readily available, and adopted by healthcare systems and providers. The current treatment regimen has several drawbacks, including prolonged treatment time to completely eradicate the bacteria (sterilization). This increases the risk of toxicity associated with long-term use of antitubercular drug. Isoniazid (INH) is a major first-line drug used for the treatment of TB, although the metabolic and morphological aberrations that it causes and emergence of its resistance on wide scale have been a matter of great concern for future treatment schedules of TB. Therefore, a suitable molecular modification of INH in the form of codrugs was performed in order to resolve these issues. Antioxidant aminothiols were selected as carriers to minimize hepatotoxic effects of INH. The hepatoprotective potential of these prodrugs was investigated in Wistar rats to prove effectiveness in abrogating liver damage caused by INH.

Research motivation

The root cause of INH toxicity is believed to be in the metabolism of INH at the N2 centre in hydrazinic chain by the enzymes N-acetyltransferases, which are responsible for acetylation of INH. This acetylation by N-acetyltransferases in humans is under genetic control and can be divided into two categories, *viz*. "fast acetylators" and "slow acetylators". The fast acetylators, in long-term treatment of INH, lead to significant lowering of drug bioavailability and consequent generation of INH resistance. Whereas in the case of slow acetylators, high levels of INH lead to serious hepatotoxicity. In both the cases, optimization of dose is a major issue. INH after metabolism in the liver produces hydrazine metabolites (nitrogen-centred free radicals). These radicals generate highly reactive oxygen species, which act as stimulators of lipid peroxidation, resulting in cell death and hepatic necrosis. Acute poisoning leads to lactic acidosis and renal failure, development of agranulocytosis, INH-induced tenosynovitis, INH-induced liver injury, and fatal INH-induced acute liver failure, to name only a few of the toxic consequences of INH. Furthermore, INH and/or its metabolites (*e.g.*, hydrazine) are associated with causing mitochondrial injury that may lead to oxidant stress in mitochondria and destruction of energy homeostasis. This specific observation inspired us to design prodrugs of INH; transiently masking the N2 centre in the hydrazinic chain of the INH moiety by using aminothiols which could serve by protecting the liver against toxic effects of INH. Previous studies have shown that aminothiols have antioxidant potential and they attenuate liver injury induced by INH, acetaminophen, fluoride, cisplatin, carbon tetrachloride and lead overdose. But, none of the studies have been based on introducing these antioxidant promoeities [N-acetyl cysteine (NAC), N-(2-mercaptopropionyl) glycine (MPG) and L-methionine (Met)] in the INH molecule *via* amide linkage at the hydrazinic centre and exploring their therapeutic potential. This study is the first to explore the hepatoprotective potential of aminothiol-INH conjugates for restoration of normal hepatic physiology in INH-intoxicated rats and their possible healing mechanism. It was foreseen that these prodrugs may find utility in safer treatment of TB.

Research objectives

The chief objective of this work was to minimize hepatotoxic effects of the antitubercular drug INH and, thereby, improve its safety profile in the management of TB. As metabolism at the hydrazinic chain of INH is responsible for possible side effects, we thought of masking the N2 centre in the hydrazinic chain transiently. Hepatoprotective action was achieved by using aminothiols such as NAC, MPG and Met as antioxidant carriers, which act by scavenging free radicals. Signs of liver injury did not manifest in the prodrug-treated groups, which was one of the important objectives of the present study. Future research could be directed at investigating the *in vivo* antimycobacterial potential of these prodrugs.

Research methods

Facile synthesis of target mutual prodrugs was accomplished through optimization of the Schotten-Baumann reaction and Boc-anhydride to avoid complex purification procedures. Spectral analysis was used for extensive characterization of synthesized prodrugs. Novel HPLC methods were developed and validated for simultaneous estimation of INH and aminothiols in the presence of intact prodrugs in order to study their release profiles in buffers of varied pH, rat homogenates of the gastrointestinal tract, blood, urine and faeces. For *in vivo* study, male Wistar rats weighing 180-220 g were fasted for 24 h. The animals were given drug solution in stipulated dose, quantity depending on the body weight of each animal. At 0 min, 30 min, 1 h, 2 h, 4 h, 6 h, 8 h, 10 hr and 24 h of treatment, 3 mL of blood was withdrawn by retro-orbital puncture into EDTA-coated tubes and centrifuged at 5000 rpm at 0-5 ℃ for 10 min. A 0.1 mL aliquot of the supernatant solution of centrifuged blood was added to an Eppendorf tube and 0.9 mL of methanol added to it for immediate plasma protein precipitation. The solution was vortexed for 2 min and then centrifuged at 5000 rpm for 10 min at 0-5 ℃ in order to precipitate solid matter present in the biological sample and other impurities. Then, 20 μL of the supernatant was injected into the HPLC instrument. Hepatoprotective potential was evaluated in male Wistar rats in a 21-d study. Doses calculated on equimolar basis were administered for 21 d to respective groups. All the animals were examined for liver function markers, antioxidant markers, biochemical parameters and liver histology. Livers of the sacrificed animals were removed and fixed in 10% buffered formalin and samples were sent for microscopic examination. Various markers like aminotransferases, superoxide dismutase, glutathione peroxidase and malondialdehyde, cholesterol and triglycerides were estimated at the end of study. Relevant statistical tests were used for analysing the data.

Research results

Activation of prodrugs by amidases in the small intestine, restoration of enzyme levels, re-establishment of the antioxidant defence system to avert the formation of excessive free radicals, regeneration of hepatocytes, maintenance of structural integrity of liver by released aminothiols and significantly notable reparation of INH-induced hepatotoxicity in Wistar rats were the promising outcomes of this study. This is the pioneer study to identify and describe the therapeutic potential of hepatoprotective prodrugs of INH in Wistar rats. These prodrugs could be explored further as an alternative to INH for treatment of TB.

Research conclusions

In the present work, the N2 centre of the hydrazinic chain in INH was transiently masked with aminothiols, as literature review revealed that antioxidant aminothiols play a vital role in restoring the antioxidant defence system of a host after a free radical-mediated destructive autocatalytic process which occurs in INH-induced hepatotoxicity. The novel hepatoprotective prodrug strategy proved to be advantageous in terms of lowering the biochemical parameters and liver function markers, and remarkably improving the levels of enzymes involved in the antioxidant defence system. This study emphasized the effectiveness of aminothiols to maintain integrity of the liver. These prodrugs have the potential to be screened further for their effectiveness in patients who are on long-term treatment with INH.

Research perspectives

This study proved that concept-based design of hepatoprotective prodrugs can be applied successfully in overcoming toxic effects of a drug. This work proved that an amide conjugation strategy can provide a potential synergistic effect in abrogation of INH-induced hepatotoxicity. Future research should be directed towards investigation of *in vivo* antimycobacterial potential and pharmacokinetic profiles in order to elucidate the exact molecular and biochemical mechanisms of these synthesized prodrugs.

ACKNOWLEDGMENTS

The authors would like to gratefully acknowledge Lupin Research Park, Lupin Ltd. (Aurangabad, India) for providing the gift sample of isoniazid and Zim Laboratories (Nagpur, India) for providing the gift sample of N-acetylcysteine.

REFERENCES

1 **WHO**. Global Tuberculosis Report. World Health Organization Report 2016

2 **Hearn MJ**, Cynamon MH. In vitro and in vivo activities of acylated derivatives of isoniazid against mycobacterium tuberculosis. *Drug Des Discov* 2003; **18**: 103-108 [PMID: 15553921 DOI: 10.1080/10559610390450705]

3 **Adhvaryu MR**, Reddy N, Vakharia BC. Prevention of hepatotoxicity due to anti tuberculosis treatment: a novel integrative approach. *World J Gastroenterol* 2008; **14**: 4753-4762 [PMID: 18720535 DOI: 10.3748/wjg.14.4753]

4 **Scharer L**, Smith JP. Serum transaminase elevations and other hepatic abnormalities in patients receiving isoniazid. *Ann Intern Med* 1969; **71**: 1113-1120 [PMID: 5361410 DOI: 10.7326/0003-4819-71-6-1113]

5 **Nolan CM**, Goldberg SV, Buskin SE. Hepatotoxicity associated with isoniazid preventive therapy: a 7-year survey from a public health tuberculosis clinic. *JAMA* 1999; **281**: 1014-1018 [PMID: 10086436 DOI: 10.1001/jama.281.11.1014]

6 **Metushi IG**, Cai P, Zhu X, Nakagawa T, Uetrecht JP. A fresh look at the mechanism of isoniazid-induced hepatotoxicity. *Clin Pharmacol Ther* 2011; **89**: 911-914 [PMID: 21412230 DOI: 10.1038/clpt.2010.355]

7 **Boelsterli UA**, Lee KK. Mechanisms of isoniazid-induced idiosyncratic liver injury: emerging role of mitochondrial stress. *J Gastroenterol Hepatol* 2014; **29**: 678-687 [PMID: 24783247 DOI: 10.1111/jgh.12516]

8 **Cassano R**, Trombino S, Ferrarelli T, Cavalcanti P, Giraldi C, Lai F, Loy G, Picci N. Synthesis, characterization and in-vitro antitubercular activity of isoniazid-gelatin conjugate. *J Pharm Pharmacol* 2012; **64**: 712-718 [PMID: 22471367 DOI: 10.1111/j.2042-7158.2012.01461.x]

9 **Horváti K**, Mezo G, Szabó N, Hudecz F, Bosze S. Peptide conjugates of therapeutically used antitubercular isoniazid-design, synthesis and antimycobacterial effect. *J Pept Sci* 2009; **15**: 385-391 [PMID: 19319854 DOI: 10.1002/psc.1129]

10 **Kakkar D**, Tiwari AK, Chuttani K, Kumar R, Mishra K, Singh H, Mishra AK. Polyethylene-glycolylated isoniazid conjugate for reduced toxicity and sustained release. *Ther Deliv* 2011; **2**: 205-212 [PMID: 22833946 DOI: 10.4155/tde.10.97]

11 **Dandawate P**, Vemuri K, Venkateswara Swamy K, Khan EM, Sritharan M, Padhye S. Synthesis, characterization, molecular docking and anti-tubercular activity of Plumbagin-Isoniazid Analog and its β-cyclodextrin conjugate. *Bioorg Med Chem Lett* 2014; **24**: 5070-5075 [PMID: 25264074 DOI: 10.1016/j.bmcl.2014.09.032]

12 **Wu ZR**, Zhi DJ, Zheng LF, Li JY, Li Y, Xie QJ, Feng N, Bao YF, Gao QY, Song Y, Li HY. Design and applications of bifunctional cinnamide derivatives as potential antimycobacterial agents with few hepatotoxic effects. *Med Chem Res* 2015; **24**: 161-170 [DOI: 10.1007/s00044-014-1112-z]

13 **Singh C**, Jodave L, Bhatt TD, Gill MS, Suresh S. Hepatoprotective agent tethered isoniazid for the treatment of drug-induced hepatotoxicity: Synthesis, biochemical and histopathological evaluation. *Toxicol Rep* 2014; **1**: 885-893 [PMID: 28962300 DOI: 10.1016/j.toxrep.2014.10.001]

14 **Hearn M**, Cynamon M, Chen M, Coppins R, Davis J, Joo-On Kang H, Noble A, Tu-Sekine B, Terrot MS, Trombino D, Thai M, Webster ER, Wilson R. Preparation and antitubercular activities in vitro and in vivo of novel Schiff bases of isoniazid. *Eur J Med Chem* 2009; **44**: 4169-4178 [PMID: 19524330 DOI: 10.1016/j.ejmech.2009.05.009]

15 **Bhilare NV**, Dhaneshwar SS, Mahadik KR. Phenolic acid-tethered isoniazid for abrogation of drug-induced hepatotoxicity: design, synthesis, kinetics and pharmacological evaluation. *Drug Deliv Transl Res* 2018; **8**: 770-779 [PMID: 29498003 DOI: 10.1007/s13346-018-0500-1]

16 **Tafazoli S**, Mashregi M, O'Brien PJ. Role of hydrazine in isoniazid-induced hepatotoxicity in a hepatocyte inflammation model. *Toxicol Appl Pharmacol* 2008; **229**: 94-101 [PMID: 18295292 DOI: 10.1016/j.taap.2008.01.002]

17 **Li S**, Tan HY, Wang N, Zhang ZJ, Lao L, Wong CW, Feng Y. The Role of Oxidative Stress and Antioxidants in Liver Diseases. *Int J Mol Sci* 2015; **16**: 26087-26124 [PMID: 26540040 DOI: 10.3390/ijms161125942]

18 **Attri S**, Rana SV, Vaiphei K, Sodhi CP, Katyal R, Goel RC, Nain CK, Singh K. Isoniazid- and rifampicin-induced oxidative hepatic injury--protection by N-acetylcysteine. *Hum Exp Toxicol* 2000; **19**: 517-522 [PMID: 11204554 DOI: 10.1191/096032700674230830]

19 **Zhang JG**, Lindup WE. Tiopronin protects against the nephrotoxicity of cisplatin in rat renal cortical slices in vitro. *Toxicol Appl Pharmacol* 1996; **141**: 425-433 [PMID: 8975767 DOI: 10.1006/taap.1996.0308]

20 **Rana SV**, Attri S, Vaiphei K, Pal R, Attri A, Singh K. Role of N-acetylcysteine in rifampicin-induced hepatic injury of young rats. *World J Gastroenterol* 2006; **12**: 287-291 [PMID: 16482631 DOI: 10.3748/wjg.v12.i2.287]

21 **Bhilare NV**, Dhaneshwar SS, Sinha AJ, Kandhare AD, Bodhankar SL. Novel Thioester Prodrug of N-acetylcysteine for Odor Masking and Bioavailability Enhancement. *Curr Drug Deliv* 2016; **13**: 611-620 [PMID: 26338258 DOI: 10.2174/1567201812666150904144607]

22 **Pinnen F**, Cacciatore I, Cornacchia C, Sozio P, Cerasa LS, Iannitelli A, Nasuti C, Cantalamessa F, Sekar D, Gabbianelli R, Falcioni ML, Di Stefano A. Codrugs linking L-dopa and sulfur-containing antioxidants: new pharmacological tools against Parkinson's disease. *J Med Chem* 2009; **52**: 559-563 [PMID: 19093882 DOI: 10.1021/jm801266x]

23 **Caylak E**, Aytekin M, Halifeoglu I. Antioxidant effects of methionine, alpha-lipoic acid, N-acetylcysteine and homocysteine on lead-induced oxidative stress to erythrocytes in rats. *Exp Toxicol Pathol* 2008; **60**: 289-294 [PMID: 18407480 DOI: 10.1016/j.etp.2007.11.004]

24 **Bhilare NV**, Dhaneshwar SS. Synthesis and evaluation of morpholinoethylester conjugate of N-acetylcysteine in ovalbumin-induced airway hyperresponsiveness in Sprague dawley rats. *Lett Drug Des Discov* 2016; **13**: 1-7 [DOI: 10.2174/1570180813666160804152912]

25 **Reed DJ**, Orrenius S. The role of methionine in glutathione biosynthesis by isolated hepatocytes. *Biochem Biophys Res Commun* 1977; **77**: 1257-1264 [PMID: 901533 DOI: 10.1016/S0006-291X(77)80115-0]

26 **Labadarios D**, Davis M, Portmann B, Williams R. Paracetamol-induced hepatic necrosis in the mouse-relationship between covalent binding, hepatic glutathione depletion and the protective effect of alpha-mercaptopropionylglycine. *Biochem Pharmacol* 1977; **26**: 31-35 [PMID: 831725 DOI: 10.1016/0006-2952(77)90126-5]

27 **Jhaumeer L**, KhodaBoccus A, Hemraz U, Sunnassee S. Use of Di-tert-butyl-dicarbonate Both as a Protecting and Activating Group in the Synthesis of Dipeptides. *Synth Commun* 2007; **37**: 4191-4197 [DOI: 10.1080/00397910701575202]

28 **Marklund S**, Marklund G. Involvement of the superoxide anion radical in the autoxidation of pyrogallol and a convenient assay for superoxide dismutase. *Eur J Biochem* 1974; **47**: 469-474 [PMID: 4215654 DOI: 10.1111/j.1432-1033.1974.tb03714.x]

29 **Chanchal SK**, Mahajan UB, Siddharth S, Reddy N, Goyal SN, Patil PH, Bommanahalli BP, Kundu CN, Patil CR, Ojha S. In vivo and in vitro protective effects of omeprazole against neuropathic pain. *Sci Rep* 2016; **6**: 30007 [PMID: 27435304 DOI: 10.1038/srep30007]

30 **Moron MS**, Depierre JW, Mannervik B. Levels of glutathione, glutathione reductase and glutathione S-transferase activities in rat lung and liver. *Biochim Biophys Acta* 1979; **582**: 67-78 [PMID: 760819 DOI: 10.1016/0304-4165(79)90289-7]

31 **Ohkawa H**, Ohishi N, Yagi K. Assay for lipid peroxides in animal tissues by thiobarbituric acid reaction. *Anal Biochem* 1979; **95**: 351-358 [PMID: 36810 DOI: 10.1016/0003-2697(79)90738-3]

32 **Reitman S**, Frankel S. A colorimetric method for the determination of serum glutamic oxalacetic and glutamic pyruvic transaminases. *Am J Clin Pathol* 1957; **28**: 56-63 [PMID: 13458125 DOI: 10.1093/ajcp/28.1.56]

33 **Sullivan DR**, Kruijswijk Z, West CE, Kohlmeier M, Katan MB. Determination of serum triglycerides by an accurate enzymatic method not affected by free glycerol. *Clin Chem* 1985; **31**: 1227-1228 [PMID: 4006196]

34 **Blum J**, Fridovich I. Inactivation of glutathione peroxidase by superoxide radical. *Arch Biochem Biophys* 1985; **240**: 500-508 [PMID: 2992378 DOI: 10.1016/0003-9861(85)90056-6]

35 **Aruoma OI**, Halliwell B, Hoey BM, Butler J. The antioxidant action of N-acetylcysteine: its reaction with hydrogen peroxide, hydroxyl radical, superoxide, and hypochlorous acid. *Free Radic Biol Med*

1989; **6**: 593-597 [PMID: 2546864 DOI: 10.1016/0891-5849(89)90066-X]
36 **Jaya DS**, Augustine J, Menon VP. Protective role of Nacetylcysteine against alcohol - and paracetamol - induced toxicity. *Ind J Clin Biochem* 1994; **9**: 64-71 [DOI: 10.1007/BF02869573]
37 **Bais B**, Saiju P. Ameliorative effect of Leucas cephalotes extract on isoniazid and rifampicin induced hepatotoxicity. *Asian Pac J Trop Biomed* 2014; **4**: S633-S638 [DOI: 10.12980/APJTB.4.2014APJTB-2014-0236]
38 **Saxena B**, Sharma S. Food Color Induced Hepatotoxicity in Swiss Albino Rats, Rattus norvegicus. *Toxicol Int* 2015; **22**: 152-157 [PMID: 26862277 DOI: 10.4103/0971-6580.172286]
39 **Tian Z**, Liu H, Su X, Fang Z, Dong Z, Yu C, Luo K. Role of elevated liver transaminase levels in the diagnosis of liver injury after blunt abdominal trauma. *Exp Ther Med* 2012; **4**: 255-260 [PMID: 23139714 DOI: 10.3892/etm.2012.575]
40 **Timmins GS**, Deretic V. Mechanisms of action of isoniazid. *Mol Microbiol* 2006; **62**: 1220-1227 [PMID: 17074073 DOI: 10.1111/j.1365-2958.2006.05467.x]
41 **Gelen V**, Şengül E, Gedikli S, Atila G, Uslu H, Makav M. The protective effect of rutin and quercetin on 5-FU-induced hepatotoxicity in rats. *Asian Pac J Trop Dis* 2017; **7**: 647-653 [DOI: 10.1016/j.apjtb.2017.06.013]
42 **Martinet W**, Knaapen MW, De Meyer GR, Herman AG, Kockx MM. Oxidative DNA damage and repair in experimental atherosclerosis are reversed by dietary lipid lowering. *Circ Res* 2001; **88**: 733-739 [PMID: 11304497 DOI: 10.1161/hh0701.088684]
43 **Peretti E**, Karlaganis G, Lauterburg BH. Acetylation of acetylhydrazine, the toxic metabolite of isoniazid, in humans. Inhibition by concomitant administration of isoniazid. *J Pharmacol Exp Ther* 1987; **243**: 686-689 [PMID: 3681700]
44 **Pal R**, Rana SV, Vaiphei K, Singh K. Isoniazid-rifampicin induced lipid changes in rats. *Clin Chim Acta* 2008; **389**: 55-60 [PMID: 18157944 DOI: 10.1016/j.cca.2007.11.028]
45 **Santhosh S**, Sini TK, Anandan R, Mathew PT. Effect of chitosan supplementation on antitubercular drugs-induced hepatotoxicity in rats. *Toxicology* 2006; **219**: 53-59 [PMID: 16337069 DOI: 10.1016/j.tox.2005.11.001]
46 **Evan Prince S**, Udhaya LB, Sunitha PS, Arumugam G. Reparation of Isoniazid and Rifampicin Combinatorial Therapy-Induced Hepatotoxic Effects by Bacopa monnieri. *Pharmacology* 2016; **98**: 29-34 [PMID: 27007136 DOI: 10.1159/000444856]
47 **Flora SJ,** Dwivedi N, Deb U, Kushwaha P, Lomash V. Effects of co-exposure to arsenic and dichlorvos on glutathione metabolism, neurological, hepatic variables and tissue histopathology in rats. *Toxicol Res* 2014; **3**: 23-31 [DOI: 10.1039/C3TX50038A]
48 **Tousson E**, Atteya Z, El-Atrash A, Jeweely OI. Abrogation by Ginkgo Byloba leaf extract on hepatic and renal toxicity induced by methotrexate in rats. *Cancer Res Treat* 2014; **2**: 44-51
49 **Grinberg L**, Fibach E, Amer J, Atlas D. N-acetylcysteine amide, a novel cell-permeating thiol, restores cellular glutathione and protects human red blood cells from oxidative stress. *Free Radic Biol Med* 2005; **38**: 136-145 [PMID: 15589382 DOI: 10.1016/j.freeradbiomed.2004.09.025]

P- Reviewer: Akbulut S, Skrypnyk IN, Zapater P **S- Editor**: Gong ZM
L- Editor: Filipodia **E- Editor**: Yin SY

World Journal of Hepatology

Submit a Manuscript: http://www.f6publishing.com

World J Hepatol 2018 July 27; 10(7): 509-516

DOI: 10.4254/wjh.v10.i7.509

ISSN 1948-5182 (online)

CASE REPORT

Hepatitis B virus subgenotype F3 reactivation with vaccine escape mutations: A case report and review of the literature

Stefan Schlabe, Kathrin van Bremen, Souhaib Aldabbagh, Dieter Glebe, Corinna M Bremer, Tobias Marsen, Walter Mellin, Veronica Di Cristanziano, Anna M Eis-Hübinger, Ulrich Spengler

Stefan Schlabe, Kathrin van Bremen, Souhaib Aldabbagh, Anna M Eis-Hübinger, Ulrich Spengler, German Center of Infectious Diseases Research (DZIF), Partner-Site Cologne-Bonn, Bonn-Cologne35392, Germany

Stefan Schlabe, Kathrin van Bremen, Ulrich Spengler, Department of Internal Medicine I, University Hospital of Bonn, Bonn 53127, Germany

Souhaib Aldabbagh, Anna M Eis-Hübinger, Institute of Virology, University Hospital of Bonn, Bonn 53127, Germany

Dieter Glebe, Corinna M Bremer, Institute of Medical Virology, Justus Liebig University Giessen, National Reference Center for Hepatitis B and D Viruses, Biomedical Research Center Seltersberg, Giessen 35392, Germany

Dieter Glebe, Corinna M Bremer, German Center of Infectious Diseases Research (DZIF), Partner-Site Giessen, Giessen 35392, Germany

Tobias Marsen, Practice of Nephrology and Dialysis, Nephrological Center Cologne-Lindenthal, Cologne 50937, Germany

Walter Mellin, Practice of Pathology and Cytology, Cologne 50931, Germany

Veronica Di Cristanziano, Institute of Virology, University Hospital of Cologne, Cologne 50935, Germany

ORCID number: Stefan Schlabe (0000-0002-7797-3674); Kathrin van Bremen (0000-0002-6701-1084); Souhaib Aldabbagh (0000-0002-6289-1756); Dieter Glebe (0000-0001-5039-0252); Corinna M Bremer (0000-0003-4811-785X); Tobias Marsen (0000-0002-4627-6577); Walter Mellin (0000-0003-0355-8942); Veronica Di Cristanziano (0000-0003-1604-8386); Anna M Eis-Hübinger (0000-0001-6567-2201); Ulrich Spengler (0000-0002-8746-2413).

Author contributions: Schlabe S and van Bremen K wrote the manuscript; Marsen T wrote the nephrological medical history, including transplantation and HBV management before transplantation; Mellin W discussed pathological findings of HBV reactivation; Eis-Hübinger AM, Aldabbagh S, Bremer CM, and Glebe D characterized the resistant virus and performed deep sequencing; Di Cristanziano V, Schlabe S, van Bremen K, Marsen T and Spengler U took care of the patient; escape mechanism and impact of second and third-generation vaccines were discussed and revised by Schlabe S, Spengler U, Eis-Hübinger AM, and Glebe D; the phylogenetic analysis and alignment were done by Eis-Hübinger AM and Aldabbagh S; all authors read and approved the final manuscript.

Informed consent statement: The patient gave informed consent for the publication of his medical history. Identifying details were omitted or anonymized.

Conflict-of-interest statement: Spengler U has consulted for AbbVie and has received a royalty from UpToDate for another study. Marsen T has received speakers honoraria from GHD Gesundheits GmbH and Fresenius Medical Care Nephrology for another study. Schlabe S has received sponsoring for educational events from Janssen for another study. All other authors state no conflict of interest.

CARE Checklist (2013) statement: The authors have read the guidelines of the CARE Checklist (2013) and the manuscript adheres to CARE Checklist guidelines.

Manuscript source: Unsolicited manuscript

Correspondence to: Stefan Schlabe, MD, Doctor, Resident, Department of Internal Medicine I, University Hospital of Bonn, Sigmund-Freud-Str. 25, Bonn 53127, Germany.stefan.schlabe@ukbonn.de
Telephone: +49-163-7477199

Received: April 6, 2018
Peer-review started: April 7, 2018
First decision: April 23, 2018
Revised: May 8, 2018
Accepted: June 7, 2018
Article in press: June 8, 2018
Published online: July 27, 2018

Abstract

Hepatitis B represents a global health threat because its chronic course and sequelae contribute to a high morbidity and mortality. Hepatitis B virus (HBV) infection can be controlled by vaccines, antiviral treatment, and by interrupting transmission. Rare vaccine escape mutants are serious because they eliminate vaccine protection. Here, we present a 74-year-old vaccinated patient with HBV reactivation 11 years after kidney transplantation. The patient was HBV-positive but HBsAg-negative prior to vaccination 6 years before transplantation. The reactivated virus was HBV genotype F3 with vaccine escape mutations G145R, P120Q, and Q129P. The patient was successfully treated with entecavir. The epidemiological reasons for this subgenotype, which is extremely rare in Western Europe, were unclear. This case illustrates that second-generation vaccines are not always effective in a specific group of patients.

Key words: Entecavir; Hepatitis B virus; Subgenotype F3; Kidney transplantation; Vaccine escape mutant G145R

Core tip: We report the first documented case of hepatitis B virus (HBV) subgenotype F3 reactivation with vaccine escape mutations in a patient after kidney transplantation. We successfully treated this patient with entecavir. This case illustrates a specific clinical situation in which the current World Health Organization HBV vaccine may be unsuccessful, and third generation vaccines should be considered.

Schlabe S, van Bremen K, Aldabbagh S, Glebe D, Bremer CM, Marsen T, Mellin W, Di Cristanziano V, Eis-Hübinger AM, Spengler U. Hepatitis B virus subgenotype F3 reactivation with vaccine escape mutations: A case report and review of the literature. *World J Hepatol* 2018; 10(7): 509-516 Available from: URL: http://www.wjgnet.com/1948-5182/full/v10/i7/509.htm DOI: http://dx.doi.org/10.4254/wjh.v10.i7.509

INTRODUCTION

Hepatitis B virus (HBV) is an enveloped virus of the *Hepadnaviridae* family. HBV is highly hepatotropic and is transmitted parenterally. There are 111.2 million cases of hepatitis[1] and 686000 hepatitis-related deaths reported worldwide each year. Long-term sequelae of hepatitis include liver cirrhosis and liver cell carcinoma, and these are responsible for the majority of hepatitis related deaths[2]. HBV has at least ten different genotypes, each with a specific geographic pattern[3].

There is no cure for chronic HBV infection. Antiviral agents are able to suppress viral replication but have to be taken permanently to prevent reactivation. A plasma-derived vaccine (first generation) was developed in 1982 and was replaced in 1986 by a recombinant monovalent yeast-derived vaccine (second generation). Global prevention strategies include vaccination at birth and during early childhood. However, 5%-10%of immunocompetent vaccines do not induce protective neutralizing antibody production (more so in immunodeficient patients)[4].

Immunization with second-generation vaccines relies on neutralizing antibody production against the "a" determinant, a hydrophilic antigenic domain (residues 100-170) of the HBV surface (S) protein. Specific single mutations, such as G145R, disrupt the structure of this epitope domain so that neutralizing antibodies (anti-HBs) cannot recognize it, thereby eliminating protection[5].

In this study, we report a case of HBV subgenotype F3 reactivation after kidney transplantation. Our findings highlight that current vaccines are not always effective against mutated HBV. Furthermore, current vaccines do not confer protection against HBV subgenotype F3, which is distantly related to those subgenotypes that current vaccines are based upon.

CASE REPORT

A 74-year-old patient was referred to the University Hospital of Bonn with acute hepatitis in March 2015. He initially presented with loss of appetite and acute watery diarrhea for 7 d. He was a frail patient, requiring long-term level Ⅲ care. Six weeks prior to admission he had slightly elevated alanine aminotransferase (ALT) levels (78 U/L) due to a urinary tract infection.

His medical history included chronic kidney failure due to tuberculous empyema, and the left kidney was resected in 1965. In May 1996, end-stage renal disease was diagnosed and hemodialysis was started. Prior to dialysis, chronic HBV infection had been diagnosed with partial seroconversion (anti-HBc and anti-HBe-positive and anti-HBs-negative). In November 1995, he tested positive for the HBV virus surface antigen (HBsAg). HBsAg declined to borderline levels in July 1996; and in May 1996, only low levels of HBV DNA viremia (9 pg/mL) were detected. Tests for HBs-Ag and HBV DNA have been repeatedly negative since July 1996. Two years later, seroconversion to anti-HBs had still not occurred, and the patient was repeatedly vaccinated with GenHBVax (January 1998, May 1998, and July 2002), which stabi-

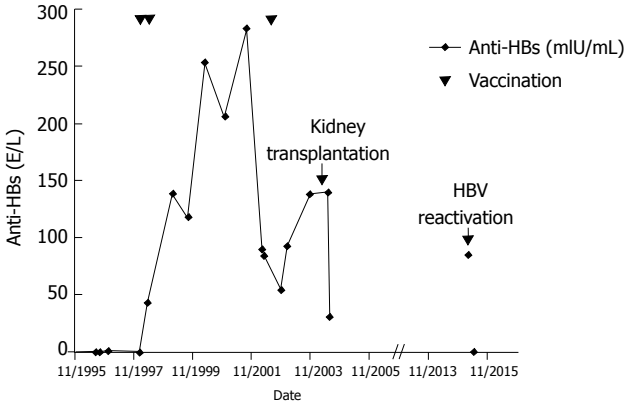

Figure 1 Course of anti-HBs levels since diagnosis of hepatitis B virus infection in 1995. Vaccine was administered in January 1998, May 1998, and July 2002. Kidney transplantation and hepatitis B virus reactivation are indicated.

lized anti-HBs levels (Figure 1).

In June 2004, he underwent cadaveric kidney transplantation and received three immunosuppressive treatments: sirolimus, tacrolimus, and methylprednisolone. This treatment was discontinued several months later because of severe side effects and was converted to 25 mg azathioprine every other day in combination with daily administration of 300 mg allopurinol plus 4 mg prednisolone with close lymphocyte monitoring. Permanent antiviral treatment was not administered. After the immunosuppressant regimen was changed, graft function remained stable with an eGFR (MDRD) grade of IIIb A1.

At admission (March 2015), his liver enzyme levels were massively elevated: ALT, 1462 U/L; aspartate aminotransferase (AST), 1459 U/L; gamma glutamyltransferase 407 U/L; lactate dehydrogenase (LDH), 616 U/L; and bilirubin, 5 mg/dL. Creatinine was elevated to 2.9 mg/dL (eGFR (MDRD) 25 mL/min). Ultrasound and CT scans excluded a tumor, thrombosis, or abscess. Serologic hepatotropic virus evaluation revealed highly replicative HBV infection with 22.5 million IU/mL HBV DNA and positive results for HBsAg (79.11 IU/mL) and anti-HBs (85.2 mIU/mL). Anti-HBe tests were also positive, while anti-HBc IgM tests were negative. Infection with hepatitis C/D viruses, CMV, and HIV was excluded. Markers of past hepatitis A/E virus, HSV, and Epstein Barr virus (EBV) infections were detected. A liver biopsy showed acute hepatitis with multiple disseminated acidophilic single cell necroses, pericentral lipofuscinosis, vacuolar lipid droplets, and minimal periportal fibrosis. The latter was interpreted as chronic toxic damage (Figure 2).

Aminotransaminase levels decreased slightly, but bilirubin peaked at 24 mg/mL 11 d after presentation. Because hepatitis B had reactivated despite high levels of anti-HBs antibodies, we initiated further analyses. Full genome analysis revealed the virus to be subgenotype F3 of genotype F (Figure 3). HBV genotype F is endemic in South America but rare in Europe. There were no reported contacts to South America, Spain, or any other epidemiological links to regions endemic for genotype F. The patient had received blood transfusions following a traffic accident with bilateral hip fracture requiring surgical procedures back in the 1960s, which may represent potential transmission routes. After kidney transplantation and revisions to the hip prosthesis, only minor surgical wound care interventions had been performed before presentation.

We found eight mutations and amino acid substitutions in the S protein, including the most common vaccine escape mutation G145R (Figure 4). Analysis of the HBV polymerase reverse transcription domain showed no known primary resistance mutations against the nucleos(t)ide analogues lamivudine, telbivudine, entecavir, tenofovir, or adefovir. Sequence analysis showed that wild-type and mutated viruses were present at a ratio of approximately 40:60 for five out of the eight identified mutations, indicating a mixed HBV population. The CD4 cell count was low (121/μL), the B cell count was strongly reduced (2/μL), and immunoglobulin levels were slightly reduced. Therefore, immunosuppressive treatment was reduced to 3 mg prednisolone, 100 mg allopurinol, and 25 mg azathioprine.

Daily treatment with 0.5 mg entecavir was initiated because of reduced kidney function. Viral replication decreased significantly and was negative 5 mo after the diagnosis (Figure 5). The entecavir dosage was later adjusted according to kidney function every fourth day. No complications with liver function were reported following treatment. Immunosuppressive treatment was changed to tacrolimus.

DISCUSSION

Reactivation of chronic hepatitis B in immunosuppressed patients is serious. In this patient, reactivation occurred approximately 11 years after immunosuppressive therapy was initiated, and no recent causes for reactivation, such as a change in immunosuppressive medication, were reported. HBV reactivation is a well described risk in renal transplant recipients. However, only one report of reactivation due to a vaccine escape mutant (HBV genotype E) in a successfully vaccinated post-transplant patient 4 years after kidney transplantation has been published[6]. Post-renal transplant patients are at risk of *de novo* HBV infections due to immunosuppression. At least two reported cases of HBV infection have been described in vaccinated kidney transplant patients carrying vaccine escape mutations[7,8]. A *de novo* infection, albeit unlikely, cannot be excluded completely in our patient.

We identified the immune escape mutation G145R in our patient. This mutation was discovered in 1988[9] and has been described in HBV genotypes A-D worldwide[10]. Reduced antibody binding is sufficient for immunologic breakthrough of HBV escape mutants[5]. We also identified a P120Q mutation in the upstream region of the HBV core gene and two different mutations at positions

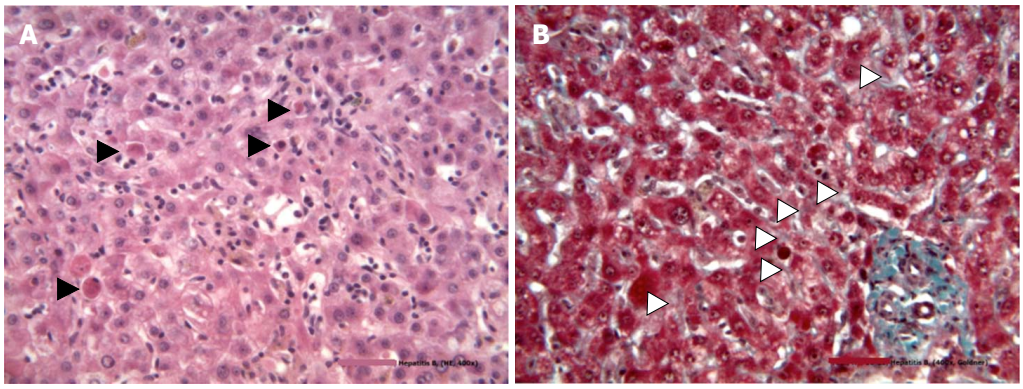

Figure 2 Hematoxylin and eosin stain of a liver specimen from the patient described in this study showing necrosis of hepatocytes (black triangles) without infiltrations and trichrome stain for fibrosis. A: Necrosis of hepatocytes; B: Trichromestain for fibrosis. Periportal fibrosis is indicated by white triangles.

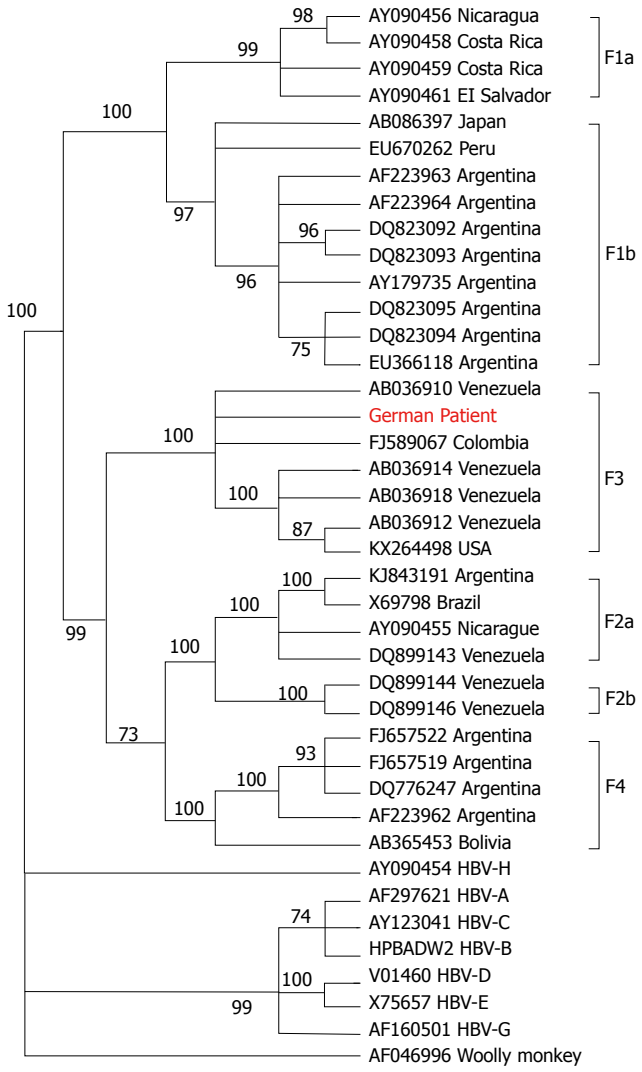

Figure 3 Phylogenetic tree of hepatitis B virus based on complete hepatitis B virus genomes. The tree was constructed using the MEGAv6.0 software package[29], (http//:www.megasoftware.net), with the neighbor-joining method with p-distance and 1000 bootstrap replicates. Bootstrap values of at least 70 are shown at the nodes. Phylogenetic analysis was performed using reference sequences from GenBank, indicated in the tree by their GenBank accession numbers. Country of virus origin is included for all genotype F sequences. Woolly monkey HBV was used as the outgroup. The sequence from the patient described in this study is presented in red. HBV: Hepatitis B virus.

Q129, Q129P, and H in our patient. Mutations at these positions have been described in immune escape variants or occult infection[10]. The combination of different mutations alters HBV antigenicity even further[11]. All eight mutations found in the case presented here and available previous reports on these specific mutations

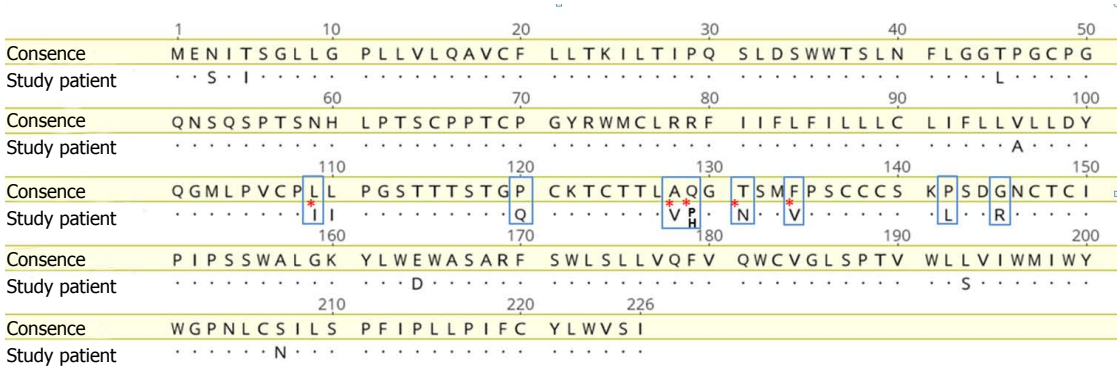

Figure 4 Vaccine escape mutations in the patient's hepatitis B virus strain. Alignment of the HBs antigen amino acid sequence (SHBs) of the patient´s strain with a HBV genotype F consensus sequence derived from the HIV-grade database (www.hiv-grade.de). Amino acids are named according to the one-letter code. Dots in the patient´s sequence represent amino acids identical to those in the consensus sequence. Positions relevant for drug resistance are indicated by blue boxes. Red asterisks denote positions in the patient´s strain (*i.e.*, 109, 128, 129, 131, and 134) where both the amino acid of the consensus strain and the vaccine escape mutation were observed. HBV: Hepatitis B virus.

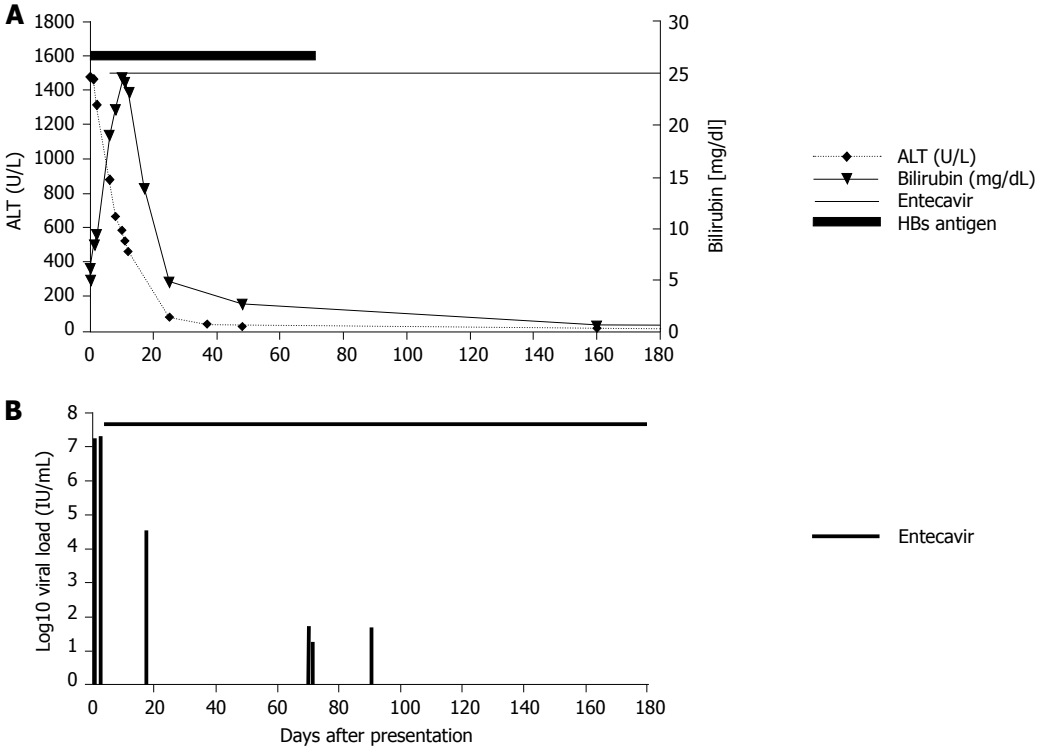

Figure 5 Course of amino transferases and bilirubin levels during acute hepatitis in March 2015 and HBV viremia levels after diagnosis of hepatitis B virus reactivation. A: Course of amino transferases and bilirubin levels during acute hepatitis in March 2015; B: Course of HBV viremia levels after diagnosis of HBV reactivation. Start of antiviral treatment is indicated. ALT: Alanine aminotransferase.

are provided in the supplemental file. Escape mutants are rare, but they can be selected by vaccination in highly endemic regions[12] and during reactivation of occult HBV.

HBV genotype F is endemic in Central and South America and has four subgenotypes, F1–F4[13]. Prevalence outside South America is very low (up to 7% in Spain[14]and 1.4% in the whole of Europe[15]). Surprisingly, the HBV genotype in our patient was subgenotype F3, subtype adw4q. The phylogenetic tree of this virus was similar to virus strains in Venezuela (Figure 3).

HBV genotype F is the most genetically divergent of the HBV genotypes[16]. It shares a close genetic and geographical association with related orthohepadnaviruses endemic in mammals of Middle and South America, like the woolly monkey, a nonhuman primate, and the Tent-making bat. This suggests an evolutionary link between these viruses in different host species[17]. The distant relationship of HBV genotype F strains with European HBV isolates has specific clinical implications. For example, the current World Health Organization (WHO) vaccine is based on the "a" determinant domain of subgenotype A2 (subtype adw2), which has a different antigen to genotype F (subtype adw4). Therefore, vaccine escape is more likely in genotype F. Moreover, HBV genotype F infections have high viral

loads and are typically HBeAg-positive in acute cases. This may facilitate breakthrough when anti-HBs titers are low[18,19]. However, only two cases of vaccine failure in patients infected with HBV subgenotype F have been reported. They were infected with genotype F1b (subtype adw4) after traveling to Northern Argentina[20] and with subgenotype F1 after traveling to Spain[21], respectively. Escape mutants were not detected in either patient, suggesting that the HBV genotype F breakthrough without the help of escape mutations. The patients described in these previous reports were vaccinated before infection. In contrast, our patient was vaccinated after HBV infection. In the 1990s, several clinical pilot trials tested vaccination in HBsAg-positive patients to induce virus-specific cellular immunity and HBsAg loss ("therapeutic vaccination") using vaccines containing HBsAg and later containing preS2/S proteins[22]. Initial results suggested a small effect on replication, seroconversion, and HBsAg loss, but the concept was later proven unsuccessful, at least with current vaccines[23]. In our case, vaccine escape was an additional negative effect of this vaccination therapy. Escape mutation selection in our patient after second-generation vaccination could be explained by: (1) incomplete neutralization of HBV genotype F by the generated antibodies; and (2) selection pressure from vaccination. To the best of our knowledge, this is the first case describing breakthrough of HBV genotype F due to G145R, P120Q, and Q129P escape mutations in a transplant setting.

The high viral load in our patient presented a substantial risk for virus transmission during blood sampling or laboratory blood work. The risk was aggravated because the virus was HBeAg-negative, which favors the development of severe and fulminant acute hepatitis due to abnormal immunopathology. Fatal outbreaks of HBeAg-negative HBV strains, even with common genotypes, have recently been reported in healthcare settings and nursing homes[24].

This case illustrates the limitations of the conventional HBV vaccine in individuals infected with escape mutant forms of the virus. These limitations include impaired immunogenicity and inability of neutralizing antibodies to recognize the virus. All available second-generation, yeast-derived vaccines are based on the non-glycosylated "a" determinant of the small surface HBV protein (SHBs). Several third-generation vaccines (Hepagene™, Bio-Hep B™, Sci-V-vac™) were developed in the 1990s and contain all three HBV envelope proteins: The SHBs, the medium (MHBs) (preS2-SHBs), and the large (LHBs) (preS1/preS2-SHBs) within subviral particles derived from mammalian cells[25]. The amino terminal of the preS1 domain contains the binding domain for sodium-dependent taurocholate co-transporting peptide (NTCP), which is the high-affinity receptor for HBV cell binding and entry[26]. PreS1-specific antibodies are interesting because the receptor-binding domain of preS1 is relatively conserved across all HBV genotypes. To date, a third-generation vaccine is not globally available; one has been on the market in Israel and in several countries in East Asia and Africa since 2001. The response rate in healthy non-responders is superior to second-generation vaccines[27] as well as in immunosuppressed post-liver transplantation patients who do not respond to second-generation vaccines[28].

In summary, we present a rare case of vaccine escape in an immunosuppressed patient infected with the rare HBV subgenotype F3 in Western Europe. This vaccine escape mutant replicated despite high levels of anti-HBs. Fortunately, antiviral agents effectively lowered the viral load and ameliorated liver inflammation. Despite this successful treatment, third-generation vaccines should be introduced as a protective measure to enhance the immunological protection of low-responders and risk groups (*e.g.*, immunosuppressed patients, patients with chronic kidney failure) and possibly induce seroconversion of HBs-Ag to anti-HBs in chronic HBeAg-negative patients with low viral loads. The HBV status of immunosuppressed patients should be carefully monitored in transplant settings to prevent possible reactivation.

ARTICLE HIGHLIGHTS

Case characteristics

A 74-year-old patient with previous hepatitis B infection presented 11 years after kidney transplantation with diarrhea, loss of appetite, and icterus.

Clinical diagnosis

The main clinical finding was acute liver dysfunction.

Differential diagnosis

The differentials of acute liver dysfunction in this patient were acute hepatitis caused by hepatitis B virus (HBV) reactivation or hepatitis D virus (HDV) superinfection or infection with another hepatotropic virus, sepsis, obstruction of bile ducts, cholangitis, tumor, abscess, or thrombosis.

Laboratory diagnosis

Laboratory results revealed acute hepatitis caused by highly replicative HBV subgenotype F3 with immune escape mutations.

Imaging diagnosis

A computed tomography (CT) scan excluded bile duct obstruction, tumor, abscess, and thrombosis.

Pathological diagnosis

Histologic examinations showed acute hepatitis with multiple disseminated acidophilic single cell necroses and pericentral lipofuscinosis, vacuolar lipid droplets, and minimal periportal fibrosis suggesting additional chronic toxic damage.

Treatment

Acute hepatitis B was treated with an antiviral medication, the nucleoside reverse transcriptase inhibitor (NRTI) entecavir (ETV).

Related reports

HBV reactivation has been reported in immunosuppressed patients, patients

with *de novo* infection, and in successfully vaccinated persons (caused by vaccine escape mutations or subgenotype F).

Term explanation

Vaccine or immune escape describes the ability of the HBV to reinfect or reactivate in the presence of neutralizing antibodies that cannot neutralize the virus.

Experiences and lessons

Acute hepatitis caused by hepatitis B infection may occur in a successfully vaccinated patient if the virus escapes antibody neutralization. Escape may be caused by escape mutations that change surface antigens or by a virus genotype that is distantly related to the virus genotype that the second-generation HBV vaccine is based on.

REFERENCES

1 **GBD 2015 Disease and Injury Incidence and Prevalence Collaborators**. Global, regional, and national incidence, prevalence, and years lived with disability for 310 diseases and injuries, 1990-2015: a systematic analysis for the Global Burden of Disease Study 2015. *Lancet* 2016; **388**: 1545-1602 [PMID: 27733282 DOI: 10.1016/S0140-6736(16)31678-6]

2 **Global Burden of Disease Study 2013 Collaborators**. Global, regional, and national incidence, prevalence, and years lived with disability for 301 acute and chronic diseases and injuries in 188 countries, 1990-2013: a systematic analysis for the Global Burden of Disease Study 2013. *Lancet* 2015; **386**: 743-800 [PMID: 26063472 DOI: 10.1016/S0140-6736(15)60692-4]

3 **Kramvis A**. Genotypes and genetic variability of hepatitis B virus. *Intervirology* 2014; **57**: 141-150 [PMID: 25034481 DOI: 10.1159/000360947]

4 **Hepatitis B vaccines.** *Wkly Epidemiol Rec* 2009; **84**: 405-419 [PMID: 19817017]

5 **Waters JA**, Kennedy M, Voet P, Hauser P, Petre J, Carman W, Thomas HC. Loss of the common "A" determinant of hepatitis B surface antigen by a vaccine-induced escape mutant. *J Clin Invest* 1992; **90**: 2543-2547 [PMID: 1281839 DOI: 10.1172/JCI116148]

6 **Le Pendeven C**, Cuzon G, Fontaine H, Zatla F, Schneider V, Amiel C, Khayat R, Nicolas JC, Soussan P. Hepatitis B escape mutant reactivation in a renal transplant patient. *J Clin Virol* 2007; **40**: 74-76 [PMID: 17652016 DOI: 10.1016/j.jcv.2007.06.009]

7 **Sayiner AA**, Agca H, Sengonul A, Celik A, Akarsu M. A new hepatitis B virus vaccine escape mutation in a renal transplant recipient. *J Clin Virol* 2007; **38**: 157-160 [PMID: 17210268 DOI: 10.1016/j.jcv.2006.12.002]

8 **Lu M**, Lorentz T. De novo infection in a renal transplant recipient caused by novel mutants of hepatitis B virus despite the presence of protective anti-hepatitis B surface antibody. *J Infect Dis* 2003; **187**: 1323-1326 [PMID: 12696014 DOI: 10.1086/373902]

9 **Zanetti AR**, Tanzi E, Manzillo G, Maio G, Sbreglia C, Caporaso N, Thomas H, Zuckerman AJ. Hepatitis B variant in Europe. *Lancet* 1988; **2**: 1132-1133 [PMID: 2460710 DOI: 10.1016/S0140-6736(88)90541-7]

10 **Coppola N**, Onorato L, Minichini C, Di Caprio G, Starace M, Sagnelli C, Sagnelli E. Clinical significance of hepatitis B surface antigen mutants. *World J Hepatol* 2015; **7**: 2729-2739 [PMID: 26644816 DOI: 10.4254/wjh.v7.i27.2729]

11 **Okamoto H**, Tsuda F, Sakugawa H, Sastrosoewignjo RI, Imai M, Miyakawa Y, Mayumi M. Typing hepatitis B virus by homology in nucleotide sequence: comparison of surface antigen subtypes. *J Gen Virol* 1988; **69**: 2575-2583 [PMID: 3171552 DOI: 10.1099/0022-1317-69-10-2575]

12 **Hsu HY**, Chang MH, Ni YH, Chen HL. Survey of hepatitis B surface variant infection in children 15 years after a nationwide vaccination programme in Taiwan. *Gut* 2004; **53**: 1499-1503 [PMID: 15361503 DOI: 10.1136/gut.2003.034223]

13 **Alvarado-Mora MV**, Pinho JR. Distribution of HBV genotypes in Latin America. *Antivir Ther* 2013; **18**: 459-465 [PMID: 23792558 DOI: 10.3851/IMP2599]

14 **Sánchez-Tapias JM**, Costa J, Mas A, Bruguera M, Rodés J. Influence of hepatitis B virus genotype on the long-term outcome of chronic hepatitis B in western patients. *Gastroenterology* 2002; **123**: 1848-1856 [PMID: 12454842 DOI: 10.1053/gast.2002.37041]

15 **Kurbanov F**, Tanaka Y, Mizokami M. Geographical and genetic diversity of the human hepatitis B virus. *Hepatol Res* 2010; **40**: 14-30 [PMID: 20156297 DOI: 10.1111/j.1872-034X.2009.00601.x]

16 **Norder H**, Hammas B, Lee SD, Bile K, Couroucé AM, Mushahwar IK, Magnius LO. Genetic relatedness of hepatitis B viral strains of diverse geographical origin and natural variations in the primary structure of the surface antigen. *J Gen Virol* 1993; **74**: 1341-1348 [PMID: 8336122 DOI: 10.1099/0022-1317-74-7-1341]

17 **Drexler JF**, Geipel A, König A, Corman VM, van Riel D, Leijten LM, Bremer CM, Rasche A, Cottontail VM, Maganga GD, Schlegel M, Müller MA, Adam A, Klose SM, Carneiro AJ, Stöcker A, Franke CR, Gloza-Rausch F, Geyer J, Annan A, Adu-Sarkodie Y, Oppong S, Binger T, Vallo P, Tschapka M, Ulrich RG, Gerlich WH, Leroy E, Kuiken T, Glebe D, Drosten C. Bats carry pathogenic hepadnaviruses antigenically related to hepatitis B virus and capable of infecting human hepatocytes. *Proc Natl Acad Sci U S A* 2013; **110**: 16151-16156 [PMID: 24043818 DOI: 10.1073/pnas.1308049110]

18 **Pezzano SC**, Torres C, Fainboim HA, Bouzas MB, Schroder T, Giuliano SF, Paz S, Alvarez E, Campos RH, Mbayed VA. Hepatitis B virus in Buenos Aires, Argentina: genotypes, virological characteristics and clinical outcomes. *Clin Microbiol Infect* 2011; **17**: 223-231 [PMID: 20545965 DOI: 10.1111/j.1469-0691.2010.03283.x]

19 **Stramer SL**, Wend U, Candotti D, Foster GA, Hollinger FB, Dodd RY, Allain JP, Gerlich W. Nucleic acid testing to detect HBV infection in blood donors. *N Engl J Med* 2011; **364**: 236-247 [PMID: 21247314 DOI: 10.1056/NEJMoa1007644]

20 **O'Halloran JA**, De Gascun CF, Dunford L, Carr MJ, Connell J, Howard R, Hall WW, Lambert JS. Hepatitis B virus vaccine failure resulting in chronic hepatitis B infection. *J Clin Virol* 2011; **52**: 151-154 [PMID: 21802353 DOI: 10.1016/j.jcv.2011.06.020]

21 **Tacke F**, Amini-Bavil-Olyaee S, Heim A, Luedde T, Manns MP, Trautwein C. Acute hepatitis B virus infection by genotype F despite successful vaccination in an immune-competent German patient. *J Clin Virol* 2007; **38**: 353-357 [PMID: 17324621 DOI: 10.1016/j.jcv.2006.12.024]

22 **Pol S**, Nalpas B, Driss F, Michel ML, Tiollais P, Denis J, Brécho C; Multicenter study group. Efficacy and limitations of a specific immunotherapy in chronic hepatitis B. *J Hepatol* 2001; **34**: 917-921 [PMID: 11451177 DOI: 10.1016/S0168-8278(01)00028-9]

23 **Cesar Aguilar J**, Y L. Immunotherapy for Chronic Hepatitis B using HBsAg-based Vaccine Formulations: From Preventive Commercial Vaccines to Therapeutic Approach Julio Cesar Aguilar. *Euroasian J Hepatogastroenterol* 2014; **4**: 92-97 [PMID: 29699355 DOI: 10.5005/jp-journals-10018-1109]

24 **Seiz PL**, Slanina H, Ziebuhr J, Gerlich WH, Glebe D, Schüttler CG. Studies of nosocomial outbreaks of hepatitis B in nursing homes in Germany suggest a major role of hepatitis B e antigen expression in disease severity and progression. *Int J Med Microbiol* 2015; **305**: 663-672 [PMID: 26338147 DOI: 10.1016/j.ijmm.2015.08.016]

25 **Shouval D**, Ilan Y, Adler R, Deepen R, Panet A, Even-Chen Z, Gorecki M, Gerlich WH. Improved immunogenicity in mice of a mammalian cell-derived recombinant hepatitis B vaccine containing pre-S1 and pre-S2 antigens as compared with conventional yeast-derived vaccines. *Vaccine* 1994; **12**: 1453-1459 [PMID: 7533967 DOI: 10.1016/0264-410X(94)90155-4]

26 **Yan H**, Zhong G, Xu G, He W, Jing Z, Gao Z, Huang Y, Qi Y, Peng B, Wang H, Fu L, Song M, Chen P, Gao W, Ren B, Sun Y, Cai T, Feng X, Sui J, Li W. Sodium taurocholate cotransporting polypeptide is a functional receptor for human hepatitis B and D virus. *Elife* 2012; **3** [PMID: 25409679 DOI: 10.7554/eLife.00049]

27 **Krawczyk A**, Ludwig C, Jochum C, Fiedler M, Heinemann FM, Shouval D, Roggendorf M, Roggendorf H, Lindemann M. Induction of a robust T- and B-cell immune response in non- and low-responders to conventional vaccination against hepatitis B by using a third generation PreS/S vaccine. *Vaccine* 2014; **32**: 5077-5082 [PMID: 24975813 DOI: 10.1016/j.vaccine.2014.06.076]

28 **Lo CM**, Lau GK, Chan SC, Fan ST, Wong J. Efficacy of a pre-S containing vaccine in patients receiving lamivudine prophylaxis after liver transplantation for chronic hepatitis B. *Am J Transplant* 2007; **7**: 434-439 [PMID: 17283489 DOI: 10.1111/j.1600-6143.2006.01636.x]

29 **Tamura K**, Stecher G, Peterson D, Filipski A, Kumar S. MEGA6: Molecular Evolutionary Genetics Analysis version 6.0. *Mol Biol Evol* 2013; **30**: 2725-2729 [PMID: 24132122 DOI: 10.1093/molbev/mst197]

P- Reviewer: Kai K, Kanda T, Saniabadi A **S- Editor**: Ji FF
L- Editor: Filipodia **E- Editor**: Tan WW

World Journal of Hepatology

Submit a Manuscript: http://www.f6publishing.com

World J Hepatol 2018 July 27; 10(7): 517-522

DOI: 10.4254/wjh.v10.i7.517

ISSN 1948-5182 (online)

CASE REPORT

Large primary hepatic gastrinoma in young patient treated with trisegmentectomy: A case report and review of the literature

Leonardo Zumerkorn Pipek, Yuri Justi Jardim, Gustavo Heluani Antunes de Mesquita, Fernanda Nii, Kayo Augusto de Almeida Medeiros, Bárbara Justo Carvalho, Diego Ramos Martines, Leandro Ryuchi Iuamoto, Daniel Reis Waisberg, Luiz Augusto Carneiro D'Albuquerque, Alberto Meyer, Wellington Andraus

Leonardo Zumerkorn Pipek, Yuri Justi Jardim, Gustavo Heluani Antunes de Mesquita, Fernanda Nii, Kayo Augusto de Almeida Medeiros, Bárbara Justo Carvalho, Diego Ramos Martines, Leandro Ryuchi Iuamoto, Faculdade de Medicina FMUSP, Universidade de São Paulo, São Paulo 05403, Brazil

Yuri Justi Jardim, Program in Global Surgery and Social Change, Department of Global Health and Social Medicine, Harvard Medical School, Boston, MA 02115, United States

Daniel Reis Waisberg, Luiz Augusto Carneiro D'Albuquerque, Alberto Meyer, Wellington Andraus, Departamento de Gastroenterologia, Hospital das Clínicas HCFMUSP, Faculdade de Medicina, Universidade de São Paulo, São Paulo 05403, Brazil

ORCID number: Leonardo Zumerkorn Pipek (0000-0001-5268-4668); Yuri Justi Jardim (0000-0001-9293-5310); Gustavo Heluani Antunes de Mesquita (0000-0002-2334-6894); Fernanda Nii (0000-0002-5254-4785); Kayo Augusto de Almeida Medeiros (0000-0001-8994-1883); Bárbara Justo Carvalho (0000-0002-7599-6610); Diego Ramos Martines (0000-0003-0559-1324); Leandro Ryuchi Iuamoto (0000-0002-6624-5815); Daniel Reis Waisberg (0000-0003-4284-0633); Luiz Augusto Carneiro D'Albuquerque (0000-0001-7607-7168); Alberto Meyer (0000-0002-8408-0508); Wellington Andraus (0000-0002-5162-138X).

Author contributions: Pipek LZ, Jardim YJ, Mesquita GHA, and Martines DR wrote the article; Nii F, Medeiros KAA, and Carvalho BJ performed the literature search; Waisberg DR and D'Albuquerque LAC identified the case and revised the manuscript for important intellectual content; Iuamoto LR, Andraus W, and Meyer A reviewed the final version of the article.

Informed consent statement: Written informed consent and permission to write this manuscript was obtained from the patient of this case report.

Conflict-of-interest statement: No potential conflicts of interest relevant to this article were reported.

Manuscript source: Unsolicited manuscript

Correspondence to: Leonardo Zumerkorn Pipek, MBBS, Faculdade de Medicina FMUSP, Universidade de São Paulo, Av Dr Arnaldo 455, São Paulo 05403, Brazil. leonardo.pipek@fm.usp.br
Telephone: +55-11-30617000
Fax: +55-11-30617000

Received: March 28, 2018
Peer-review started: March 29, 2018
First decision: April 23, 2018
Revised: April 25, 2018
Accepted: May 30, 2018
Article in press: May 31, 2018
Published online: July 27, 2018

Abstract

Primary hepatic gastrinoma is a rare disease, with fewer than 40 cases reported in the medical literature. Because it is located in an organ in which metastases are common, its diagnosis is difficult. We report a case of a 19 years old male patient with a history of gastric

ulcers since the age of nine. Following gastric surgery, an antrectomy and a vagotomy, there was some alleviation of symptoms. Subsequently, the patient reported various intermittent episodes of diarrhea, diffuse abdominal pain, and vomiting. The patient underwent tomography, which revealed the presence of a hepatic mass measuring 19.5 cm × 12.5 cm × 17 cm. Primary hepatic gastrinoma was diagnosed based on laboratory examinations that indicated hypergastrinemia and a positron emission tomography/magnetic resonance study with somatostatin analogue that confirmed the liver as the primary site. After hepatic trisegmentectomy (Ⅱ, Ⅲ, Ⅳ, Ⅴ, Ⅷ), the patient's symptoms improved. The case is notable for the presence of a rare tumor with uncommon dimensions.

Key words: Gastrinoma; Primary hepatic gastrinoma; Zollinger-Ellison syndrome; Hepatic trisegmentectomy; Gastric surgery

Core tip: Primary hepatic gastrinoma is a very rare disease. Due to its location in an organ in which metastases are common, its diagnosis is difficult. We report a case of a 19 years old male patient with a history of gastric ulcers since the age of nine. Hypergastrinemia and a PET/MR study with somatostatin analogue confirmed that the liver was the primary site. After hepatic trisegmentectomy, the patient's symptoms improved. The case is notable for the presence of a rare tumor with uncommon dimensions.

Pipek LZ, Jardim YJ, Mesquita GHA, Nii F, Medeiros KAA, Carvalho BJ, Martines DR, Iuamoto LR, Waisberg DR, D'Albuquerque LAC, Meyer A, Andraus W. Large primary hepatic gastrinoma in young patient treated with trisegmentectomy: A case report and review of the literature. *World J Hepatol* 2018; 10(7): 517-522 Available from: URL: http://www.wjgnet.com/1948-5182/full/v10/i7/517.htm DOI: http://dx.doi.org/10.4254/wjh.v10.i7.517

INTRODUCTION

Zollinger-Ellison syndrome[1] is characterized by gastric hypersecretion, resulting in peptic disease and diarrhea[2]. Diagnosis is confirmed by gastrin levels of over 1000 pg/mg. This syndrome was first described by Zollinger and Ellison[2] in 1955. With an incidence of around 0.5 to 2 per million, the majority of patients are diagnosed between 20 and 50 years of age, with a higher prevalence among men. The majority of gastrinomas are sporadic, and 20%-30% are associated with type 1 endocrine neoplasias, NEM-1[3].

The classical clinical presentation of the syndrome is the presence of abdominal pain (75%) and chronic diarrhea (73%). Half of patients present with burning as a result of gastroesophageal reflux. There is still a significant population (17%-25%) that presents with weight loss and gastrointestinal bleeding[4]. Over 90% of cases of gastrinomas are present in the so-called "gastrinoma triangle", delimited by the cystic duct, the junction between the second and third portions of the duodenum, and the junction between the colon and the pancreatic body. Occasionally, gastrinomas have also been described in other areas, including lymph nodes, biliary tree, ovaries, kidneys, heart, gallbladder, omentum, and liver[5-7]. This article describes a case of primary hepatic gastrinoma in a 19 years old hypergastremic patient who underwent hepatic trisegmentectomy to remove the tumor.

CASE REPORT

A male patient, 19 years of age, was referred as a result of intermittent abdominal pain over the previous 10 years. He reported an attack of diffuse abdominal pain for 1 month at the age of nine. At that time, a gastric ulcer was diagnosed, and due to the failure of clinical treatment, he underwent antrectomy with vagotomy in another service. In the years following the surgery, the patient presented sporadic episodes of non-specific diffuse abdominal pain associated with nausea and vomiting. Diarrhea was also present, but dyspeptic characteristics were not. During that time, emergency treatment was sought with regularity, with improvement following clinical treatment. A loss of around 16 kg of body weight was reported over the year prior to admission to our service (from 68 to 52 kg).

Upper digestive endoscopy was carried out. In the third distal, close to the esophageal transition, the mucosa was pearlescent and thickened, which was associated with confluent erosions larger than 5 mm. This covered 100% of the circumference of the organ, with ulcerations and fibrin (intense erosive distal esophagitis-Los Angeles Class D). Furthermore, an image compatible with extrinsic compression of the stomach was revealed (Figure 1).

Computed tomography (CT) and magnetic resonance (Figure 2) were carried out, showing increased dimensions of the liver, as the result of a voluminous expansive hypervascularized lesion with necrotic central areas. Involvement in the portal vein was identified, and the mass mainly occupied the central portion of the liver and hilum, affecting segments Ⅰ, Ⅱ, Ⅲ, Ⅳ, Ⅷ and measuring 19.5 cm × 12.5 cm × 17.0 cm.

A biopsy was carried out with the following immunohistochemical characteristics: cytokeratin 7 negative, cytokeratin 20 negative, chromogranin positive, synaptophysin positive, CD99 positive, Hep par 1 negative, polyclonal CEA positive (standard cytoplasma and membrane), and Ki 67 positive (around 5%). It was concluded that the profile was compatible with a well-defined neuroendocrine tumor (NET Grade 2). The diagnosis was confirmed by the discovery of gastrin hypersecretion, *via* chemiluminescence, with a resulting

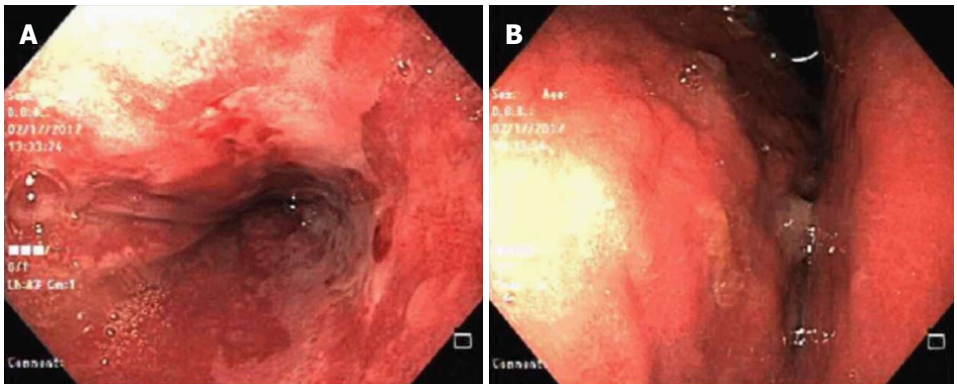

Figure 1 Upper digestive endoscopy showing intense erosive distal esophagitis and extrinsic compression of the stomach. A: Intense erosive distal esophagitis; B: Extrinsic compression of the stomach.

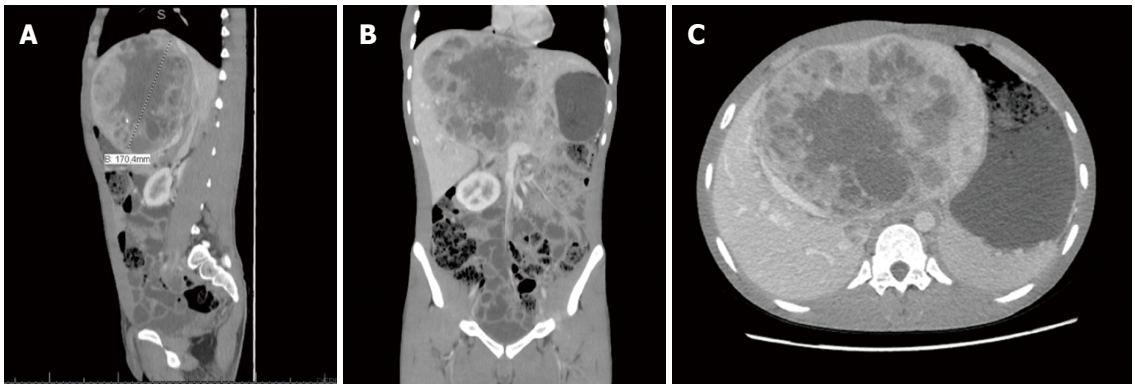

Figure 2 The computed tomography of hepatic lesion. A and B: Computed tomography showing a voluminous heterogeneous hepatic lesion, with a neoplasic aspect and dimensions 19.5 cm × 12.5 cm × 17.0 cm; C: Compression of the right hepatic vein.

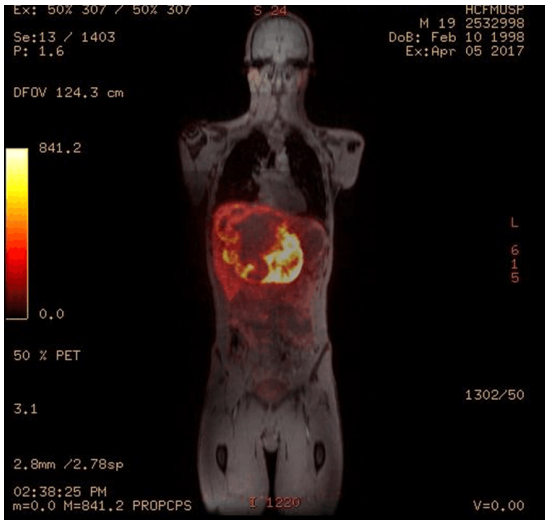

Figure 3 Positron emission tomography associated with magnetic resonance with somatostatin analogue confirmed that the liver was the primary site of the tumor.

value of 6709.0 pg/mL.

Considering that the liver is a common location for metastasis, it was important to define whether or not the tumor was primary. To do this, positron emission tomography associated with magnetic resonance was carried out - PET-MR - with somatostatin analogue (Figure 3). The examination was carried out following the administration of 2.7 mCi of Galium-68-DOTA-Octreotate (68Ga-DOTATATE) intravenously. The examination showed a relatively well-defined expansive lesion on the liver, with lobulated contours, situated in the left lobe. Heterogeneity in T2 and an anomalously high concentration of radiopharmacus was noted. It was heterogeneously distributed, with central and peripheral areas with hypoconcentration of radiotracer (which can correspond to necrosis/liquefaction), measuring around 18.1 cm × 11.3 cm at the largest axes. Contact and constriction of the inferior vena cava, which was permeable, were sustained. There were no signs of invasion of the head or body of the pancreas.

From these examinations it was possible to confirm the diagnosis of primary hepatic gastrinoma and to recommend surgical resection. Prior to the surgical procedure, there were a number of intracavity adherences. Hepatic trisegmentation (Ⅱ, Ⅲ, Ⅳ, Ⅴ, Ⅷ) was carried out (Figure 4), identifying a large volume mass, mainly occupying the left lobe of the liver. Segments Ⅴ and Ⅷ were most affected, with atrophy in segment Ⅱ, as well as compensatory hypertrophy in segments Ⅵ and Ⅶ. The remaining liver maintained approximately 80% of the volume of a functional liver. The

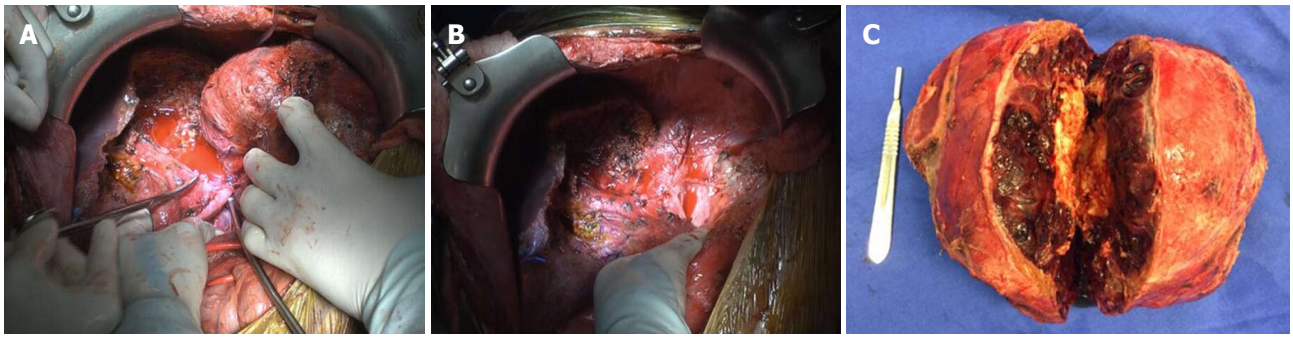

Figure 4 Intraoperative appearances. A: After hepatic posterior sector mass separation; B: Aspect of the remaining liver after surgical removal; C: Surgical piece.

patient was readmitted in the early postoperative phase with abdominal pains and leaking of bile through the drain due to a biliary fistula. The patient was submitted to a surgical procedure with a good outcome. Six months after the resection, the patient was well, had no relapses, and had a gastrin level of 40.5 pg/mL. At 1 year after the surgery, exam showed a gastrin level of 89.2 pg/mL. The normal range of gastrin is 13 to 115 pg/mL.

DISCUSSION

Zollinger-Ellison syndrome (ZES) is predominantly sporadic, although in 20%-30% of cases its origin is type 1 multiple endocrine neoplasia (MEN1). MEN 1 is a genetic disease that occurs in the gene MEN1, leading to the formation of various neoplasias; pancreatic endocrine tumors, pituitary adenomas, and hyperplasia of the parathyroid are the most prevalent. Despite the evidence of ulcers in this patient at the age of nine, ZES should be considered, principally because of the patient's history and hypergastrinemia. There was no report of the occurrence of MEN1 together with primary hepatic gastrinoma, including in our case.

Gastropancreatic neuroendocrine neoplasias, which can cause ZES, are classified according to their prognosis. Well-defined neuroendocrine tumors have a clinical course that is much less aggressive and can be subclassified as G1 (Ki-67 < 3) and G2 (Ki-67 of 3%-20%), according to the Ki-67 index that assesses the level of differentiation of cells in tissue. Poorly defined tumors are in category G3, presenting Ki-67 > 20%. Histopathological analysis of the patient's tumor revealed a Ki-67 of 5% (G2)[8]. The most common gastrinomas, duodenal and pancreatic, present a mean diameter of 1 and 3 cm, respectively[9]. The tumor in this case had dimensions of 19.5 cm × 12.5 cm × 17.0 cm.

Primary ectopic gastrinomas are neuroendocrine tumors located outside of the triangle of gastrinoma and are responsible for less than 10% of cases. One specific site in which they occur is the liver, with only 26 cases described in the literature in a review from 2012[10]. In recent years, there were a few more cases described, but the total number is still very low. According to a recent study[11], in ZES patients, primary gastrinomas of the liver were the second most common extrapancreatic, extraintestinal site for a primary gastrinoma and may metastasize to regional lymph nodes. Compared with typical ZES patients, the epidemiology of primary hepatic gastrinoma is a little different. The patients are generally affected much younger, with a predominance of males and no association with MEN 1, as it was in our case[12].

This rare hepatic gastrinoma is slow growing, with around 65% of cases malignant and 30%-40% of those cases being metastatic at initial presentation. This relatively high rate of metastases arises from the difficulty of diagnosis, especially in palliative care and hepatic metastases[13]. Despite this, our patient did not present metastases in radiological examinations.

A clinical presentation of ZES similar to gastroesophageal reflux can lead to treatment with proton-pump inhibitors. This medication masks the symptoms and alters gastrin levels, prolonging the time necessary to identify the real cause of the disease. A study[14] showed that prior to widespread use of proton-pump inhibitors (before 1985), the rate of metastases was only 19%. Ten years later, this number had risen to 55%. Prior to the advent of proton-pump inhibitors, partial and full gastrectomies were common to reduce the incidence of ulcers. In the report of this case, the fact that the patient had previously undergone antrectomy with vagotomy meant that his symptoms were less apparent than they would otherwise have been.

A second factor that can complicate diagnosis is related to the morphofunctional characteristics of the liver. It is known that the liver is a common site of metastasis for a variety of tumors, and classifying the neoplasia as primarily hepatic requires some examinations to confirm the absence of other primary sites. One of the examinations currently used is PEC/CT with 68 gallium-dotatate. This radiopharmacum is associated with computerized tomography and is a somatostatin analogue, which allows the identification of tumors[15]. The sensitivity of the examination was 93% (95%CI: ± 2%) and the specificity was 91% (95%CI: 82%-97%), as identified in a meta-analysis[9]. Once the neuroendocrine tumors present somatostatin receptors, it is possible to confirm whether the hepatic

gastrinoma is primary or the result of metastasis[16,17]. In this case, the existence of a single focus in the liver combined with a high level of gastrin highly suggested it as a primary site. Is important to emphasize the importance of the follow up of gastrin levels to ensure that there is not a small small duodenal primary gastrinoma that could not have been detected in the PET/CT and surgery[11].

Despite few reported cases, surgical resection should be the treatment of choice and, furthermore, the only chance of a cure. The rate of success in these cases is 86%, and 60% present early postoperative eugastrinemia, 40% after five years. In the event that surgery is not possible, such as in cases of diffuse metastasis or comorbidities, it is possible to follow conventional treatment: Ablation by radiofrequency, chemotherapy (doxorubicin, streptozocin, 5-fluorouracil), interferon, and transplantation[13]. A study with 160 patients with gastrinoma showed that 15-year disease-related survival was 98% for operated and 74% for unoperated (P = 0.0002)[18].

In conclusion, primary hepatic gastrinomas are extremely rare tumors that cause Zollinger-Ellison syndrome. Due to their clinical presentation and the liver being a significant site of metastases, diagnosis of the disease is time consuming and difficult. Following diagnosis, the treatment of choice is surgery, and, in cases where there are no metastases, the prognosis is good. Therefore, it is important to diagnose properly the primary gastrinoma.

ARTICLE HIGHLIGHTS

Case characteristics

Primary hepatic gastrinoma in a 19 years old hypergastremic patient who underwent hepatic trisegmentectomy to remove the tumor.

Clinical diagnosis

Primary hepatic gastrinoma.

Differential diagnosis

Gastrointestinal tumors, MEN 1.

Laboratory diagnosis

Gastrin levels were 6709.0 pg/mL before surgery. After the procedure it was 40.5 pg/mL.

Imaging diagnosis

Computed tomography (CT) showed a voluminous heterogeneous hepatic lesion, with a neoplasic aspect and dimensions 19.5 cm × 12.5 cm × 17.0 cm.

Pathological diagnosis

Histopathological analysis of the patient's tumor revealed a Ki-67 of 5% (G2).

Treatment

Hepatic trisegmentectomy.

Term explanation

Gastrinoma: A gastrinoma is a tumor that secretes an excess of gastrin, leading to ulceration in the duodenum, stomach, and the small intestine.

Experiences and lessons

Primary hepatic gastrinoma is a very difficult to diagnose. Meticulous examination is necessary for appropriate diagnosis and treatment.

ACKNOWLEDGEMENTS

The authors are thankful to Justin Axel-Berg for the English corrections.

REFERENCES

1 **Ellison EC**, Johnson JA. The Zollinger-Ellison syndrome: a comprehensive review of historical, scientific, and clinical considerations. *Curr Probl Surg* 2009; **46**: 13-106 [PMID: 19059523 DOI: 10.1067/j.cpsurg.2008.09.001]

2 **Zollinger RM**, Ellison EH. Primary peptic ulcerations of the jejunum associated with islet cell tumors of the pancreas. *Ann Surg* 1955; **142**: 709-723; discussion, 724-728 [PMID: 13259432 DOI: 10.1097/00000658-195510000-00015]

3 **Bergsland E**. Zollinger-Ellison syndrome (gastrinoma): Clinical manifestations and diagnosis. Available from: URL: https://www.uptodate.com/contents/zollinger-ellison-syndrome-gastrinoma-clinical-manifestations-and-diagnosis?source=search_result&search=gastrinomaselectedTitle=1~90

4 **Roy PK**, Venzon DJ, Shojamanesh H, Abou-Saif A, Peghini P, Doppman JL, Gibril F, Jensen RT. Zollinger-Ellison syndrome. Clinical presentation in 261 patients. *Medicine* (Baltimore) 2000; **79**: 379-411 [PMID: 11144036 DOI: 10.1097/00005792-200011000-00004]

5 **Smyrniotis V**, Kehagias D, Kostopanagiotou G, Tripolitsioti P, Paphitis A. Primary hepatic gastrinoma. *Am J Gastroenterol* 1999; **94**: 3380-3382 [PMID: 10566761 DOI: 10.1111/j.1572-0241.1999.3380a.x]

6 **Thompson NW**, Vinik AI, Eckhauser FE, Strodel WE. Extrapancreatic gastrinomas. *Surgery* 1985; **98**: 1113-1120 [PMID: 4071387]

7 **Norton JA**, Alexander HR, Fraker DL, Venzon DJ, Gibril F, Jensen RT. Possible primary lymph node gastrinoma: occurrence, natural history, and predictive factors: a prospective study. *Ann Surg* 2003; **237**: 650-657; discussion 657-9 [PMID: 12724631 DOI: 10.1097/01.SLA.0000064375.51939.48]

8 **Klimstra DS**, Yang Z. Pathology classification, and grading of neoplasms arising in the digestive system. Available from: URL: https://www.uptodate.com/contents/pathology-classification-and-grading-of-neuroendocrine-tumors-arising-in-the-digestive-system?source=search_result&search=gastrinoma%20ki-67&selectedTitle=1~150

9 **Ogawa S**, Wada M, Fukushima M, Shimeno N, Inoue S, Chung H, Fujita M, Suginoshita Y, Okada A, Inokuma T, Yagi S, Ito K, Imai Y. Case of primary hepatic gastrinoma: Diagnostic usefulness of the selective arterial calcium injection test. *Hepatol Res* 2015; **45**: 823-826 [PMID: 25145887 DOI: 10.1111/hepr.12404]

10 **Harvey A**, Pasieka JL, Al-Bisher H, Dixon E. Primary hepatic gastrinoma causing zollinger-ellison syndrome: a rare and challenging diagnosis. *Cancers (Basel)* 2012; **4**: 130-140 [PMID: 24213231 DOI: 10.3390/cancers4010130]

11 Incidence and Prognosis of Primary Gastrinomas in the Hepatobiliary Tract. *JAMA Surg* 2018; 153: e175083 [PMID: 29365025 DOI: 10.1001/jamasurg.2017.5083]

12 **Moriura S**, Ikeda S, Hirai M, Naiki K, Fujioka T, Yokochi K, Gotou S. Hepatic gastrinoma. *Cancer* 1993; **72**: 1547-1550 [PMID: 8348490 DOI: 10.1002/1097-0142(19930901)72:5<1547::AID-CNCR2820720510>3.0.CO;2-C]

13 **Tsalis K**, Vrakas G, Vradelis S, Dimoulas A, Pilavaki M, Papaemmanouil S, Micheli A, Lazarides C, Kartalis G. Primary hepatic gastrinoma: Report of a case and review of literature. *World J Gastrointest Pathophysiol* 2011; **2**: 26-30 [PMID: 21607163 DOI: 10.4291/wjgp.v2.i2.26]

14 **Evans JT**, Nickles S, Hoffman BJ. Primary hepatic gastrinoma: an

unusual case of zollinger-ellison syndrome. *Gastroenterol Hepatol* (NY) 2010; **6**: 53-56 [PMID: 20567542]

15 **Treglia G**, Castaldi P, Rindi G, Giordano A, Rufini V. Diagnostic performance of Gallium-68 somatostatin receptor PET and PET/CT in patients with thoracic and gastroenteropancreatic neuroendocrine tumours: a meta-analysis. *Endocrine* 2012; **42**: 80-87 [PMID: 22350660 DOI: 10.1007/s12020-012-9631-1]

16 **Mojtahedi A**, Thamake S, Tworowska I, Ranganathan D, Delpassand ES. The value of (68)Ga-DOTATATE PET/CT in diagnosis and management of neuroendocrine tumors compared to current FDA approved imaging modalities: a review of literature. *Am J Nucl Med Mol Imaging* 2014; **4**: 426-434 [PMID: 25143861]

17 **Deppen SA**, Liu E, Blume JD, Clanton J, Shi C, Jones-Jackson LB, Lakhani V, Baum RP, Berlin J, Smith GT, Graham M, Sandler MP, Delbeke D, Walker RC. Safety and Efficacy of 68Ga-DOTATATE PET/CT for Diagnosis, Staging, and Treatment Management of Neuroendocrine Tumors. *J Nucl Med* 2016; **57**: 708-714 [PMID: 26769865 DOI: 10.2967/jnumed.115.163865]

18 **Norton JA**, Fraker DL, Alexander HR, Gibril F, Liewehr DJ, Venzon DJ, Jensen RT. Surgery increases survival in patients with gastrinoma. *Ann Surg* 2006; **244**: 410-419 [PMID: 16926567 DOI: 10.1097/01.sla.0000234802.44320.a5]

P- Reviewer: Gencdal G, Jensen RT, Kaya M, Luo GH, Ozenirler S, Singh S, Tsuchiya A **S- Editor**: Ji FF **L- Editor**: Filipodia **E- Editor**: Tan WW

World Journal of Hepatology

Submit a Manuscript: http://www.f6publishing.com

World J Hepatol 2018 July 27; 10(7): 523-529

DOI: 10.4254/wjh.v10.i7.523

ISSN 1948-5182 (online)

CASE REPORT

Hepatectomy for gallbladder-cancer with unclassified anomaly of right-sided ligamentum teres: A case report and review of the literature

Toru Goto, Hiroaki Terajima, Takehito Yamamoto, Yoichiro Uchida

Toru Goto, Hiroaki Terajima, Takehito Yamamoto, Yoichiro Uchida, Department of Gastroenterological Surgery and Oncology, Tazuke Kofukai Medical Research Institute, Kitano Hospital, Osaka 530-8480, Japan

ORCID number: Toru Goto (0000-0002-8215-6839); Hiroaki Terajima (0000-0001-7938-6345); Takehito Yamamoto (0000-0002-2236-7124); Yoichiro Uchida (0000-0003-2266-7722).

Author contributions: Goto T, Terajima H and Uchida Y managed the patient and performed the operation; Goto T collected the clinical data, designed this report and wrote the paper; Terajima H and Yamamoto T helped draft and revise the manuscript.

Informed consent statement: The patient provided informed written consent for publication of this case report.

Conflict-of-interest statement: The authors declare that no conflicts of interest are associated with this manuscript.

CARE Checklist (2013) statement: The authors have read the CARE Checklist (2013), and the manuscript was prepared and revised according to the CARE Checklist (2013).

Manuscript source: Unsolicited manuscript

Correspondence to: Hiroaki Terajima, MD, PhD, Chief Doctor, Surgeon, Chief Director, Department of Gastroenterological Surgery and Oncology, Tazuke Kofukai Medical Research Institute, Kitano Hospital, 2-4-20 Ohgimachi, Kita-ku, Osaka 530-8480, Japan. h-terashima@kitano-hp.or.jp
Telephone: +81-6-63128824
Fax: +81-6-63128867

Received: February 19, 2018
Peer-review started: February 19, 2018
First decision: March 2, 2018
Revised: March 27, 2018
Accepted: May 30, 2018
Article in press: May 30, 2018
Published online: July 27, 2018

Abstract

Right-sided ligamentum teres (RSLT) is a congenital anomaly in which the right umbilical ligament becomes dominant and anomalous ramifications of the hepatic vessels and biliary system are present. A male patient in his 70s was diagnosed with advanced gallbladder cancer directly infiltrating the right hepatic duct (RHD), together with RSLT. Preoperative three-dimensional simulation of the liver based on multiple detector computed tomography images after cholangiography revealed ramifications of all segmental portal veins from the portal trunk and discordance of the arterial and biliary branching patterns of segment 8. Fusion analysis of the biliary architecture and segmental volumetry showed that the RHD drained segments 1r, 5, 6, and 7. We successfully performed a modified right-sided hepatectomy sparing segment 8 (*i.e.*, resection of the RHD drainage territory), with negative surgical margins. This report is the first to describe major hepatectomy for advanced gallbladder cancer with RSLT.

Key words: Right-sided ligamentum teres; Hepatectomy; Gallbladder cancer; Preoperative liver simulation; Anomaly of the portal vein

Core tip: Right-sided ligamentum teres (RSLT) is a congenital anomaly that involves anomalous ramifications of the

hepatic vessels and biliary system. A male in his 70s with RSLT was diagnosed with advanced gallbladder cancer directly infiltrating the right hepatic duct (RHD). Based on preoperative liver simulation, we successfully performed a modified right-sided hepatectomy sparing segment 8, which corresponded to resection of the RHD drainage territory (segments 1r, S5, S6, and S7), with negative surgical margins. This report is the first to describe major hepatectomy for advanced gallbladder cancer with RSLT.

Goto T, Terajima H, Yamamoto T, Uchida Y. Hepatectomy for gallbladder-cancer with unclassified anomaly of right-sided ligamentum teres: A case report and review of the literature. *World J Hepatol* 2018; 10(7): 523-529 Available from: URL: http://www.wjgnet.com/1948-5182/full/v10/i7/523.htm DOI: http://dx.doi.org/10.4254/wjh.v10.i7.523

INTRODUCTION

Right-sided ligamentum teres (RSLT) is a rare congenital anomaly in which the umbilical ligament on the left side atrophies and the right ligament becomes dominant at the 7-mm embryo stage[1]. The incidence of RSLT has been reported to be 0.2%-1.2% in adults[1,2]. RSLT is associated with anomalous ramifications in the arterial, portal vein, and biliary systems; therefore, precise evaluation of the branching patterns of the vascular and biliary architecture is required to avoid injuring the hepatic vasculature of the remnant liver[3-5]. Recent papers have demonstrated the significance of three-dimensional (3D) liver simulation before hepatectomy in RSLT patients to determine surgical strategies, such as the hepatectomy procedure and the cutting plane[6-8]. For gallbladder cancer, macroscopically complete surgical resection with negative microscopic margins remains the only potentially curative treatment, and major hepatectomy, such as extended right hepatectomy, is usually required for locally advanced gallbladder cancer[9]. This case report is the first to describe major hepatectomy for advanced gallbladder cancer concomitant with RSLT.

CASE REPORT

A male patient in his 70s was incidentally diagnosed with a gallbladder tumor by computed tomography (CT) during a preoperative examination of an inguinal hernia. He had no appreciable disease and had a good exercise tolerance. Laboratory tests showed normal levels of carcinoembryonic antigen and CA19-9. Hyperbilirubinemia was not observed. The indocyanine green (ICG) retention rate at 15 min was 3.6%; the normal range is less than 10%[10]. The patient's Child-Turcotte-Pugh score was 5 points, Grade A[11]. An abdominal contrast-enhanced CT scan showed an atrophied gallbladder with tumor-like localized wall thickness enhanced by contrast medium, strongly suggesting the possibility of gallbladder cancer. The gallbladder was attached to the left side of the liver and complicated variations of the intrahepatic vascular architecture were detected, suggesting RSLT (Figure 1A-E). Endoscopic retrograde gallbladder drainage (ERGBD) was performed for cytological examination of bile in the gallbladder and adenocarcinoma was detected two consecutive times (Figure 1F). To prevent obstructive jaundice and to evaluate horizontal extension of the tumor along the bile duct, ERGBD was switched to endoscopic nasobiliary drainage (ENBD) one week later. Two ENBD tubes were placed both in the right hepatic duct (RHD) and the left hepatic duct (LHD). ENBD tube cholangiography demonstrated a severe stenotic change of the RHD, and the confluence of the LHD and the common bile duct was intact (Figure 1G-I). No metastases of lymph nodes and distant organs were detected by CT scanning. Based on these findings, the patient was diagnosed with advanced gallbladder cancer with direct infiltration of the RHD rather than hilar cholangiocarcinoma. The gallbladder carcinoma was classified as cStage ⅢA (T3; right bile duct, N0, M0) according to the Union for International Cancer Control system[12]. Considering the patient's eligibility for radical surgery, we finally determined that right-sided major hepatectomy with resection of the RHD drainage territory was required.

Preoperative simulation was performed to plan the hepatectomy using multiple detector CT (MDCT) with a slice thickness of 1 mm after contrast cholangiography through an ENBD tube. After a quarto-phase (non-contrast, arterial, portal venous, and hepatic venous phases) contrast study was performed, two-dimensional CT images were transferred to a workstation (SYNAPSE VINCENT: FUJIFILM Medical Co., Ltd., Tokyo, Japan), and 3D images were automatically constructed for some areas and manually constructed for other areas. The intrahepatic vasculature was reconstructed at the 4th order division level (Figure 2A) and was verified by 4 liver surgeons independently. We labeled each sub-segment following the Couinaud classification[13] and the Brisbane 2000 terminology of Liver Anatomy and Resections[14] to define the anatomical divisions of the liver (Figure 2B and C). All segmental portal branches were separately ramified from the portal trunk (Figure 2D). No arterial anomalies were detected (Figure 2E). Bile duct analysis demonstrated that the bile duct of segment 8 (B8) was ramified from the LHD, and the RHD drained segments 5, 6, and 7. The bile duct of the right side of segment 1 (B1r) was ramified from the RHD, and the bile duct of the left side (B1l) was ramified from the LHD (Figure 2F).

Based on this simulation, resection of the gallbladder bed and the RHD drainage territory (segments 1r, 5, 6, and 7) was planned (Figure 3). The future liver remnant (FLR) volume was 605 mL. The plasma clearance rate of ICG in the FLR (calculated as the plasma clearance rate of ICG × the proportion of the FLR) was 0.131; 0.05 is the cut-off value for predicting mortality and morbidity[15]. The functional count rate of the FLR according to technetium-99m diethylenetriamine pentaacetic acid galactosyl human serum albumin scintigraphy was 50.2%[16]. The hepatic artery of segment 8 (A8) branched from the

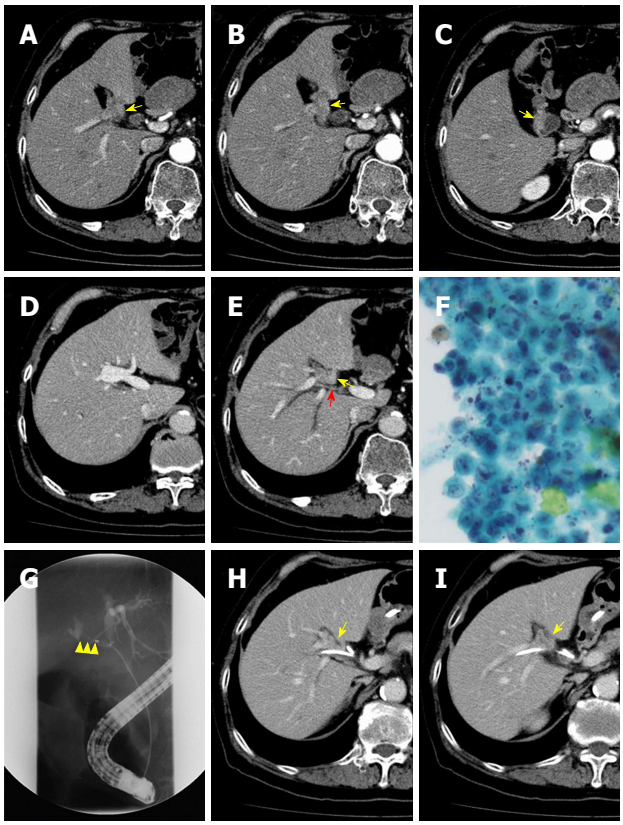

Figure 1 Contrast-enhanced computed tomography, cytological examination of bile, and endoscopic retrograde cholangiography. A, B and C: The highly atrophied gallbladder (yellow arrow) had tumor-like localized wall thickness enhanced by contrast medium; D: The cul-de-sac of the right-sided umbilical portion is shown; E: The gallbladder (yellow arrow) is located on the left-sided liver bed. Direct infiltration of the tumor into the right hepatic artery (red arrow) is not evident; F: Cytological examination of bile obtained from endoscopic retrograde gallbladder drainage demonstrated atypical cells with a high nucleo-cytoplasmic ratio, strongly suggesting adenocarcinoma; G: Endoscopic retrograde cholangiography shows severe stenosis of the right hepatic duct (yellow arrowhead); H and I: The gallbladder tumor (yellow arrow) directly spreads to the nearby right hepatic duct where an endoscopic nasobiliary tube was placed.

right hepatic artery, while B8 branched from the LHD.

During laparotomy, the gallbladder was located on the left side of the RSLT (Figure 4). After mobilization of the right lobe, lymphadenectomy of the hepatoduodenal ligament was performed. The common bile duct and LHD were divided, resulting in pathologically negative surgical margins, followed by parenchymal dissection of the gallbladder bed. All portal and arterial branches of segments 5 to 8 were extrahepatically separated and taped. Each pedicle was temporarily clamped, and the intrahepatic blood flow was simultaneously monitored via ultrasonography. After dividing all inflow vessels of segments 5 to 7, the demarcation line was detected as preoperatively simulated (Figure 5). The liver parenchyma was transected using a Cavitron ultrasonic surgical aspirator and saline-coupled bipolar electrocautery[17], with an intermittent Pringle maneuver. After dividing the right hepatic vein, the specimen was excised (Figure 6). Hepaticojejunostomy to the LHD and jejunojejunostomy were conducted, and the operation was successfully completed as planned (Figure 7). The surgical time was 682 min, and the estimated blood loss was 430 g.

Pathological examinations demonstrated well-differentiated tubular adenocarcinoma of the gallbladder with direct invasion of the liver parenchyma and the RHD (Figure 8). The tumor cell invaded to the RHD wall, but not into the lumen. Surgical margins were pathologically negative, and the tumor was classified as pStage Ⅲ A (T3; liver bed and right bile duct, N0, M0). Postoperative contrast-enhanced CT showed no ischemic regions in the remnant liver, including the spared segment 8. The patient was discharged 8 d after surgery without any complications more severe than a Grade Ⅱ Clavien-Dindo classification[18]. Five months after surgery, solitary liver metastasis in segment 2, far from the surgical stump, was detected during adjuvant chemotherapy with gemcitabine. The liver metastasis disappeared on imaging analysis after 2 cycles of chemotherapy with gemcitabine plus cisplatin (GC). The patient underwent ileocecal resection for primary ascending colon cancer 7 months after surgery; thereafter, an additional 13 cycles of GC therapy were continued. Multiple mediastinal lymph node metastases were identified 18 mo after surgery, and second-line chemotherapy with S-1 was introduced. The patient has currently survived 26 months after hepatectomy.

DISCUSSION

This report is the first to describe major hepatectomy for curative resection of advanced gallbladder cancer with RSLT. Preoperative simulation enabled visualization of the complicated anatomical findings of the intrahepatic vascular and biliary architecture and provided valuable assistance in performing resection of the RHD drainage territory without injuring the hepatic vasculature of the remnant liver.

The anomalies associated with RSLT may lead to several surgical problems during hepatectomy. In the most common cases (*e.g.*, an independent ramification of the right lateral portal pedicle), a surgeon's misunderstanding and ligation of the left portal trunk result in a lack of portal flow in two-thirds of the whole liver during left hepatectomy[3]. Therefore, awareness of the type of anomaly is important before planning hepatectomy for patients with RSLT[1,3,4]. In 1997, Nagai *et al*[1] reported two types of portal vein classifications of RSLT, and later, Shindoh *et al*[3] and Nishitai *et al*[4] demonstrated the classification of arterial, portal, and biliary ramifications. Portal ramification patterns were classified into three types: Independent right lateral, bifurcation, and trifurcation. Our case may be defined as an unclassified type because four sectional portal branches did not exist, and all subsegmental branches were directly ramified from the portal trunk. In the bifurcation type, P4 runs from the right paramedian branch to the left paramedian area beyond the middle hepatic vein (MHV). However, our case showed that P4 was ramified from the main portal trunk and did not run beyond the MHV. Therefore,

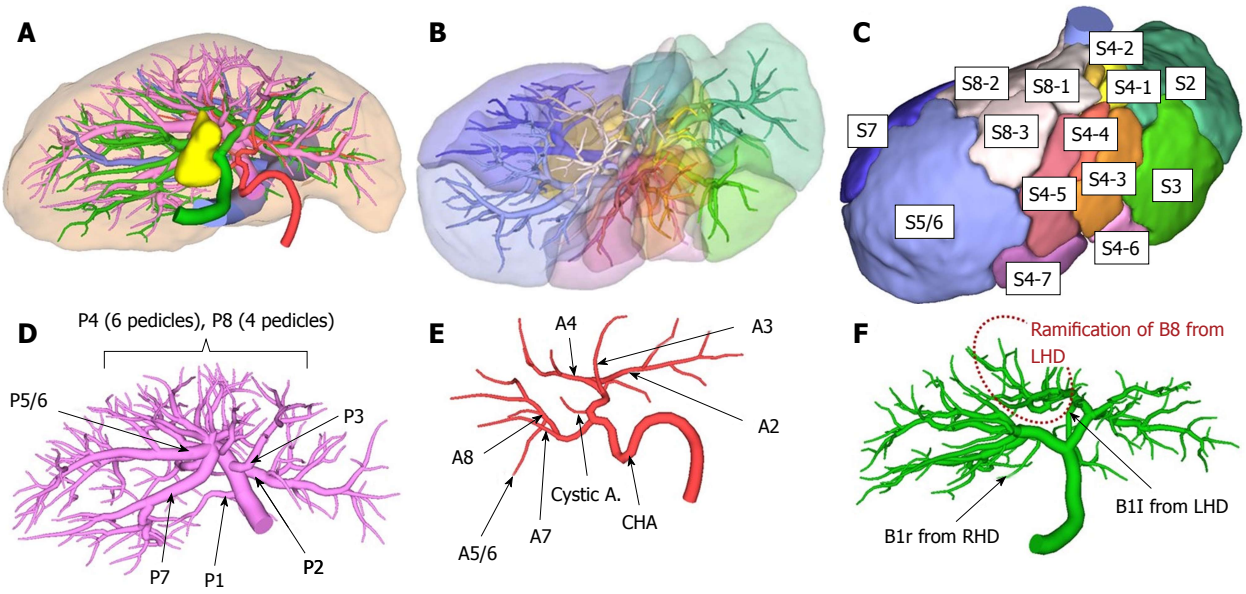

Figure 2 Preoperative simulation. A: An "all-in-one" simulation image. The intrahepatic vasculature was reconstructed at the 4th order division level (red: hepatic artery, pink: portal vein, green: bile duct, yellow: Gallbladder, blue: hepatic vein); B and C: Simulated segmentation based on the portal venous flow. Couinaud's definition was referred to for the naming of each segment; D: All segmental portal branches were ramified from the portal trunk. Interestingly, a common trunk of P5 and P6 was present; E: Hepatic arterial ramification without anomalous anatomy; F: The bile duct of segment 8 (B8) was ramified from the left hepatic duct, not from the right hepatic duct. RHD: Right hepatic duct; LHD: Left hepatic duct.

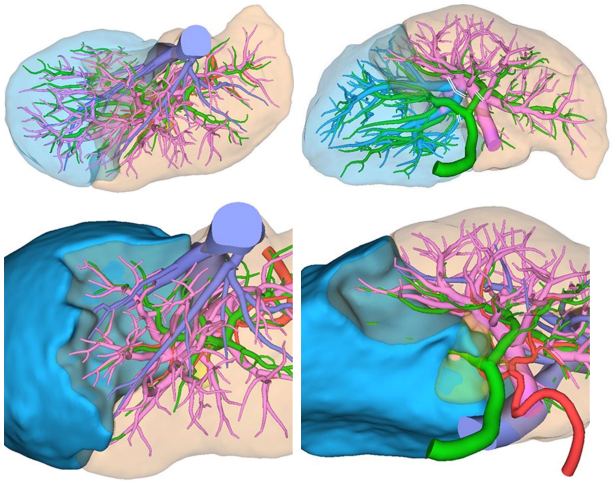

Figure 3 Simulation of modified right-sided hepatectomy. The resection area corresponded to the drainage territory of the right hepatic duct (segments 1r, 5, 6, and 7, blue area).

performing a conventional anatomical hepatectomy was difficult, and each subsegmental portal vein branch from the portal trunk had to be identified and divided. Hepatic arterial ramification patterns are classified into 3 types: Independent ramification of the left hepatic artery, common trunk formation between the left hepatic artery and the ventral branch of the right paramedian artery, and replaced left hepatic artery from the left gastric artery. Our case is classified as the first type. Intrahepatic bile duct confluence patterns are classified into 4 types: Symmetrical, independent right lateral, total left, and total right. Our case corresponds to the independent right lateral type, in which the LHD drains the right paramedian section.

No specific relationship has been reported among the patterns of the biliary, portal, and arterial ramifications in RSLT livers[4]. Embryologically, the portal ramifications induce restructuring of the ductal plate that surrounds them in the future intrahepatic ducts, which results in a periportal position of the intrahepatic bile ducts[19]. In principle, the formation of hepatic arteries follows the portal venous tributaries, and dissociations between the portal venous system and bile duct system have been reported[20]. Therefore, an uncorrelated pattern of portal vein and bile tree ramifications is possible. In our case, however, the arterial ramification pattern differed from the biliary confluence pattern; A8 was ramified from the right hepatic artery, and B8 entered into the LHD. This report is the first to describe an artery and bile duct that were not parallel. If the vascular and biliary anatomies of the expected remnant liver in major hepatectomy with hilar lymphadenectomy for hepatobiliary malignancies are extremely complicated, as in this case, hepatic resection with the Glissonian approach[6] is difficult to perform. Step-by-step extrahepatic division of all vasculature through hilar dissection based on precise preoperative simulation is the safest and most secure surgical strategy, as described in this paper.

Anomalies of the intrahepatic portal vein are not rare[2,21]. However, in our case, all subsegmental portal veins were ramified from the portal trunk extrahepatically. Therefore, we could intentionally encircle all portal branches in accordance with the detailed preoperative simulation. Although conventional right hepatectomy was also planned as an alternative, the infiltration of the tumor to the right hepatic artery was not evident from

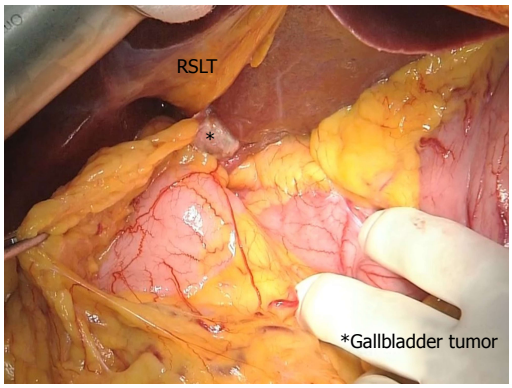

Figure 4 Hepatic hilar view during the operation. The gallbladder was located at the left side of the right-sided ligamentum teres (RSLT).

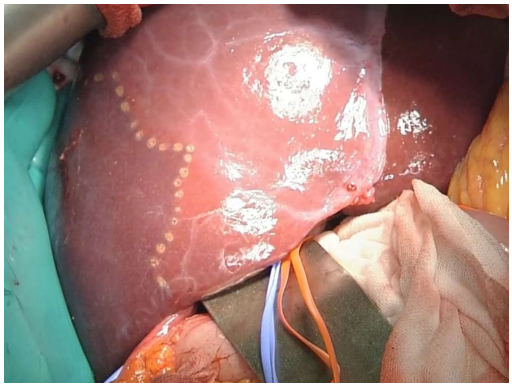

Figure 5 Demarcation line after dividing all arterial and portal branches of segments 1r, 5, 6, and 7.

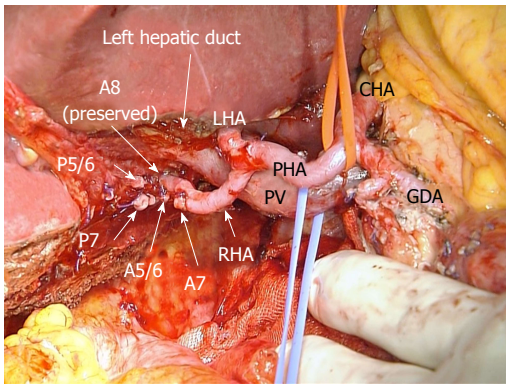

Figure 6 Final view of the hepatic hilum after hepatectomy. The portal and hepatic arterial branches of segment 8 were preserved. A common trunk of P5 and P6 was detected during the operation, which was confirmed by ischemic changes in S5 and S6 after clamping the target branch.

the intraoperative findings; therefore, modified right-sided hepatectomy was possible, as simulated.

Liver simulation, particularly 3D modeling and virtual planning, offers a new approach to liver resection, as reported by several groups[22-24]. Liver simulation has led to significantly shorter surgical times, and the predicted liver volume to be resected appears to correlate well with the actual resected liver weight[23]. Preoperative

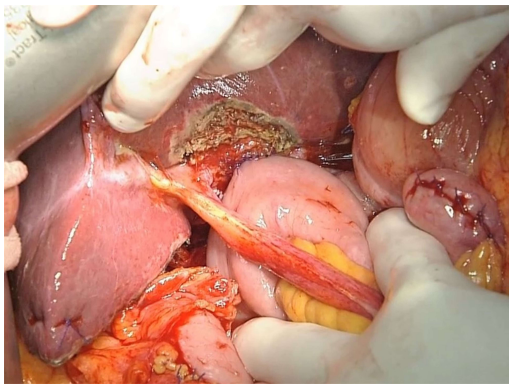

Figure 7 Final view after hepaticojejunostomy. The ligamentum teres originated from the main portal trunk and ran between S4-6 and S4-7.

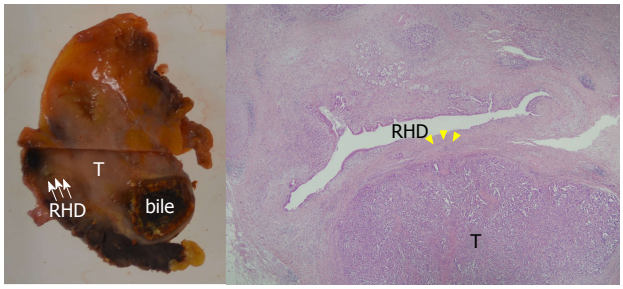

Figure 8 Pathological examination. Pathological examination shows well-differentiated tubular adenocarcinoma of the gallbladder (T) with direct invasion of the liver parenchyma and the right hepatic duct (RHD: white arrow). The tumor cell invaded to the RHD wall, but not into the lumen (yellow arrowhead) (hematoxylin eosin saffron, original magnification × 20).

simulation has become a common practice in Japan because simulation software has been developed and has become commercially available, and the cost of preoperative liver simulation has been covered by national health care insurance since 2012[25]. The fusion image of the portal vein and bile duct is useful for hepatectomy with RSLT because both the symmetrical type and the total left type of bile duct confluence patterns are similar to the ramification pattern of the normal liver, and cholangiography alone may provide misleading information for the operation[4]. The fusion image from one examination modality is referred to as an "all-in-one" (bile ducts, arteries, and portal veins) 3D image, in which MDCT is performed after cholangiography using carbon dioxide or iodine[24]. We strongly recommend structuring "all-in-one" 3D simulation images when planning hepatectomy with RSLT to evaluate the horizontal and perpendicular spreading of a tumor and its influence on the surrounding intrahepatic vasculature.

A systematic review of preoperative liver simulation and navigation has demonstrated the characteristics of the ideal simulation and navigation tool[26]. Simulation can accurately predict the liver volume to be resected, even by complicated anatomical resection procedures, and permits stereotactic measurement of the length of the surgical margin, which could not be estimated previously[27]. In this case, the most useful contribution

of liver simulation was the combination of volumetry with the 3D structure of the intrahepatic vasculature. Using volumetry, we could not only calculate the cubic content but also visualize the parenchymal shape that each subsegmental portal branch dominated. By comparing each subsegmental area with the 3D structure of the right-sided biliary trees, we could exactly determine the hepatic territory to be resected and divide the portal pedicles in the proper sequence, as simulated. Simulation also enabled us to perform a parenchyma-preserving hepatectomy, which may contribute to safe and curative resection in selected cases with liver neoplasm in the right anterior resection region[28]. Takamoto *et al*[29] demonstrated accurate, completed drawings and surgical strategies for malignant liver tumors to execute anatomic segmentectomy and subsegmentectomy using 3D simulation. We also successfully performed parenchyma-preserving anatomical resection at the 3rd order division level for oncologically curative resection based on a precise preoperative analysis. The current 3D simulation system cannot be used as a real-time navigation tool during surgery[29], and the development of new technology is ongoing.

In conclusion, 3D simulation based on precise intrahepatic vascular and biliary analysis enabled accurate and oncologically curative hepatic resection, even in a patient with rare anatomical anomalies.

ARTICLE HIGHLIGHTS

Case characteristics

A healthy and asymptomatic male in his 70s was incidentally diagnosed with a gallbladder tumor by preoperative computed tomography (CT) scanning for an inguinal hernia.

Clinical diagnosis

The patient, who had right-sided ligamentum teres (RSLT) with abnormal vascular anomaly, was diagnosed with advanced gallbladder cancer invading the right hepatic duct (RHD, cStage Ⅲ A, T3; right bile duct, N0, M0).

Differential diagnosis

Based on 2 important findings, including a solid tumor-like appearance of the highly atrophied gallbladder by CT scanning and cytological evidence of adenocarcinoma from bile obtained by endoscopic retrograde gallbladder drainage rather than endoscopic nasobiliary drainage, advanced gallbladder cancer with infiltration of the RHD was more convincing than hilar cholangiocarcinoma as a preoperative diagnosis.

Laboratory diagnosis

Laboratory tests revealed that tumor markers and liver function were within the normal ranges.

Imaging diagnosis

Preoperative three-dimensional liver simulation based on multiple detector computed tomography scanning combined with endoscopic nasobiliary tube cholangiography revealed that all segmental portal veins were independently ramified from the portal trunk and that the RHD drained the right-sided liver except for segment 8 (segments 1r, 5, 6, and 7).

Pathological diagnosis

Pathological examination showed well-differentiated tubular adenocarcinoma of the gallbladder invading the hepatic parenchyma and the RHD.

Treatment

The patient was treated with extended hepatectomy of the RHD drainage territory (segments 1r, 5, 6, and 7) without injuring the hepatic vasculature of the remnant liver based on preoperative liver simulation.

Related reports

Shindoh *et al* demonstrated anomalous vascular architecture with right-sided ligamentum teres (RSLT) and Ome *et al* reported major hepatectomy for RSLT patients. Shindoh J, Akahane M, Satou S, Aoki T, Beck Y, Hasegawa K, Sugawara Y, Ohtomo K, Kokudo N. Vascular architecture in anomalous right-sided ligamentum teres: Three-dimensional analyses in 35 patients. *HPB* (Oxford) 2012; **14**: 32-41 [PMID: 22151449 DOI: 10.1111/j.1477-2574.2011.00398.x]. Ome Y, Kawamoto K, Park TB, Ito T. Major hepatectomy using the glissonean approach in cases of right umbilical portion. *World J Hepatol* 2016; **8**: 1535-1540 [PMID: 28008345 DOI: 10.4254/wjh.v8.i34.1535].

Term explanation

RSLT is a congenital anomaly in which the umbilical ligament on the left side atrophies, and it is associated with anomalous ramifications in the artery, portal vein, and biliary systems.

Experiences and lessons

Preoperative 3D liver simulation based on precise intrahepatic vascular and biliary analysis enabled accurate and oncologically curative hepatic resection, even in a patient with rare anatomical anomalies.

ACKNOWLEDGMENTS

We thank Naomi Matsuzaki MD, a specialist in pathology, for her pathological diagnosis.

REFERENCES

1 **Nagai M**, Kubota K, Kawasaki S, Takayama T, BandaiY, Makuuchi M. Are left-sided gallbladders really located on the left side? *Ann Surg* 1997; **225**: 274-280 [PMID: 9060583 DOI: 10.1097/00000658-199703000-00006]

2 **Maetani Y**, Itoh K, Kojima N, Tabuchi T, Shibata T, Asonuma K, Tanaka K, Konishi J. Portal vein anomaly associated with deviation of the ligamentum teres to the right and malposition of the gallbladder. *Radiology* 1998; **207**: 723-728 [PMID: 9609896 DOI: 10.1148/radiology.207.3.9609896]

3 **Shindoh J**, Akahane M, Satou S, Aoki T, Beck Y, Hasegawa K, Sugawara Y, Ohtomo K, Kokudo N. Vascular architecture in anomalous right-sided ligamentum teres: three-dimensional analyses in 35 patients. *HPB* (Oxford) 2012; **14**: 32-41 [PMID: 22151449 DOI: 10.1111/j.1477-2574.2011.00398.x]

4 **Nishitai R**, Shindoh J, Yamaoka T, Akahane M, Kokudo N, Manaka D. Biliary architecture of livers exhibiting right-sided ligamentum teres: an indication for preoperative cholangiography prior to major hepatectomy. *HPB* (Oxford) 2016; **18**: 929-935 [PMID: 27594117 DOI: 10.1016/j.hpb.2016.08.002]

5 **Kawai K**, Koizumi M, Honma S, Tokiyoshi A, Kodama K. Right ligamentum teres joining to the right branch of the portal vein. *Anat Sci Int* 2008; **83**: 49-54 [PMID: 18402088 DOI: 10.1111/j.1447-073X.2007.00168.x]

6 **Ome Y**, Kawamoto K, Park TB, Ito T. Major hepatectomy using the glissonean approach in cases of right umbilical portion. *World J Hepatol* 2016; **8**: 1535-1540 [PMID: 28008345 DOI: 10.4254/wjh.v8.i34.1535]

7 **Abe T**, Kajiyama K, Harimoto N, Gion T, Shirabe K, Nagaie T. Resection of metastatic liver cancer in a patient with a left-sided gallbladder and intrahepatic portal vein and bile duct anomalies: A case report. *Int J Surg Case Rep* 2012; **3**: 147-150 [PMID: 22365920 DOI: 10.1016/j.ijscr.2012.01.003]

8 **Sakaguchi T**, Suzuki S, Morita Y, Oishi K, Suzuki A, Fukumoto K, Inaba K, Takehara Y, Baba S, Nakamura S, Konno H. Hepatectomy

for metastatic liver tumors complicated with right umbilical portion. *Hepatogastroenterology* 2011; **58**: 984-987 [PMID: 21830428]
9 **Fairweather M**, Balachandran VP, D'Angelica MI. Surgical management of biliary tract cancers. *Chin Clin Oncol* 2016; **5**: 63 [PMID: 27829277 DOI: 10.21037/cco.2016.10.03]
10 **Hemming AW**, Scudamore CH, Shackleton CR, Pudek M, Erb SR. Indocyanine green clearance as a predictor of successful hepatic resection in cirrhotic patients. *Am J Surg* 1992; **163**: 515-518 [PMID: 1575310 DOI: 10.1016/0002-9610(92)90400-L]
11 **Pugh RN**, Murray-Lyon IM, Dawson JL, Pietroni MC, Williams R. Transection of the oesophagus for bleeding oesophageal varices. *Br J Surg* 1973; **60**: 646-649 [PMID: 4541913 DOI: 10.1002/bjs.1800600817]
12 **Sobin LH**, Gospodarowicz MK, Wittekind C. TNM classification of malignant tumours. Hoboken, NJ: John Wiley Sons, 2011
13 **Couinaud C**. Le foie: Études anatomiques et chirurgicales. Paris: Masson Cie, 1957
14 **Pang YY**. The Brisbane 2000 terminology of liver anatomy and resections. HPB 2000; 2:333-39. *HPB* (Oxford) 2002; **4**: 99; author reply 99-99; author reply 100 [PMID: 18332933 DOI: 10.1080/13651820276037848 9]
15 **Yokoyama Y**, Nishio H, Ebata T, Igami T, Sugawara G, Nagino M. Value of indocyanine green clearance of the future liver remnant in predicting outcome after resection for biliary cancer. *Br J Surg* 2010; **97**: 1260-1268 [PMID: 20602507 DOI: 10.1002/bjs.7084]
16 **Nanashima A**, Abo T, Kudo T, Sakamoto I, Hayashi H, Murakami G, Takeshita H, Hidaka S, Kido Y, Nagayasu T. Usefulness of examining hepatic functional volume using technetium-99m galactosyl serum albumin scintigraphy in hepatocellular carcinoma. *Nucl Med Commun* 2013; **34**: 478-488 [PMID: 23458853 DOI: 10.1097/MNM.0b013e32835f945f]
17 **Yamamoto Y**, Ikai I, Kume M, Sakai Y, Yamauchi A, Shinohara H, Morimoto T, Shimahara Y, Yamamoto M, Yamaoka Y. New simple technique for hepatic parenchymal resection using a Cavitron Ultrasonic Surgical Aspirator and bipolar cautery equipped with a channel for water dripping. *World J Surg* 1999; **23**: 1032-1037 [PMID: 10512943 DOI: 10.1007/s002689900619]
18 **Dindo D**, Demartines N, Clavien PA. Classification of surgical complications: a new proposal with evaluation in a cohort of 6336 patients and results of a survey. *Ann Surg* 2004; **240**: 205-213 [PMID: 15273542 DOI: 10.1097/01.sla.0000133083.54934.ae]
19 **Cheynel N**, Arnal E, Rat P, Benoit L, Trouilloud P, Favre JP. Absence of the portal bifurcation at the hilum of the liver due to intrahepatic origin of the left branch of the portal vein. *Surg Radiol Anat* 2001; **23**: 355-357 [PMID: 11824139 DOI: 10.1007/s00276-001-0355-9]
20 **Hsu SL**, Chen TY, Huang TL, Sun CK, Concejero AM, Tsang LL, Cheng YF. Left-sided gallbladder: its clinical significance and imaging presentations. *World J Gastroenterol* 2007; **13**: 6404-6409 [PMID: 18081230 DOI: 10.3748/wjg.v13.i47.6404]
21 **Sanli EC**, Kurtoglu Z, Kara A, Uzmansel D. Left sided-right portal joined round ligament with an anomaly of the intrahepatic portal vein. *Saudi Med J* 2006; **27**: 1897-1900 [PMID: 17143372]
22 **Miyamoto R**, Oshiro Y, Hashimoto S, Kohno K, Fukunaga K, Oda T, Ohkohchi N. Three-dimensional imaging identified the accessory bile duct in a patient with cholangiocarcinoma. *World J Gastroenterol* 2014; **20**: 11451-11455 [PMID: 25170235 DOI: 10.3748/wjg.v20.i32.11451]
23 **Nakayama K**, Oshiro Y, Miyamoto R, Kohno K, Fukunaga K, Ohkohchi N. The Effect of Three-Dimensional Preoperative Simulation on Liver Surgery. *World J Surg* 2017; **41**: 1840-1847 [PMID: 28271263 DOI: 10.1007/s00268-017-3933-7]
24 **Okuda Y**, Taura K, Seo S, Yasuchika K, Nitta T, Ogawa K, Hatano E, Uemoto S. Usefulness of operative planning based on 3-dimensional CT cholangiography for biliary malignancies. *Surgery* 2015; **158**: 1261-1271 [PMID: 26054319 DOI: 10.1016/j.surg.2015.04.021]
25 **Mise Y**, Tani K, Aoki T, Sakamoto Y, Hasegawa K, Sugawara Y, Kokudo N. Virtual liver resection: computer-assisted operation planning using a three-dimensional liver representation. *J Hepatobiliary Pancreat Sci* 2013; **20**: 157-164 [PMID: 23135735 DOI: 10.1007/s00534-012-0574-y]
26 **Hallet J**, Gayet B, Tsung A, Wakabayashi G, Pessaux P; 2nd International Consensus Conference on Laparoscopic Liver Resection Group. Systematic review of the use of pre-operative simulation and navigation for hepatectomy: current status and future perspectives. *J Hepatobiliary Pancreat Sci* 2015; **22**: 353-362 [PMID: 25728031 DOI: 10.1002/jhbp.220]
27 **Yamanaka J**, Okada T, Saito S, Kondo Y, Yoshida Y, Suzumura K, Hirano T, Iimuro Y, Fujimoto J. Minimally invasive laparoscopic liver resection: 3D MDCT simulation for preoperative planning. *J Hepatobiliary Pancreat Surg* 2009; **16**: 808-815 [PMID: 19466379 DOI: 10.1007/s00534-009-0112-8]
28 **Kurimoto A**, Yamanaka J, Hai S, Kondo Y, Sueoka H, Ohashi K, Asano Y, Hirano T, Fujimoto J. Parenchyma-preserving hepatectomy based on portal ramification and perfusion of the right anterior section: preserving the ventral or dorsal area. *J Hepatobiliary Pancreat Sci* 2016; **23**: 158-166 [PMID: 26744104 DOI: 10.1002/jhbp.317]
29 **Takamoto T**, Hashimoto T, Ogata S, Inoue K, Maruyama Y, Miyazaki A, Makuuchi M. Planning of anatomical liver segmentectomy and subsegmentectomy with 3-dimensional simulation software. *Am J Surg* 2013; **206**: 530-538 [PMID: 23809675 DOI: 10.1016/j.amjsurg.2013.01.041]

P- Reviewer: Barreto SG, Kanazawa A, Kai K, Ramia JM, Shindoh J
S- Editor: Ji FF **L- Editor**: A **E- Editor**: Yin SY

Published by **Baishideng Publishing Group Inc**
7901 Stoneridge Drive, Suite 501, Pleasanton, CA 94588, USA
Telephone: +1-925-223-8242
Fax: +1-925-223-8243
E-mail: bpgoffice@wjgnet.com
Help Desk: http://www.f6publishing.com/helpdesk
http://www.wjgnet.com